



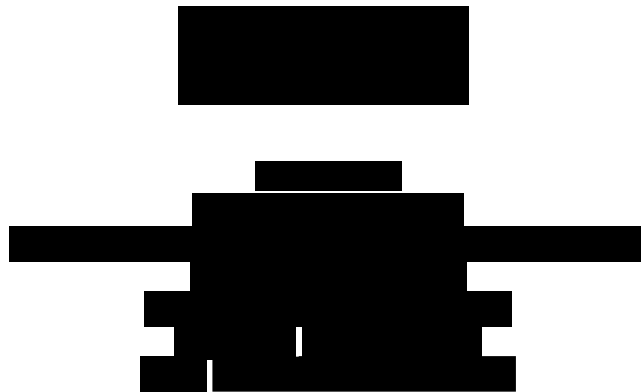
**Application to Amend the Australia New Zealand Food Standards Code  
Schedule 26 - Food Produced Using Gene Technology**

**OECD Unique Identifier - DP-915635-4**

DP915635 Maize

Submitting company:

Corteva Agriscience Australia Pty Ltd



March 2023

**© 2023 Pioneer Hi-Bred International, Inc., member of Corteva Agriscience group of companies, All Rights Reserved.** <sup>®</sup>, <sup>TM</sup>, <sup>SM</sup> Trademarks and service marks of Corteva Agriscience and its affiliated

This document is protected by copyright law. This document and material is for use only by the regulatory authority for the purpose that it is submitted by Pioneer Hi-Bred International, Inc., member of Corteva Agriscience group of companies, ("Corteva Agriscience"), its affiliates, or its licensees and only with the explicit consent of Corteva Agriscience. Except in accordance with law, any other use of this material, without prior written consent of Corteva Agriscience, is strictly prohibited. The intellectual property, information, and materials described in or accompanying this document are proprietary to Corteva Agriscience. By submitting this document, Corteva Agriscience does not grant any party or entity not authorized by Corteva Agriscience any right or license to the information or intellectual property described in this document.

## SUMMARY

Corteva Agriscience is a publicly traded, global pure-play agriculture company that provides farmers around the world with the most complete portfolio in the industry - including a balanced and diverse mix of seed, crop protection and digital solutions focused on maximizing productivity to enhance yield and profitability. With some of the most recognized brands in agriculture and an industry-leading product and technology pipeline well positioned to drive growth, the company is committed to working with stakeholders throughout the food system as it fulfils its promise to enrich the lives of those who produce and those who consume, ensuring progress for generations to come. Corteva Agriscience became an independent public company on June 1, 2019 and was previously the Agriculture Division of DowDuPont. More information can be found at [www.corteva.com](http://www.corteva.com).

Corteva Agriscience Australia Pty Ltd, member of Corteva Agriscience group of companies, is submitting this application to FSANZ to vary the Code to approve food uses of insect-resistant and herbicide-tolerant maize (*Zea mays L.*) event DP-915635-4 (referred to as DP915635 maize), a new food produced using gene technology.

DP915635 maize was genetically modified to express the IPD079Ea protein for control of susceptible corn rootworm (CRW) pests, the phosphinothricin acetyltransferase (PAT) protein for tolerance to glufosinate herbicide, and the phosphomannose isomerase (PMI) protein that was used as a selectable marker. The IPD079Ea protein is presented to FSANZ for review for the first time. The PAT and PMI proteins present in DP915635 maize are found in several approved events that are currently in commercial use.

This application presents information supporting the safety and nutritional comparability of DP915635 maize. The molecular characterization analyses conducted on DP915635 maize demonstrated that the introduced genes are integrated at a single locus, stably inherited across multiple generations, and segregate according to Mendel's law of genetics. The allergenic and toxic potential of the IPD079Ea protein were evaluated, and the IPD079Ea protein was found unlikely to be allergenic or toxic to humans or animals. The PAT and PMI proteins present in DP915635 maize are found in several approved events that are currently in commercial use. In accordance with the Application Handbook, only the updated bioinformatics analysis has been provided for these two proteins. The results confirm PAT and PMI proteins as unlikely to cause an adverse effect on humans or animals. A compositional equivalence assessment demonstrated that the nutrient composition of DP915635 maize forage and grain is comparable to that of conventional maize, represented by non-genetically modified (non-GM) near-isoline maize and non-GM commercial maize.

Overall, data and information contained herein support the conclusion that DP915635 maize containing the IPD079Ea, PAT, and PMI proteins is as safe and nutritious as non-GM maize for food and feed uses.

## TABLE OF CONTENTS

<b>SUMMARY</b> .....	<b>2</b>
<b>Table of Contents</b> .....	<b>3</b>
<b>List of Tables</b> .....	<b>5</b>
<b>List of Figures</b> .....	<b>7</b>
<b>Checklists</b> .....	<b>9</b>
<b>Statutory Declaration</b> .....	<b>11</b>
<b>General Information on the Application</b> .....	<b>12</b>
Applicant .....	12
Purpose of the application.....	12
Justification for the application .....	12
D(a) Need for the proposed change .....	12
D(b) Advantage of the genetically modified food .....	13
D.1 Regulatory impact.....	13
<b>A. Technical information on the food produced using gene technology</b> .....	<b>16</b>
A.1 Nature and identity of the genetically modified food .....	16
A.1.(a) Description of the GM organisms, nature and purpose of the genetic modification .....	16
A.1.(b) GM Organism Identification .....	16
A.1.(c) Trade name .....	16
A.2 History of use of the host and donor organisms.....	17
A.2.(a) Donor Organisms .....	17
A.2.(b) Host Organism .....	18
A.3 The nature of the genetic modification .....	19
A.3(a) Transformation Method .....	19
A.3(b) Description of the construct and the transformation vectors used .....	38
A.3(c) Molecular characterisation .....	38
A.3(d) Breeding process .....	54
A.3(e) Stability of the genetic changes .....	56
<b>B. Characterisation and safety assessment of new substances</b> .....	<b>65</b>
B.1 Characterisation and safety assessment of new substances .....	65
B.2 New proteins.....	65
IPD079Ea protein.....	65
PAT protein.....	89
PMI protein.....	98
B.3 Other (non-protein) new substances.....	107
B.4 Novel herbicide metabolites in GM herbicide-tolerant plants .....	107
B.5 Compositional analyses of the food produced using gene technology .....	107
<b>C. Information related to the nutritional impact of the food</b> .....	<b>124</b>
<b>D. Other Information</b> .....	<b>124</b>
Overall Risk Assessment Conclusions for DP915635 Maize .....	124

<b>References</b> .....	<b>125</b>
<b>Study index</b> .....	<b>132</b>
<b>Appendix A. Methods for Southern-by-Sequencing Analysis</b> .....	<b>134</b>
<b>Appendix B. Methods for Southern Blot Analysis</b> .....	<b>156</b>
<b>Appendix C. Methods for Multi-Generation Segregation Analysis</b> .....	<b>158</b>
<b>Appendix D. Methods for Sanger Sequencing Analysis</b> .....	<b>160</b>
<b>Appendix E. Methods for Characterization of IPD079Ea Protein</b> .....	<b>164</b>
<b>Appendix F. Methods for Characterization of PAT Protein</b> .....	<b>175</b>
<b>Appendix G. Methods for Characterization of PMI Protein</b> .....	<b>178</b>
<b>Appendix H. Methods for Trait Expression Analyses</b> .....	<b>181</b>
<b>Appendix I. Methods for Nutrient Composition Analysis</b> .....	<b>185</b>

## LIST OF TABLES

Table 1. List of Genetic Elements in Plasmids Used for Landing Pad Transformation and Their Presence in DP915635 Maize .....	20
Table 2. List of Genetic Elements in PHP83175 T-DNA and Their Presence in DP915635 Maize .....	26
Table 3. Description of the Genetic Elements in Plasmid PHP83175 .....	32
Table 4. Description of the Genetic Elements in the T-DNA Region from Plasmid PHP83175 .....	33
Table 5. Maize Endogenous Elements in Plasmids and DP915635 Insertion .....	42
Table 6. DP915635 Maize and Control Maize SbS Junction Reads .....	43
Table 7. SbS Junction Reads at Single Nucleotide Changes .....	44
Table 8. Generations and Comparators Used for Analysis of DP915635 Maize .....	55
Table 9. Description of DNA Probes Used for Southern Hybridization .....	57
Table 10. Predicted and Observed Hybridization Bands on Southern Blots; <i>Pvu</i> II Digest .....	57
Table 11. Summary of Genotypic and Phenotypic Segregation Results for Five Generations of DP915635 Maize .....	64
Table 12. Tryptic Peptides of DP915635 Maize-Derived IPD079Ea Protein Identified Using LC-MS Analysis .....	71
Table 13. Chymotryptic Peptides of DP915635 Maize-Derived IPD079Ea Protein Identified Using LC-MS Analysis .....	72
Table 14. Combined Sequence Coverage of Identified Tryptic and Chymotryptic Peptides of DP915635 Maize-Derived IPD079Ea Protein Using LC-MS Analysis .....	73
Table 15. Tryptic Peptides of Microbially Derived IPD079Ea Protein Identified Using LC-MS Analysis .....	74
Table 16. Chymotryptic Peptides of Microbially Derived IPD079Ea Protein Identified Using LC-MS Analysis .....	75
Table 17. Combined Sequence Coverage of Identified Tryptic and Chymotryptic Peptides of Microbially Derived IPD079Ea Protein Using LC-MS Analysis .....	76
Table 18. N-Terminal Amino Acid Sequence Analysis of IPD079Ea Protein .....	77
Table 19. Biological Activity of Heat-Treated IPD079Ea Protein in Artificial Diet Fed to Western Corn Rootworm .....	79
Table 20. Summary of IPD079Ea Protein <i>In Vitro</i> Pepsin Resistance Assay Results .....	79
Table 21. Summary of IPD079Ea Protein <i>In Vitro</i> Pancreatin Resistance Assay Results .....	82
Table 22. Identified Tryptic and Chymotryptic Peptides of DP915635 Maize-Derived PAT Protein Using LC-MS Analysis .....	94
Table 23. Combined Sequence Coverage of Identified Tryptic and Chymotryptic Peptides of DP915635 Maize-Derived PAT Protein Using LC-MS Analysis .....	95
Table 24. N-Terminal Amino Acid Sequence Analysis of DP915635 Maize-Derived PAT Protein .....	95
Table 25. Identified Tryptic Peptides of DP915635 Maize-Derived PMI Protein Using LC-MS Analysis .....	102
Table 26. Identified Chymotryptic Peptides of DP915635 Maize-Derived PMI Protein Using LC-MS Analysis .....	103
Table 27. Combined Sequence Coverage of Identified Tryptic and Chymotryptic Peptides of DP915635 Maize-Derived PMI Protein Using LC-MS Analysis .....	104
Table 28. Across-Sites Summary of IPD079Ea Protein Concentrations in DP915635 Maize .....	107
Table 29. Across-Sites Summary of PAT Protein Concentrations in DP915635 Maize .....	108
Table 30. Across-Sites Summary of PMI Protein Concentrations in DP915635 Maize .....	108
Table 31. Outcome of the Nutrient Composition Assessment for DP915635 Maize .....	110
Table 32. Proximate, Fiber, and Mineral Results for DP915635 Maize Forage .....	113
Table 33. Proximate and Fiber Results for DP915635 Maize Grain .....	114
Table 34. Fatty Acid Results for DP915635 Maize Grain .....	115
Table 35. Number of Fatty Acid Sample Values Below the Lower Limit of Quantification for DP915635 Maize Grain .....	117
Table 36. Amino Acid Results for DP915635 Maize Grain .....	117
Table 37. Mineral Results for DP915635 Maize Grain .....	119
Table 38. Number of Mineral Sample Values Below the Lower Limit of Quantification for DP915635 Maize Grain .....	120
Table 39. Vitamin Results for DP915635 Maize Grain .....	121
Table 40. Number of Vitamin Sample Values Below the Lower Limit of Quantification for DP915635 Maize Grain .....	122
Table 41. Secondary Metabolite and Anti-Nutrient Results for DP915635 Maize Grain .....	122
Table 42. Number of Secondary Metabolite and Anti-Nutrient Sample Values Below the Lower Limit of Quantification for DP915635 Maize Grain .....	123

Table D.1. PCR Amplification Conditions .....	161
Table D.2. Restriction Enzyme Digests of Topo Clone DNA Containing PCR Fragment F .....	162
Table E.1. Control Samples for Simulated Gastric Fluid (SGF) Digestibility Analysis .....	170
Table E.2. Control Samples for Simulated Intestinal Fluid (SIF) Digestibility Analysis .....	172
Table H.1. Maize Growth Stage Descriptions .....	181
Table I.1. Methods for Compositional Analysis .....	187

## LIST OF FIGURES

Figure 1. Schematic Diagram of Plasmid PHP73878.....	21
Figure 2. Schematic Diagram of the T-DNA Region from Plasmid PHP73878.....	22
Figure 3. Schematic Diagram of Plasmid PHP70605.....	23
Figure 4. Schematic Diagram of Plasmid PHP21139.....	24
Figure 5. Schematic Diagram of Plasmid PHP21875.....	25
Figure 6. Schematic Diagram of Plasmid PHP83175.....	27
Figure 7. Schematic Diagram of the T-DNA Region from Plasmid PHP83175.....	28
Figure 8. Schematic Diagram of the DP915635 Maize Insertion.....	29
Figure 9. Southern by Sequencing (SbS) Process Flow Diagram.....	39
Figure 10. Schematic Diagram of the DNA Insertion in DP915635 Maize.....	44
Figure 11. SbS Results for Control Maize.....	46
Figure 12. SbS Results for Positive Control Samples.....	48
Figure 13. SbS Results for DP915635 Maize (Plant ID 385269369).....	50
Figure 14. Diagram of the Insert and Genomic Border Regions Sequenced in DP915635 Maize.....	51
Figure 15. Event Development Process of DP915635 Maize.....	54
Figure 16. Breeding Diagram for DP915635 Maize and Generations Used for Analysis.....	55
Figure 17. Map of Plasmid PHP83175 for Southern Analysis.....	58
Figure 18. Map of PHP83175 T-DNA for Southern Analysis.....	59
Figure 19. Map of Insertion in DP915635 Maize for Southern Analysis.....	60
Figure 20. Southern Blot Analysis of DP915635 Maize; <i>Pvu</i> II Digest with <i>ipd079Ea</i> Probe.....	61
Figure 21. Southern Blot Analysis of DP915635 Maize; <i>Pvu</i> II Digest with <i>mo-pat</i> Probe.....	62
Figure 22. Southern Blot Analysis of DP915635 Maize; <i>Pvu</i> II Digest with <i>pmi</i> Probe.....	63
Figure 23. Deduced Amino Acid Sequence of the IPD079Ea Protein.....	65
Figure 24. SDS-PAGE Analysis of IPD079Ea Protein.....	67
Figure 25. Western Blot Analysis of IPD079Ea Protein.....	68
Figure 26. Glycosylation Analysis of DP915635 Maize-Derived IPD079Ea Protein.....	69
Figure 27. Glycosylation Analysis of Microbially Derived IPD079Ea Protein.....	70
Figure 28. Amino Acid Sequence of DP915635 Maize-Derived IPD079Ea Protein Indicating Tryptic and Chymotryptic Peptides Identified Using LC-MS Analysis.....	73
Figure 29. Amino Acid Sequence of Microbially Derived IPD079Ea Protein Indicating Chymotryptic Peptides Identified Using LC-MS Analysis.....	76
Figure 30. SDS-PAGE Analysis of IPD079Ea Protein in Simulated Gastric Fluid Digestion Time Course.....	80
Figure 31. Western Blot Analysis of IPD079Ea Protein in Simulated Gastric Fluid Digestion Time Course.....	81
Figure 32. SDS-PAGE Analysis of IPD079Ea Protein in Simulated Intestinal Fluid Digestion Time Course.....	83
Figure 33. Western Blot Analysis of IPD079Ea Protein in Simulated Intestinal Fluid Digestion Time Course.....	84
Figure 34. SDS-PAGE Analysis of IPD079Ea Protein in a Sequential Digestion with Simulated Gastric Fluid and Simulated Intestinal Fluid.....	86
Figure 35. Alignment of the Deduced Amino Acid Sequence of PAT Protein Encoded by <i>pat</i> and <i>mo-pat</i> Genes.....	89
Figure 36. SDS-PAGE Analysis of DP915635 Maize-Derived PAT Protein.....	91
Figure 37. Western Blot Analysis of PAT Protein.....	92
Figure 38. Glycosylation Analysis of the DP915635 Maize-Derived PAT Protein.....	94
Figure 39. Identified Tryptic and Chymotryptic Peptide Amino Acid Sequence of DP915635 Maize-Derived PAT Protein Using LC-MS Analysis.....	95
Figure 40. Deduced Amino Acid Sequence of the PMI Protein.....	98
Figure 41. SDS-PAGE Analysis of DP915635 Maize-Derived PMI Protein.....	99
Figure 42. Western Blot Analysis of DP915635 Maize-Derived PMI Protein.....	101
Figure 43. Glycosylation Analysis of DP915635 Maize-Derived PMI Protein.....	102

Figure 44. Amino Acid Sequence of DP915635 Maize-Derived PMI Protein Indicating the Identified Tryptic and Chymotryptic Peptide Using LC-MS Analysis .....	105
Figure A.1. SbS Results for DP915635 Maize (Plant ID 385269371) .....	139
Figure A.2. SbS Results for DP915635 Maize (Plant ID 385269372) .....	141
Figure A.3. SbS Results for DP915635 Maize (Plant ID 385269373) .....	143
Figure A.4. SbS Results for DP915635 Maize (Plant ID 385269375) .....	145
Figure A.5. SbS Results for DP915635 Maize (Plant ID 385269367) .....	147
Figure A.6. SbS Results for DP915635 Maize (Plant ID 385269368) .....	149
Figure A.7. SbS Results for DP915635 Maize (Plant ID 385269370) .....	151
Figure A.8. SbS Results for DP915635 Maize (Plant ID 385269374) .....	153
Figure A.9. SbS Results for DP915635 Maize (Plant ID 385269376) .....	155
Figure D.1. Map of Fragment F Indicating Restriction Enzyme Cut Sites.....	162

## CHECKLISTS

General requirements (3.1.1)		
Check	Page No.	Mandatory requirements
		A Form of application
<input checked="" type="checkbox"/>		<input checked="" type="checkbox"/> <i>Application in English</i> <input checked="" type="checkbox"/> <i>Executive Summary (separated from main application electronically)</i> <input checked="" type="checkbox"/> <i>Relevant sections of Part 3 clearly identified</i> <input checked="" type="checkbox"/> <i>Pages sequentially numbered</i> <input checked="" type="checkbox"/> <i>Electronic copy (searchable)</i> <input checked="" type="checkbox"/> <i>All references provided</i>
<input checked="" type="checkbox"/>	12	B Applicant details
<input checked="" type="checkbox"/>	12	C Purpose of the application
		D Justification for the application
<input checked="" type="checkbox"/>	12	<input checked="" type="checkbox"/> <i>Regulatory impact information</i> <input checked="" type="checkbox"/> <i>Impact on international trade</i>
		E Information to support the application
<input checked="" type="checkbox"/>		<input checked="" type="checkbox"/> <i>Data requirements</i>
		F Assessment procedure
<input checked="" type="checkbox"/>		<input checked="" type="checkbox"/> <i>General</i> <input type="checkbox"/> <i>Major</i> <input type="checkbox"/> <i>Minor</i> <input type="checkbox"/> <i>High level health claim variation</i>
		G Confidential commercial information
<input checked="" type="checkbox"/>		<input checked="" type="checkbox"/> <i>CCI material separated from other application material</i> <input checked="" type="checkbox"/> <i>Formal request including reasons</i> <input checked="" type="checkbox"/> <i>Non-confidential summary provided</i>
		H Other confidential information
<input checked="" type="checkbox"/>		<input checked="" type="checkbox"/> <i>Confidential material separated from other application material</i> <input checked="" type="checkbox"/> <i>Formal request including reasons</i>
		I Exclusive Capturable Commercial Benefit
<input type="checkbox"/>		<input type="checkbox"/> <i>Justification provided</i>
		J International and other national standards
<input checked="" type="checkbox"/>		<input checked="" type="checkbox"/> <i>International standards</i>
		<input type="checkbox"/> <i>Other national standards</i>
<input checked="" type="checkbox"/>	11	K Statutory Declaration
		L Checklist/s provided with application
<input checked="" type="checkbox"/>	9	<input checked="" type="checkbox"/> <i>3.1.1 Checklist</i> <input checked="" type="checkbox"/> <i>All page number references from application included</i> <input checked="" type="checkbox"/> <i>Any other relevant checklists for Chapters 3.2–3.7</i>

### Foods produced using gene technology (3.5.1)

Check	Page No.	Mandatory requirements
<input checked="" type="checkbox"/>	16	A.1 Nature and identity
<input checked="" type="checkbox"/>	17	A.2 History of use of host and donor organisms
<input checked="" type="checkbox"/>	19	A.3 Nature of genetic modification
<input checked="" type="checkbox"/>	65	B.1 Characterisation and safety assessment
<input checked="" type="checkbox"/>	65	B.2 New proteins
<input checked="" type="checkbox"/>	107	B.3 Other (non-protein) new substances
<input checked="" type="checkbox"/>	107	B.4 Novel herbicide metabolites in GM herbicide-tolerant plants
<input checked="" type="checkbox"/>	107	B.5 Compositional analyses
<input checked="" type="checkbox"/>	124	C Nutritional impact of GM food
<input checked="" type="checkbox"/>	124	D Other information

## STATUTORY DECLARATION

### STATUTORY DECLARATION

*Statutory Declarations Act 1959*<sup>1</sup>

I, [REDACTED] Regulatory Manager of Corteva Agriscience, Level 9, 67 Albert Ave, Chatswood, NSW 2067  
make the following declaration under the *Statutory Declarations Act 1959*:

1. the information provided in this application fully sets out the matters required
2. the information provided in this application is true to the best of my knowledge and belief
3. no information has been withheld that might prejudice this application, to the best of my knowledge and belief

I understand that a person who intentionally makes a false statement in a statutory declaration is guilty of an offence under section 11 of the *Statutory Declarations Act 1959*, and I believe that the statements in this declaration are true in every particular.

[REDACTED]

[Signature of person making the declaration]

[REDACTED]

<sup>1</sup> <http://www.comlaw.gov.au/Series/C1959A00052>.

## GENERAL INFORMATION ON THE APPLICATION

The chapter numbering follows section numbers from the FSANZ Application Handbook (Chapters 3.1 and 3.5.1).

### APPLICANT

This application is submitted by:

[REDACTED]  
[REDACTED]  
[REDACTED]  
[REDACTED]  
[REDACTED]

The primary contact is:

[REDACTED]  
[REDACTED]  
[REDACTED]  
[REDACTED]  
[REDACTED]

[REDACTED]  
[REDACTED]  
[REDACTED]  
[REDACTED]

### PURPOSE OF THE APPLICATION

Corteva Agriscience Australia Pty Ltd, member of Corteva Agriscience group of companies (herein referred to as Corteva), has developed DP915635 maize (OECD Unique Identifier DP-915635-4), a new event that has been transformed to express the IPD079Ea, PAT, and PMI proteins.

As a result of this application, Corteva seeks an amendment of Standard 1.5.2 *Food produced using gene technology* by inserting the following into table to Schedule 26 3(4) after the last entry: *herbicide-tolerant and insect-protected corn line DP915635*.

### JUSTIFICATION FOR THE APPLICATION

#### D(a) Need for the proposed change

Corteva is a member of Excellence Through Stewardship™ (ETS). Corteva has developed the new maize event DP915635, which is being commercialized in accordance with the ETS Product Launch Stewardship Guidance and in compliance with Corteva policies regarding stewardship of GM products. In line with these guidelines, Corteva's process for launches of new products includes a longstanding process to evaluate export market information, value chain consultations, and regulatory functionality. Corteva's application to amend Standard 1.5.2 with respect to DP915635 is in support of these policies.

## **D(b) Advantage of the genetically modified food**

DP915635 maize was genetically modified to express the IPD079Ea protein for control of susceptible corn rootworm (CRW) pests, the phosphinothricin acetyltransferase (PAT) protein for tolerance to glufosinate herbicide, and the phosphomannose isomerase (PMI) protein that was used as a selectable marker.

Maize has multiple downstream uses for feed, fuel, and food that are significant for the global supply of this crop commodity. The introduction of insect-resistant and herbicide-tolerant DP915635 maize is intended to help growers keep pace with increasing maize demand globally. The United States is one of the world's largest maize producers and a leading exporter of maize. The United States is one of the world's largest maize producers and a leading exporter of maize. In 2020, more than 14 billion bushels of maize were produced in the United States from approximately 90 million planted acres, valued at nearly \$60 billion ([NCGA, 2020](#); [USDA-NASS, 2020](#)). One of the most serious pests of maize in the United States is Western corn rootworm (WCR; *Diabrotica virgifera virgifera*), with economic losses of greater than \$1 billion annually from both management costs and yield loss ([Metcalf, 1986](#); [PHI, 2010](#); [Shrestha et al., 2018](#)).

### **Insect resistance**

WCR damage has historically been managed with crop rotation, broad-spectrum soil insecticides, and transgenic crops expressing crystalline (Cry) proteins, such as Cry3-class and Cry34/35 classes proteins, developed from *Bacillus thuringiensis* (*Bt*). As adoption of *Bt* maize has increased, the selection pressure on target insects to develop resistance has become greater ([Cullen et al., 2013](#)). Insect resistance to transgenic traits can reduce the efficacy of the traits over time, increasing costs of maize production and/or reducing yield. As reduced performance of Cry3 Cry34/35 classes proteins in maize has been reported in the scientific literature ([Gassmann et al., 2016](#); [Jakka et al., 2016](#)), differentiated modes of action (MOA) are important for maintaining sustainable and durable CRW management ([Gassmann et al., 2016](#); [Niu et al., 2017](#)). The IPD079Ea protein expressed in DP915635 maize has been demonstrated to be efficacious against susceptible CRW pests, including WCR, and provides a new MOA that is separate and distinct from the currently available *Bt* protein-based MOAs for CRW control. DP915635 maize provides farmers with an additional control option for CRW pests to help protect maize grain yield.

### **Herbicide tolerance**

The PAT protein is tolerant to the herbicidal active ingredient glufosinate-ammonium ([CERA - ILSI Research Foundation, 2016](#)). DP915635 maize provides farmers with an additional control option for herbicide management practices.

#### **D.1 Regulatory impact**

Corteva have developed the new maize line DP915635, which will be commercialized in accordance with the ETS Product Launch Stewardship Guidance and in compliance with Corteva policies regarding stewardship of GM products. In line with these guidelines, Corteva's product launch process for launches of new products includes a longstanding process to evaluate export market information, value chain consultations, and regulatory functionality. Growers and end-users must take all steps within their control to follow appropriate stewardship requirements and confirm their buyer's acceptance of the grain or other material being purchased.

Refer to the OECD Consensus Document on Compositional Considerations for New Varieties of Maize (*Zea mays*): Key Food and Feed Nutrients, Anti-nutrients and Secondary Plant Metabolites ([OECD, 2002](#)), for the following aspects of the food uses of maize:

- Production of maize for food and feed
- Processing of maize

- Wet Milling
- Dry Milling
- Masa Production
- Feed Processing

The majority of grain and forage derived from maize is used for animal feeds. Less than 10% of maize grain is processed for human food products. Maize grain is also processed into industrial products, such as ethyl alcohol by fermentation and highly refined starch by wet-milling to produce starch and sweetener products. In addition to milling, maize germ can be processed to obtain maize oil.

Domestic production of maize in Australia (ca. 440,000 t) and New Zealand is supplemented by import of a small amount of maize-based products, largely as high-fructose maize syrup, which is not currently manufactured in either Australia or New Zealand. Such products are processed into breakfast cereals, baking products, extruded confectionery and maize chips. Other maize products such as maize starch are also imported. This is used by the food industry for the manufacture of dessert mixes and canned foods ([www.grdc.com.au](http://www.grdc.com.au)).

#### **D.1.1 Costs and benefits for industry, consumers and government**

Corteva launches new products in accordance with the Corteva Product Launch Policy and Excellence Through Stewardship Product Launch Guidance . Our long-standing, multi-faceted approach includes evaluating export market information, performing value-chain consultations and consideration of regulatory functionality. Innovative technologies like DP915635 maize are designed to deliver exceptional value and needed performance to the farmers that produce grain from these products, along with helping farmers provide enough safe, nutritious food to meet global demand. In line with these guidelines, our approach to responsible launches of new products includes a long-standing process to evaluate export market information, value chain consultations, regulatory functionality, preparedness to meet product ramp up and demand plans, and other factors. Corteva continues to advocate for a global synchronous, science-based and predictable regulatory system. We also encourage farmers, industry, and consumer groups to continue to advocate for the acceptance of new, innovative technologies that help to improve farm productivity and profitability and contribute to the global economy and environmental sustainability.

Corteva does not develop nor import direct food or feed products into the Australian or New Zealand markets. The proposed amendment to the Standard, however, may result in increasing Australia and New Zealand's access to international grain food and markets while supporting Corteva's sale of seed in markets where DP915635 maize is to be cultivated. In this sense, and in an effort to maintain transparency with FSANZ, Corteva acknowledges that there may be a capturable commercial benefit to Corteva as defined in Section 8 of the FSANZ Act. Any relevant local costs are made up of Corteva personnel time both locally and globally as well as the direct fees associated with the submission.

Most of the sweet corn consumed in Australia is grown domestically. Domestic production of corn in Australia and New Zealand is supplemented by importation of a small amount of corn-based products usually frozen or canned, largely as high-fructose corn syrup, which is not currently manufactured in either Australia or New Zealand ([www.grdc.com.au](http://www.grdc.com.au)). Although not requiring a FSANZ approval for livestock feed, from time to time, mainly during periods of drought where local supply of feed grain is limited, maize is imported from the United States for use as stock feed, predominantly in the pig and poultry markets. This variation to the Standard permits the import and use of food derived or developed from DP915635 maize. This offers benefits to the industry and consumers in Australia and New Zealand, which result from the advantages of DP915635 maize available to growers in cultivation countries (see Section D(b) Advantage of the genetically modified food of the dossier).

While Corteva does not possess quantitative data, which would allow it to estimate the benefits in monetary terms, DP915635 is anticipated to contribute to the maintenance of stable global maize supply, choice and affordability for consumers. No specific costs associated with the approval of DP915635 for Australian and New Zealand consumers have been identified.

Similarly, an analysis in monetary terms for the grain and food industry is hard to determine, however, Australian and New Zealand importers are expected to benefit from trade access, which the approval of DP915635 will support (see Section D.1.2 Impact on international trade of the dossier). Compliance with import requirements is also anticipated to be simplified when sourcing from markets in which DP915635 is commercialized as a seed product. The only identified costs associated with the approval of DP915635 for Australian and New Zealand industry is meeting their GM labelling requirements for those foods derived from DP915635 maize which trigger them, similarly to other existing GM maize varieties.

No dollar value of the costs and benefits for the governments can be assigned with the available information. However, from the government perspective, approval of DP915635 maize will avoid potential trade disruption or instances of non-compliance related to the regulation of GM foods. No costs associated with the approval of DP915635 for Australian and New Zealand governments have been identified.

#### **D.1.2 Impact on international trade**

The addition of DP915635 maize to Schedule 26 is anticipated to facilitate imports of maize from the applicable cultivation countries. Without such an approval, grain handlers may undertake a scientifically unnecessary and costly activities to segregate DP915635 maize and food products derived from it for Australian markets. Therefore, amending the Food Code to include DP915635 maize is anticipated to have a positive impact on Australian access to international commodity trade markets.

## A. TECHNICAL INFORMATION ON THE FOOD PRODUCED USING GENE TECHNOLOGY

### A.1 NATURE AND IDENTITY OF THE GENETICALLY MODIFIED FOOD

#### A.1.(a) Description of the GM organisms, nature and purpose of the genetic modification

DP915635 maize was genetically modified to produce the IPD079Ea protein for control of susceptible corn rootworm (CRW) pests, the phosphinothricin acetyltransferase (PAT) protein for tolerance to the herbicidal active ingredient glufosinate-ammonium, and the phosphomannose isomerase (PMI) protein that was used as a selectable marker.

The IPD079Ea protein, encoded by the *ipd079Ea* gene from *Ophioglossum pendulum*, confers control of CRW pests when expressed in plants by causing disruption of the midgut epithelium ([Boeckman et al., 2022](#); [Carlson et al., 2022](#)). IPD079Ea is an insecticidal protein containing a Membrane Attack Complex/Perforin and Cholesterol-Dependent Cytolysin domain (MACPF/CDC). The MACPF/CDC proteins are widespread in nature and are found across multiple kingdoms of life including Bacteria and Eukaryotes ([Anderluh et al., 2014](#)). There exists a large single superfamily of MACPF proteins. However, there are important distinctions related to function, evolutionary selection, and sequence homology across MACPF proteins that remain to be understood. In plants, MACPF proteins play a role in plant development and plant responses to environmental stresses ([Yu et al., 2020](#)). Some MACPF proteins bind to receptors on the cell membrane of target cells and form transmembrane pores ([Rosado et al., 2008](#)).

The function of the MACPF protein IPD079Ea in *O. pendulum* remains to be understood, but based on evidence from the field, this protein may play a role in plant defense or plant development. The IPD079Ea protein has a pore-forming function and binds to receptors present in the midgut epithelial cells of CRW. Insecticidal activity is caused by disruption of the midgut epithelial cells.

The PAT protein, encoded by a maize-optimized version of the phosphinothricin acetyltransferase (*mo-pat*) gene from *Streptomyces viridochromogenes*, confers tolerance to the herbicidal active ingredient glufosinate-ammonium at current labeled rates by acetylating phosphinothricin to an inactive form. The PAT protein present in DP915635 maize is identical to the corresponding protein found in a number of approved events across several different crops that are currently commercialized and have a history of safe use ([CERA - ILSI Research Foundation, 2011](#); [CERA - ILSI Research Foundation, 2016](#); [Hérouet et al., 2005](#)).

The phosphomannose isomerase (PMI) protein, encoded by the *pmi* gene from *Escherichia coli*, serves as a selectable marker in plant tissue during transformation which allows for tissue growth using mannose as the carbon source. The PMI protein is found in several approved events that are currently in commercial use ([ISAAA, 2020](#)).

#### A.1.(b) GM Organism Identification

In accordance with OECD's "Guidance for the Designation of a Unique Identifier for Transgenic Plants", this event has an OECD identifier of DP-915635-4, also referred to as DP915635 maize.

#### A.1.(c) Trade name

Maize event DP915635 is at pre-commercialization stage and has not yet been assigned a commercial product name.

## A.2 HISTORY OF USE OF THE HOST AND DONOR ORGANISMS

### A.2.(a) Donor Organisms

#### ***Ophioglossum pendulum*: donor of the *ipd079Ea* gene**

- Class: Polypodiophyta
- Order: Ophioglossales
- Family: Ophioglossaceae
- Genus: *Ophioglossum* L.
- Species: *O. pendulum* L.

*Ophioglossum pendulum* is known as Old World adders-tongue fern because, like the other species in this family, the vascular stalk grows in the shape of a snake's tongue. Ferns are among the oldest living organisms on the planet and, with the exception of Antarctica, are globally distributed ([Fernández, 2011](#)). The order Ophioglossales contains one family, Ophioglossaceae (the adder's-tongue family), which is divided into five genera ([USDA-NRCS, 2020](#)). The genus *Ophioglossum* L., containing approximately fifty species ([Kew Science, 2020a](#)), is native to many parts of North, Central, and South America, Africa, Europe, Asia, and Australia ([Kew Science, 2020a](#)). *O. pendulum* specifically has been introduced in the state of Florida in the United States ([USDA-NRCS, 2020](#)), and is native to India, Australia, parts of Africa, and southeast Asia ([Kew Science, 2020b](#)).

While there are some anecdotal accounts of *Ophioglossum* ferns being used for medicinal applications or for food, these accounts are limited. There are no reports of *O. pendulum* being poisonous to humans or livestock.

#### ***Streptomyces viridochromogenes*: donor of the *mo-pat* gene**

- Class: Actinobacteria (high G+C Gram-positive bacteria)
- Order: Actinomycetales
- Family: Streptomycetaceae
- Genus: *Streptomyces*
- Species: *S. viridochromogenes*
- Strain: Tü494

*Streptomyces. viridochromogenes* is a Gram-positive, saprophytic, aerobic bacterium commonly found in soil. *S. viridochromogenes* is not considered pathogenic to humans or animals and is not known to be an allergen or toxin. *S. viridochromogenes* produces the tripeptide L-phosphinothricyl-L-alanyl-alanine (L-PPT), which was developed as a non-selective herbicide ([OECD, 1999](#)).

#### ***Escherichia coli*: donor of the *pmi* gene**

- Class: Gammaproteobacteria
- Order: Enterobacteriales
- Family: Enterobacteriaceae
- Genus: *Escherichia*
- Species: *E. coli*
- Strain: K-12

*Escherichia coli* (*E. coli*) is a Gram-negative, facultatively anaerobic, rod-shaped bacterium. The strain *E. coli* K-12 is a strain which has been debilitated, does not normally colonize the human intestine and has a poor survival rate in the environment. *E. coli* K-12 has a history of safe use in human drug and specialty chemical production ([US-EPA, 1997](#)).

**A.2.(b) Host Organism**

Information relating to maize, the host organism, was included in previous safety assessments prepared by FSANZ. Repeating it is not considered necessary in this submission.

## A.3 THE NATURE OF THE GENETIC MODIFICATION

### A.3(a) Transformation Method

DP915635 maize was developed by site-specific integration (SSI; [Anand et al., 2019](#)) using two sequential transformation steps to (1) insert an integration site sequence (referred to as a “landing pad” sequence) at a specific location of the maize genome using microprojectile bombardment and a clustered regularly interspaced short palindromic repeats-Cas9 (CRISPR-Cas9)-mediated targeted insertion process, and (2) insert, via recombination, the intended expression cassettes from the plasmid PHP83175 T-DNA region into the landing pad in the maize genome using *Agrobacterium*-mediated transformation. After each transformation step, a line containing only the intended insertion with no unintended plasmid-derived sequences was selected for the next step in the process. The use of SSI for targeted transgene insertion has advantages compared to random transformation by allowing the ability to pre-select the insertion location to avoid endogenous gene disruption and pre-test the genomic location for agronomic neutrality ([Gao et al., 2020](#)). Thus, the SSI approach can simplify risk assessment of the event intended for commercialization as it concerns potential for insertional effects.

#### First Transformation Step: Insertion of Landing Pad from PHP73878

The first transformation step utilized microprojectile co-bombardment with four plasmids (PHP73878, PHP70605, PHP21139, and PHP21875) to deliver the various components needed for transformation and improved plant regeneration (Table 1; Figure 1 - Figure 5). During this transformation step, the landing pad sequence was inserted into the maize genome using a CRISPR-Cas9-mediated targeted insertion process, during which the RNA-guided DNA endonuclease, Cas9, binds to a defined target location based on RNA-DNA interaction with a specific DNA sequence.

Following microprojectile co-bombardment, the following genetic elements were expressed: the *zm-45CR1* guide RNA and *cas9* gene from plasmid PHP70605 (Figure 3), the *zm-wus2* gene from plasmid PHP21139 (Figure 4), and the *zm-odp2* gene from plasmid PHP21875 (Figure 5). Expression of the *zm-45CR1* guide RNA directed the Cas9 protein, an RNA-guided DNA endonuclease, to produce a double-stranded DNA break between the continuous, endogenous *zm-SEQ158* and *zm-SEQ159* sequences in the maize genome. These endogenous sequences are identical to the *zm-SEQ158* and *zm-SEQ159* sequences flanking the landing pad sequence in plasmid PHP73878 (Figure 1). The landing pad was inserted into the maize genome by a native cellular mechanism known as homology-directed repair (HDR). During HDR, crossovers (homologous recombination) occurred between the *zm-SEQ158* and *zm-SEQ159* sequences in PHP73878 and the identical endogenous *zm-SEQ158* and *zm-SEQ159* sequences in the maize genome, thus introducing the landing pad sequence into the maize genome at the targeted location. The introduced landing pad sequence consists of the *loxP* site, *ubiZM1* promoter including the 5' untranslated region (5' UTR) and intron, FRT1 recombination target site, *nptII* gene, *pinII* terminator, and FRT6 recombination target site (Figure 2). The transient expression of the WUS protein from plasmid PHP21139 and the ODP2 protein from plasmid PHP21875 allowed for the improved regeneration of maize plants from the transformation process.

Table 1 presents the relevant genetic elements used in this transformation step and indicates whether they are present in the final DP915635 maize event.

Maize plants were regenerated after transformation. A maize line that contained the landing pad sequence but did not contain unintended plasmid DNA sequences was selected and advanced to the next step in the transformation process.

**Table 1. List of Genetic Elements in Plasmids Used for Landing Pad Transformation and Their Presence in DP915635 Maize**

Plasmid	Genetic Element	Description	Presence in DP915635
<b>PHP73878</b>	<i>zm</i> -SEQ158	Genomic recognition site for HDR	Yes <sup>a</sup>
	<i>loxP</i>	Cre recombination site	Yes
	<i>ubiZM1</i>	Promoter region	Yes
	FRT1	Flippase recombination target site	Yes
	<i>nptII</i>	Neomycin phosphotransferase gene	No
	<i>pinII</i> terminator	Terminator	No
	FRT6	Flippase recombination target site	Yes
<b>PHP70605</b>	<i>zm</i> -SEQ159	Genomic recognition site for HDR	Yes <sup>a</sup>
	<i>cas9</i> exons 1 and 2	Cas9 endonuclease gene	No
	<i>zm</i> -45CR1 guide RNA	The single guide RNA for directing the Cas9 endonuclease to a targeted location	No
<b>PHP21139</b>	<i>zm-wus2</i>	Developmental gene for regeneration	No
<b>PHP21875</b>	<i>zm-odp2</i>	Developmental gene for regeneration	No

<sup>a</sup> The *zm*-SEQ158 and *zm*-SEQ159 are continuous, endogenous sequences in the maize genome, which are not considered to be part of the inserted DNA in DP915635 maize. Their role in PHP73878 was targeting of the landing pad sequence between the endogenous *zm*-SEQ158 and *zm*-SEQ159 sequences in the maize genome.

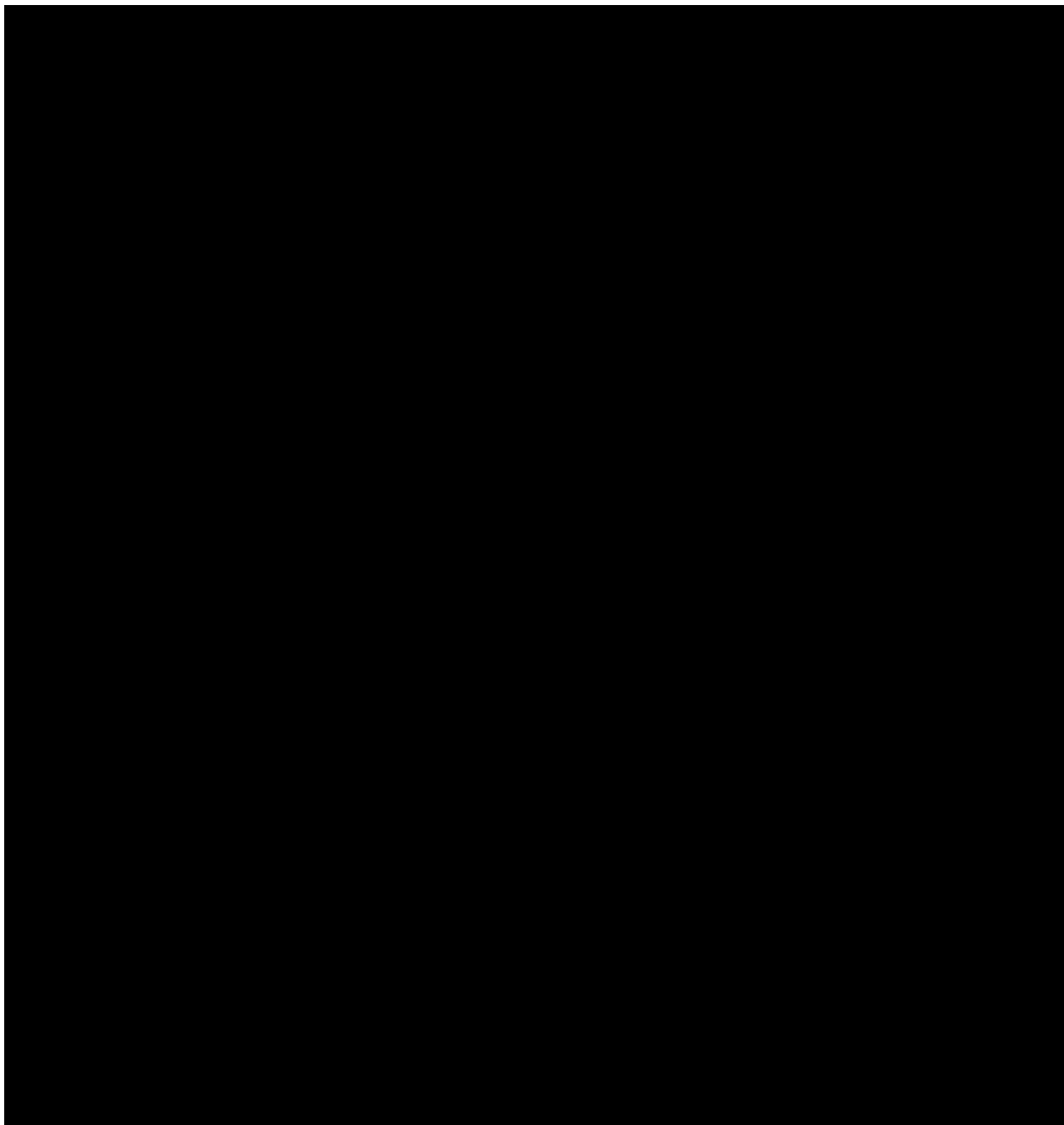


**Figure 1. Schematic Diagram of Plasmid PHP73878**

Schematic diagram of plasmid PHP73878 containing the *nptII* gene cassette, along with the *zm*-SEQ158, *loxP* site, FRT1, FRT6, and *zm*-SEQ159 elements. The portion flanked by the *zm*-SEQ158 and *zm*-SEQ159 sequences, referred to as a “landing pad”, was inserted into the maize genome during homology-directed repair (HDR) following a Cas9 endonuclease-mediated double-stranded break. The size of plasmid PHP73878 is [REDACTED] bp. In a subsequent transformation step, the region between the FRT1 and FRT6 recombination sites was replaced by SSI with the intended *pmi*, *mo-pat*, and *ipd079Ea* gene cassettes from the PHP83175 T-DNA (Figure 7) that is flanked by the same FRT1 and FRT6 sites.



**Figure 2. Schematic Diagram of the T-DNA Region from Plasmid PHP73878**

Schematic diagram of the T-DNA region from plasmid PHP73878 containing the *nptII* gene cassette. The size of the T-DNA is [redacted] bp.



**Figure 3. Schematic Diagram of Plasmid PHP70605**

Schematic diagram of plasmid PHP70605 containing the *cas9* gene cassette and the *zm-45CR1* guide RNA cassette. The size of plasmid PHP70605 is [REDACTED] bp. Plasmid PHP70605 was used during transformation to express the Cas9 endonuclease to create a double-stranded break at a genomic location specified by the *zm-45CR1* guide RNA but was not incorporated into the genome of the maize line used for the second transformation step.



**Figure 4. Schematic Diagram of Plasmid PHP21139**

Schematic diagram of plasmid PHP21139 containing the *zm-wus2* gene cassette. The size of plasmid PHP21139 is [redacted] bp. Plasmid PHP21139 was used to enhance transformation and plant regeneration but was not incorporated into the genome of the maize line used for the second transformation step.

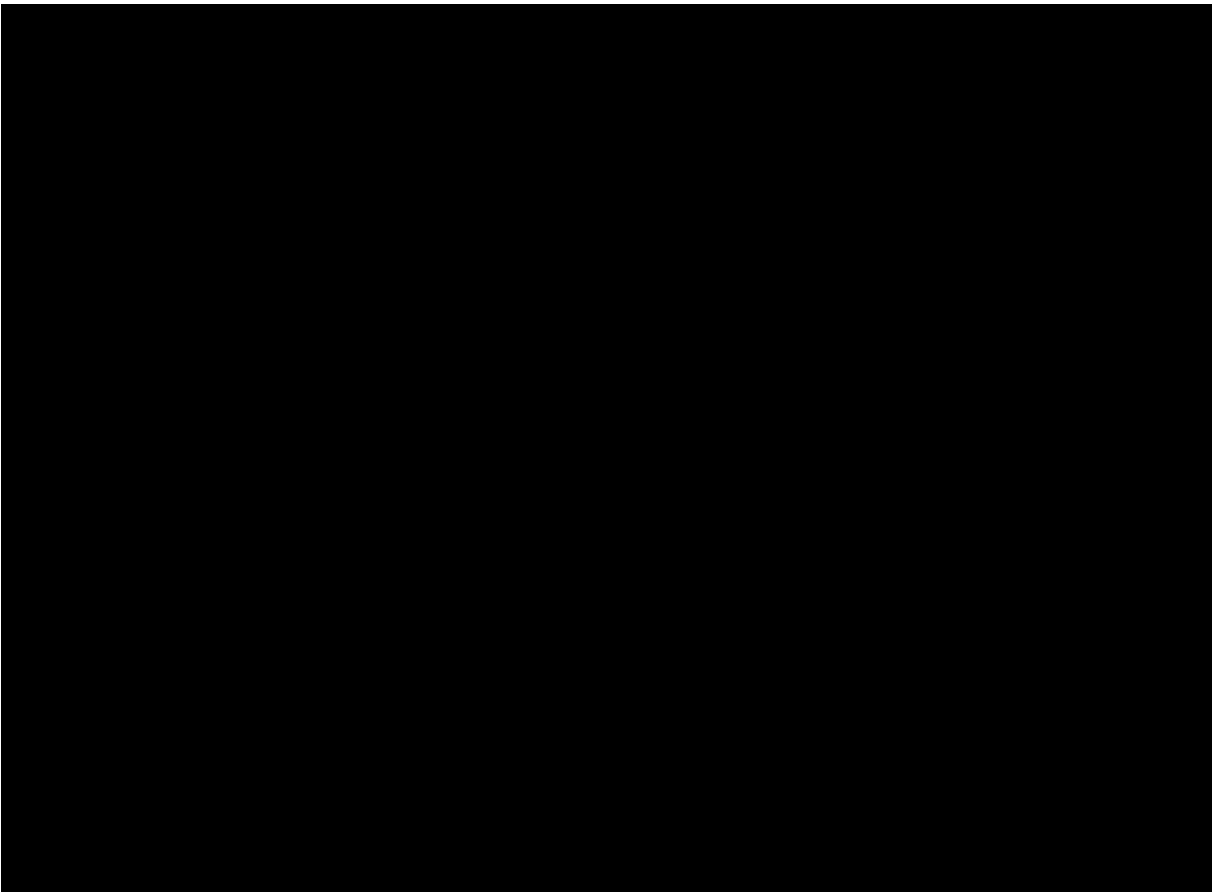


**Figure 5. Schematic Diagram of Plasmid PHP21875**

Schematic diagram of plasmid PHP21875 containing the *zm-odp2* gene cassette. The size of plasmid PHP21875 is [REDACTED] bp. Plasmid PHP21875 was used to enhance transformation and plant regeneration but was not incorporated into the genome of the maize line used for the second transformation step.

## Second Transformation Step: Site-Specific Integration of Expression Cassettes from PHP83175 T-DNA

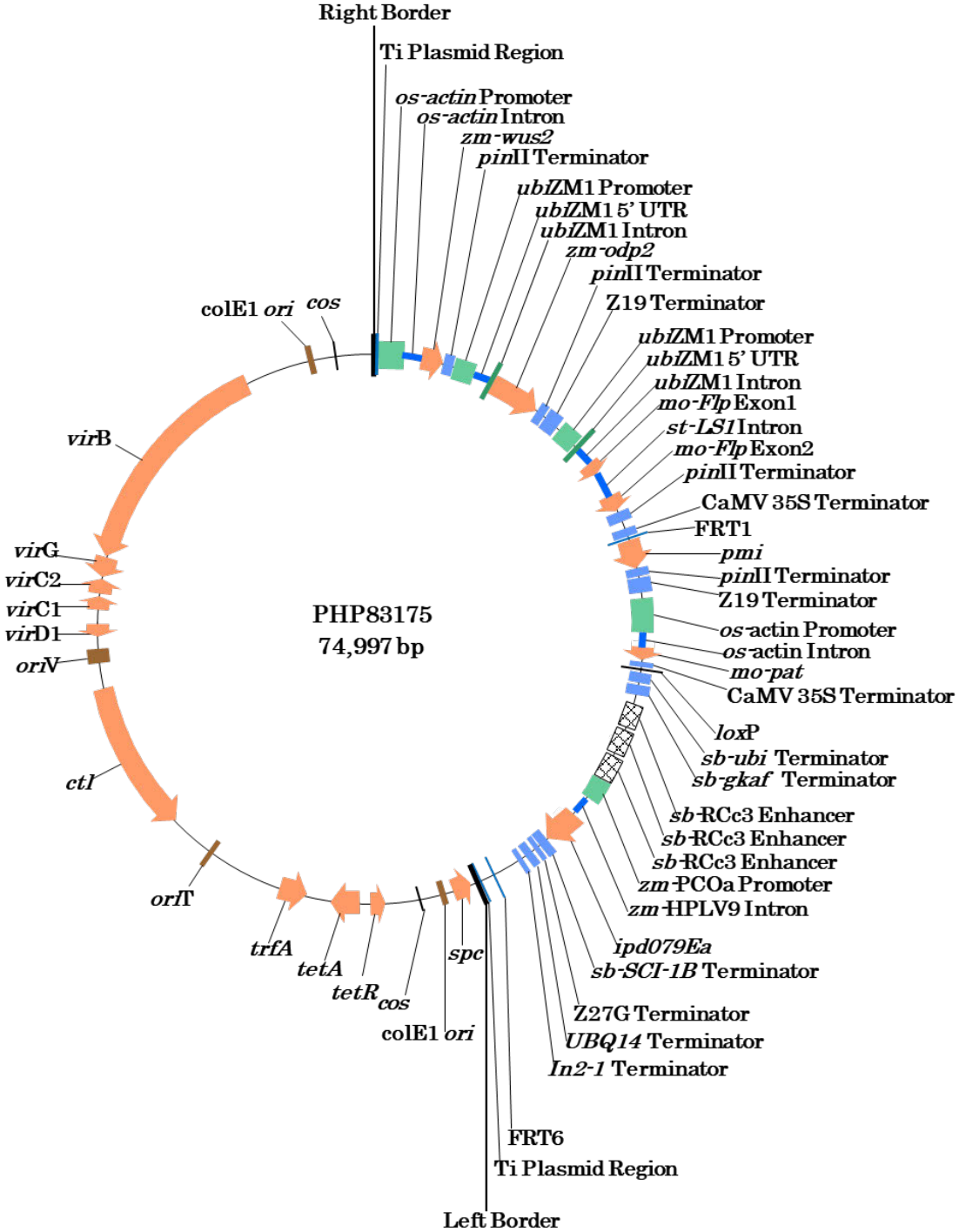
The second transformation step used to create DP915635 maize utilized *Agrobacterium*-mediated transformation with plasmid PHP83175 (Figure 6) to convey the PHP83175 T-DNA (Figure 7) into the plant cell nucleus; however, the T-DNA did not integrate entirely into the genome. Rather, the FLP recombinase encoded by the *mo-Flp* gene in the T-DNA (outside of the FRT1 and FRT6 sites) exchanged the *nptII* gene and *pinII* terminator in the landing pad for the intended trait gene cassettes (*pmi*, *mo-pat*, and *ipd079Ea*) located between the FRT1 and FRT6 sites in the PHP83175 T-DNA region, resulting in the inserted DNA in DP915635 maize (Figure 8). The *ubiZM1* promoter region in the landing pad adjacent to the FRT1 site facilitates the expression of the *pmi* gene used for selection. Expression of the *zm-wus2* and *zm-odp2* gene cassettes produces the WUS and ODP2 proteins which allow for improved regeneration of maize plants following transformation. During this transformation, the *zm-wus2*, *zm-odp2*, and *mo-Flp* genes were transiently expressed without integration into the maize genome. The result of this SSI process was the T0 plant containing the DP915635 maize insertion (Figure 8).

Table 2 lists the relevant genetic elements within the PHP83175 T-DNA and indicates whether they are present in the final DP915635 maize event.

Maize plants were regenerated after transformation. A maize line that contained the intended expression cassettes for DP915635 maize but did not contain unintended plasmid DNA sequences was selected and advanced to the next step in the event development process.

**Table 2. List of Genetic Elements in PHP83175 T-DNA and Their Presence in DP915635 Maize**

Genetic Element	Description	Presence in DP915635
Right Border	T-DNA right border	No
<i>zm-wus2</i>	Developmental gene for regeneration	No
<i>zm-odp2</i>	Developmental gene for regeneration	No
<i>mo-Flp</i>	Maize-optimized flippase gene	No
FRT1	Flippase recombination target site	Yes
<i>pmi</i>	Phosphomannose isomerase gene	Yes
<i>mo-pat</i>	Maize-optimized phosphinothricin acetyltransferase gene	Yes
<i>loxP</i>	Cre recombination site	Yes
<i>ipd079Ea</i>	Insect protection protein gene	Yes
FRT6	Flippase recombination target site	Yes
Left Border	T-DNA left border	No



**Figure 6. Schematic Diagram of Plasmid PHP83175**

Schematic diagram of plasmid PHP83175 containing the *pmi*, *mo-pat*, and *ipd079Ea* gene cassettes intended for incorporation into the DP915635 maize genome, and the *zm-wus2*, *zm-odp2*, and *mo-Flp* gene cassettes not intended for incorporation into the DP915635 maize genome. The size of plasmid PHP83175 is 74,997 bp.



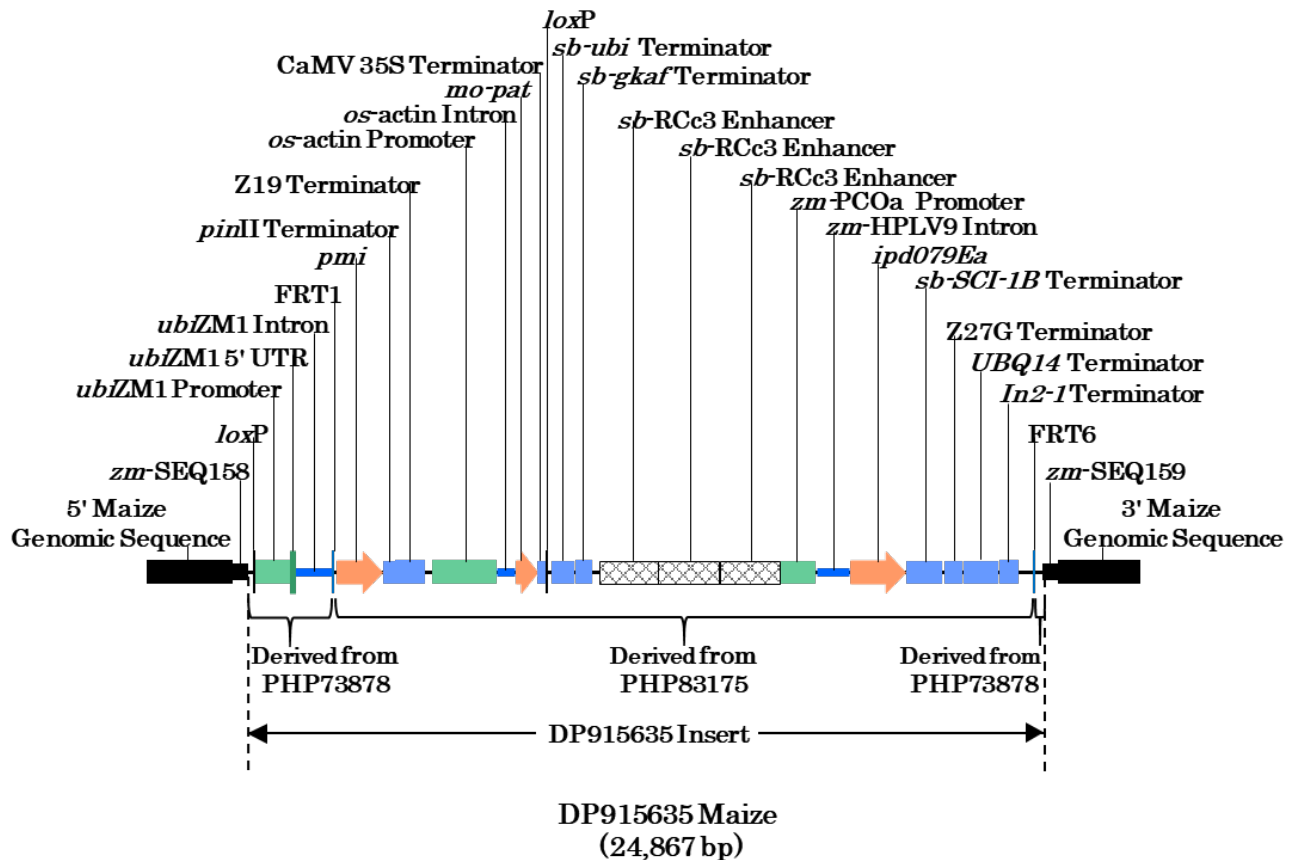


**Figure 8. Schematic Diagram of the DP915635 Maize Insertion**

Schematic diagram of the insertion (indicated by dashed vertical lines) in the DP915635 maize genome following SSI at the FRT1 and FRT6 sites. The size of the inserted DNA in DP915635 maize is 20,564 bp, and it includes sequences from the T-DNA region of plasmids PHP83175 (Figure 7) and PHP73878 (Figure 2). The flanking maize genomic regions are represented by horizontal black bars. Although the *zm-SEQ158* and *zm-SEQ159* are present in PHP73878, they are derived from the maize genome and appear in their natural context in the chromosome, so are considered to be part of the flanking maize genome and are not included as part of the insertion.

## Description of the T-DNA Region of Binary Plasmid PHP83175

The T-DNA of plasmid PHP83175 contains a total of six gene cassettes, of which three gene cassettes (*ipd079Ea*, *mo-pat*, and *pmi*; Figure 7) are intended for incorporation into the DP915635 maize genome, and the remaining three gene cassettes (*zm-wus2*, *zm-odp2*, and *mo-Flp*) are transiently expressed without integration into the maize genome. Further description of the gene cassettes included in the T-DNA of plasmid PHP83175 is provided below. The PHP83175 T-DNA also contains two FLP recombinase target sequences, FRT1 and FRT6 sites ([Proteau et al., 1986](#)), as well as one *loxP* ([Dale and Ow, 1990](#)) and four *attB* recombination sites ([Cheo et al., 2004](#); [Hartley et al., 2000](#); [Katzen, 2007](#)). Summaries of the genetic elements within plasmid PHP83175 and the T-DNA region of plasmid PHP83175 are provided in Table 3 and Table 4, respectively.

- The *zm-wus2* gene cassette contains the maize *Wuschel2* (*wus2*) gene ([Mayer et al., 1998](#)) encoding the WUS protein. The expressed WUS protein enhances tissue regeneration during transformation ([Lowe et al., 2016](#)). The WUS protein is 302 amino acids in length and has a molecular weight of approximately 31 kDa. Expression of the *zm-wus2* gene is controlled by the promoter and intron region of the rice (*Oryza sativa*) actin (*os-actin*) gene (GenBank accession CP018159; GenBank accession EU155408.1), in conjunction with the presence of the terminator region from the potato (*Solanum tuberosum*) proteinase inhibitor II (*pinII*) gene ([An et al., 1989](#); [Keil et al., 1986](#)).
- The *zm-odp2* gene cassette contains the maize ovule development protein 2 (*odp2*) gene (GenBank accession XM008676474) encoding the ODP2 protein. The expressed ODP2 protein enhances the regeneration of maize plants from tissue culture after transformation (U.S. Patent 8420893). The ODP2 protein is 710 amino acids in length and has a molecular weight of approximately 74 kDa. Expression of the *zm-odp2* gene is controlled by the promoter region from the maize ubiquitin gene 1 (*ubiZM1*) including the 5' untranslated region (5' UTR) and intron ([Christensen et al., 1992](#)). The terminator for the *zm-odp2* gene is a second copy of the *pinII* terminator. An additional terminator is present between the second and third cassettes: the terminator region from the maize 19-kDa zein (Z19) gene (GenBank accession KX247647; [Dong et al., 2016](#)). This additional terminator element is intended to minimize any potential transcriptional interference with the downstream cassettes. Transcriptional interference is defined as the transcriptional suppression of one gene on another when both are in close proximity ([Shearwin et al., 2005](#)). The placement of one or multiple transcriptional terminators between gene cassettes has been shown to reduce the occurrence of transcriptional interference ([Greger et al., 1998](#)).
- The *mo-Flp* gene cassette contains maize-optimized exon 1 and exon 2 of the flippase (*Flp*) gene ([Dymecki, 1996](#)) from *Saccharomyces cerevisiae*, separated by an intron region from the potato *LS1* (*st-LS1*) gene ([Eckes et al., 1986](#)). The expressed FLP protein facilitates site specific recombination during transformation. The FLP protein is 423 amino acids in length and has a molecular weight of approximately 49 kDa. Expression of the *mo-Flp* gene is controlled by a second copy of the *ubiZM1* promoter, the 5' UTR and intron, in conjunction with a third copy of the *pinII* terminator. An additional terminator is present between the third and fourth cassettes to minimize potential transcriptional interference: the 35S terminator region from the cauliflower mosaic virus genome (CaMV 35S terminator; [Franck et al., 1980](#); [Guilley et al., 1982](#)).
- The *pmi* gene cassette contains the phosphomannose isomerase (*pmi*) gene from *Escherichia coli* ([Negrotto et al., 2000](#)). The expressed PMI protein in plant tissue serves as a selectable marker during transformation which allows for tissue growth using mannose as the carbon source. The PMI protein is 391 amino acids in length and has a molecular weight of approximately 43 kDa. As present in the T-DNA region of PHP83175, the *pmi* gene lacks a promoter, but its location next to the flippase recombination target site, FRT1, allows post-recombination expression by an appropriately-placed promoter. The terminator for the *pmi* gene is a

fourth copy of the *pinII* terminator. An additional Z19 terminator present between the fourth and fifth cassettes is intended to minimize potential transcriptional interference between cassettes.

- The *mo-pat* gene cassette contains a maize-optimized version of the phosphinothricin acetyltransferase gene (*mo-pat*) from *Streptomyces viridochromogenes* ([Wohlleben et al., 1988](#)) encoding the PAT protein. The expressed PAT protein confers tolerance to phosphinothricin. The PAT protein is 183 amino acids in length and has a molecular weight of approximately 21 kDa. Expression of the *mo-pat* gene is controlled by a second copy of the promoter and intron region of the *os-actin* gene (GenBank accession CP018159; GenBank accession EU155408.1), in conjunction with a second copy of the CaMV35S terminator. Two additional terminators are present between the fifth and sixth cassettes to minimize potential transcriptional interference: the terminator regions from the sorghum (*Sorghum bicolor*) ubiquitin (*sb-ubi*) gene (Phytozome gene ID Sobic.004G049900.1; US Patent 9725731) and  $\gamma$ -kafarin (*sb-gkaf*) gene ([de Freitas et al., 1994](#)), respectively.
- The *ipd079Ea* gene cassette contains the insecticidal protein gene, *ipd079Ea*, from *Ophioglossum pendulum* ([WO Patent 2017/023486; Allen et al., 2017](#)). The expressed IPD079Ea protein in plants is effective against certain coleopteran pests by causing disruption of the midgut epithelium. The IPD079Ea protein is 479 amino acids in length and has a molecular weight of approximately 52 kDa. Expression of the *ipd079Ea* gene is controlled by three copies of the enhancer region, showing root-specific activity, from the sorghum (*Sorghum bicolor*) root cortical RCc3 (*sb-RCc3*) gene (WO Patent 2012/112411; [Diehn and Peterson-Burch, 2012](#)) followed by the promoter region upstream of a *Zea mays* PCO118362 mRNA sequence (*zm-PCOa*) identified as having root-specific activity (WO Patent 2017/222821; [Crow et al., 2017](#)) and the intron region from the *Zea mays* ortholog of a rice (*Oryza sativa*) hypothetical protein (*zm-HPLV9*) gene, a predicted *Zea mays* calmodulin 5 gene (Phytozome gene ID Zm00008a029682) (WO Patent 2016/109157; [Abbitt and Shen, 2016](#)). The terminator for the *ipd079Ea* gene is the terminator region from the sorghum (*Sorghum bicolor*) subtilisin-chymotrypsin inhibitor 1B (*sb-SCI-1B*) gene (WO Patent 2018/102131; [Abbitt et al., 2018](#)). Three additional terminators are present to minimize potential transcriptional interference: the terminator region from the maize W64 line 27-kDa gamma zein (Z27G) gene ([Das et al., 1991; Liu et al., 2016](#)), the terminator region from the *Arabidopsis thaliana* ubiquitin 14 (*UBQ14*) gene ([Callis et al., 1995](#)), and the terminator region from the maize *In2-1* gene ([Hershey and Stoner, 1991](#)).

**Table 3. Description of the Genetic Elements in Plasmid PHP83175**

Region	Location on Plasmid (bp to bp)	Genetic Element	Size (bp)	Description
T-DNA	1 – 32,069		32,069	See Table 4 for information on the elements in this region
Plasmid Construct	32,070 – 56,953	Includes Elements Below	24,884	DNA from various sources for plasmid construction and plasmid replication
	33,245 – 34,033 (complementary)	<i>spc</i>	789	Spectinomycin resistance gene from bacteria ( <a href="#">Fling et al., 1985</a> )
	35,156 – 35,525 (complementary)	<i>colE1 ori</i>	370	Origin of replication region from <i>Escherichia coli</i> ( <a href="#">Tomizawa et al., 1977</a> )
	36,619 – 36,632	<i>cos</i>	14	Cohesive ends from lambda bacteriophage DNA ( <a href="#">Komari et al., 1996</a> )
	38,337 – 38,987 (complementary)	<i>tetR</i>	651	Tetracycline resistance regulation gene from bacteria ( <a href="#">Komari et al., 1996</a> )
	39,093 – 40,292	<i>tetA</i>	1,200	Tetracycline resistance gene from bacteria ( <a href="#">Komari et al., 1996</a> )
	41,565 – 42,713 (complementary)	<i>trfA</i>	1,149	Trans-acting replication gene from bacteria ( <a href="#">Komari et al., 1996</a> )
	46,495 – 46,861 (complementary)	<i>oriT</i>	367	Origin of transfer region from bacteria ( <a href="#">Komari et al., 1996</a> )
	48,478 – 54,748 (complementary)	<i>ctl</i>	6,271	Central control operon region from bacteria ( <a href="#">Komari et al., 1996</a> )
	55,756 – 56,466 (complementary)	<i>oriV</i>	711	Origin of replication region from bacteria ( <a href="#">Komari et al., 1996</a> )
Ti Plasmid Backbone	56,954 – 71,770	Includes Elements Below	14,817	Virulence ( <i>vir</i> ) gene region and intergenic regions from Ti plasmid of <i>Agrobacterium tumefaciens</i> ( <a href="#">Komari et al., 1996</a> )
	57,267 – 57,710 (complementary)	<i>virD1</i>	444	Virulence gene from <i>Agrobacterium tumefaciens</i> important for T-DNA insertion into genome
	57,979 – 58,673	<i>virC1</i>	695	Virulence gene from <i>Agrobacterium tumefaciens</i> important for T-DNA insertion into genome
	58,676 – 59,284	<i>virC2</i>	609	Virulence gene from <i>Agrobacterium tumefaciens</i> important for T-DNA insertion into genome
	59,395 – 60,198 (complementary)	<i>virG</i>	804	Virulence gene from <i>Agrobacterium tumefaciens</i> important for T-DNA insertion into genome
	60,330 – 69,765 (complementary)	<i>virB</i>	9,436	Virulence operon region from <i>Agrobacterium tumefaciens</i> important for T-DNA insertion into genome
Plasmid Construct	71,771 – 74,997	Includes Elements Below	3,227	DNA from various sources for plasmid construction and plasmid replication
	72,066 – 72,435 (complementary)	<i>colE1 ori</i>	370	Origin of replication region from <i>Escherichia coli</i> ( <a href="#">Tomizawa et al., 1977</a> )

Region	Location on Plasmid (bp to bp)	Genetic Element	Size (bp)	Description
	73,528 – 73,541	<i>cos</i>	14	Cohesive ends from lambda bacteriophage DNA ( <a href="#">Komari et al., 1996</a> )

Table 4. Description of the Genetic Elements in the T-DNA Region from Plasmid PHP83175

Gene Cassette	Location on T-DNA (bp to bp)	Genetic Element	Size (bp)	Description
	1 – 25	Right Border (RB)	25	T-DNA Right Border from the <i>Agrobacterium tumefaciens</i> Ti plasmid ( <a href="#">Komari et al., 1996</a> )
	26 – 75	Ti Plasmid Region	50	Sequence from the <i>Agrobacterium tumefaciens</i> Ti plasmid ( <a href="#">Komari et al., 1996</a> )
	76 – 415	Intervening Sequence	340	DNA sequence used for cloning
zm-wus2 gene cassette	416 – 2,097	<i>os-actin</i> Promoter	1,682	Promoter region from the <i>Oryza sativa</i> (rice) actin gene (GenBank accession CP018159; GenBank accession EU155408.1)
	2,098 – 2,566	<i>os-actin</i> Intron	469	Intron region from the <i>Oryza sativa</i> (rice) actin gene (GenBank accession CP018159; GenBank accession EU155408.1)
	2,567 – 2,571	Intervening Sequence	5	DNA sequence used for cloning
	2,572 – 3,480	<i>zm-wus2</i>	909	<i>Wuschel 2</i> gene from <i>Zea mays</i> ( <a href="#">Lowe et al., 2016</a> ; <a href="#">Mayer et al., 1998</a> )
	3,481 – 3,481	Intervening Sequence	1	DNA sequence used for cloning
	3,482 – 3,792	<i>pinII</i> Terminator	311	Terminator region from the <i>Solanum tuberosum</i> (potato) proteinase inhibitor II gene ( <a href="#">An et al., 1989</a> ; <a href="#">Keil et al., 1986</a> )
	3,793 – 3,862	Intervening Sequence	70	DNA sequence used for cloning
zm-odp2 gene cassette	3,863 – 4,762	<i>ubiZM1</i> Promoter	900	Promoter region from the <i>Zea mays</i> ubiquitin gene 1 ( <a href="#">Christensen et al., 1992</a> )
	4,763 – 4,845	<i>ubiZM1</i> 5' UTR	83	5' untranslated region from the <i>Zea mays</i> ubiquitin gene 1 ( <a href="#">Christensen et al., 1992</a> )
	4,846 – 5,858	<i>ubiZM1</i> Intron	1,013	Intron region from the <i>Zea mays</i> ubiquitin gene 1 ( <a href="#">Christensen et al., 1992</a> )
	5,859 – 5,876	Intervening Sequence	18	DNA sequence used for cloning
	5,877 – 8,009	<i>zm-odp2</i>	2,133	Ovule development protein 2 gene from <i>Zea mays</i> (GenBank accession XM008676474; US Patent 8420893)

Gene Cassette	Location on T-DNA (bp to bp)	Genetic Element	Size (bp)	Description
	8,010 – 8,078	Intervening Sequence	69	DNA sequence used for cloning
	8,079 – 8,389	<i>pinII</i> Terminator	311	Terminator region from the <i>Solanum tuberosum</i> (potato) proteinase inhibitor II gene ( <a href="#">An et al., 1989</a> ; <a href="#">Keil et al., 1986</a> )
	8,390 – 8,405	Intervening Sequence	16	DNA sequence used for cloning
	8,406 – 9,147	Z19 Terminator	742	Terminator region from the <i>Zea mays</i> 19-kDa zein gene (GenBank accession KX247647; <a href="#">Dong et al., 2016</a> )
	9,148 – 9,168	Intervening Sequence	21	DNA sequence used for cloning
mo-Flp gene cassette	9,169 – 10,068	<i>ubiZM1</i> Promoter	900	Promoter region from the <i>Zea mays</i> ubiquitin gene 1 ( <a href="#">Christensen et al., 1992</a> )
	10,069 – 10,151	<i>ubiZM1</i> 5' UTR	83	5' untranslated region from the <i>Zea mays</i> ubiquitin gene 1 ( <a href="#">Christensen et al., 1992</a> )
	10,152 – 11,164	<i>ubiZM1</i> Intron	1,013	Intron region from the <i>Zea mays</i> ubiquitin gene 1 ( <a href="#">Christensen et al., 1992</a> )
	11,165 – 11,194	Intervening Sequence	30	DNA sequence used for cloning
	11,195 – 11,828	<i>mo-Flp</i> Exon1	634	Maize-optimized exon 1 of the flippase gene from <i>Saccharomyces cerevisiae</i> ( <a href="#">Dymecki, 1996</a> )
	11,829 – 12,017	<i>st-LS1</i> Intron	189	Intron region from the <i>Solanum tuberosum</i> (potato) <i>LS1</i> gene ( <a href="#">Eckes et al., 1986</a> )
	12,018 – 12,655	<i>mo-Flp</i> Exon2	638	Maize-optimized exon 2 of the flippase gene from <i>Saccharomyces cerevisiae</i> ( <a href="#">Dymecki, 1996</a> )
	12,656 – 12,660	Intervening Sequence	5	DNA sequence used for cloning
	12,661 – 12,971	<i>pinII</i> Terminator	311	Terminator region from the <i>Solanum tuberosum</i> (potato) proteinase inhibitor II ( <a href="#">An et al., 1989</a> ; <a href="#">Keil et al., 1986</a> )
	12,972 – 13,025	Intervening Sequence	54	DNA sequence used for cloning
	13,026 – 13,046	<i>attB4</i>	21	Bacteriophage lambda integrase recombination site ( <a href="#">Cheo et al., 2004</a> )
	13,047 – 13,125	Intervening Sequence	79	DNA sequence used for cloning
	13,126 – 13,319	CaMV 35S Terminator	194	35S terminator region from the cauliflower mosaic virus genome ( <a href="#">Franck et al., 1980</a> ; <a href="#">Guilley et al., 1982</a> )
	13,320 – 13,334	Intervening Sequence	15	DNA sequence used for cloning

Gene Cassette	Location on T-DNA (bp to bp)	Genetic Element	Size (bp)	Description
	13,335 – 13,382	FRT1	48	Flippase recombination target site from <i>Saccharomyces cerevisiae</i> ( <a href="#">Proteau et al., 1986</a> )
	13,383 – 13,400	Intervening Sequence	18	DNA sequence used for cloning
<i>pmi</i> gene cassette	13,401 – 14,616	<i>pmi</i>	1,216	Phosphomannose isomerase gene from <i>Escherichia coli</i> including 5' and 3' untranslated regions (UTR) ( <a href="#">Negrotto et al., 2000</a> ) as described below: 5' UTR at bp 13,401-13,404 (4 bp long) Coding sequence at bp 13,405-14,580 (1,176 bp long) 3' UTR at bp 14,581-14,616 (36 bp long)
	14,617 – 14,626	Intervening Sequence	10	DNA sequence used for cloning
	14,627 – 14,937	<i>pinII</i> Terminator	311	Terminator region from the <i>Solanum tuberosum</i> (potato) proteinase inhibitor II gene ( <a href="#">An et al., 1989</a> ; <a href="#">Keil et al., 1986</a> )
	14,938 – 14,947	Intervening Sequence	10	DNA sequence used for cloning
	14,948 – 15,689	Z19 Terminator	742	Terminator region from the <i>Zea mays</i> 19-kDa zein gene (GenBank accession KX247647; <a href="#">Dong et al., 2016</a> )
	15,690 – 15,892	Intervening Sequence	203	DNA sequence used for cloning
<i>mo-pat</i> gene cassette	15,893 – 17,574	<i>os-actin</i> Promoter	1,682	Promoter region from the <i>Oryza sativa</i> (rice) actin gene (GenBank accession CP018159; GenBank accession EU155408.1)
	17,575 – 18,043	<i>os-actin</i> Intron	469	Intron region from the <i>Oryza sativa</i> (rice) actin gene (GenBank accession CP018159; GenBank accession EU155408.1)
	18,044 – 18,058	Intervening Sequence	15	DNA sequence used for cloning
	18,059– 18,610	<i>mo-pat</i>	552	Maize-optimized phosphinothricin acetyltransferase gene from <i>Streptomyces viridochromogenes</i> ( <a href="#">Wohlleben et al., 1988</a> )
	18,611 – 18,628	Intervening Sequence	18	DNA sequence used for cloning
	18,629 – 18,822	CaMV 35S Terminator	194	35S terminator region from the cauliflower mosaic virus genome ( <a href="#">Franck et al., 1980</a> ; <a href="#">Guilley et al., 1982</a> )
	18,823 – 18,843	Intervening Sequence	21	DNA sequence used for cloning
	18,844 – 18,877	<i>loxP</i>	34	Bacteriophage P1 recombination site recognized by Cre recombinase ( <a href="#">Dale and Ow, 1990</a> )
	18,878 – 18,973	Intervening Sequence	96	DNA sequence used for cloning

Gene Cassette	Location on T-DNA (bp to bp)	Genetic Element	Size (bp)	Description
	18,974 – 19,557	<i>sb-ubi</i> Terminator	584	Terminator region from the <i>Sorghum bicolor</i> (sorghum) ubiquitin gene (Phytozome gene ID Sobic.004G049900.1; US Patent 9725731; <a href="#">Abbitt, 2017</a> )
	19,558 – 19,598	Intervening Sequence	41	DNA sequence used for cloning
	19,599 – 20,062	<i>sb-gkaf</i> Terminator	464	Terminator region from the <i>Sorghum bicolor</i> (sorghum) γ-kafarin gene ( <a href="#">de Freitas et al., 1994</a> )
	20,063 – 20,095	Intervening Sequence	33	DNA sequence used for cloning
	20,096 – 20,119	<i>attB1</i>	24	Bacteriophage lambda integrase recombination site from the Invitrogen Gateway <sup>®</sup> cloning system ( <a href="#">Hartley et al., 2000</a> ; <a href="#">Katzen, 2007</a> )
	20,120 – 20,157	Intervening Sequence	38	DNA sequence used for cloning
ipd079Ea gene cassette	20,158 – 21,738	<i>sb-RcC3</i> Enhancer	1,581	Enhancer region, showing root-specific activity, from the <i>Sorghum bicolor</i> (sorghum) root cortical RCc3 ( <i>sb-RcC3</i> ) gene (WO Patent 2012/112411; <a href="#">Diehn and Peterson-Burch, 2012</a> )
	21,739 – 21,744	Intervening Sequence	6	DNA sequence used for cloning
	21,745 – 23,325	<i>sb-RcC3</i> Enhancer	1,581	Enhancer region, showing root-specific activity, from the <i>Sorghum bicolor</i> (sorghum) root cortical RCc3 ( <i>sb-RcC3</i> ) gene (WO Patent 2012/112411; <a href="#">Diehn and Peterson-Burch, 2012</a> )
	23,326 – 23,338	Intervening Sequence	13	DNA sequence used for cloning
	23,339 – 24,922	<i>sb-RcC3</i> Enhancer	1,584	Enhancer region, showing root-specific activity, from the <i>Sorghum bicolor</i> (sorghum) root cortical RCc3 ( <i>sb-RcC3</i> ) gene (WO Patent 2012/112411; <a href="#">Diehn and Peterson-Burch, 2012</a> )
	24,923 – 25,833	<i>zm-PCOa</i> Promoter	911	Promoter region upstream of a <i>Zea mays</i> PCO118362 mRNA sequence identified as having root-specific activity (WO Patent 2017/222821; <a href="#">Crow et al., 2017</a> )
	25,834 – 25,851	Intervening Sequence	18	DNA sequence used for cloning
	25,852 – 26,707	<i>zm-HPLV9</i> Intron	856	Intron region from the <i>Zea mays</i> ortholog of an <i>Oryza sativa</i> (rice) hypothetical protein ( <i>zm-HPLV9</i> ) gene, a predicted <i>Zea mays</i> calmodulin 5 gene (Phytozome gene ID Zm00008a029682, WO Patent 2016109157; <a href="#">Abbitt and Shen, 2016</a> )
	26,708 – 26,716	Intervening Sequence	9	DNA sequence used for cloning

Gene Cassette	Location on T-DNA (bp to bp)	Genetic Element	Size (bp)	Description
	26,717 – 28,156	<i>ipd079Ea</i>	1,440	Insecticidal protein gene from <i>Ophioglossum pendulum</i> (WO Patent 2017/023486; <a href="#">Allen et al., 2017</a> )
	28,157 – 28,173	Intervening Sequence	17	DNA sequence used for cloning
	28,174 – 29,126	<i>sb-SCI-1B</i> Terminator	953	Terminator region of the <i>Sorghum bicolor</i> (sorghum) subtilisin-chymotrypsin inhibitor 1B gene (WO Patent 2018/102131; <a href="#">Abbitt et al., 2018</a> )
	29,127 – 29,172	Intervening Sequence	46	DNA sequence used for cloning
	29,173 – 29,632	Z27G Terminator	460	Terminator region from the <i>Zea mays</i> W64 line 27-kDa gamma zein gene ( <a href="#">Das et al., 1991</a> ; <a href="#">Liu et al., 2016</a> )
	29,633– 29,638	Intervening Sequence	6	DNA sequence used for cloning
	29,639 – 30,540	<i>UBQ14</i> Terminator	902	Terminator region from the <i>Arabidopsis thaliana</i> ubiquitin 14 gene ( <a href="#">Callis et al., 1995</a> )
	30,541 – 30,546	Intervening Sequence	6	DNA sequence used for cloning
	30,547 – 31,040	<i>In2-1</i> Terminator	494	Terminator region from the <i>Zea mays In2-1</i> gene ( <a href="#">Hershey and Stoner, 1991</a> )
	31,041 – 31,097	Intervening Sequence	57	DNA sequence used for cloning
	31,098 – 31,121	<i>attB2</i>	24	Bacteriophage lambda integrase recombination site from the Invitrogen Gateway® cloning ( <a href="#">Hartley et al., 2000</a> ; <a href="#">Katzen, 2007</a> )
	31,122 – 31,268	Intervening Sequence	147	DNA sequence used for cloning
	31,269 – 31,289 (complementary)	<i>attB3</i>	21	Bacteriophage lambda integrase recombination site ( <a href="#">Cheo et al., 2004</a> )
	31,290 – 31,524	Intervening Sequence	235	DNA sequence used for cloning
	31,525 – 31,572	FRT6	48	Modified flippase recombination target site from <i>Saccharomyces cerevisiae</i> ( <a href="#">Proteau et al., 1986</a> )
	31,573 – 31,987	Intervening Sequence	415	DNA sequence used for cloning
	31,988 – 32,044	Ti Plasmid Region	57	Sequence from the <i>Agrobacterium tumefaciens</i> Ti plasmid ( <a href="#">Komari et al., 1996</a> )
	32,045 – 32,069	Left Border (LB)	25	T-DNA Left Border from the <i>Agrobacterium tumefaciens</i> Ti plasmid ( <a href="#">Komari et al., 1996</a> )

### **A.3(b) Description of the construct and the transformation vectors used**

Please refer to Section A.3(a) *Transformation Method* for the vectors used in transformation and to Table 3 for a description of the genetic elements in Plasmid PHP83175, Figure 6 for the map of Plasmid PHP83175, Table 4 for the description of the genetic elements in the T-DNA region from Plasmid PHP83175 and Figure 7 for the map of the T-DNA region from Plasmid PHP83175.

### **A.3(c) Molecular characterisation**

Characterization of the inserted DNA in DP915635 maize was conducted using a Next Generation Sequencing (NGS) method known as Southern-by-Sequencing (SbS™ technology, hereafter referred to as SbS) to determine the insertion copy number and organization within the plant genome and to confirm the absence of plasmid backbone and other unintended sequences. Southern blot analysis was performed to confirm stable genetic inheritance of the inserted *ipd079Ea*, *mo-pat*, and *pmi* gene cassettes across multiple generations during the breeding process. Segregation analysis was conducted for five generations of DP915635 maize to confirm stable Mendelian inheritance. Sanger sequencing was conducted to determine the DNA sequence of the DP915635 insert and flanking genomic regions. Additionally, a bioinformatic assessment was conducted to evaluate the potentially-expressed peptides within an insertion or crossing the boundary between an insertion and its genomic borders for similarity to known and putative allergens and toxins.

Based on the SbS analysis described below, it was determined that a single copy of the inserted DNA with the expected organization (Figure 8. Schematic Diagram of the DP915635 Maize Insertion), and that no additional insertions, plasmid backbone, or other unintended plasmid sequences are present in DP915635 maize. In addition, Southern blot analysis across five breeding generations confirmed the stable genetic inheritance of the DNA insertion in DP915635 maize. Segregation analysis across five breeding generations confirmed a stable Mendelian inheritance pattern. Sanger sequencing was conducted to determine the DNA sequence of the DP915635 insert and flanking genomic regions.

#### **Southern-by-Sequencing (SbS) Analysis to Determine Insertion Copy Number and Organization and Confirm the Absence of Plasmid Backbone and Other Unintended Plasmid Sequences ([PHI-2020-044 study](#))**

SbS analysis utilizes probe-based sequence capture, Next Generation Sequencing (NGS) techniques, and bioinformatics procedures to capture, sequence, and identify inserted DNA within the maize genome. By compiling a large number of unique sequencing reads and mapping them against the transformation plasmid and control maize genome, unique junctions due to inserted DNA are identified in the bioinformatics analysis and used to determine the number of insertions within the plant genome, verify insertion intactness, and confirm the absence of plasmid backbone sequences.

The SbS technique (Figure 9) utilizes capture probes homologous to the transformation plasmid to isolate genomic DNA that hybridizes to the probe sequences ([Zastrow-Hayes et al., 2015](#)). Captured DNA is then sequenced using a Next Generation Sequencing (NGS) procedure and the results are analyzed using bioinformatics tools. During the analysis, junction reads are identified as those sequence reads where part of the read shows exact homology to the plasmid DNA sequence while the rest of the read does not match the contiguous plasmid. Junctions may occur between inserted DNA and genomic DNA, or between insertions of two plasmid-derived DNA sequences that are not contiguous in the transformation plasmid. Multiple sequence reads are generated for each junction and are compiled into a consensus sequence for the junction. By compiling a large number of unique sequencing reads and comparing them to the transformation plasmid and control maize genome, unique junctions due to inserted DNA are identified. A unique junction is defined as one in which the 20 bp plasmid-derived sequence and the 30 bp

adjacent sequence are the same across multiple reads, although the overall length of the multiple reads for that junction will vary due to the sequencing process. The number of unique junctions is related to the number of plasmid insertions present in the maize genome (for example, a single T-DNA insertion is expected to have two unique junctions). Detection of additional unique junctions beyond the two expected for a single insertion would indicate the presence of rearrangements or additional insertions derived from plasmid DNA. Absence of any junctions indicates there are no detectable insertions within the maize genome.

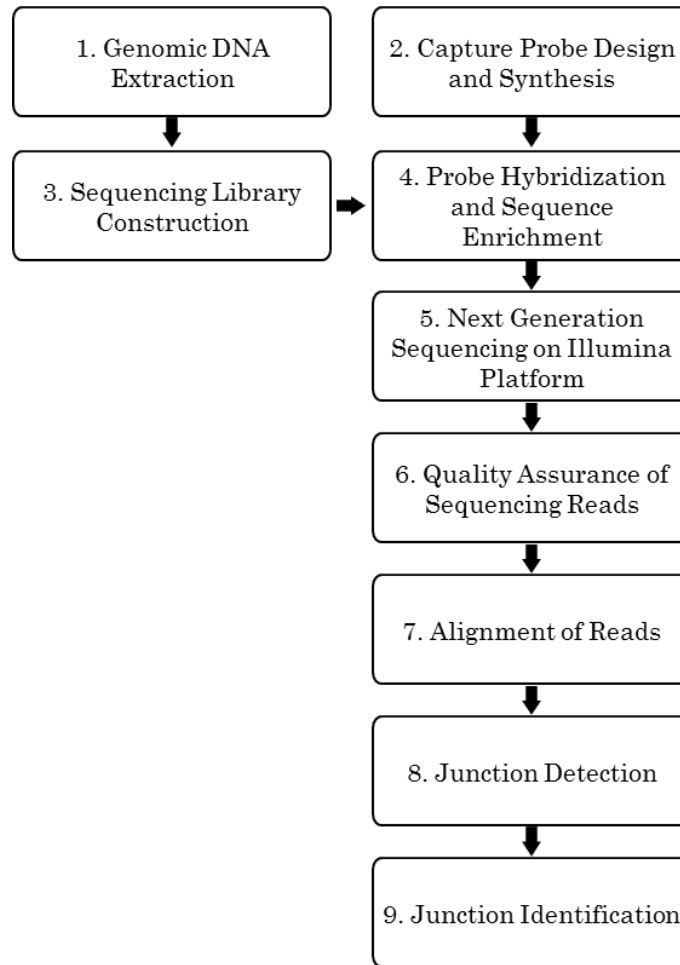


**Figure 9. Southern by Sequencing (SbS) Process Flow Diagram**

The T1 generation of DP915635 maize was analyzed by SbS, using full-coverage probes comprising the entire sequences of the trait plasmid PHP83175, the landing pad plasmid PHP73878, and the helper plasmids PHP70605, PHP21139, and PHP21875, to determine the insertion copy number and intactness and to confirm the absence of plasmid backbone sequences or unintended plasmid integration. SbS was also performed on non-GM near-isoline PHR03 maize as a control, and on positive control samples of each plasmid to confirm that the assay could reliably detect plasmid fragments spiked into control maize genomic DNA at a level equivalent to one copy of plasmid per genome copy. Based on the results obtained from the SbS analysis, a schematic diagram of the DP915635 insertion was developed and is provided in Figure 10.

Several genetic elements in the plasmids used in the positive control samples are derived from maize and thus the homologous elements in the PHR03 maize genome will be captured by the full-coverage probes used in the SbS analysis. These endogenous elements (*zm*-SEQ158, *ubiZM1* promoter, 5' UTR, and intron, *zm*-SEQ159, *zm-U6 pol III* promoter and terminator, *zm*-45CR1 guide RNA, *In2-2* promoter, *zm-wus2*, *In2-1* terminator, *zm-odp2*, Z19 terminator, *zm*-PCOa promoter, *zm*-HPLV9 intron, and Z27G terminator; Table 5, Figure 1 - Figure 7) will have sequencing reads in the SbS results due to the homologous elements in the PHR03 maize genome. However, if no junctions are detected, these sequencing reads only indicate the presence of the endogenous elements in their normal context of the maize genome and are not from inserted DNA.

SbS analysis results for the control maize are shown in Figure 11 and the positive control samples are presented in Figure 12. Example SbS results for one positive plant from the DP915635 T1 generation are presented in Figure 13. The SbS results for the remaining 9 plants tested are presented in Appendix A.

#### *SbS Analysis of the PHR03 Control Maize*

Sequencing reads were detected in the PHR03 control maize (Figure 11); however, coverage above background level (35x) was obtained only for the endogenous genetic elements derived from the maize genome, along with reads to some regions of the *sb*-RCc3 enhancer elements in the *ipd079Ea* cassette. These sequence reads were due to capture and sequencing of these genetic elements in their normal context within the PHR03 control maize genome (Table 5). Capture of the *sb*-RCc3 enhancer elements occurred due to homology of the sorghum-derived elements to sequences in the maize genome. Variation in coverage of the endogenous elements or *sb*-RCc3 enhancer regions is due to sequence variations between the PHR03 control maize and the maize or sorghum varieties from which the genetic elements in the five plasmids were derived. No junctions were detected between plasmid sequences and the maize genome (Table 6), indicating that there are no plasmid DNA insertions in the control maize, and the sequence reads were solely due to the endogenous or homologous genetic elements present in the PHR03 control maize genome.

#### *SbS Analysis of the Positive Control Samples Containing Spiked-in Plasmid DNA*

SbS analysis of the positive control samples containing spiked-in plasmid DNA resulted in sequence coverage across the entire length of each plasmid (Figure 12), indicating that the SbS assay utilizing the full-coverage probe library is sensitive enough to detect PHP83175, PHP73878, PHP70605, PHP21139, or PHP21875 sequences at a concentration equivalent to one copy of plasmid per copy of the maize genome. No junctions were detected between plasmid and genomic sequences (Table 6), indicating that the sequence reads were due to either the spiked-in plasmid or the endogenous maize genetic elements that were detected in the PHR03 control maize.

#### *SbS Analysis of the T1 Generation of DP915635 Maize*

SbS analysis of ten plants of the T1 generation of DP915635 maize resulted in five plants that contained the intended insertion (Table 6, Figure 13; and Appendix A - Figures A1 to A4). Each of these plants contained two unique genome-insertion junctions, one at each end of the intended insertion, that were identical across the five plants. The insertion, derived from PHP73878 and PHP83175, starts with the 5' junction at bp 1 and ends with the 3' junction at bp 20,564 (Figure 8). The number of sequence reads at the 5' and 3' junctions is provided in Table 6. There were no other junctions between PHP83175, PHP73878, PHP70605, PHP21139, or PHP21875 plasmid sequences and the

maize genome detected in the plants, indicating that there are no additional plasmid-derived insertions present in DP915635 maize.

A single nucleotide change was identified in all five plants in the *ubiZM1* promoter of the *pmi* cassette that differs from the expected insertion sequence (Variations panel of panel A of Figure 13; Appendix A - Figures A1 to A4). As this change is in all five positive plants, it was determined to be present in the initial transformed plant. An additional single nucleotide change was identified in the *os-actin* promoter of one plant (Appendix A - Figure A2); as this is the only occurrence in the plants analyzed, it is likely due to a spontaneous change during the breeding process. Furthermore, this change was not detected in the Sanger sequencing of the DP915635 maize insert and border regions in a later breeding generation. The read depth enabling identification of the single nucleotide changes is provided in Table 7. Alignments of the reads from the five positive plants to the five plasmid maps (Figure 13; Appendix A - Figures A1 to A4) show coverage of the genetic elements found in the intended insertion, along with coverage of the endogenous elements in the plasmids that were not incorporated into the insertion (*zm*-SEQ158, *zm*-SEQ159, *zm-U6 pol III* promoter and terminator, *zm-45CR1* guide RNA, *In2-2* promoter, *zm-wus2*, and *zm-odp2*). Reads also aligned to the *pinII* terminator elements located outside of the intended insertion regions in PHP83175, PHP73878, PHP70605, and PHP21875 although these elements were not incorporated into the insertion. The NGS reads that aligned to these copies of the *pinII* terminator are from fragments containing the *pinII* terminator in the *pmi* cassette of the intended insertion; however, the reads from this single copy align to all copies of the *pinII* terminator in the plasmid maps. Similarly, reads aligned to the CaMV 35S terminator elements in the *mo-Fip* cassette and to the *os-actin* promoter and intron region of the *zm-wus2* cassette in PHP83175 due to the presence of identical elements in the *mo-pat* cassette of the intended insertion.

There were no unexpected junctions between non-contiguous regions of the intended insertion identified, indicating that there are no rearrangements or truncations in the inserted DNA. Furthermore, there were no junctions between maize genome sequences and the backbone sequence of any of the plasmids involved in the production of DP915635 maize, demonstrating that no plasmid backbone or other unintended plasmid sequences were incorporated into DP915635 maize.

Each of the five DP915635 maize plants from the T1 generation that were determined to be negative for the DP915635 insertion yielded sequencing reads (Table 6 and Appendix A - Figures A5 to A9) that matched the reads in the control maize, indicating the reads were due to the same sequences detected by the probes in the control maize. There were no junctions between plasmid sequences and the maize genome detected in these plants, indicating that these plants did not contain any insertions derived from PHP83175, PHP73878, PHP70605, PHP21139, or PHP21875.

SbS analysis of the T1 generation of DP915635 maize demonstrated that DP915635 maize contains a single copy of the inserted DNA derived from PHP83175 and PHP73878, and that no additional insertions or plasmid backbone sequences are present in its genome.

Additional details regarding analytical methods for SbS analysis are provided in Appendix A.

Detailed methods and results are provided in the [PHI-2020-044 study](#).

**Table 5. Maize Endogenous Elements in Plasmids and DP915635 Insertion**

Number <sup>a</sup>	Name of Endogenous Element <sup>b</sup>	Present in Plasmid(s) or Insertion
1	<i>zm</i> -SEQ158 <sup>c</sup>	PHP73878
2	<i>ubiZM1</i> promoter, 5' UTR, and intron	PHP73878, PHP70605, PHP21875, PHP83175, DP915635 insertion
3	<i>zm</i> -SEQ159 <sup>c</sup>	PHP73878
4	<i>zm-U6 pol III</i> promoter	PHP70605
5	<i>zm-45CR1</i> guide RNA	PHP70605
6	<i>zm-U6 pol III</i> terminator	PHP70605
7	<i>In2-2</i> promoter	PHP21139
8	<i>zm-wus2</i>	PHP21139; PHP83175
9	<i>In2-1</i> terminator	PHP21139, PHP83175, DP915635 insertion
10	<i>zm-odp2</i>	PHP21875, PHP83175
11	Z19 terminator	PHP83175, DP915635 insertion
12	<i>zm-PCOa</i> promoter	PHP83175, DP915635 insertion
13	<i>zm-HPLV9</i> intron	PHP83175, DP915635 insertion
14	Z27G terminator	PHP83175, DP915635 insertion

<sup>a</sup> The numbers indicating endogenous genetic elements are shown as circled numbers found below linear construct maps in Figure 11 - Figure 13 and Appendix A Figures A1 to A9.

<sup>b</sup> As shown in the plasmid and T-DNA maps in Figure 1 - Figure 7 and the intended insertion map in Figure 8.

<sup>c</sup> As the *zm*-SEQ158 and *zm*-SEQ159 are found in their native context in the maize genome, they are considered part of the flanking genomic regions and not part of the DP915635 insertion (Figure 8).

**Table 6. DP915635 Maize and Control Maize SbS Junction Reads**

Sample Description	Total Reads at 5' Junction <sup>a</sup>	Unique Reads at 5' Junction <sup>b</sup>	Total Reads at 3' Junction <sup>c</sup>	Unique Reads at 3' Junction <sup>d</sup>	DP915635 Insertion
DP915635 Maize Plant ID 385269367	0	0	0	0	-
DP915635 Maize Plant ID 385269368	0	0	0	0	-
DP915635 Maize Plant ID 385269369	560	184	622	176	+
DP915635 Maize Plant ID 385269370	0	0	0	0	-
DP915635 Maize Plant ID 385269371	571	174	601	186	+
DP915635 Maize Plant ID 385269372	439	161	457	177	+
DP915635 Maize Plant ID 385269373	546	190	628	181	+
DP915635 Maize Plant ID 385269374	0	0	0	0	-
DP915635 Maize Plant ID 385269375	527	181	539	176	+
DP915635 Maize Plant ID 385269376	0	0	0	0	-
PHR03 Control Maize	0	0	0	0	-
PHP831759 Positive Control	0	0	0	0	-
PHP21139 Positive Control	0	0	0	0	-
PHP21875 Positive Control	0	0	0	0	-
PHP70605 Positive Control	0	0	0	0	-
PHP73878 Positive Control	0	0	0	0	-

<sup>a</sup> Total number of sequence reads across the 5' junction of the DP915635 insertion.

<sup>b</sup> Unique sequence reads establishing the location of the 5' genomic junction of the DP915635 insertion (Figure 8). Multiple identical NGS supporting reads are condensed into each unique read.

<sup>c</sup> Total number of sequence reads across the 3' junction of the DP915635 insertion.

<sup>d</sup> Unique sequence reads establishing the location of the 3' genomic junction of the DP915635 insertion (Figure 8). Multiple identical NGS supporting reads are condensed into each unique read.

**Table 7. SbS Junction Reads at Single Nucleotide Changes**

Sample Description	Read Depth at <i>ubiZM1</i> Promoter Single Nucleotide Change <sup>a</sup>	Read Depth at <i>os-Actin</i> Promoter Single Nucleotide Change <sup>b</sup>
DP915635 Maize Plant ID 385269369	81	NA
DP915635 Maize Plant ID 385269371	99	NA
DP915635 Maize Plant ID 385269372	94	726
DP915635 Maize Plant ID 385269373	89	NA
DP915635 Maize Plant ID 385269375	110	NA

<sup>a</sup> Total number of unique reads enabling identification of the single nucleotide change in the *ubiZM1* promoter of all five plants containing the DP915635 insert.

<sup>b</sup> Total number of unique reads enabling identification of the single nucleotide change in the *os-actin* promoter of plant 385269372. NA=Not Applicable; this single nucleotide change was not present in these plants.

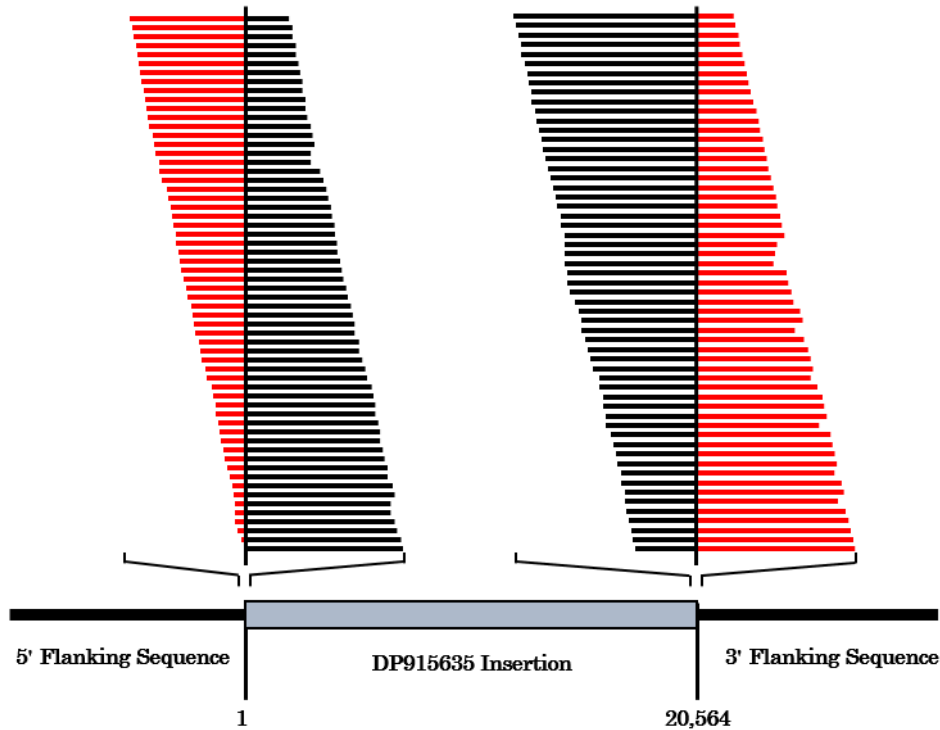
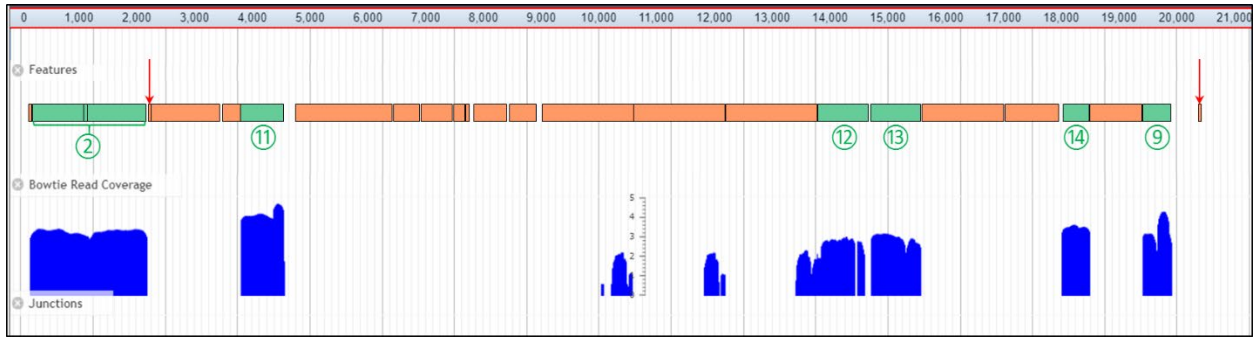


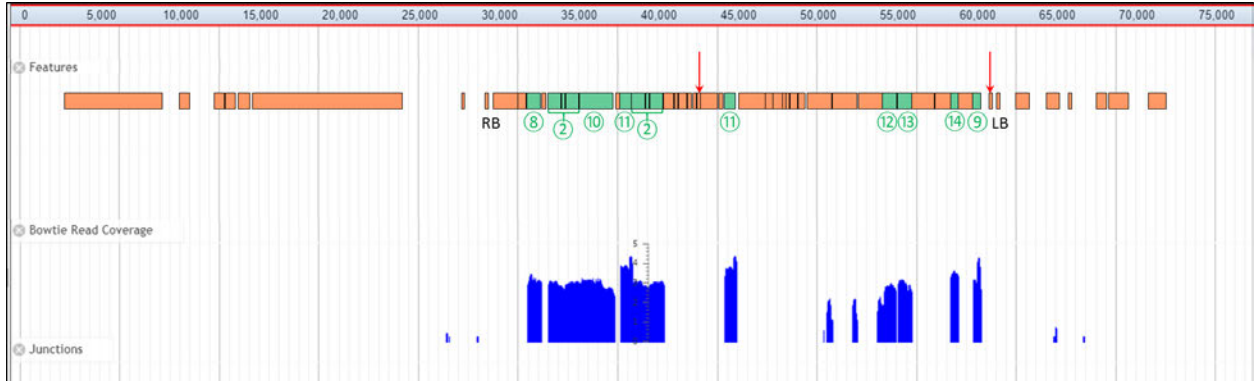
**Figure 10. Schematic Diagram of the DNA Insertion in DP915635 Maize**

Schematic diagram of the DNA insertion in DP915635 maize based on the SbS analysis described. The flanking maize genomic regions, including *zm-SEQ158* and *zm-SEQ159*, are indicated in the map by black bars. A single copy of the insertion, derived from *PHP73878* and *PHP83175* and shown by the gray box, is integrated into the DP915635 maize genome. Vertical lines show the locations of the two-unique genome-insertion junctions. The numbers below the map indicate the bp location of the junction nucleotide in reference to the sequence of the intended insertion (Figure 8). Representative individual sequencing reads across the junctions are shown as stacked lines above each junction (not to scale); red indicates genomic flanking sequence and black indicates inserted DNA sequence within each read.

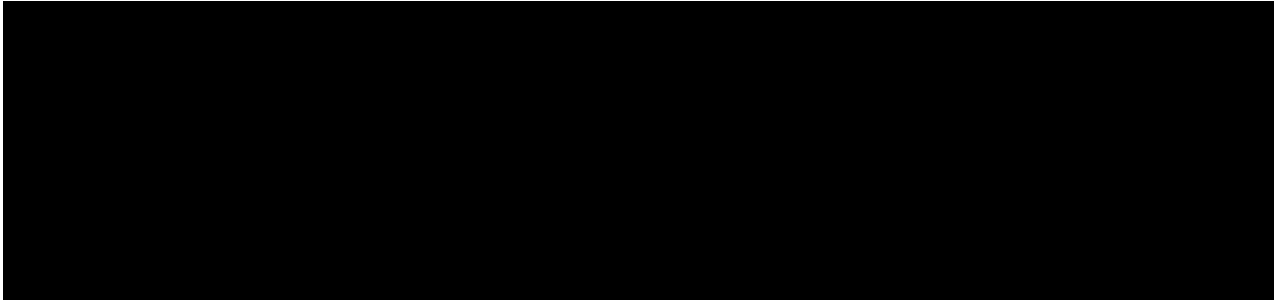
### A. Alignment to Intended Insertion



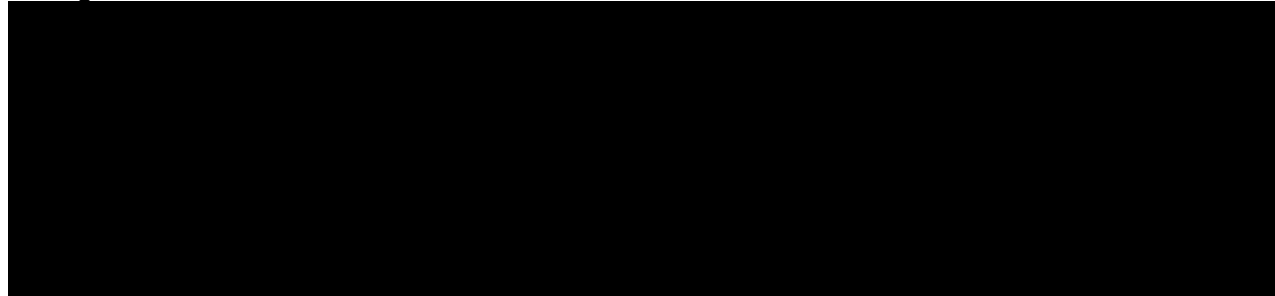
### B. Alignment to PHP83175



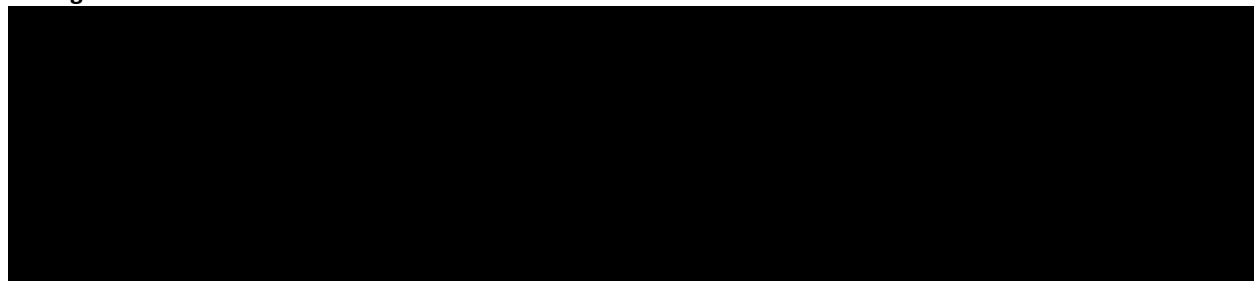
### C. Alignment to PHP73878



### D. Alignment to PHP70605



#### E. Alignment to PHP21139



#### F. Alignment to PHP21875

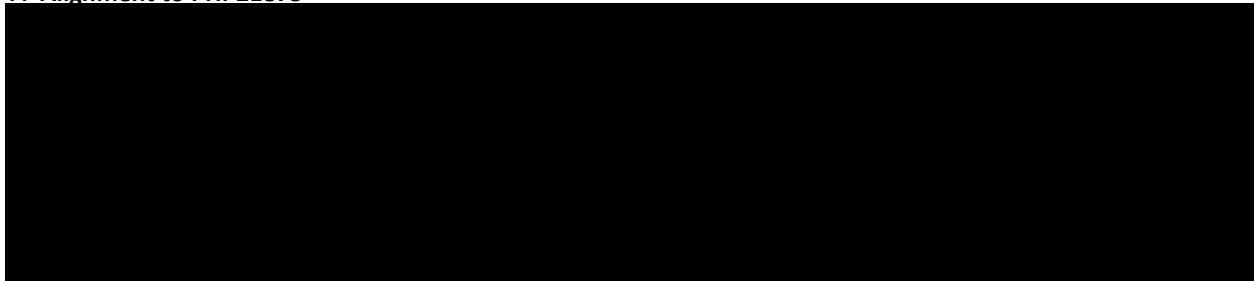
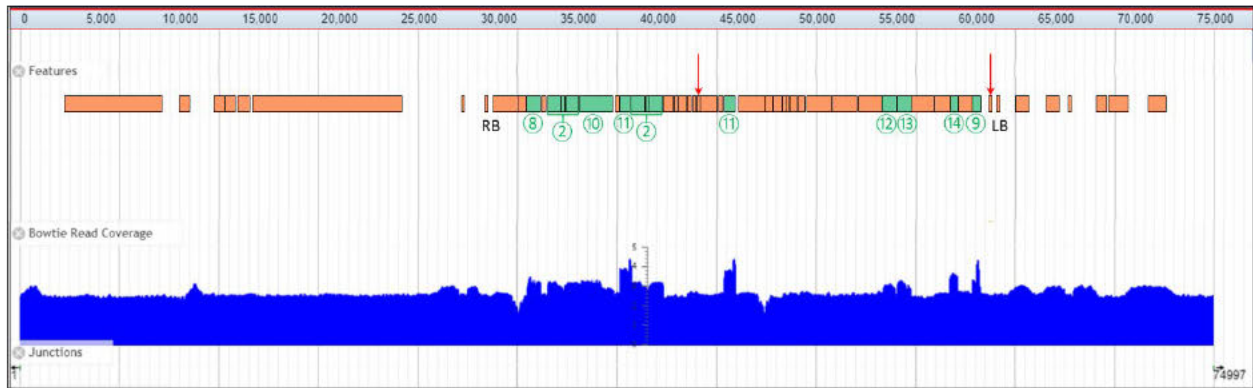


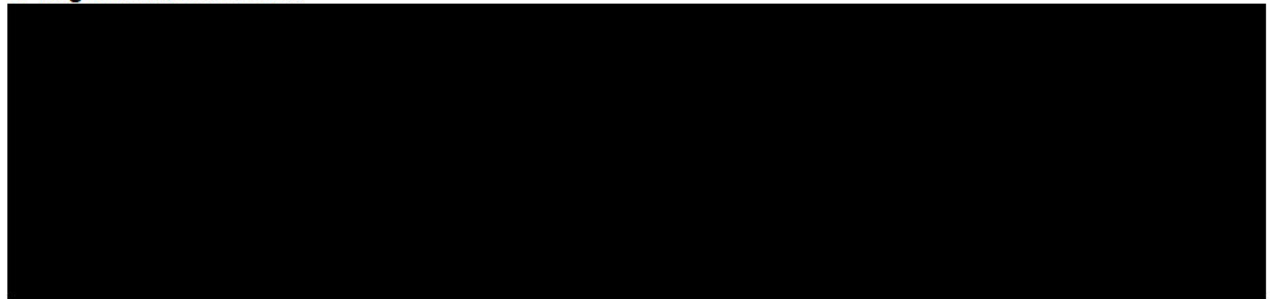
#### Figure 11. SbS Results for Control Maize

The blue coverage graph shows the number of individual NGS reads aligned at each point on the intended insertion or construct using a logarithmic scale at the middle of the graph. Green bars above the coverage graph indicate endogenous genetic elements in each plasmid derived from the maize genome (identified by numbers, Table 5), while tan bars indicate genetic elements derived from other sources. The absence of any junctions between plasmid and genomic sequences indicates that there are no insertions or plasmid backbone sequence present in the PHR03 control maize. FRT sites are indicated by red arrows. A) SbS results for PHR03 control maize aligned against the intended insertion (20,564 bp; Figure 8). Coverage above background level (35x) was obtained only for regions derived from or showing homology to maize endogenous elements. Variation in coverage of the endogenous elements is due to some sequence variation between the control maize and the source of the corresponding genetic elements. As no junctions were detected between plasmid sequences and the maize genome, there are no DNA insertions identified in the PHR03 control maize, and the sequence reads are solely due to the endogenous elements or homologous elements present in the PHR03 genome. B) SbS results aligned against the plasmid PHP83175 sequence (74,997 bp; Figure 6). Coverage was obtained only for the endogenous elements or those with homology to endogenous elements. C) SbS results aligned against the plasmid PHP73878 sequence [REDACTED] bp; Figure 1). Coverage was obtained only for the endogenous elements. D) SbS results aligned against the plasmid PHP70605 sequence [REDACTED] bp; Figure 3). E) SbS results aligned against the plasmid PHP21139 sequence [REDACTED] bp; Figure 4). Coverage was obtained only for the endogenous elements. F) SbS results aligned against the plasmid PHP21875 sequence [REDACTED] bp; Figure 5). Coverage was obtained only for the endogenous elements.

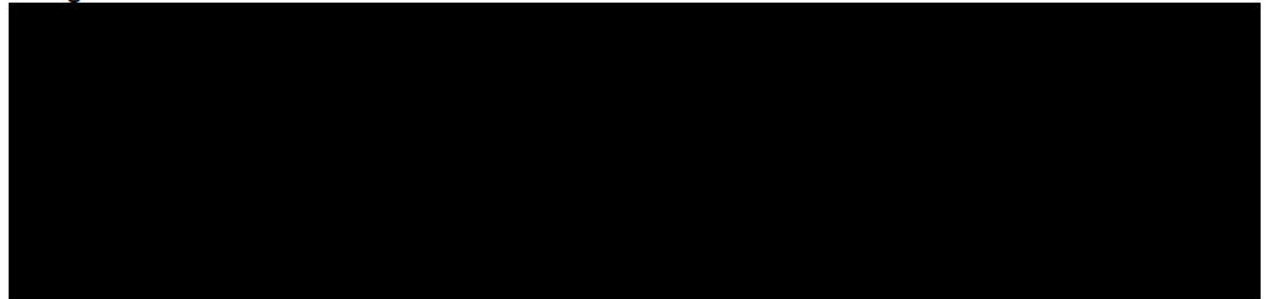
### A. Alignment to PHP83175



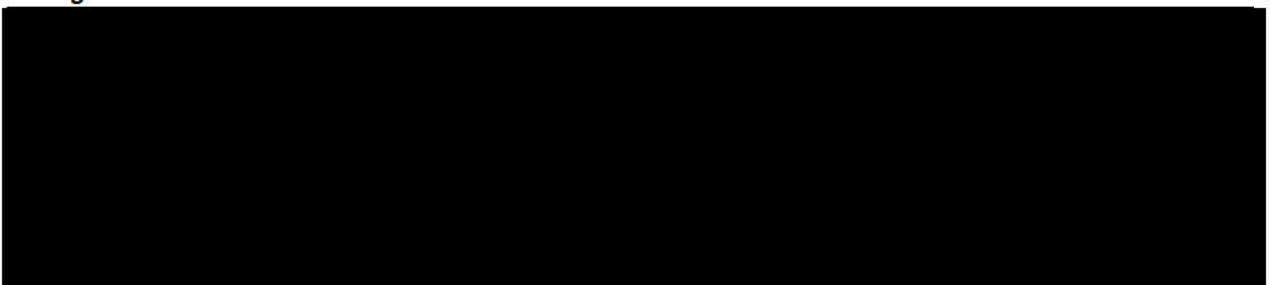
### B. Alignment to PHP73878



### C. Alignment to PHP70605



### D. Alignment to PHP21139



## E. Alignment to PHP21875

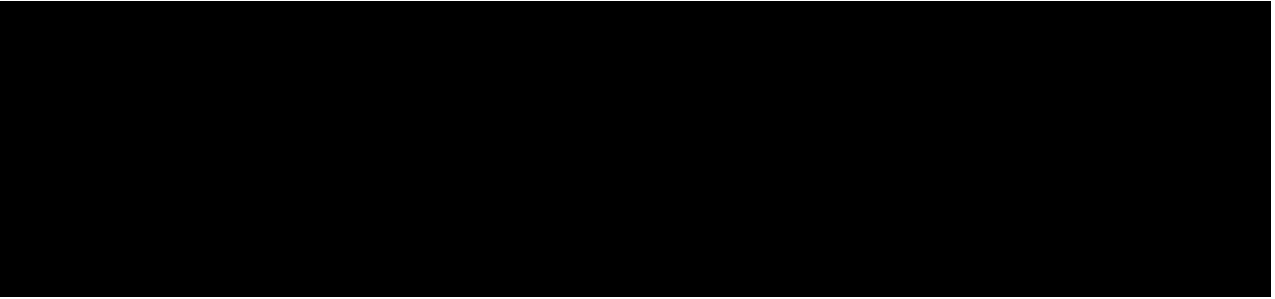
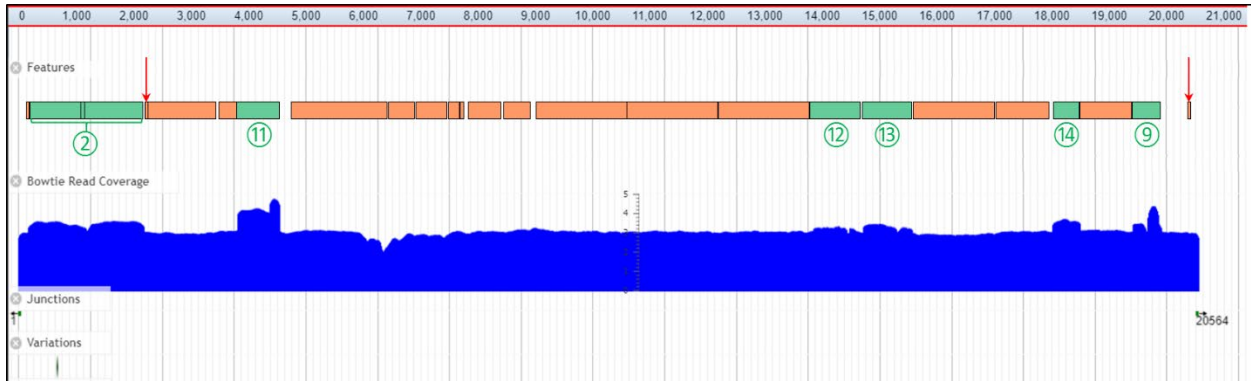


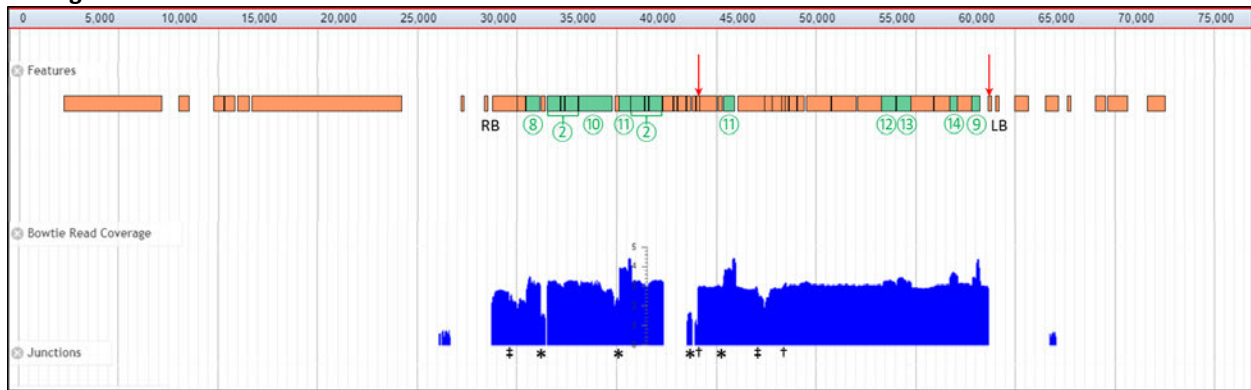
### Figure 12. SbS Results for Positive Control Samples

The positive control samples consisted of control maize DNA spiked with each plasmid at a level corresponding to one copy of plasmid per copy of the maize genome. The blue coverage graph shows the number of individual NGS reads aligned at each point on the intended insertion or construct using a logarithmic scale at the middle of the graph. Green bars above the coverage graph indicate endogenous genetic elements in the plasmid derived from the maize genome (identified by numbers, Table 5), while tan bars indicate genetic elements derived from other sources. FRT sites are indicated by red arrows. Junctions shown at the bottom of each graph are artifacts of mapping a circular plasmid to a linear map and show the start and end points of the plasmid sequence but do not indicate actual insertions in genomic DNA. **A)** SbS results of the PHP83175 positive control sample aligned against PHP83175 (74,997 bp; Figure 6). Coverage was obtained across the full length of the plasmid, indicating successful capture of PHP83175 sequences by the SbS probe library. **B)** SbS results of the PHP73878 positive control sample aligned against PHP73878 [REDACTED] bp; Figure 1). Coverage was obtained across the full length of the plasmid, indicating successful capture of PHP73878 sequences by the SbS probe library. **C)** SbS results of the PHP70605 positive control sample aligned against PHP70605 [REDACTED] bp; Figure 3). Coverage was obtained across the full length of the plasmid, indicating successful capture of PHP70605 sequences by the SbS probe library. **D)** SbS results of the PHP21139 positive control sample aligned against PHP21139 [REDACTED] bp; Figure 4). Coverage was obtained across the full length of the plasmid, indicating successful capture of PHP21139 sequences by the SbS probe library. **E)** SbS results of the PHP21875 positive control sample aligned against PHP21875 [REDACTED] bp; Figure 5). Coverage was obtained across the full length of the plasmid, indicating successful capture of PHP21875 sequences by the SbS probe library.

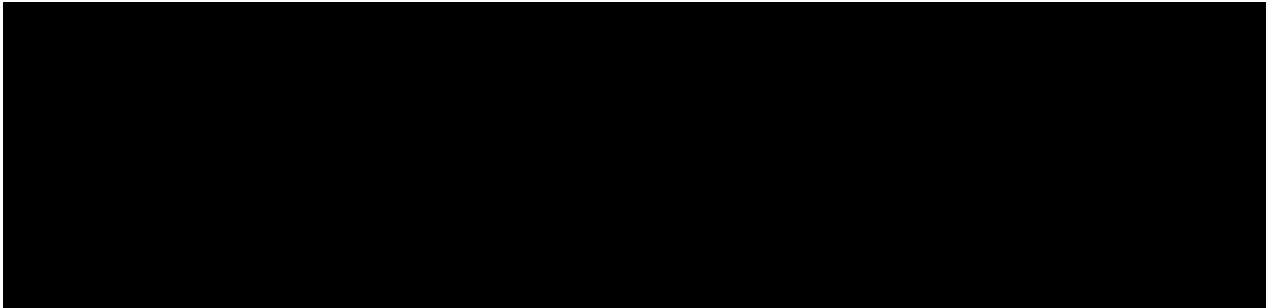
### A. Alignment to Intended Insertion



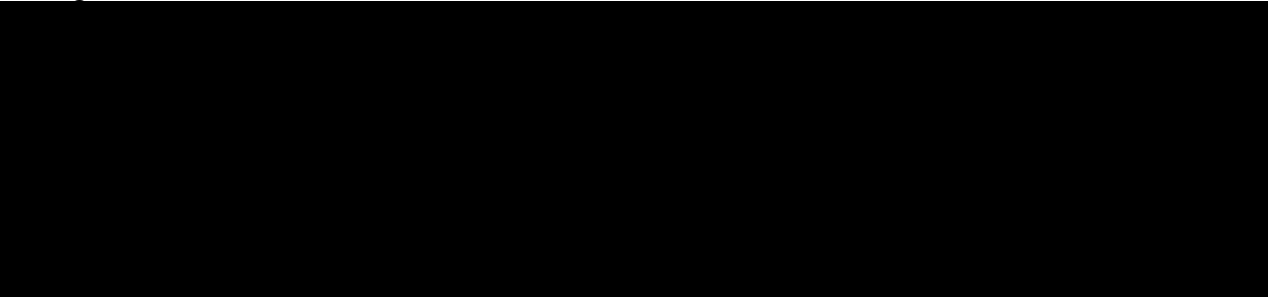
### B. Alignment to PHP83175



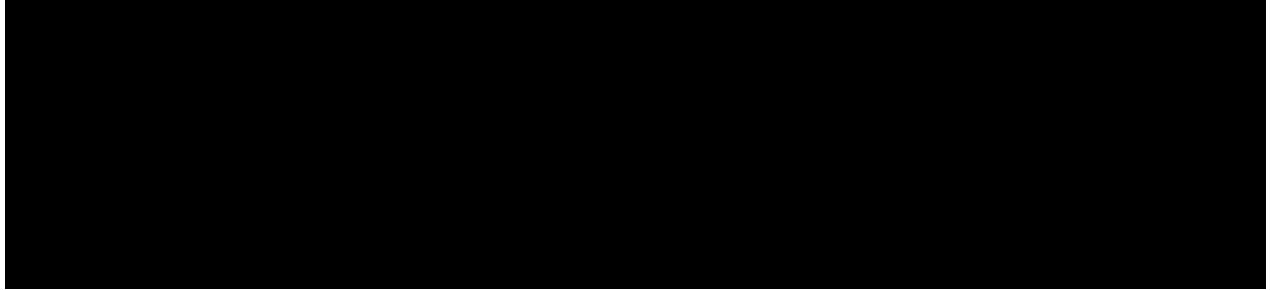
### C. Alignment to PHP73878



### D. Alignment to PHP70605



#### F. Alignment to PHP21139



#### F. Alignment to PHP21875

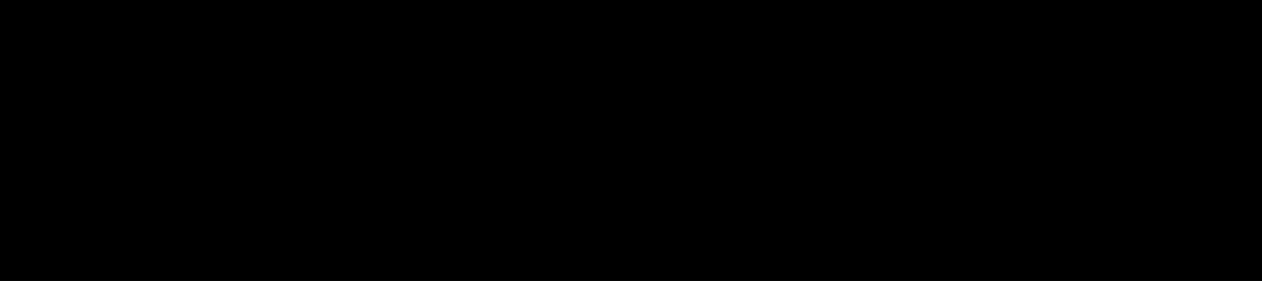


#### Figure 13. SbS Results for DP915635 Maize (Plant ID 385269369)

The blue coverage graph shows the number of individual NGS reads aligned at each point on the intended insertion or construct using a logarithmic scale at the middle of the graph. Green bars above the coverage graph indicate endogenous genetic elements in each plasmid derived from the maize genome (identified by numbers, Table 5), while tan bars indicate genetic elements derived from other sources. FRT sites are indicated by red arrows. **A)** SbS results aligned against the intended insertion (20,564 bp; Figure 8), indicating that this plant contains the intended insertion. Arrows below the graph indicate the two plasmid-to-genome sequence junctions identified by SbS; the numbers below the arrows refer to the bp location of the junction relative to the intended insertion (Figure 8). The presence of only two junctions demonstrates the presence of a single insertion in the DP915635 maize genome. The Variations panel indicates the location of a single nucleotide change identified in all plants containing the insertion. **B)** SbS results aligned against the plasmid PHP83175 sequence (74,997 bp; Figure 6). Coverage was obtained for the elements between FRT1 and FRT6 transferred into DP915635 maize (region between the red arrows at top of graph). Coverage was also obtained for the endogenous elements in the region between the RB and FRT1 that were not transferred into the DP915635 maize genome, and to the *pinII* terminator (\*), CaMV35S terminator (†), and *os-actin* promoter and intron (‡) elements outside of the FRT sites due to alignment of reads derived from identical elements in the final insertion to all copies of these elements in PHP83175. **C)** SbS results aligned against the plasmid PHP73878 sequence [redacted] bp; Figure 1). Coverage was obtained for *zm*-SEQ158, *zm*-SEQ159, and the elements found in the intended insertion (between *zm*-SEQ158 to FRT1 and between FRT6 to *zm*-SEQ159), along with the *pinII* terminator element (\*) in PHP73878 due to alignment of reads derived from the *pinII* terminator in the *pmi* cassette of the intended insertion to the copy of this element in PHP73878. **D)** SbS results aligned against the plasmid PHP70605 sequence [redacted] bp; Figure 3). Coverage was obtained only for the endogenous elements along with the *pinII* terminator element (\*). **E)** SbS results aligned against the plasmid PHP21139 sequence [redacted] bp; Figure 4). Coverage was obtained only for the endogenous elements. **F)** SbS results aligned against the plasmid PHP21875 sequence [redacted] bp; Figure 5). Coverage was obtained for the endogenous elements along with the *pinII* terminator element (\*). The absence of any junctions other than to the intended insertion indicates that there are no additional insertions or backbone sequence present in DP915635 maize.

#### Sequence of Insert and Genomic Border Regions ([PHI-2019-245 study](#))

Sequence characterization analysis was performed to determine the DNA sequence of the DP915635 insert and flanking genomic regions. It should be noted that while DNA sequencing provides certain molecular information, the exact nucleotide sequence should not be viewed as static. Spontaneous mutations are a very common phenomenon in plants, presenting a biological mechanism of adaptation to constantly changing environment ([Weber et al., 2012](#)). Spontaneous mutations can occur in any part of the plant genome and in both non-GM and GM plants ([Waigmann et al., 2013](#)). In GM plants, there is no scientific basis to expect that the frequency of spontaneous mutations in transgenic insert or flanking genomic regions would be greater than in the rest of the plant genome, or that they would have a differential impact on safety ([La Paz et al., 2010](#); [Waigmann et al., 2013](#)).

To sequence the DP915635 insert and flanking genomic regions, PCR primers were designed to amplify nine overlapping PCR products spanning the insert and the 5' and 3' flanking genomic regions (Figure 14). The overlapping consensus sequences from all PCR fragments were then used to assemble the final bi-directional consensus sequence for the entirety of the DP915635 insert and genomic borders. The total length of sequence determined in DP915635 maize is 24,867 bp, comprised of 2,257 bp of the 5' flanking genomic sequence, 2,046 bp of the 3' flanking genomic sequence, and 20,564 bp of inserted DNA.

The sequence of the DP915635 insert was compared to the intended landing pad sequence from plasmid PHP73878 and the T-DNA sequence from plasmid PHP83175. The DP915635 insert was confirmed to have the expected sequences from PHP73878 and PHP83175 except for a single nucleotide A to C change at bp 2,931 in the *ubiZM1* promoter of the landing pad sequence.

Additional details regarding analytical methods for Sanger sequencing analysis are provided in Appendix D.

Detailed methods and results are provided in the [PHI-2019-245 study](#).

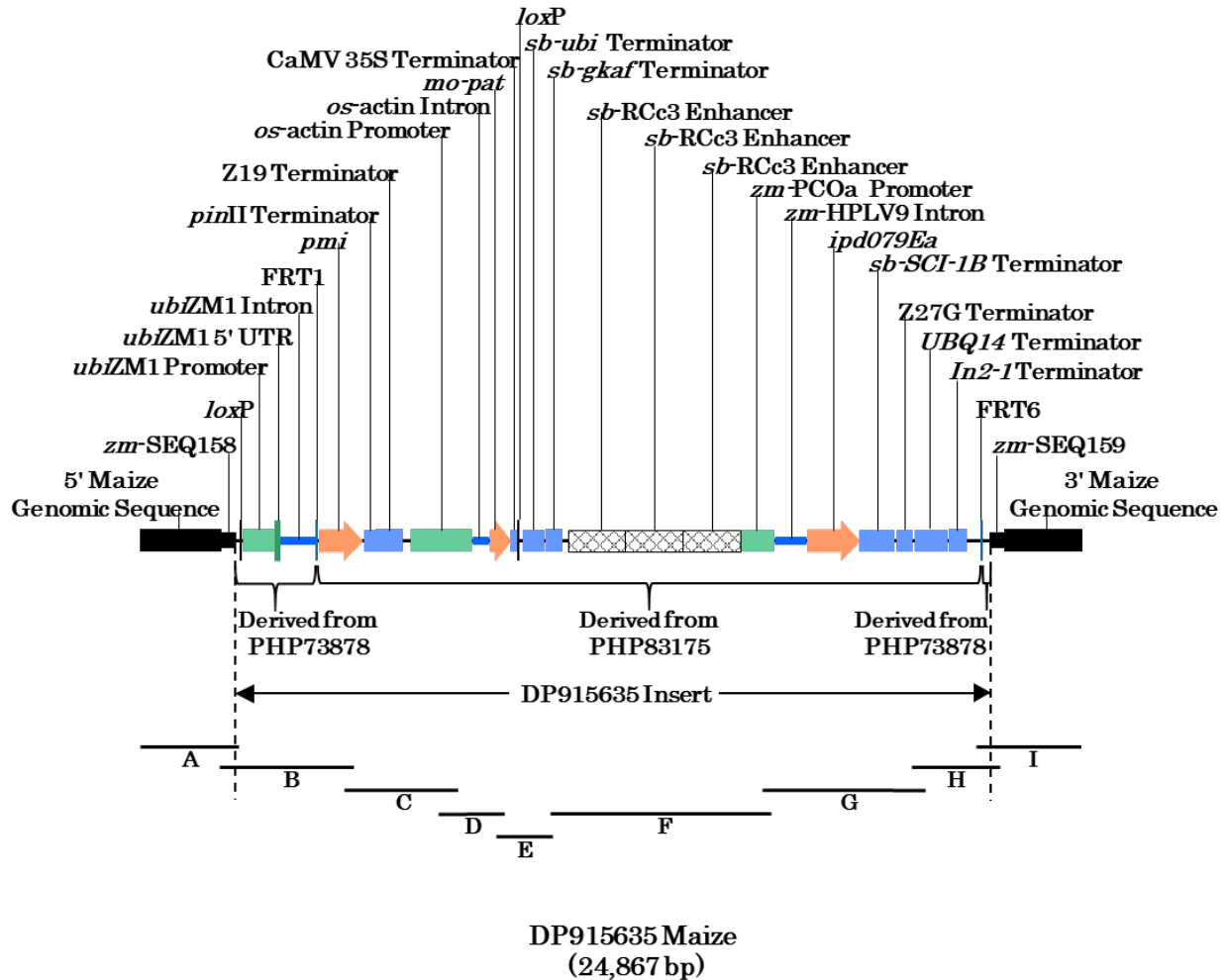


Figure 14. Diagram of the Insert and Genomic Border Regions Sequenced in DP915635 Maize

Nine overlapping PCR fragments (A, B, C, D, E, F, G, H, and I) covering the inserted DNA and genomic border regions were amplified from genomic DNA of DP915635 maize. Each black horizontal bar represents the relative position of the PCR fragment, and the vertical dash lines represent the genomic border and insert junctions. The total length of confirmed sequence for the DP915635 insert and flanking genomic regions is 24,867 bp, comprised of 2,257 bp of the 5' flanking genomic sequence, 2,046 bp of the 3' flanking genomic sequence, and 20,564 bp of the inserted DNA.

#### **Open Reading Frame Analysis of the Insert/Border Junctions ([PHI-2020-213/222 study](#))**

Assessing potentially-expressed peptides within an insertion or crossing the boundary between an insertion and its genomic borders for similarity to known and putative allergens and toxins is a critical part of the weight-of-evidence approach used to evaluate the safety of genetically-modified plant products ([Codex Alimentarius Commission, 2003](#)). Here, a bioinformatics assessment of potentially-expressed peptides (i.e., translations of open reading frames [ORFs]) was conducted following established international criteria ([Codex Alimentarius Commission, 2003](#); [FAO/WHO, 2001](#)). All potentially-expressed peptides of length  $\geq 30$  amino acids that are within the DP915635 insertion or that cross the boundary between the insertion and its genomic borders were identified and evaluated.

Ninety-two (92) translations of ORFs  $\geq 30$  amino acids were identified for the DP915635 maize sequence.

The potential allergenicity of the translations of ORFs was assessed by comparison of their sequences to the sequences in the Comprehensive Protein Allergen Resource (COMPARE) 2020 database (January 2020). The COMPARE database is compiled through a collaborative effort of the Health and Environmental Sciences Institute (HESI) Protein Allergens, Toxins, and Bioinformatics (PATB) Committee. This database is peer-reviewed and contains 2,248 sequences. Two searches were performed to assess for potential allergenicity of the translations of ORFs:

1. A search between the translations of ORFs and protein sequences in the COMPARE database was conducted with FASTA using default parameters, except that the *E*-value was set to 0.0001. The returned alignments were inspected to identify any displaying  $\geq 35\%$  identity over an alignment length of  $\geq 80$  amino acids.
2. A search between the translations of ORFs and protein sequences in the COMPARE database was conducted to identify any contiguous 8-amino acid matches to an allergen.

No alignments were returned between a translation of an ORF and any protein sequence in the COMPARE database.

One contiguous 8-amino acid match (DLSDKETT) was found between the translated ORF corresponding to the PMI protein sequence in DP915635 maize (frame DP915635\_7) and the sequence of an allergen (a putative alpha-parvalbumin from frog, GenBank Accession CAC83047.1; [Hilger et al., 2002](#)). Comprehensive analysis of this match strongly indicates that this is a false positive and is unlikely to represent a cross-reactive risk.

No other translations of ORFs displayed any contiguous 8-amino acid matches to an allergen in the database.

Collectively, these data indicate that no allergenicity concern arose from the bioinformatics assessment of DP915635 maize.

The potential toxicity of the translations of ORFs was assessed by comparison of their sequences to the sequences in an internal toxin database. The internal toxin database is a subset of sequences found in UniProtKB/Swiss-Prot. To produce the internal toxin database, the proteins in UniProtKB/Swiss-Prot are filtered for molecular function by keywords that could imply toxicity or adverse health effects (e.g., toxin, hemagglutinin, vasoactive, etc.). The internal toxin database is updated annually. The search between the translations of ORFs and protein sequences in

the internal toxin database was conducted with BLASTP using default parameters, except that the *E*-value was set to 0.0001 and all the alignments at or below the *E*-value threshold were returned.

No alignments were returned between the translations of ORFs and any protein sequence in the internal toxin database. Therefore, no toxicity concerns arose from the bioinformatics assessment of the translations of ORFs.

Bioinformatics evaluation of DP915635 maize did not generate biologically relevant amino acid sequence similarities to known allergens, toxins, or other proteins that would be harmful to humans or animals.

Detailed methods and results are provided in the [PHI-2020-213/222 study](#).

#### **Event-Specific Detection Methodology (PHI-2020-154 study)**

An event-specific quantitative real-time PCR method was developed and validated for detection of event DP-915635-4 in maize. The event-specific assay for DP915635 maize is designed to amplify the target sequence at the 3' junction between the DP915635 maize insertion and the maize genomic DNA. The binding site of the forward primer is within the transgenic insertion, the binding site of the reverse primer is within the maize genomic DNA, and the binding site of the probe spans the junction of the transgenic insertion and the maize genomic DNA. [REDACTED]

Detailed methods and results are provided in the [PHI-2020-154 study](#).

#### **Conclusions on the Characterization of the Inserted DNA in DP915635 Maize**

SbS analysis confirmed that DP915635 maize contains a single copy of the inserted DNA with the expected organization. SbS analysis results also showed no additional insertions, plasmid backbone, or other unintended plasmid sequences were present in DP915635 maize. As the data presented in A.3(e) *Stability of the genetic changes* Southern blot analysis of five generations of DP915635 maize confirmed that the inserted DNA in DP915635 maize is stable and equivalent across multiple generations during the breeding process. Segregation analysis confirmed that the inserted DNA segregated as a single locus according to Mendelian rules of inheritance across five generations of DP915635 maize, and the stability of the insertion and of the herbicide tolerance phenotype was demonstrated in these populations.

Sanger sequencing analyses determined the sequences of the inserted DNA and the flanking genomic border regions in DP915635 maize. The total length of sequence determined in DP915635 maize is 24,867 bp, comprised of 2,257 bp of the 5' flanking genomic border sequence, 2,046 bp of the 3' flanking genomic border sequence, and 20,564 bp of inserted DNA (consisting, from the 5' end to the 3' end, of 2,211 bp from plasmid PHP73878, 18,190 bp from plasmid PHP83175, and another 163 bp from plasmid PHP73878).

A bioinformatics evaluation of the DP915635 maize insert did not generate biologically relevant amino acid sequence similarities to known allergens, toxins, or other proteins that would be harmful to humans or animals.

Together, these analyses confirmed that a single copy of the inserted DNA, with no plasmid backbone sequences or other unintended sequences is present in the DP915635 maize genome. The introduced genes were stably inherited across multiple generations, and segregate according to Mendel's law of inheritance. Sanger sequencing analyses determined the sequences of the inserted DNA and flanking genomic regions in DP915635 maize. Bioinformatic analyses support the conclusion that there is unlikely to be allergenicity or toxicity concerns regarding

the putative translated ORFs at the DP915635 insertion site. Additionally, an event-specific quantitative real-time PCR detection method was developed and validated for DP915635 maize.

#### A.3(d) Breeding process

Plants that were regenerated from transformation and tissue culture (designated T0 plants) were selected for further characterization. Refer to Figure 15 for a schematic overview of the transformation and event development process for DP915635 maize.

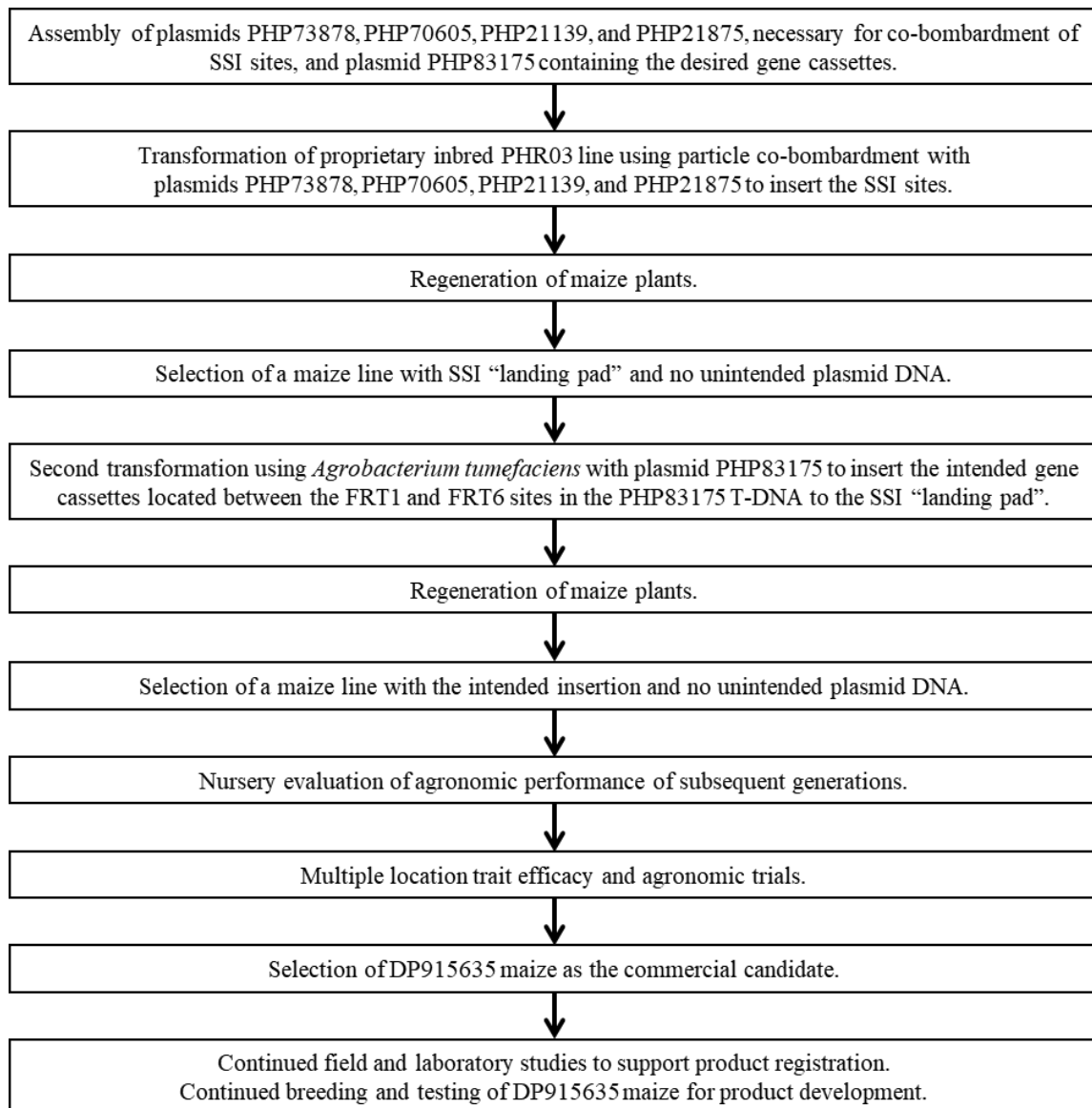
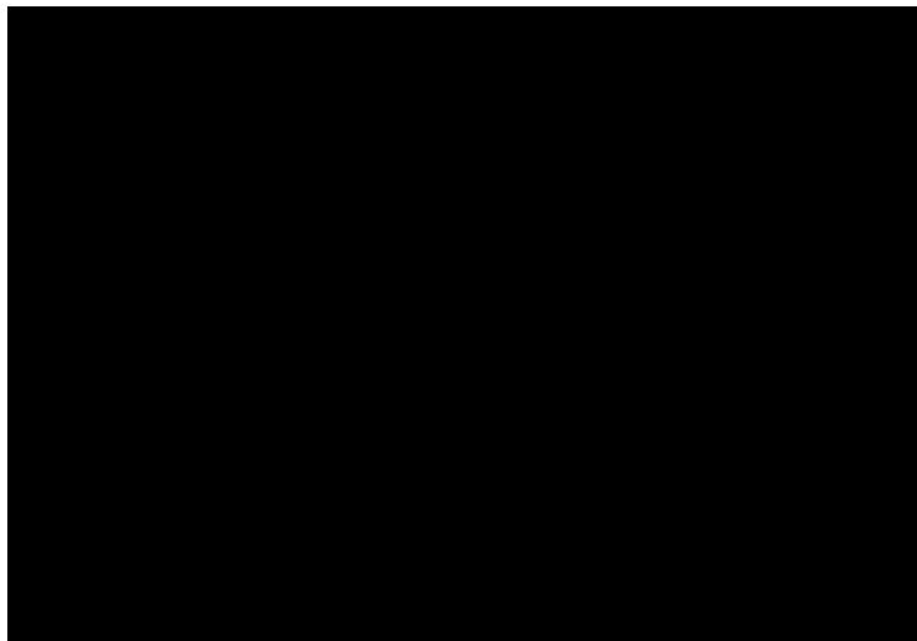


Figure 15. Event Development Process of DP915635 Maize

The subsequent breeding of DP915635 maize proceeded as indicated in Figure 16 to produce specific generations for the characterization and assessments conducted, as well as for the development of commercial maize lines. Table 8 provides the generations used for each characterization study.



**Figure 16. Breeding Diagram for DP915635 Maize and Generations Used for Analysis**

The breeding steps to produce the generations used for characterization, assessment, and the development of commercial lines are shown schematically. Proprietary inbred PHR03 was used for transformation to produce DP915635 maize.

**Table 8. Generations and Comparators Used for Analysis of DP915635 Maize**

Analysis	Seed Generation(s) Used	Comparators
Insertion copy number, insertion organization, and the absence of plasmid backbone and other unintended plasmid sequences by SbS	T1	PHR03
Insertion stability by Southern Blot	T1, T2, T3, T4, T5	PHR03
Sanger sequencing	T4	PHR03
Mendelian Inheritance by multi-generation segregation analysis	F1 (PHR03/PHR1J), T2, T3, T4, T5	N/A
Composition and Expression Analysis	F1 (PH1KTF/PHR03)	PH1KTF/PHR03

#### Selection of Comparators

For the characterization of DP915635 maize, proprietary maize inbred (PHR03) and F1 hybrid (PH1KTF/PHR03) lines were used as experimental controls (Table 8). The control lines selected are non-genetically modified (non-GM) and

represent the genetics of the maize lines used to produce the DP915635 maize generations used in analysis (Figure 16).

In addition, conventionally bred (conventional) non-GM maize hybrid lines (i.e., reference lines), were used to obtain tolerance intervals for compositional analyses. These maize hybrids were chosen to represent a wide range of conventional non-GM varieties that could be planted commercially. These tolerance intervals help represent the normal range of variation of the maize crop for compositional analytes and further helped to determine the comparability of DP915635 maize to conventional non-GM maize.

### A.3(e) Stability of the genetic changes

#### Southern Analysis to Determine Stable Genetic Inheritance across Generations ([PHI-2020-114 study](#))

Southern blot analysis was performed on five generations of DP915635 maize to evaluate the stability of the inserted *ipd079Ea*, *mo-pat*, and *pmi* gene cassettes across multiple generations.

Restriction enzyme *Pvu* II (indicated in Figure 17 and Figure 18) was selected to verify the stability of the DP915635 maize insertion across the five generations (T1, T2, T3, T4, and T5) of DP915635 maize plants. *Pvu* II was selected because there is a single *Pvu* II restriction site within the DP915635 maize insertion, which provides a means to uniquely identify the event, as additional sites would be in the adjacent flanking genomic DNA (Figure 19). Genomic DNA samples from the five generations of DP915635 maize and control maize plants were digested with *Pvu* II and hybridized with the *ipd079Ea*, *mo-pat*, and *pmi* gene probes for Southern analysis. Hybridization patterns of these probes exhibited event-specific bands unique to the DP915635 maize insertion, and thus provided a means of verification that the genomic border regions of the DP915635 maize insertion were not changed across the five generations during breeding. Plasmid PHP83175 was added to control maize DNA, digested with *Pvu* II, and included on the blot to verify successful probe hybridization. The probes used for Southern hybridization are described in Table 9 and shown in Figure 17.

Hybridization of the *ipd079Ea* probes to *Pvu* II-digested genomic DNA resulted in a single band of approximately 6,500 bp in all five generations of DP915635 maize samples analyzed (Table 10, Figure 20). This result confirmed that the 3' border fragment, containing the *ipd079Ea* gene in the DP915635 maize insertion, is intact and stable across the five generations of DP915635 maize. The lanes containing PHP83175 plasmid DNA showed the expected band of 7,037 bp, confirming successful hybridization of the *ipd079Ea* probes.

Hybridization of the *mo-pat* and *pmi* probes to *Pvu* II-digested genomic DNA resulted in a consistent band of approximately 15,000 bp in all five generations of DP915635 maize (Table 10, Figure 21 and Figure 22, respectively). These results confirmed that the 5' border fragment, containing the *mo-pat* and *pmi* genes in the DP915635 maize insertion, is intact and stable across the five generations of DP915635 maize. The lanes containing PHP83175 plasmid DNA showed the expected band of 19,295 bp, confirming successful hybridization of the *mo-pat* and *pmi* probes.

The presence of equivalent bands from hybridization with each of the *ipd079Ea*, *mo-pat*, and *pmi* probes within the plants from all five generations analyzed confirms that the inserted DNA in DP915635 maize is consistent and stable across multiple generations during the breeding process.

Additional details regarding analytical methods for Southern analysis are provided in Appendix B.

Detailed methods and results are provided in the [PHI-2020-114 study](#).

**Table 9. Description of DNA Probes Used for Southern Hybridization**

Genetic Element/ Probe Name	Probe Length bp	Position on PHP83175 T-DNA (bp to bp) <sup>a</sup>
<i>pmi</i> <sup>b</sup>	569	13,393 to 13,961
	660	13,931 to 14,590
<i>mo-pat</i>	582	18,040 to 18,621
<i>ipd079Ea</i> <sup>c</sup>	712	26,717 to 27,428
	750	27,411 to 28,160

<sup>a</sup> The probe position is based on the PHP83175 T-DNA map (Figure 18).

<sup>b</sup> and <sup>c</sup> These probes comprise two fragments that are combined in a single hybridization solution.

**Table 10. Predicted and Observed Hybridization Bands on Southern Blots; *Pvu* II Digest**

Probe Name	Predicted and Observed Fragment Size from Plasmid PHP83175 (bp) <sup>a</sup>	Predicted Fragment Size from Intended Insertion Map of DP915635 Maize (bp) <sup>b</sup>	Observed Fragment Size in DP915635 Maize <sup>c</sup> (bp)	Figure
<i>ipd079Ea</i>	7,037	>6,211	~6,500	Figure 20
<i>mo-pat</i>	19,295	>14,353	~15,000	Figure 21
<i>pmi</i>	19,295	>14,353	~15,000	Figure 22

<sup>a</sup> Predicted and observed fragment sizes based on the PHP83175 plasmid map (Figure 17).

<sup>b</sup> Predicted sizes based on the DP915635 insertion map (Figure 19).

<sup>c</sup> Observed fragment sizes are approximated from the DIG-labeled DNA Molecular Weight Marker III and VII fragments on the Southern blots. Due to inability to determine the exact sizes on the blot, all approximated values are rounded to the nearest 100 bp.

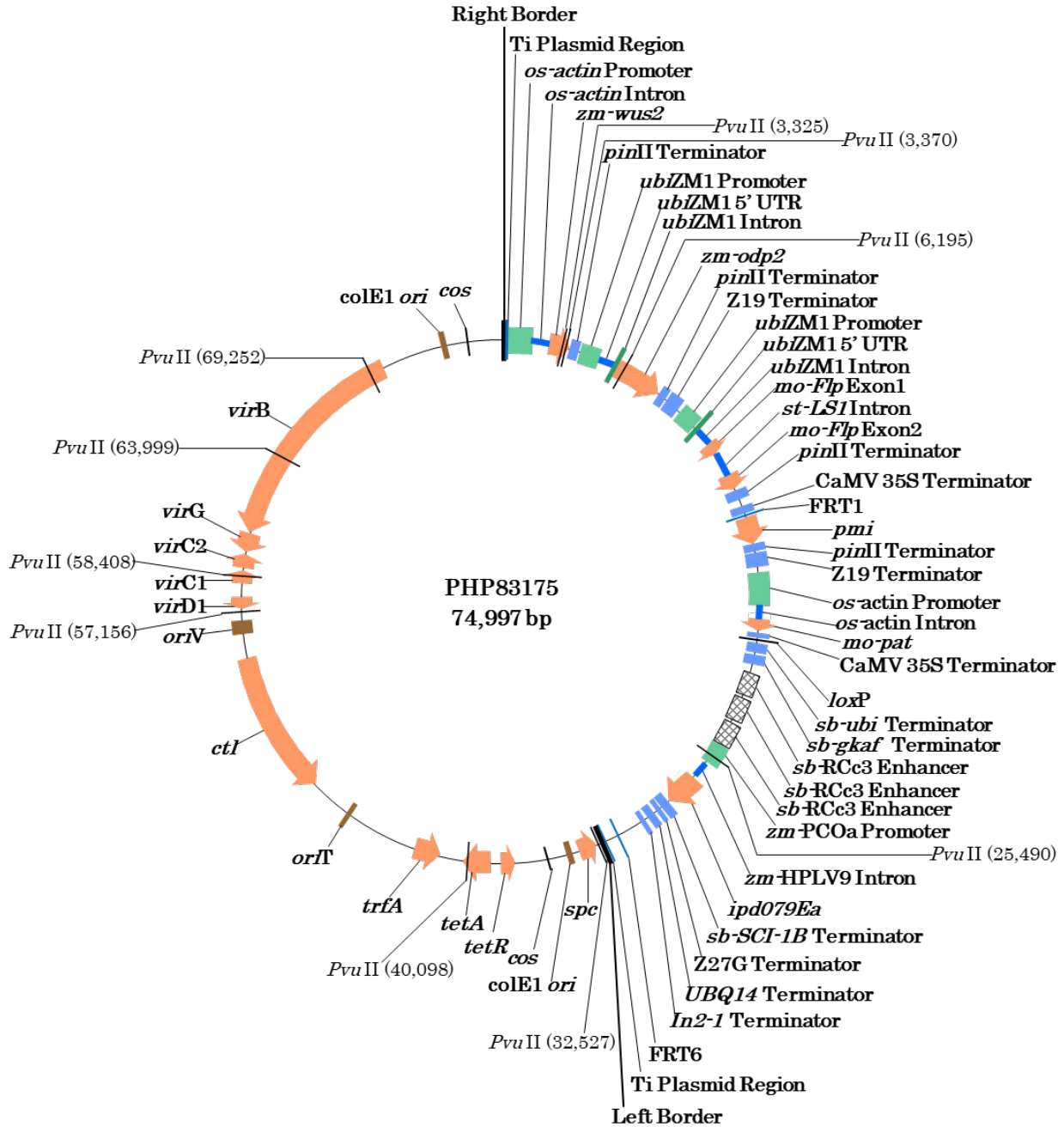


**Figure 17. Map of Plasmid PHP83175 for Southern Analysis**

Plasmid map of PHP83175 indicating Pvu II restriction enzyme sites with base pair positions, and containing the *pmi*, *mo-pat*, and *ipd079Ea* gene cassettes intended for incorporation into the maize genome, and the *zm-wus2*, *zm-odp2*, and *mo-Flp* gene cassettes not intended for incorporation into the maize genome. FRT1 and FRT6 sites flank the intended insert from PHP83175 T-DNA (Figure 19) that provided the elements transferred during SSI. The size of plasmid PHP83175 is 74,997 bp.

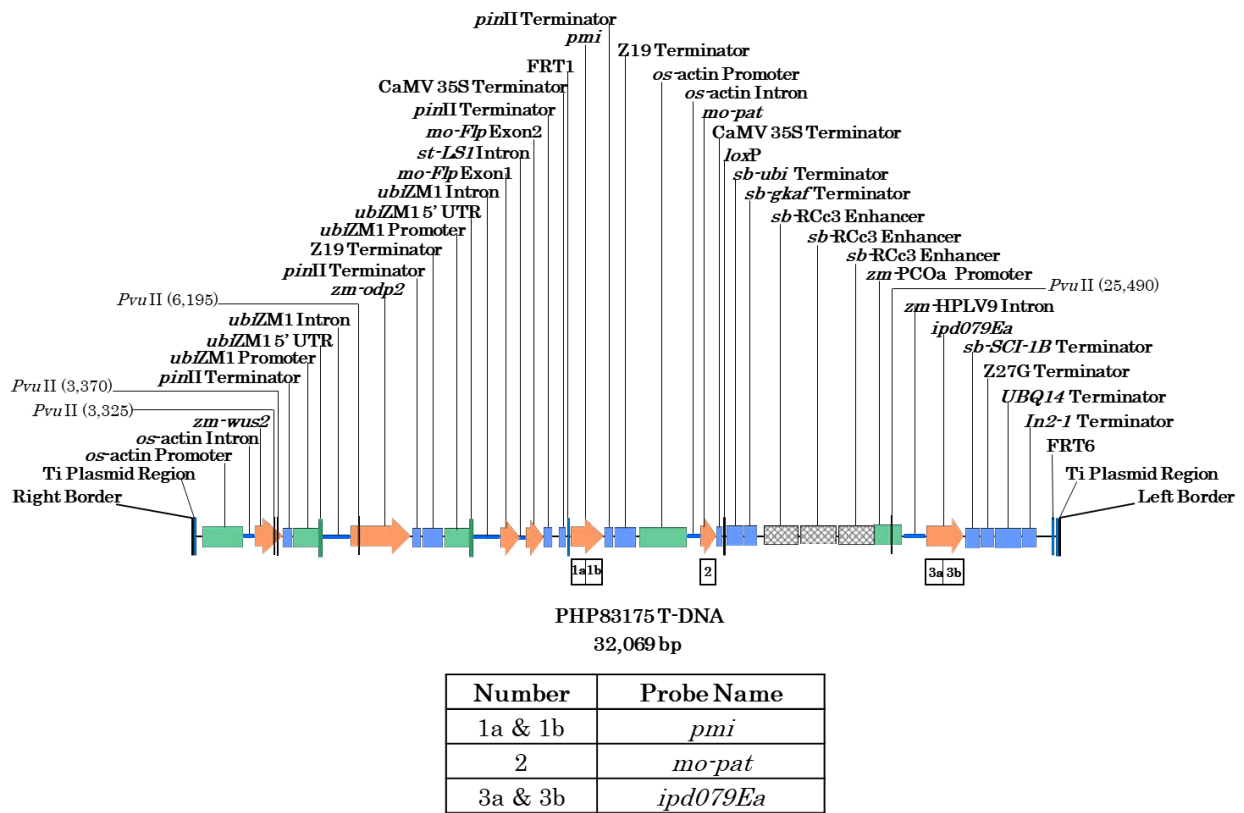
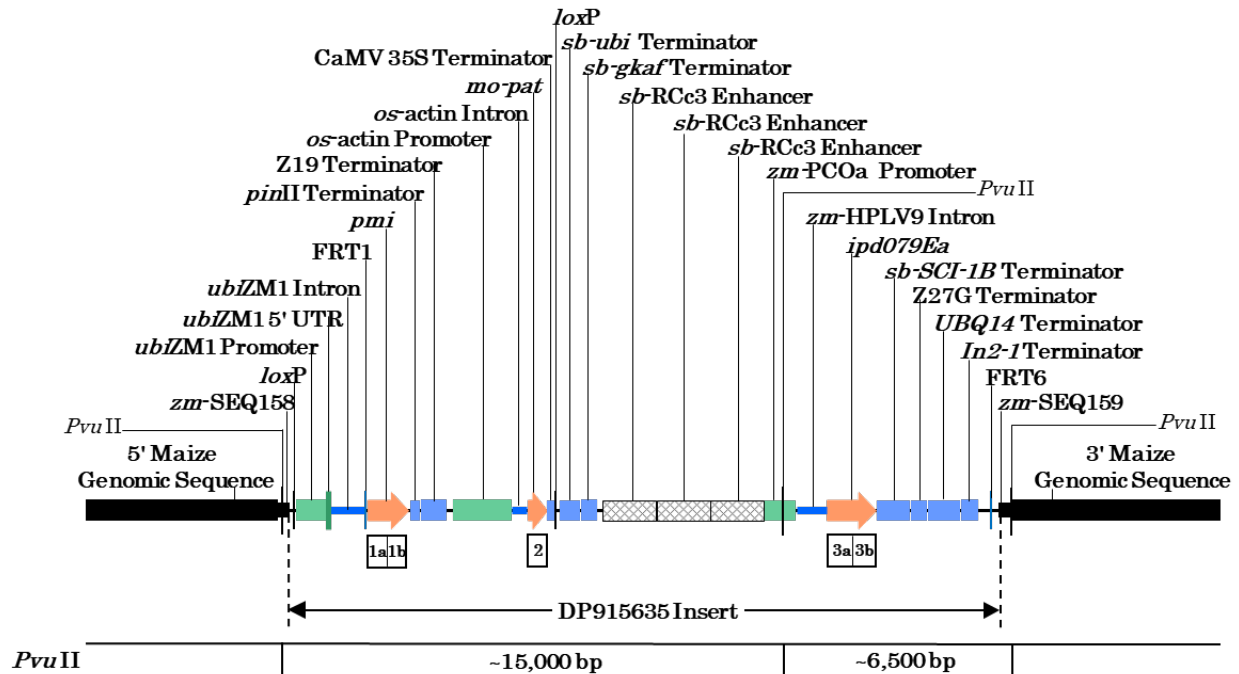


**Figure 18. Map of PHP83175 T-DNA for Southern Analysis**

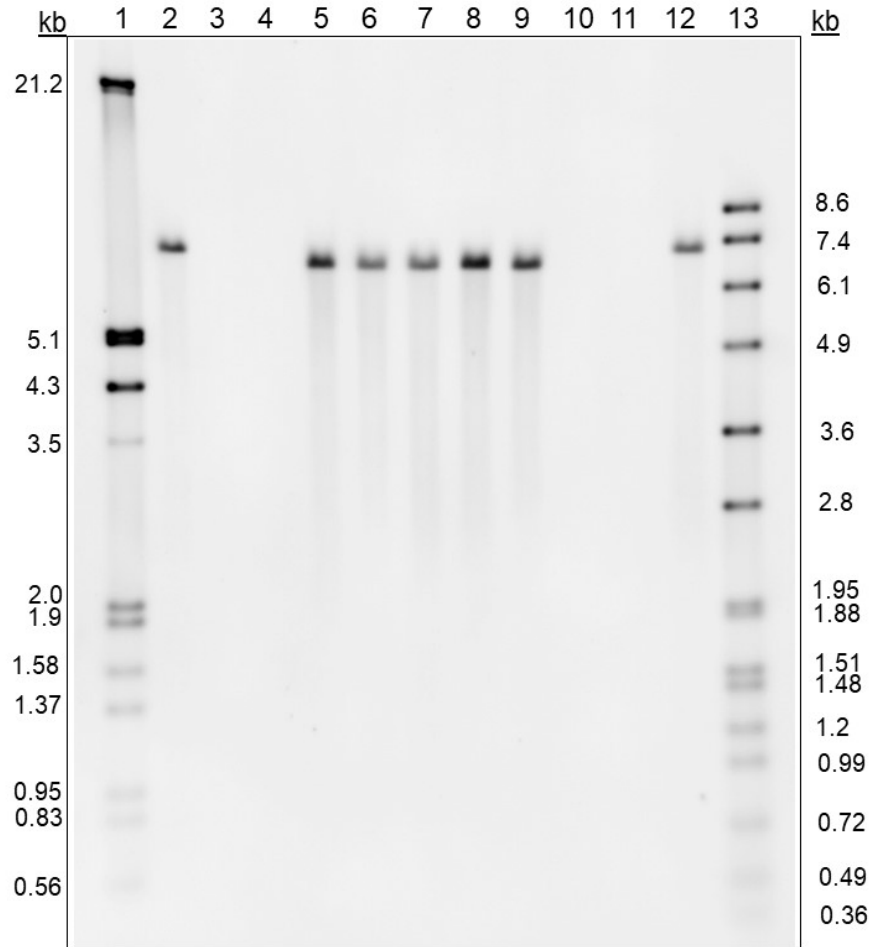
Map of the PHP83175 T-DNA indicating the Pvu II restriction enzyme sites, the *pmi*, *mo-pat*, and *ipd079Ea* gene cassettes located between the FRT1 and FRT6 sites intended for insertion into the landing pad, and the *zm-wus2*, *zm-odp2*, and *mo-Flp* gene cassettes outside the FRT1 and FRT6 sites not intended for insertion into the landing pad. The size of the PHP83175 T-DNA region is 32,069 bp. The portion of the T-DNA between the FRT1 and FRT6 sites is incorporated in the final DNA insertion (Figure 19). The locations of the Southern blot probes are shown by the boxes below the map.



Probe	Probe Name
1a & 1b	<i>pmi</i>
2	<i>mo-pat</i>
3a & 3b	<i>ipd079Ea</i>

**Figure 19. Map of Insertion in DP915635 Maize for Southern Analysis**

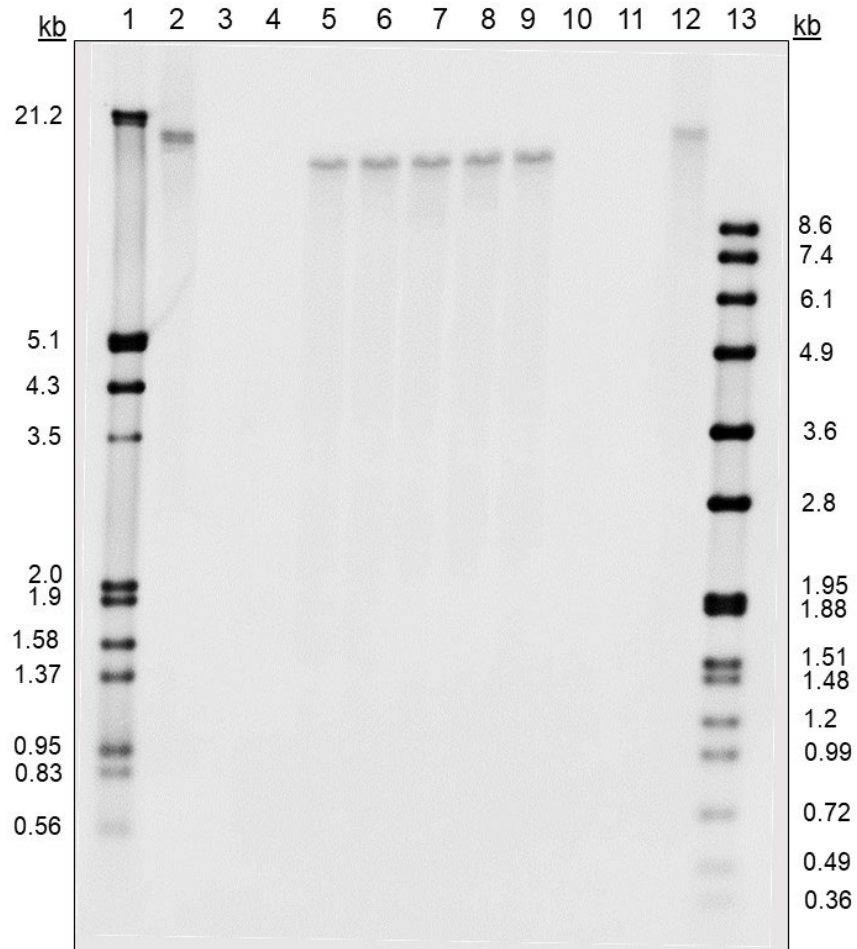
Map of the inserted DNA in the DP915635 maize genome following SSI integration of the gene cassettes from the PHP83175 T-DNA (Figure 18). The DP915635 maize insert comprises sequences from two sources: the parts of the landing pad outside the FRT1 and FRT6 sites and the sequences from the PHP83175 T-DNA within the FRT1 and FRT6 sites (with *pmi*, *mo-pat*, and *ipd079Ea* gene cassettes). The flanking maize genomic DNA is represented by the horizontal black rectangular bars. The locations of the Southern blot probes are shown by the boxes below the map. The locations of restriction enzyme sites in the flanking maize genomic DNA are not to scale. The Pvu II restriction sites are indicated with the sizes of observed fragments on Southern blots shown below the map in base pairs (bp). The locations of restriction enzyme sites in the flanking maize genomic DNA are not to scale.



Lane	Sample	Lane	Sample
1	DIG-labeled DNA marker III	8	DP915635 maize T4 generation
2	1 copy of PHP83175 + PHR03 control maize	9	DP915635 maize T5 generation
3	PHR03 control maize	10	Blank
4	Blank	11	PHR03 control maize
5	DP915635 maize T1 generation	12	1 copy of PHP83175 + PHR03 control maize
6	DP915635 maize T2 generation	13	DIG-labeled DNA marker VII
7	DP915635 maize T3 generation		

**Figure 20. Southern Blot Analysis of DP915635 Maize; *Pvu* II Digest with *ipd079Ea* Probe**

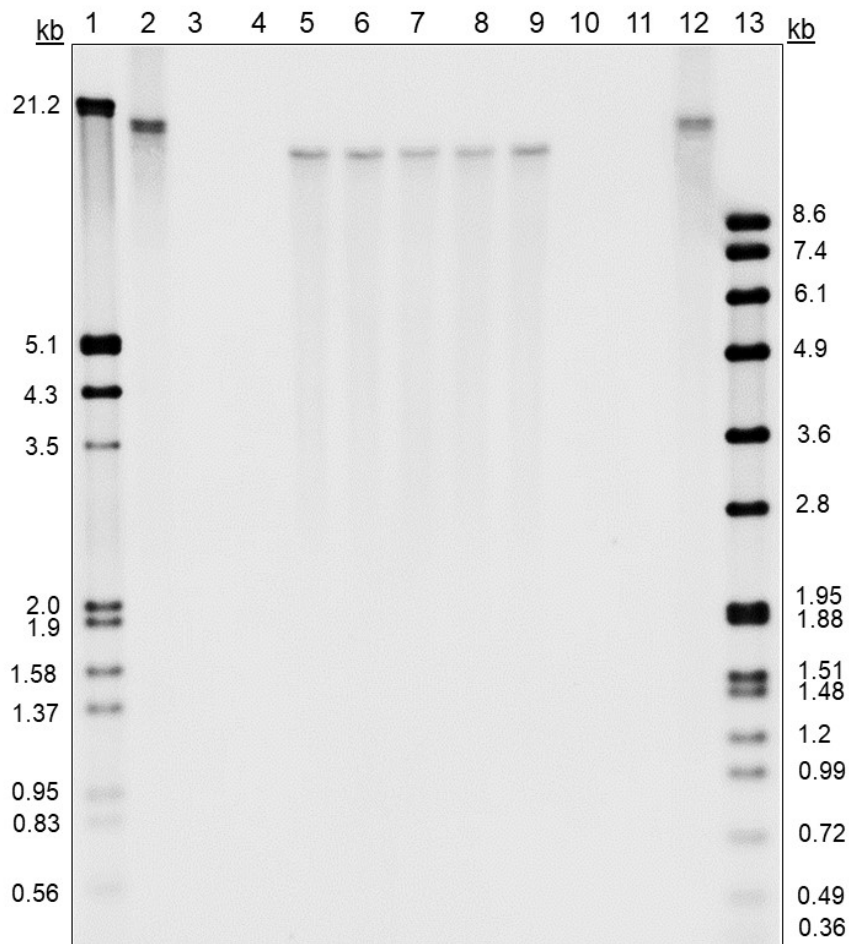
Genomic DNA isolated from leaf tissues of DP915635 maize from T1, T2, T3, T4, and T5 generations, and PHR03 control maize plants, was digested with *Pvu* II and hybridized to the *ipd079Ea* probe. Approximately 10 µg of genomic DNA was digested and loaded per lane. Positive control lanes include PHP83175 plasmid DNA at approximately one gene copy number and 10 µg of control maize DNA. Sizes of the DIG-labeled DNA Molecular Weight Marker III and VII are indicated adjacent to the blot image in kilobases (kb).



Lane	Sample	Lane	Sample
1	DIG-labeled DNA marker III	8	DP915635 maize T4 generation
2	1 copy of PHP83175 + PHR03 control maize	9	DP915635 maize T5 generation
3	PHR03 control maize	10	Blank
4	Blank	11	PHR03 control maize
5	DP915635 maize T1 generation	12	1 copy of PHP83175 + PHR03 control maize
6	DP915635 maize T2 generation	13	DIG-labeled DNA marker VII
7	DP915635 maize T3 generation		

**Figure 21. Southern Blot Analysis of DP915635 Maize; *Pvu* II Digest with *mo-pat* Probe**

Genomic DNA isolated from leaf tissues of DP915635 maize from T1, T2, T3, T4, and T5 generations, and PHR03 control maize plants, was digested with *Pvu* II and hybridized to the *mo-pat* probe. Approximately 10 µg of genomic DNA was digested and loaded per lane. Positive control lanes include PHP83175 plasmid DNA at approximately one gene copy number and 10 µg of control maize DNA. Sizes of the DIG-labeled DNA Molecular Weight Marker III and VII are indicated adjacent to the blot image in kilobases (kb).



Lane	Sample	Lane	Sample
1	DIG-labeled DNA marker III	8	DP915635 maize T4 generation
2	1 copy of PHP83175 + PHR03 control maize	9	DP915635 maize T5 generation
3	PHR03 control maize	10	Blank
4	Blank	11	PHR03 control maize
5	DP915635 maize T1 generation	12	1 copy of PHP83175 + PHR03 control maize
6	DP915635 maize T2 generation	13	DIG-labeled DNA marker VII
7	DP915635 maize T3 generation		

**Figure 22. Southern Blot Analysis of DP915635 Maize; *Pvu* II Digest with *pmi* Probe**

Genomic DNA isolated from leaf tissues of DP915635 maize from T1, T2, T3, T4, and T5 generations, and PHR03 control maize plants, was digested with *Pvu* II and hybridized to the *pmi* probe. Approximately 10 µg of genomic DNA was digested and loaded per lane. Positive control lanes include PHP83175 plasmid DNA at approximately one gene copy number and 10 µg of control maize DNA. Sizes of the DIG-labeled DNA Molecular Weight Marker III and VII are indicated adjacent to the blot image in kilobases (kb).

### Multi-Generation Segregation Analysis ([PHI-2019-127 study](#))

Segregation analysis was performed on five generations of DP915635 maize to confirm the Mendelian inheritance pattern of the inserted DNA during the breeding process. The observed inheritance pattern predicts the segregation of these genes and/or traits as a single unit and as a single genetic locus throughout the commercial breeding process. A total of 100 maize plants from each generation of DP915635 maize (F1, T2, T3, T4, and T5 generations) were analyzed using genotypic and phenotypic analyses. The selected maize generations represent a range of different crossing, backcrossing, and selfing points in a typical maize breeding program.

The genotypic analyses utilized a quantitative polymerase chain reaction (qPCR) assay to confirm the presence or absence of the DP915635 insertion and the *ipd079Ea*, *mo-pat*, and *pmi* genes in DP915635 maize leaf samples. The phenotypic analysis utilized a visual herbicide injury evaluation to confirm the presence or absence of tolerance to glufosinate-ammonium for each individual plant. The individual results for each plant were compared to the qPCR results to verify co-segregation of genotype with phenotype.

A chi-square statistical test (at the 0.05 significance level) was conducted for the qPCR results of the segregating generations of DP915635 maize to compare the observed segregation ratios to the expected segregation ratios of 1:1 for the F1 generation, and 3:1 for the T2 and T3 generations. A chi-square test was not performed for the T4 and T5 generations of DP915635 maize as all plants were identified as positive (i.e., not segregating) as expected for a homozygous generation.

A summary of segregation results for DP915635 maize is provided in Table 11. For each individual plant, all genotypic results (i.e., PCR results) matched the corresponding phenotypic result (i.e., herbicide tolerance result). No statistically significant differences were found between the observed and expected segregation ratios for each of the three segregating generations of DP915635 maize.

The results of the multi-generation segregation analysis demonstrated that the inserted DNA in DP915635 maize segregated together and in accordance with Mendelian rules of inheritance for a single genetic locus, indicating stable integration of the insert into the maize genome and a stable genetic inheritance pattern across breeding generations.

Additional details regarding analytical methods for the multi-generation segregation analysis are provided in Appendix C.

Detailed methods and results are provided in the [PHI-2019-127 study](#).

**Table 11. Summary of Genotypic and Phenotypic Segregation Results for Five Generations of DP915635 Maize**

Generation	Expected Segregation Ratio	Observed Segregation <sup>a</sup>			Statistical Analysis	
	(Positive:Negative)	Positive	Negative	Total	Chi-Square <sup>b</sup>	P-Value
F1	1:1	47	53	100	0.36	0.5485
T2	3:1	79	21	100	0.85	0.3556
T3	3:1	74	26	100	0.05	0.8174
T4	Homozygous	100	0	100	--	--
T5	Homozygous	100	0	100	--	--

<sup>a</sup> Genotypic analyses were conducted for each plant to confirm the presence or absence of event DP-915635-4 and the *ipd079Ea*, *mo-pat*, and *pmi* genes. Phenotypic analysis was conducted for each plant to confirm the presence or absence of a glufosinate-tolerant phenotype. All genotypic results matched the corresponding phenotypic result for each plant analyzed.

<sup>b</sup> Degrees of freedom = 1. A chi-square value greater than 3.84 (P-value less than 0.05) would indicate a significant difference.

## B. CHARACTERISATION AND SAFETY ASSESSMENT OF NEW SUBSTANCES

### B.1 CHARACTERISATION AND SAFETY ASSESSMENT OF NEW SUBSTANCES

There are no new substances associated with DP915635 maize other than the three proteins (see Section B.2 below).

### B.2 NEW PROTEINS

#### IPD079Ea protein

##### Amino Acid Sequence of the IPD079Ea Protein

The deduced amino acid sequence from the translation of the *ipd079Ea* gene is 479 amino acids in length and has a molecular weight of approximately 52 kDa (Figure 23).

```
1   MAEPNKGKAP  AMKNVAKPST  KRLIPSSIAA  SSQTSANALT  EPLPGSDAIG
51  QSYDAFGFFA  NPRSIMKELF  EFSPQEEIVV  EGNTWLLSSD  FVYTAIRDTE
101 TSTVSRRTKD  DYSKELAVKV  KLSGSYGYFS  ASVESDFSQS  ISDATDTTYT
151 SVRTHVNKWR  LSLKDDVGAL  RSKLLPGVKQ  ALATMDATQL  FDTFGTHYVS
201 EVLVGGRADY  VATTKTSAFS  SSTSISVAAE  ASFQSIAGGE  VSPEKVLAE
251 MLRENSSTRL  YALGGSALPN  ITDPATYNAW  LESIDTIPVF  CGFTQNSLKS
301 ISELADSAQR  RDALAKASQS  YIPSYVTRPA  VVGLEVIISD  SNSESPYPGY
351 TRIDYDLNRN  AGGKYVFLCY  KQKNISVGGD  ADAITDVLVV  YGNDRNPSVP
401 SGYTKIDKDL  NSGAGGKYIY  FCYSKDKRKQ  EEGLPIRGLR  VVGPHPTSVA
    PYGFSKIDID  LNMGAGGDFI  YLCKSRHLE*
```

**Figure 23. Deduced Amino Acid Sequence of the IPD079Ea Protein**

The deduced amino acid sequence from the translation of the *ipd079Ea* gene from plasmid PHP83175. The asterisk (\*) indicates the translational stop codon. The full-length protein is 479 amino acids in length and has a molecular weight of approximately 52 kDa.

##### Function and Activity of the IPD079Ea Protein

The IPD079Ea protein, encoded by the *ipd079Ea* gene, confers control of certain coleopteran pests when expressed in plants by causing disruption of the midgut epithelium. The *ipd079Ea* gene was identified and cloned from *Ophioglossum pendulum* L.

##### Characterization of IPD079Ea Protein Derived from DP915635 Maize and Microbial Systems

The IPD079Ea protein was purified from DP915635 maize leaf tissue using immuno-affinity chromatography. The maize derived IPD079Ea protein was characterized in the [PHI-2020-146 study](#).

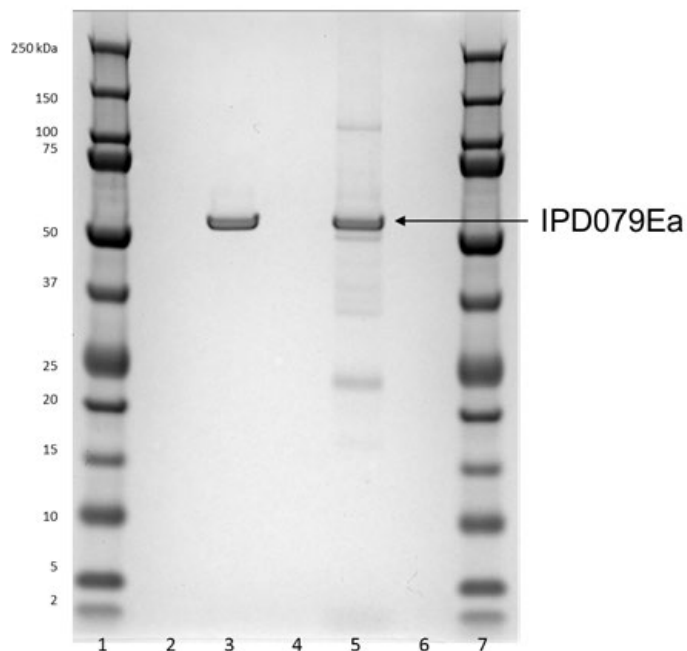
In order to have sufficient amounts of purified IPD079Ea protein for the multiple studies required to assess its safety, the IPD079Ea protein was expressed in an *Escherichia coli* protein expression system as a fusion protein with an N-terminal histidine tag. The microbially derived protein was purified using nickel affinity chromatography, and the histidine tag was cleaved with thrombin. Thrombin was removed using heparin Sepharose column chromatography. The microbially derived protein was characterized in the [PHI-2019-187 study](#).

The biochemical characteristics of the microbially derived IPD079Ea protein and the DP915635 maize-expressed IPD079Ea protein were characterized using sodium dodecyl sulfate polyacrylamide gel electrophoresis (SDS-PAGE), western blot, glycosylation, mass spectrometry, and N-terminal amino acid sequence analyses. For the microbially derived protein, the bioactivity was verified by insect bioassays. The results demonstrated that the IPD079Ea protein derived from DP915635 maize is of the expected molecular weight, immunoreactivity, lack of glycosylation, and amino acid sequence. The microbially derived IPD079Ea protein was demonstrated to be equivalent to the DP915635 maize-derived IPD079Ea protein for use in safety testing.

#### *SDS-PAGE Analysis*

Samples of the IPD079Ea protein derived from DP915635 maize and microbially derived IPD079Ea protein purified from a microbial expression system were analyzed by SDS-PAGE (cite study reports). As expected, the IPD079Ea proteins migrated as a band consistent with the expected molecular weight of approximately 52 kDa, as shown in Figure 24.

Additional details regarding SDS-PAGE analytical methods are provided in Appendix E.



Lane	Sample Identification
1	Pre-stained Protein Molecular Weight Marker <sup>a</sup>
2	1X LDS/DTT Sample Buffer Blank
3	Microbially Derived IPD079Ea Protein <sup>b</sup>
4	1X LDS/DTT Sample Buffer Blank
5	DP915635 Maize-Derived IPD079Ea Protein <sup>c</sup>
6	1X LDS/DTT Sample Buffer Blank
7	Pre-stained Protein Molecular Weight Marker <sup>a</sup>

Note: kilodalton (kDa).

<sup>a</sup> Molecular weight markers were included to provide a visual estimate that migration was within the expected range of the predicted molecular weight.

<sup>b</sup> Protein Lot PCF-0049; diluted to 1 µg per lane.

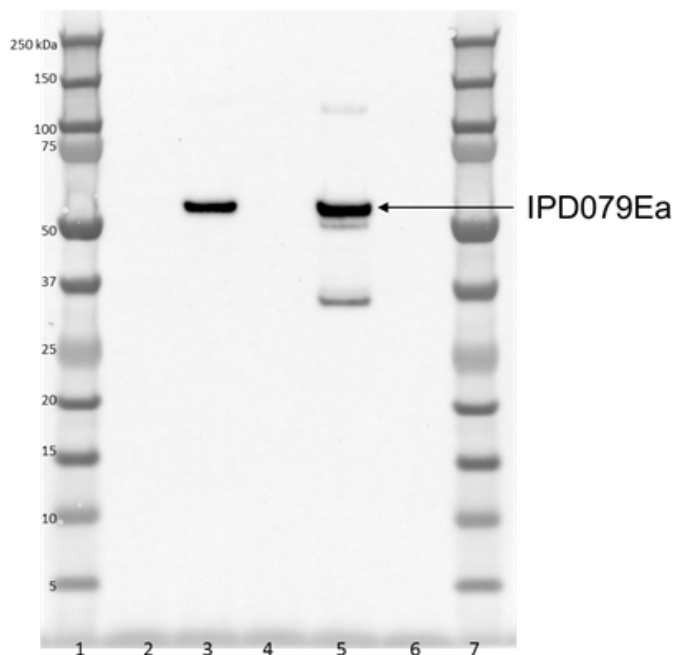
<sup>c</sup> After 1:2 dilution.

**Figure 24. SDS-PAGE Analysis of IPD079Ea Protein**

#### *Western Blot Analysis*

Samples of the IPD079Ea protein derived from DP915635 maize and the IPD079Ea protein purified from a microbial expression system were analyzed by Western blot (cite study reports). As expected, all IPD079Ea protein samples were immunoreactive to an IPD079Ea monoclonal antibody and visible as a predominant band consistent with the expected molecular weight of approximately 52 kDa, as shown in Figure 25.

Additional details regarding Western blot analytical methods are provided in Appendix E.



Lane	Sample Identification
1	Pre-stained Protein Molecular Weight Marker <sup>a</sup>
2	1X LDS/DTT Sample Buffer Blank
3	Microbially Derived IPD079Ea Protein <sup>b</sup>
4	1X LDS/DTT Sample Buffer Blank
5	DP915635 Maize-Derived IPD079Ea Protein <sup>c</sup>
6	1X LDS/DTT Sample Buffer Blank
7	Pre-stained Protein Molecular Weight Marker <sup>a</sup>

Note: kilodalton (kDa).

<sup>a</sup> Molecular weight markers were included to provide a visual estimate that migration was within the expected range of the predicted molecular weight.

<sup>b</sup> Protein Lot PCF-0049; Diluted to 10 ng per lane.

<sup>c</sup> After 1:100 dilution.

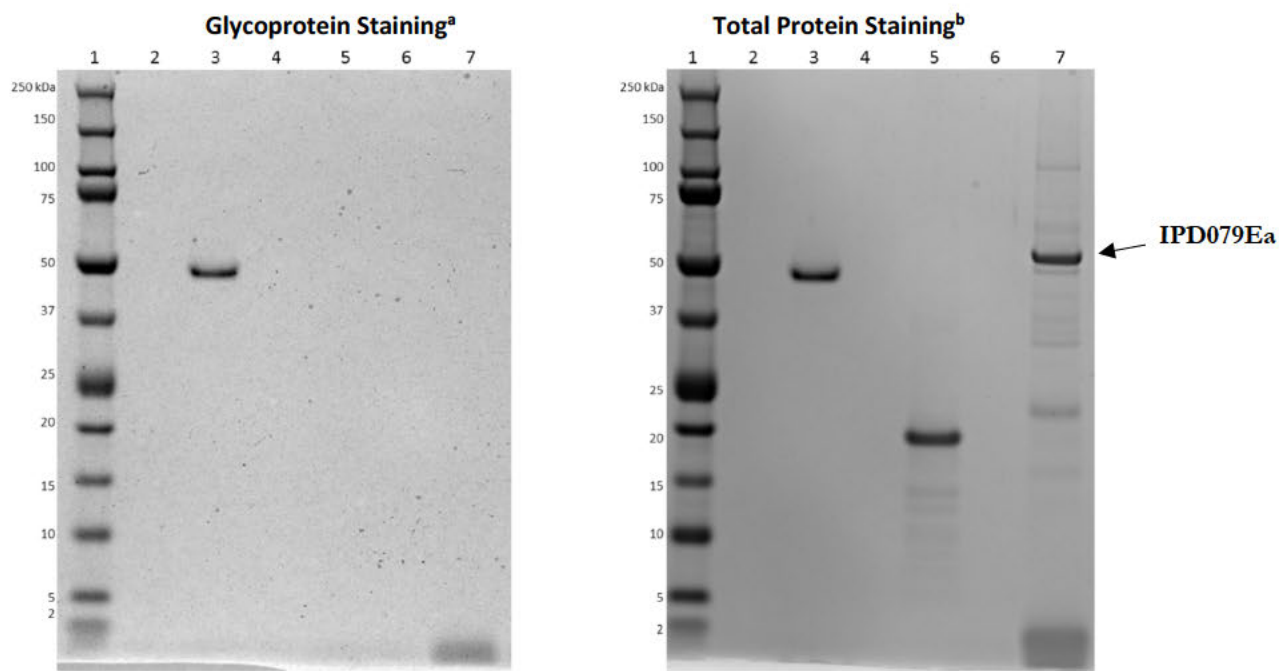
**Figure 25. Western Blot Analysis of IPD079Ea Protein**

### *Protein Glycosylation Analysis*

Samples of the IPD079Ea protein purified from DP915635 maize leaf tissue and the IPD079Ea protein purified from a microbial expression system were analyzed by SDS-PAGE (cite study reports). Each gel also included a positive control (horseradish peroxidase) and negative control (soybean trypsin inhibitor). The gels were then stained using a Pierce Glycoprotein Staining Kit to visualize any glycoproteins. The gels were imaged and then stained with GelCode Blue stain reagent to visualize all protein bands.

Glycosylation was not detected for the IPD079Ea proteins (Figure 26 and Figure 27). The horseradish peroxidase positive control was clearly visible as a stained band. The soybean trypsin inhibitor negative control was not stained by the glycoprotein stain.

Additional details regarding glycosylation analytical methods are provided in Appendix E.



Lane	Sample Identification
1	Pre-stained Protein Molecular Weight Marker <sup>c</sup>
2	1X LDS/DTT Sample Buffer Blank
3	Horseradish Peroxidase (1.0 µg)
4	1X LDS/DTT Sample Buffer Blank
5	Soybean Trypsin Inhibitor (1.0 µg)
6	1X LDS/DTT Sample Buffer Blank
7	DP915635 Maize-Derived IPD079Ea Protein <sup>d</sup>

Note: kilodalton (kDa) and microgram (µg).

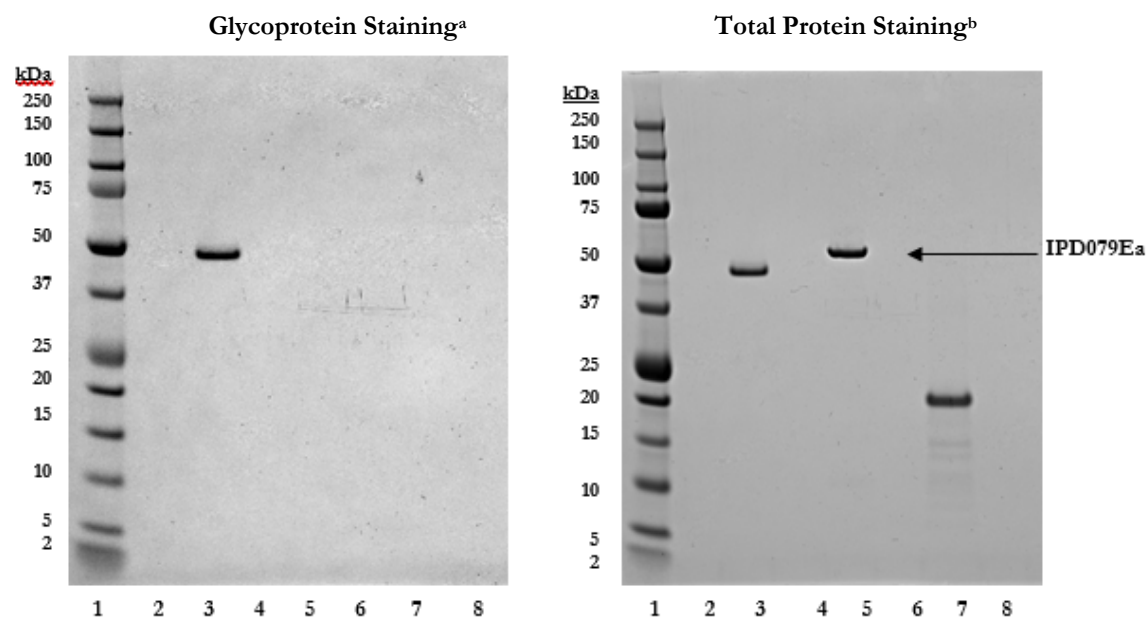
<sup>a</sup> Gel was stained with glycoprotein staining reagent.

<sup>b</sup> Gel was stained with glycoprotein staining reagent followed by staining with Coomassie Blue Reagent for total proteins.

<sup>c</sup> Molecular weight markers were included to provide a visual estimate that migration was within the expected range of the predicted molecular weight.

<sup>d</sup> After 1:2 dilution.

**Figure 26. Glycosylation Analysis of DP915635 Maize-Derived IPD079Ea Protein**



Lane	Sample Identification
1	Pre-stained Protein Molecular Weight Marker <sup>c</sup>
2	1X LDS Sample Buffer Blank
3	Positive Control: Horseradish Peroxidase (1 µg)
4	1X LDS Sample Buffer Blank
5	Microbially Derived IPD079Ea Protein (1 µg)
6	1X LDS Sample Buffer Blank
7	Negative Control: Soybean Trypsin Inhibitor (1 µg)
8	1X LDS Sample Buffer Blank

Note: kilodalton (kDa), microgram (µg).

<sup>a</sup> Gel was stained with glycoprotein staining reagent.

<sup>b</sup> Gel was stained with glycoprotein staining reagent followed by staining with Coomassie Blue Reagent for total proteins.

<sup>c</sup> Molecular weight markers were included to provide a visual estimate that migration was within the expected range of the predicted molecular weight.

**Figure 27. Glycosylation Analysis of Microbially Derived IPD079Ea Protein**

#### *Mass Spectrometry Peptide Mapping Analysis*

Samples of the IPD079Ea protein purified from DP915635 maize leaf tissue and the IPD079Ea protein purified from a microbial expression system were analyzed by SDS-PAGE. Protein bands were stained with Coomassie stain reagent, and bands containing IPD079Ea protein were excised for each sample.

The excised IPD079Ea protein bands were digested with trypsin or chymotrypsin. Digested samples were analyzed with ultra-performance liquid chromatography-mass spectrometry (LC-MS). The resulting MS data was used to search and match the peptides from the expected IPD079Ea protein sequence, and the combined sequence coverage was calculated. The identified tryptic and chymotryptic peptides for DP915635 maize-derived IPD079Ea protein are shown in Table 12 and Table 13, respectively. The combined sequence coverage was 94.8% (453/478) of the expected amino acid sequence of the DP915635 maize derived IPD079Ea protein (Table 14 and Figure 28). The identified tryptic and chymotryptic peptides for microbially derived IPD079Ea protein are shown in Table 15 and Table 16, respectively. The combined sequence coverage was 96% (463/481) of the expected amino acid sequence of the microbially derived IPD079Ea protein (Table 17 and Figure 29).

Additional details regarding peptide mapping analytical methods are provided in Appendix E.

**Table 12. Tryptic Peptides of DP915635 Maize-Derived IPD079Ea Protein Identified Using LC-MS Analysis**

Matched Residue Position	Experimental Mass <sup>a</sup>	Theoretical Mass <sup>b</sup>	Identified Peptide Sequence
1–12	1211.5919	1211.5968	AEPNKGKGGAPAMK <sup>c</sup>
6–12	630.3154	630.3159	GGAPAMK
13–20	843.4784	843.4814	NVAKPSTK
22–62	4168.0274	4168.0389	LIPSSIAASSQTSANALTEPLPGSDAIGQSYDAFGFFANPR
97–105	994.4521	994.4567	DTETSTVSR
107–113	855.3957	855.3974	TKDDYSK
121–152	3427.5155	3427.5216	LSGSYGYFSASVESDFSQSISDATDTTYTSVR
160–170	1185.6693	1185.6717	LSLKDDVGALR
164–170	744.3755	744.3766	DDVGALR
171–178	840.5409	840.5433	SKLLPGVK
173–178	625.4156	625.4163	LLPGVK
179–206	3042.4638	3042.4757	QALATMDATQLFDTFGTHYVSEVLVGG <sup>d</sup>
207–214	867.4314	867.4338	ADYVATTK
215–245	3018.4198	3018.4306	TSAFSSSTSISVAAEASFQSIAGGEVSPESK
246–252	846.46	846.4633	VLAEMLR <sup>d</sup>
299–309	1175.5744	1175.5782	SISELADSAQR
352–358	907.4372	907.4399	IDYDLNR
364–370	991.481	991.4837	YVFLCYK
373–394	2262.1029	2262.1128	NISVGGDADAITDVLVVGNDR
373–404	3292.6089	3292.6212	NISVGGDADAITDVLVVGNDRNPSPVPSGYTK
395–404	1048.5141	1048.5189	NPSVPSGYTK
417–424	1142.5053	1142.5107	YIYFCYSK
428–436	1068.5913	1068.5927	KQEEGLPIR
429–436	940.4952	940.4978	QEEGLPIR
440–455	1641.8469	1641.8515	VVGPHPTSVAPYGF <sup>c</sup> SK
456–473	2013.9468	2013.954	IDIDLNMGAGGDFIYLCK

<sup>a</sup> The experimental mass is the uncharged mass calculated from the mass to charge ratio of the observed ion.

<sup>b</sup> The theoretical mass is the *in silico* generated mass that matches closest to the experimental mass.

<sup>c</sup> The N-terminus was acetylated.

<sup>d</sup> This peptide was modified by methionine oxidation (Oxidation-M).

**Table 13. Chymotryptic Peptides of DP915635 Maize-Derived IPD079Ea Protein Identified Using LC-MS Analysis**

Matched Residue Position	Experimental Mass <sup>a</sup>	Theoretical Mass <sup>b</sup>	Identified Peptide Sequence
39–52	1433.6624	1433.6674	TEPLPGSDAIGQSY
59–69	1304.6876	1304.6911	ANPRSIMKELF
69–84	1909.8641	1909.8734	FEFSPQEEIVVEGNTW
70–84	1762.7991	1762.805	EFSPQEEIVVEGNTW
72–84	1486.6892	1486.694	SPQEEIVVEGNTW
116–121	656.4576	656.4585	AVKVKL
129–148	2109.8797	2109.8862	SASVESDFSQISDATDTTY
137–148	1287.542	1287.5467	SQSISDATDTTY
159–169	1185.6662	1185.6717	RLSLKDDVGAL
161–169	916.4834	916.4866	SLKDDVGAL
163–169	716.3689	716.3705	KDDVGAL
170–181	1308.8216	1308.8241	RSKLLPGVKQAL
174–181	824.5102	824.512	LPGVKQAL
182–190	996.4547	996.4586	ATMDATQLF
182–193	1359.5953	1359.6017	ATMDATQLFDTF
191–197	839.3428	839.345	DTFGTHY
194–202	1003.4939	1003.4975	GTHYVSEVL
198–209	1263.6402	1263.6459	VSEVLVGGRADY
203–209	736.3487	736.3504	VGGRADY
210–218	924.489	924.4917	VATTKTSAF
219–232	1342.6212	1342.6252	SSSTSISVAEASF
233–247	1499.7753	1499.7831	QSIAGGEVSPESKVL
233–251	1943.975	1943.9874	QSIAGGEVSPESKVLAEML
248–259	1405.6956	1405.6983	AEMLRENSSTRL
248–260	1568.7571	1568.7616	AEMLRENSSTRLY
260–276	1722.8428	1722.8465	YALGGSALPNITDPATY
261–276	1559.7778	1559.7831	ALGGSALPNITDPATY
263–276	1375.6571	1375.662	GGSALPNITDPATY
280–289	1132.5961	1132.6016	LESIDTIPVF
290–297	925.3932	925.3964	CGFTQNSL
293–303	1218.6402	1218.6456	TQNSLKSISEL
298–303	675.3789	675.3803	KSISEL
298–313	1758.9203	1758.9224	KSISELADSAQRRDAL
304–320	1836.9048	1836.9078	ADSAQRRDALAKASQSY
314–320	753.3634	753.3657	AKASQSY
321–333	1370.7861	1370.7922	IPSYVTRPAVVGL
325–333	910.5558	910.56	VTRPAVVGL
325–347	2428.237	2428.2486	VTRPAVVGLEVIISDSNSESPPY
325–349	2648.3191	2648.3334	VTRPAVVGLEVIISDSNSESPPYGY
334–349	1755.777	1755.7839	EVIISDSNSESPPYGY
348–354	886.4158	886.4185	GYTRIDY
350–354	666.333	666.3337	TRIDY
355–364	1106.5453	1106.5468	DLNRNAGGKY
357–364	878.4322	878.4358	NRNAGGKY
370–387	1842.9646	1842.9687	KQKNISVGGDADAITDVL
370–390	2204.1632	2204.1689	KQKNISVGGDADAITDVLVY

Matched Residue Position	Experimental Mass <sup>a</sup>	Theoretical Mass <sup>b</sup>	Identified Peptide Sequence
391–402	1261.5631	1261.5687	GNDRNPSVPSGY
403–417	1565.8008	1565.8049	TKIDKDLNSGAGGKY
423–438	1853.0445	1853.0482	SKDKRKQEEGLPIRGL
439–451	1378.7335	1378.7357	RVVGPHTSVAPY
472–478	928.4521	928.4549	CKSRHLE

<sup>a</sup> The experimental mass is the uncharged mass calculated from the mass to charge ratio of the observed ion.

<sup>b</sup> The theoretical mass is the *in silico* generated mass that matches closest to the experimental mass.

**Table 14. Combined Sequence Coverage of Identified Tryptic and Chymotryptic Peptides of DP915635 Maize-Derived IPD079Ea Protein Using LC-MS Analysis**

Protease	% Coverage	Combined % Coverage
Trypsin	64	94.8
Chymotrypsin	73	

**1** AEPNKGGA MKNVAKPSTK RLIPSSIAAS SQTANALTE PLPGSDAIGQ  
**51** SYDAFGFFAN PRSIMKELFE FSPQEEIVVE GNTWLLSSDF VYTAIRDTE  
**101** STVSRRTKDD YSKELAVKVK LSGSYGYFSA SVESDFSQSI SDATDTTYTS  
**151** VRTHVKNKWR LSLKDDVGLR SKLLPGVKQA LATMDATQLF DTFGTHYVSE  
**201** VLVGGRADYV ATTKTSAFSS STSISVAAEA SFQSIAGGEV SPESKVLAE  
**251** LRENSSTRLY ALGGSALPNI TDPATYN<sup>AWL</sup> ESIDTIPVFC GFTQNSLKSI  
**301** SELADSAQRR DALAKASQSY IPSYVTRPAV VGLEVIISDS NSESPPYGYT  
**351** RIDYDLNRNA GGKYVFLCYK QKNISVGGDA DAITDVLVY GNDRNPSVPS  
**401** GYTKIDKDLN SGAGGKYIYF CYSKDKRKQE EGLPIRGLRV VGPHTSVAP  
**451** YGFSKIDIDL NMGAGGDFIY LCKSRHLE

Gray shading	Gray-shaded type indicates DP915635 maize-derived IPD079Ea peptides identified using LC-MS analysis.
Amino acid residue abbreviations	alanine (A), aspartic acid (D), glutamic acid (E), phenylalanine (F), glycine (G), histidine (H), isoleucine (I), lysine (K), leucine (L), methionine (M), asparagine (N), proline (P), glutamine (Q), arginine (R), serine (S), threonine (T), tryptophan (W), tyrosine (Y), and valine (V).

**Figure 28. Amino Acid Sequence of DP915635 Maize-Derived IPD079Ea Protein Indicating Tryptic and Chymotryptic Peptides Identified Using LC-MS Analysis**

**Table 15. Tryptic Peptides of Microbially Derived IPD079Ea Protein Identified Using LC-MS Analysis**

Matched Residue Position	Experimental Mass <sup>a</sup>	Theoretical Mass <sup>b</sup>	Identified Peptide Sequence
1–8	832.3708	832.3749	GSMAEPNK
1–15	1444.6759	1444.6802	GSMAEPNKGAPAMK
9–15	630.3147	630.3159	GGAPAMK
16–23	843.4783	843.4814	NVAKPSTK
24–65	4324.1157	4324.14	RLIPSSIAASSQTSANALTEPLPGSDAIGQSYDAFGFFANPR
25–65	4168.018	4168.039	LIPSSIAASSQTSANALTEPLPGSDAIGQSYDAFGFFANPR
100–108	994.4514	994.4567	DTETSTVSR
110–116	855.3936	855.3974	TKDDYSK
112–121	1166.5757	1166.5819	DDYSKELAVK
124–155	3427.5015	3427.5216	LSGSYGYFSASVESDFSQSISDATDTTYTSVR
163–173	1185.6644	1185.6717	LSLKDDVGALR
167–173	744.3748	744.3766	DDVGALR
174–181	840.5401	840.5433	SKLLPGVK
182–209	3042.4575	3042.4757	QALATMDATQLFDTFGTHYVSEVLVGG <sup>c</sup>
210–217	867.4312	867.4338	ADYVATTK
218–248	3018.4128	3018.4306	TSAFSSSTSISVAEASFQSIAGGEVSPESK
249–255	830.4652	830.4684	VLAEMLR
302–312	1175.5713	1175.5782	SISELADSAQR
302–313	1331.6774	1331.6793	SISELADSAQRR
319–354	3901.9098	3901.9374	ASQSYIPSYVTRPAVVGLEVIISDSNSESPPYGYTR
355–361	907.4359	907.4399	IDYDLNR
367–373	991.4788	991.4837	YVFLCYK
376–397	2262.098	2262.1128	NISVGGDADAITDVLVYVGNDR
376–407	3292.5985	3292.6212	NISVGGDADAITDVLVYVGNDRNPSVPSGYTK
398–407	1048.5139	1048.5189	NPSVPSGYTK
408–419	1173.5976	1173.599	IDKDLNSGAGGK
411–419	817.3895	817.393	DLNSGAGGK
420–427	1142.5053	1142.5107	YIYFCYSK
431–439	1068.5869	1068.5927	KQEGLPIR
432–439	940.4941	940.4978	QEGLPIR
443–458	1641.8439	1641.8515	VVGPHTSVAPYGFASK
459–476	2013.9396	2013.954	IDIDLNMGAGGDFIYLCK

Note: A (alanine), D (aspartic acid), E (glutamic acid), F (phenylalanine), G (glycine), H (histidine), I (isoleucine), K (lysine), L (leucine), M (methionine), N (asparagine), P (proline), Q (glutamine), R (arginine), S (serine), T (threonine), W (tryptophan), Y (tyrosine), and V (valine).

<sup>a</sup> The experimental mass is the uncharged mass calculated from the mass to charge ratio of the observed ion.

<sup>b</sup> The theoretical mass is the *in silico* generated mass that matches closest to the experimental mass.

<sup>c</sup> This peptide was modified by methionine oxidation (Oxidation-M).

**Table 16. Chymotryptic Peptides of Microbially Derived IPD079Ea Protein Identified Using LC-MS Analysis**

Matched Residue Position	Experimental Mass <sup>a</sup>	Theoretical Mass <sup>b</sup>	Identified Peptide Sequence
42–55	1433.6572	1433.6674	TEPLPGSDAIGQSY
62–72	1304.682	1304.6911	ANPRSIMKELF
73–87	1762.7896	1762.805	EFSPQEEIVVEGNTW
132–151	2109.8716	2109.8862	SASVESDFSQSISDATDTTY
140–151	1287.5385	1287.5467	SQSISDATDTTY
152–161	1226.6489	1226.652	TSVRTHVNKW
162–172	1185.6641	1185.6717	RLSLKDDVGAL
164–172	916.4816	916.4866	SLKDDVGAL
173–184	1308.82	1308.8241	RSKLLPGVKQAL
177–184	824.51	824.512	LPGVKQAL
185–193	996.4526	996.4586	ATMDATQLF
185–196	1359.5912	1359.6017	ATMDATQLFDTF
194–200	839.3419	839.345	DTFGTHY
194–205	1366.6314	1366.6405	DTFGTHYVSEVL
197–205	1003.4918	1003.4975	GTHYVSEVL
197–212	1721.8267	1721.8373	GTHYVSEVLVGGGRADY
201–212	1263.6363	1263.6459	VSEVLVGGGRADY
206–212	736.3485	736.3504	VGGGRADY
206–221	1642.8219	1642.8315	VGGGRADYVATTKTSAF
213–221	924.489	924.4917	VATTKTSAF
222–235	1342.6168	1342.6252	SSSTSISVAAEASF
222–250	2824.3766	2824.3978	SSSTSISVAAEASFQSIAGGEVSPESKVL
236–250	1499.7716	1499.7831	QSIAGGEVSPESKVL
236–254	1943.9673	1943.9874	QSIAGGEVSPESKVLAEML
251–262	1405.6922	1405.6983	AEMLRNSSTRL
251–263	1568.7532	1568.7616	AEMLRNSSTRLY
255–263	1124.5502	1124.5574	RENSSTRLY
263–279	1722.835	1722.8465	YALGGSALPNITDPATY
264–279	1559.7724	1559.7831	ALGGSALPNITDPATY
266–279	1375.6537	1375.662	GGSALPNITDPATY
283–292	1132.5955	1132.6016	LESIDTIPVF
283–295	1496.7102	1496.7221	LESIDTIPVFCGF
293–300	925.392	925.3964	CGFTQNSL
296–306	1218.6364	1218.6456	TQNSLKSISEL
296–316	2302.1751	2302.1877	TQNSLKSISELADSAQRRDAL
301–306	675.3783	675.3803	KSISEL
301–316	1758.9127	1758.9224	KSISELADSAQRRDAL
301–323	2494.2612	2494.2775	KSISELADSAQRRDALAKASQSY
307–323	1836.9043	1836.9078	ADSAQRRDALAKASQSY
317–323	753.3632	753.3657	AKASQSY
324–336	1370.7836	1370.7922	IPSYVTRPAVVGL
351–357	886.415	886.4185	GYTRIDY
353–367	1754.8644	1754.87	TRIDYDLNRNAGGKY
358–367	1106.5457	1106.5468	DLNRNAGGKY
358–369	1352.6802	1352.6837	DLNRNAGGKYVF
360–367	878.4325	878.4358	NRNAGGKY

Matched Residue Position	Experimental Mass <sup>a</sup>	Theoretical Mass <sup>b</sup>	Identified Peptide Sequence
371–393	2527.2475	2527.2628	CYKQKNISVGGDADAITDVLVVY
373–390	1842.9594	1842.9687	KQKNISVGGDADAITDVL
373–393	2204.1542	2204.1689	KQKNISVGGDADAITDVLVVY
394–405	1261.5589	1261.5687	GNDRNPSVPSGY
406–420	1565.7963	1565.8049	TKIDKDLNSGAGGKY
406–422	1841.9439	1841.9523	TKIDKDLNSGAGGKYIY
426–441	1853.0351	1853.0482	SKDKRKQEEGLPIRGL
442–454	1378.7315	1378.7357	RVVGPHTSVAPY
475–481	928.4499	928.4549	CKSRHLE

Note: A (alanine), D (aspartic acid), E (glutamic acid), F (phenylalanine), G (glycine), H (histidine), I (isoleucine), K (lysine), L (leucine), M (methionine), N (asparagine), P (proline), Q (glutamine), R (arginine), S (serine), T (threonine), W (tryptophan), Y (tyrosine), and V (valine).

<sup>a</sup> The experimental mass is the uncharged mass calculated from the mass to charge ratio of the observed ion.

<sup>b</sup> The theoretical mass is the *in silico* generated mass that matches closest to the experimental mass.

**Table 17. Combined Sequence Coverage of Identified Tryptic and Chymotryptic Peptides of Microbially Derived IPD079Ea Protein Using LC-MS Analysis**

Protease	% Coverage	Combined % Coverage
Trypsin	76	96
Chymotrypsin	72	

1 **GSMAEPNKGK** **APAMKNVAKP** **STKRLIPSSI** **AASSQTSANA** **LTEPLPGSDA**  
51 **IGQSYDAFGF** **FANPRSIMKE** **LFEFSPQEEI** **VVEGNTWLLS** **SDFVYTAIRD**  
101 **TETSTVSRRT** **KDDYSKELAV** **KVKLSGSYGY** **FSASVESDFS** **QSISDATDTT**  
151 **YTSVRTHVNK** **WRLSLKDDVG** **ALRSKLLPGV** **KQALATMDAT** **QLFDTFGTHY**  
201 **VSEVLVGGRA** **DYVATTKTSA** **FSSSTSISVA** **AEASFQSIAG** **GEVSPESKVL**  
251 **AEMLRENSST** **RLYALGGSAL** **PNITDPATYN** **AWLESIDTIP** **VFCGFTQNSL**  
301 **KSISELADSA** **QRRDALAKAS** **QSYIPSYVTR** **PAVVGLEVII** **SDSNSSEPPY**  
351 **GYTRIDYDLN** **RNAGGKYVFL** **CYKQKNISVG** **GDADAITDVL** **VVYGNDRNPS**  
401 **VPSGYTKIDK** **DLNSGAGGKY** **IYFCYSKDKR** **KQEEGLPIRG** **LRVVGPHPTS**  
451 **VAPYGFSKID** **IDLNMGAGGD** **FIYLCKSRHL** **E**

Gray shading	Gray-shaded type indicates microbially derived IPD079Ea peptides identified using LC-MS analysis.
Amino acid residue abbreviations	A (alanine), D (aspartic acid), E (glutamic acid), F (phenylalanine), G (glycine), H (histidine), I (isoleucine), K (lysine), L (leucine), M (methionine), N (asparagine), P (proline), Q (glutamine), R (arginine), S (serine), T (threonine), W (tryptophan), Y (tyrosine), and V (valine).

**Figure 29. Amino Acid Sequence of Microbially Derived IPD079Ea Protein Indicating Chymotryptic Peptides Identified Using LC-MS Analysis**

#### *N-Terminal Amino Acid Sequence Analysis*

The Edman sequencing analysis of the DP915635 maize-derived IPD079Ea sample indicated the N-terminus of the protein was blocked. The N-terminal peptide was identified as AEPNKGKAPAMK from the tryptic digestion of the protein (Table 18), indicating the N-terminal methionine was absent as expected ([Dummitt et al., 2003](#); [Sherman et al., 1985](#)). The analysis of the microbially derived IPD079Ea protein using Edman sequencing identified an N-terminal

sequence (GSMAEPNKG), matching amino acid residues 1-10 of the expected sequence of the microbially derived IPD079Ea protein.

Additional details regarding N-terminal amino acid sequence analytical methods are provided in Appendix E.

**Table 18. N-Terminal Amino Acid Sequence Analysis of IPD079Ea Protein**

Description		Amino Acid Sequence
DP915635 Maize-Derived IPD079Ea Protein	Deduced Sequence <sup>a</sup>	M - A - E - P - N - K - G - G - A - P - A - M - K
	Observed Sequence	A - E - P - N - K - G - G - A - P - A - M - K
Microbially Derived IPD079Ea Protein <sup>b</sup>	Theoretical Sequence	G - S - M - A - E - P - N - K - G - G
	Observed Sequence	G - S - M - A - E - P - N - K - G - G

Note: G (glycine), S (serine), M (methionine), A (alanine), E (glutamic acid), P (proline), N (asparagine), K (lysine).

<sup>a</sup> Deduced amino acid sequence from the translation of the *ipd079Ea* gene from plasmid PHP83175.

<sup>b</sup> The extra G and S remain following thrombin cleavage and removal of the N-terminal His tag used for protein purification.

### Allergenicity and Toxicity Analyses of the IPD079Ea Protein

A weight-of-evidence approach was applied to determine the allergenic and toxic potential of the IPD079Ea protein expressed in DP915635 maize, including an assessment of the following: a bioinformatic comparison of the amino acid sequence of IPD079Ea protein to known or putative protein allergen and toxin sequences, evaluation of the stability of the IPD079Ea protein using in vitro gastric and intestinal digestion models, determination of the IPD079Ea protein glycosylation status, evaluation of the heat lability of the IPD079Ea protein using a sensitive insect bioassay, and an evaluation of acute toxicity in mice following oral exposure to IPD079Ea protein. A summary of the safety assessment for IPD079Ea protein has recently been published ([Carlson et al., 2022](#)).

#### *Bioinformatic Analysis of Homology to Known or Putative Allergens ([PHI-2020-106/201 study](#))*

Assessing newly expressed proteins for potential cross-reactivity with known or putative allergens is an important part of the weight-of-evidence approach used to evaluate the safety of these proteins in genetically-modified plant products ([Codex Alimentarius Commission, 2003](#)). In this study, a bioinformatic assessment of the IPD079Ea protein sequence for potential cross-reactivity with known or putative allergens was conducted according to relevant guidelines ([Codex Alimentarius Commission, 2003](#); [FAO/WHO, 2001](#)).

Two separate searches for the IPD079Ea protein sequence were performed using the Comprehensive Protein Allergen Resource (COMPARE) 2020 database (January 2020) available at <http://comparedatabase.org>. This peer-reviewed database is a collaborative effort of the Health and Environmental Sciences Institute (HESI) Protein Allergens, Toxins, and Bioinformatics (PATB) Committee and is comprised of 2,248 sequences.

The first search used the IPD079Ea protein sequence as the query in a FASTA v35.4.4 ([Pearson and Lipman, 1988](#)) search against the allergen sequences. The search was conducted using default parameters, except the *E*-score threshold was set to  $10^{-4}$ . An *E*-score threshold of  $10^{-4}$  has been shown to be an appropriate value for allergenicity

searches ([Mirsky et al., 2013](#)). The generated alignments were examined to identify any that are a length of 80 or greater and possess a sequence identity of  $\geq 35\%$ . The second search used the FUZZPRO program (Emboss Package v6.4.0) to identify any contiguous 8-residue identical matches between the IPD079Ea protein sequence and the allergen sequences.

Results of the search of the IPD079Ea protein sequence against the COMPARE database of known and putative allergen sequences found no alignments that were a length of 80 or greater with a sequence identity of  $\geq 35\%$ . No contiguous 8-residue matches between the IPD079Ea protein sequence and the allergen sequences were identified in the second search. Collectively, these data indicate that no allergenicity concern arose from the bioinformatics assessment of the IPD079Ea protein

#### *Bioinformatic Analysis of Homology to Known or Putative Toxins ([PHI-2020-105/211 study](#))*

Assessing newly expressed proteins for potential toxicity is an important part of the weight-of-evidence approach used to evaluate the safety of these proteins in genetically modified plant products ([Codex Alimentarius Commission, 2003](#)). The potential toxicity of the IPD079Ea protein was assessed by comparison of its sequence to the sequences in an internal toxin database. The internal toxin database is a subset of sequences found in UniProtKB/Swiss-Prot (<https://www.uniprot.org/>). To produce the internal toxin database, the proteins in UniProtKB/Swiss-Prot are filtered for molecular function by keywords that could imply toxicity or adverse health effects (e.g., toxin, hemagglutinin, vasoactive, etc.). The internal toxin database is updated annually.

The search between the IPD079Ea protein sequence and protein sequences in the internal toxin database was conducted with BLASTP using default parameters, except that low complexity filtering was turned off, the *E*-value threshold was set to  $10^{-4}$ , and unlimited alignments were returned.

No alignments with an *E*-value  $\leq 10^{-4}$  were returned between the IPD079Ea protein sequence and any protein sequence in the internal toxin database. Therefore, no toxicity concern arose from the bioinformatics assessment of the IPD079Ea protein.

#### *Thermolability Analysis ([PHI-2020-030 study](#))*

Thermal stability of the IPD079Ea protein was characterized by determining the biological activity of heat-treated IPD079Ea protein incorporated in an artificial diet fed to western corn rootworm (WCR; *Diabrotica virgifera virgifera*). Purified IPD079Ea protein was incubated at various temperatures for approximately 30 minutes before incorporation into the artificial diet. WCR larvae were exposed via oral ingestion to the diets in a 7-day bioassay. A positive control diet containing unheated IPD079Ea protein and a bioassay control diet containing water were included in the bioassay to verify assay performance. After seven days, statistical analyses were conducted to evaluate WCR mortality of the heat-treated test groups relative to the unheated test group.

The results demonstrated that IPD079Ea protein heated for approximately 30 minutes at temperatures of 50 °C or higher were inactive against WCR when incorporated in an artificial insect diet (Table 19).

Additional details regarding thermolability analytical methods are provided in Appendix E.

Detailed methods and results are provided in the [PHI-2020-030 study](#).

**Table 19. Biological Activity of Heat-Treated IPD079Ea Protein in Artificial Diet Fed to Western Corn Rootworm**

Treatment	Treatment Description	Test Dosing Solution Incubation Condition	Total Number of Observations <sup>a</sup>	Number of Surviving Organisms	Mortality (%)	Fisher's Exact Test P-Value
1	Bioassay Control Diet	NA	29	28	3.45	--
2	Unheated Control Diet	Unheated	21	1	95.2	--
3	Test Diet	25 °C	28	1	96.4	0.8214
4	Test Diet	50 °C	28	27	3.57	<0.0001 <sup>b</sup>
5	Test Diet	75 °C	29	28	3.45	<0.0001 <sup>b</sup>
6	Test Diet	95 °C	30	30	0	<0.0001 <sup>b</sup>

Note: Test diets and the unheated control diet contained a targeted concentration of 50 ng IPD079Ea protein per mg diet wet weight. Not applicable (NA); the bioassay control diet was not incubated.

<sup>a</sup> Organisms counted as missing during the bioassay, or wells containing more than one organism, were not included in the total number of observations for a given treatment.

<sup>b</sup> A statistically significant difference (P-value < 0.05) was observed in comparison to Treatment 2.

#### *Digestibility Analysis with Simulated Gastric Fluid (PHI-2020-165 study)*

Simulated gastric fluid (SGF) containing pepsin at pH ~1.2 was used to assess the susceptibility of the IPD079Ea protein to proteolytic digestion by pepsin *in vitro*. The IPD079Ea protein was incubated in SGF for 0, 0.5, 1, 2, 5, 10, 20, 30, and 60 minutes. A positive control (bovine serum albumin) and a negative control ( $\beta$ -lactoglobulin) were included in the assay and were incubated in SGF for 0, 1, and 60 minutes. After incubation in SGF, the samples were analyzed by SDS-PAGE. Coomassie-based stain or western blot was used to detect protein bands.

A summary of the SGF results is provided in Table 20. The IPD079Ea protein migrating at ~52 kDa was rapidly digested (within 0.5 minutes) in SGF as demonstrated by both SDS-PAGE and western blot analysis (Figure 30 and Figure 31). Some low molecular weight bands on the SDS-PAGE gel remained detectable in the IPD079Ea protein samples for up to 60 minutes in SGF. The bovine serum albumin control substance disappeared rapidly (less than one minute) in SGF and the  $\beta$ -lactoglobulin control persisted through the 60-minute time course, verifying that the assay performed as expected.

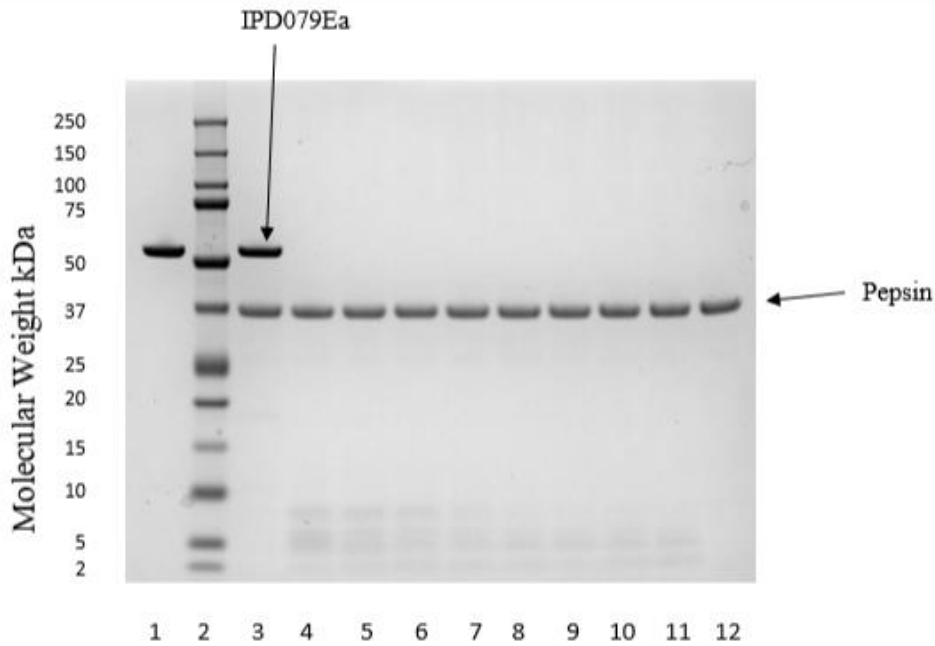
Additional details regarding SGF analytical methods are provided in Appendix E.

Detailed methods and results are provided in the [PHI-2020-165 study](#).

**Table 20. Summary of IPD079Ea Protein *In Vitro* Pepsin Resistance Assay Results**

Protein	Approximate Molecular Weight (kDa)	Digestion Time Determined by SDS-PAGE (minutes)	Digestion Time Determined by Western Blot (minutes)
IPD079Ea Protein	52	≤ 0.5	≤ 0.5
Bovine Serum Albumin (positive control)	66	≤ 1	NA
$\beta$ -Lactoglobulin (negative control)	18	> 60	NA

Note: Kilodalton (kDa), sodium dodecyl sulfate polyacrylamide gel electrophoresis (SDS-PAGE), and not applicable (NA).

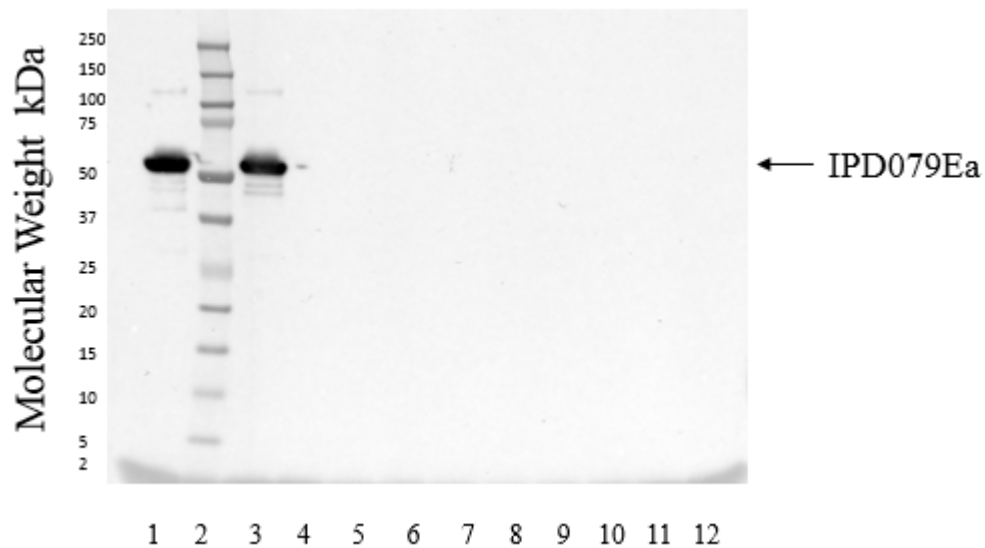


Lane	Sample Descriptions
1	IPD079Ea protein in water, Time 0
2	Pre-stained protein molecular weight marker <sup>a</sup>
3	IPD079Ea protein in SGF, Time 0
4	IPD079Ea protein in SGF, 0.5 minutes
5	IPD079Ea protein in SGF, 1 minute
6	IPD079Ea protein in SGF, 2 minutes
7	IPD079Ea protein in SGF, 5 minutes
8	IPD079Ea protein in SGF, 10 minutes
9	IPD079Ea protein in SGF, 20 minutes
10	IPD079Ea protein in SGF, 30 minutes
11	IPD079Ea protein in SGF, 60 minutes
12	SGF Control, 60 minutes

Note: kilodalton (kDa), sodium dodecyl sulfate polyacrylamide gel electrophoresis (SDS-PAGE), and simulated gastric fluid (SGF).

<sup>a</sup> Molecular weight markers were included to provide a visual estimate that migration was within the expected range of the predicted molecular weight.

**Figure 30. SDS-PAGE Analysis of IPD079Ea Protein in Simulated Gastric Fluid Digestion Time Course**



Lane	Sample Descriptions
1	IPD079Ea protein in water, Time 0
2	Pre-stained protein molecular weight marker <sup>a</sup>
3	IPD079Ea protein in SGF, Time 0
4	IPD079Ea protein in SGF, 0.5 minutes
5	IPD079Ea protein in SGF, 1 minute
6	IPD079Ea protein in SGF, 2 minutes
7	IPD079Ea protein in SGF, 5 minutes
8	IPD079Ea protein in SGF, 10 minutes
9	IPD079Ea protein in SGF, 20 minutes
10	IPD079Ea protein in SGF, 30 minutes
11	IPD079Ea protein in SGF, 60 minutes
12	SGF Control, 60 minutes

Note: kilodalton (kDa) and simulated gastric fluid (SGF).

<sup>a</sup> Molecular weight markers were included to provide a visual estimate that migration was within the expected range of the predicted molecular weight.

**Figure 31. Western Blot Analysis of IPD079Ea Protein in Simulated Gastric Fluid Digestion Time Course**

*Digestibility Analysis with Simulated Intestinal Fluid (PHI-2020-175 study)*

Simulated intestinal fluid (SIF) containing pancreatin at ~pH 7.5 was used to assess the susceptibility of the IPD079Ea protein to proteolytic digestion by pancreatin in vitro. IPD079Ea protein was incubated in SIF for 0, 0.5, 1, 2, 5, 10, 20, 30, and 60 minutes. A positive control ( $\beta$ -lactoglobulin) and a negative control (bovine serum albumin) were included in the assay and were incubated in SIF for 0, 1, and 60 minutes. After incubation in SIF, the samples were analyzed by SDS-PAGE. Coomassie-based stain or western blot was used to detect protein bands.

A summary of the SIF assay results is provided in Table 21. The IPD079Ea protein migrating at ~52 kDa was gradually digested in SIF as demonstrated by both SDS-PAGE and western blot analysis (Figure 32 and Figure 33, respectively),

although a band remained visible after 60 minutes. Fragments at lower molecular weights also remained detectable throughout the digestion. The  $\beta$ -lactoglobulin positive control was largely digested after 60 minutes in SIF and the bovine serum albumin control persisted through the 60-minute time course, verifying that the assay performed as expected.

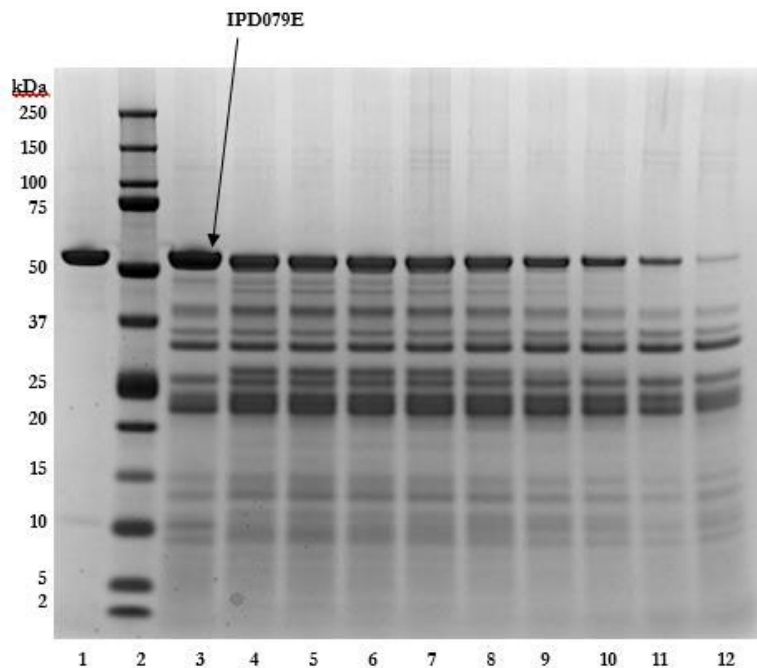
Additional details regarding SIF analytical methods are provided in Appendix E.

Detailed methods and results are provided in the [PHI-2020-175 study](#).

**Table 21. Summary of IPD079Ea Protein *In Vitro* Pancreatin Resistance Assay Results**

Protein	Approximate Molecular Weight (kDa)	Digestion Time Determined by SDS-PAGE (minutes)	Digestion Time Determined by Western Blot (minutes)
IPD079Ea Protein	52	> 60	> 60
Bovine Serum Albumin (negative control)	66	> 60	NA
$\beta$ -Lactoglobulin (positive control)	18	$\leq 1$	NA

Note: Kilodalton (kDa), sodium dodecyl sulfate polyacrylamide gel electrophoresis (SDS-PAGE), not applicable (NA).

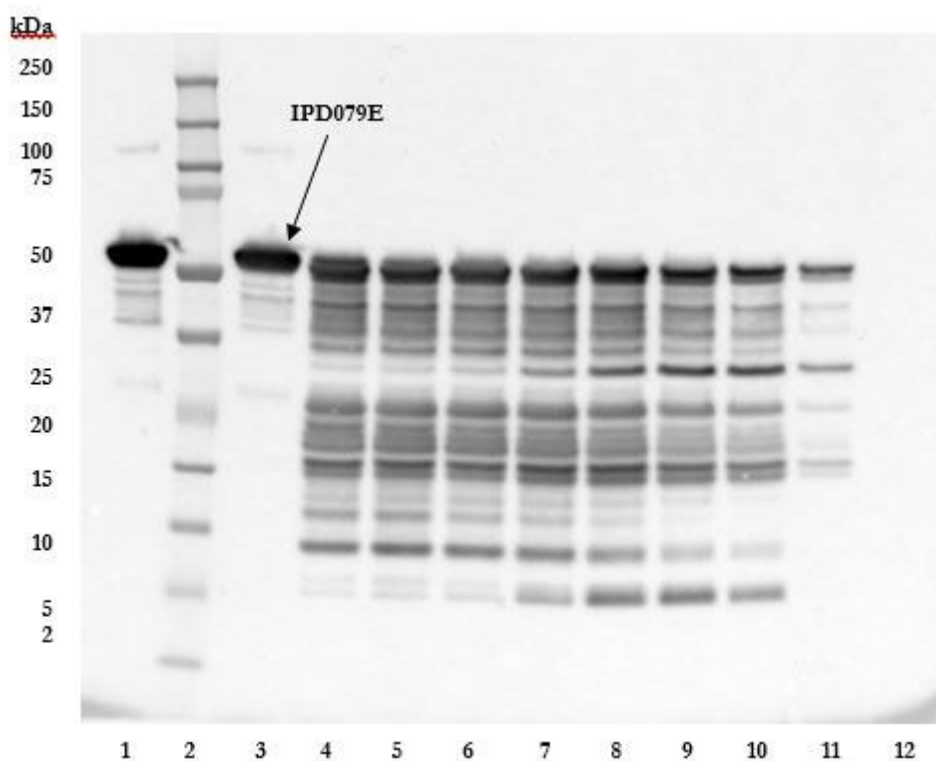


Lane	Sample Descriptions
1	IPD079Ea protein in water, Time 0
2	Pre-stained protein molecular weight marker <sup>a</sup>
3	IPD079Ea protein in SIF, Time 0
4	IPD079Ea protein in SIF, 0.5 minutes
5	IPD079Ea protein in SIF, 1 minute
6	IPD079Ea protein in SIF, 2 minutes
7	IPD079Ea protein in SIF, 5 minutes
8	IPD079Ea protein in SIF, 10 minutes
9	IPD079Ea protein in SIF, 20 minutes
10	IPD079Ea protein in SIF, 30 minutes
11	IPD079Ea protein in SIF, 60 minutes
12	SIF Control, 60 minutes

Note: kilodalton (kDa), sodium dodecyl sulfate polyacrylamide gel electrophoresis (SDS-PAGE), and simulated intestinal fluid (SIF).

<sup>a</sup> Molecular weight markers were included to provide a visual estimate that migration was within the expected range of the predicted molecular weight.

**Figure 32. SDS-PAGE Analysis of IPD079Ea Protein in Simulated Intestinal Fluid Digestion Time Course**



Lane	Sample Descriptions
1	IPD079Ea protein in water, Time 0
2	Pre-stained protein molecular weight marker <sup>a</sup>
3	IPD079Ea protein in SIF, Time 0
4	IPD079Ea protein in SIF, 0.5 minutes
5	IPD079Ea protein in SIF, 1 minute
6	IPD079Ea protein in SIF, 2 minutes
7	IPD079Ea protein in SIF, 5 minutes
8	IPD079Ea protein in SIF, 10 minutes
9	IPD079Ea protein in SIF, 20 minutes
10	IPD079Ea protein in SIF, 30 minutes
11	IPD079Ea protein in SIF, 60 minutes
12	SIF Control, 60 minutes

Note: kilodalton (kDa) and simulated intestinal fluid (SIF).

<sup>a</sup> Molecular weight markers were included to provide a visual estimate that migration was within the expected range of the predicted molecular weight.

**Figure 33. Western Blot Analysis of IPD079Ea Protein in Simulated Intestinal Fluid Digestion Time Course**

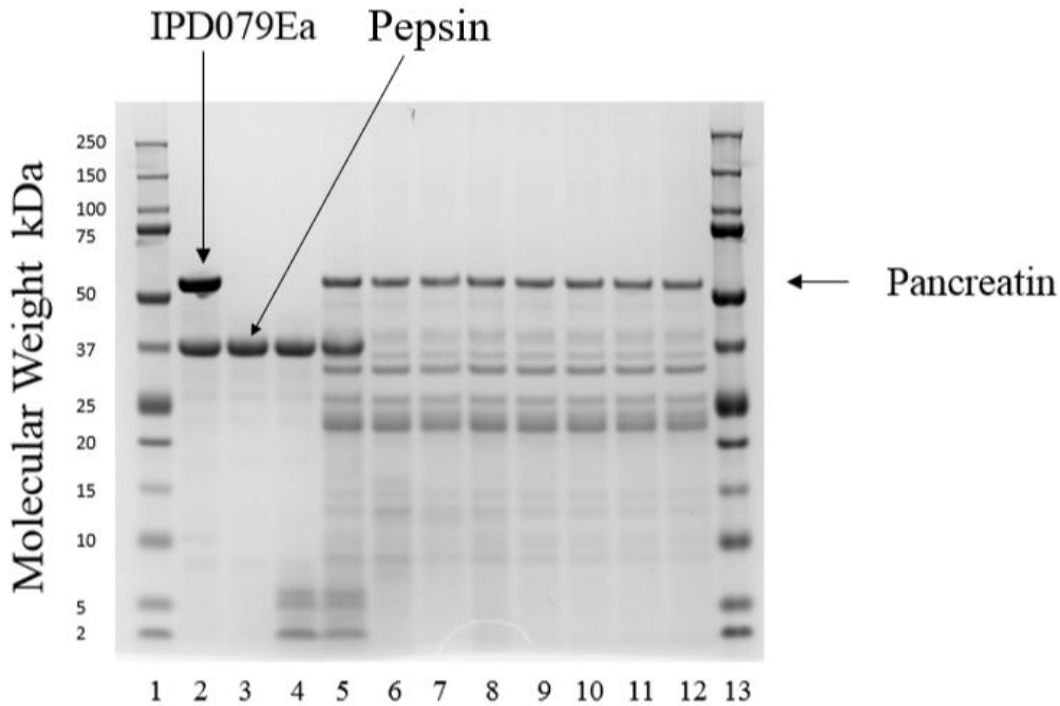
*Sequential Digestibility Analysis with Simulated Gastric Fluid (SGF) and Simulated Intestinal Fluid (SIF) ([PHI-2020-174 study](#))*

Simulated gastric fluid (SGF) containing pepsin at pH ~1.2 and simulated intestinal fluid (SIF) containing pancreatin at ~pH 7.5 were used to assess the susceptibility of the IPD079Ea protein to proteolytic digestion by pepsin followed by pancreatin *in vitro*. The IPD079Ea protein was incubated for 10 minutes in SGF and then incubated for 0, 0.5, 1, 2, 5, 10, 20 and 30 minutes in SIF. After incubation in SIF, the samples were analyzed by SDS-PAGE.

The IPD079Ea protein migrating at ~52 kDa was rapidly digested ( $\leq 0.5$  min), as demonstrated by SDS-PAGE (Figure 34). Some low molecular weight bands on the SDS-PAGE gel remained detectable in the IPD079Ea protein samples for up to 60 minutes in SGF (Figure 31). During sequential pepsin and pancreatin digestion of IPD079Ea protein, the low molecular weight bands observed after digestion in SGF for 10 minutes were rapidly digested ( $< 0.5$  minutes) during sequential SIF digestion.

Additional details regarding analytical methods are provided in Appendix E.

Detailed methods and results are provided in the [PHI-2020-174 study](#).



Lane	Sample Descriptions
1	Pre-stained Protein Molecular Weight Marker <sup>a</sup>
2	IPD079Ea Protein in SGF, Time 0
3	SGF Only; 10 minutes
4	IPD079Ea Protein in SGF, 10 minutes
5	IPD079Ea Protein in SGF 10 minutes, SIF Time 0
6	IPD079Ea Protein in SGF 10 minutes, SIF 30 seconds
7	IPD079Ea Protein in SGF 10 minutes, SIF 1 minute
8	IPD079Ea Protein in SGF 10 minutes, SIF 2 minutes
9	IPD079Ea Protein in SGF 10 minutes, SIF 5 minutes
10	IPD079Ea Protein in SGF 10 minutes, SIF 10 minutes
11	IPD079Ea Protein in SGF 10 minutes, SIF 20 minutes
12	IPD079Ea Protein in SGF 10 minutes, SIF 30 minutes
13	Pre-stained Protein Molecular Weight Marker <sup>a</sup>

Note: kilodalton (kDa), sodium dodecyl sulfate polyacrylamide gel electrophoresis (SDS-PAGE), and simulated gastric fluid (SGF).

<sup>a</sup> Molecular weight markers were included to provide a visual estimate that migration was within the expected range of the predicted molecular weight.

**Figure 34. SDS-PAGE Analysis of IPD079Ea Protein in a Sequential Digestion with Simulated Gastric Fluid and Simulated Intestinal Fluid**

*Glycoprotein Analysis (PHI-2020-146 study)*

As stated previously in the results from glycoprotein staining analysis confirmed the absence of glycosylation for IPD079Ea protein derived from DP915635 maize tissue.

#### *Evaluation of the Acute Toxicity of IPD079Ea Protein (PHI-2019-224)*

A study was conducted to evaluate the acute toxicity of the test substance, IPD079Ea protein, in [REDACTED] mice following oral exposure at the limit dose of 5000 mg/kg body weight (adjusted for IPD079Ea content). IPD079Ea protein and Bovine Serum Albumin (BSA) protein were each reconstituted in deionized water. Vehicle control, BSA control, and IPD079Ea test substance formulations were administered orally by gavage in a split dose, separated by approximately four hours; the BSA control was administered at an equivalent target dose to that of the test substance. The mice were fasted prior to and throughout the dosing procedure.

Body weights were evaluated on test days 1 (prior to fasting and shortly prior to administration of the first dose), 2, 3, 5, 8, and 15. Clinical signs were evaluated seven times on test day 1 (distributed before and after each dose) and daily thereafter. On test day 15, all surviving mice were euthanized and given a gross pathological examination.

There were no test substance-related deaths. One vehicle control female was sacrificed on test day 3 (unscheduled) due to clinical signs of dehydration, hypoactivity, and swollen shoulder and body weight loss. This animal was observed grossly with a ventral esophageal perforation, which was consistent with gavage trauma and considered to be the cause of death. All remaining animals survived until scheduled sacrifice. There were no test substance-related clinical observations and all surviving animals gained weight during the 2-week observation period prior to sacrifice. One BSA control male had a swollen abdomen on test day 15, and this animal was observed grossly to have large preputial glands filled with viscous green fluid.

Under the conditions of this study, intragastric exposure of IPD079Ea protein to male and female mice at 5000 mg/kg body weight did not result in mortality or other evidence of acute oral toxicity, based on evaluation of body weight, clinical signs, and gross pathology. Therefore, the acute oral toxicity tolerant dose and the LD<sub>50</sub> of IPD079Ea protein was determined to be greater than 5000 mg/kg body weight.

#### **Conclusions on the Safety of IPD079Ea Protein in DP915635 Maize**

In conclusion, protein characterization results via SDS-PAGE, western blot, glycosylation, mass spectrometry, and N-terminal amino acid sequence analysis, have demonstrated that the IPD079Ea protein derived from DP915635 maize is of the expected molecular weight, immunoreactivity, lack of glycosylation, and amino acid sequence. Microbially derived IPD079Ea protein was demonstrated to be equivalent to the DP915635 maize-derived IPD079Ea protein for use in safety testing.

The allergenic and toxic potential of the IPD079Ea protein was assessed using a bioinformatic comparison of the amino acid sequence of the IPD079Ea protein to known or putative protein allergen and toxin sequences, evaluation of the stability of the IPD079Ea protein using *in vitro* gastric and intestinal digestion models, determination of the IPD079Ea protein glycosylation status, evaluation of the heat lability of the IPD079Ea protein using a sensitive insect bioassay, and an evaluation of acute toxicity in mice following oral exposure to IPD079Ea protein.

The bioinformatic comparisons of the IPD079Ea protein sequence to known and putative allergen and toxin sequences showed that the IPD079Ea protein is unlikely to be allergenic or toxic for humans or animals. The IPD079Ea protein migrating at ~52 kDa was rapidly digested in SGF. The protein was gradually digested in SIF, and some bands remained visible after 60 minutes. The low molecular weight bands remaining from SGF digestion were rapidly digested (< 0.5 minutes) in sequential SIF. The IPD079Ea protein was not glycosylated. The IPD079Ea protein heated for approximately 30 minutes at targeted temperatures of 50 °C or higher was inactive against WCR when

incorporated in an artificial diet. The acute oral toxicity assessment determined the LD<sub>50</sub> of IPD079Ea protein to be greater than 5000 mg/kg. These data support the conclusion that the IPD079Ea protein in DP915635 maize is as safe as conventional maize for the food and feed supply.

Based on this weight of evidence, consumption of the IPD079Ea protein is unlikely to cause an adverse effect on humans or animals.

## PAT protein

### Amino Acid Sequence of the PAT Protein

The gene encoding the PAT protein in DP915635 maize, referred to as the *mo-pat* gene, was isolated from *Streptomyces viridochromogenes* with codon-optimization for expression in maize. The deduced amino acid sequence from the translation of the *mo-pat* gene is identical to the deduced amino acid sequence from the translation of the *pat* gene. The PAT protein encoded by the *pat* and *mo-pat* genes is 183 amino acids in length and has a molecular weight of approximately 21 kDa (Figure 35).

PAT ( <i>pat</i> )	1	MSPERRPVEI	RPATAADMAA	VCDIVNHYIE	TSTVNFRTPEP	QTPQEWIDDL
PAT ( <i>mo-pat</i> )	1	MSPERRPVEI	RPATAADMAA	VCDIVNHYIE	TSTVNFRTPEP	QTPQEWIDDL
PAT ( <i>pat</i> )	51	ERLQDRYPWL	VAEVEGVVAG	IAYAGPWKAR	NAYDWTVEST	VYVSHRHQRL
PAT ( <i>mo-pat</i> )	51	ERLQDRYPWL	VAEVEGVVAG	IAYAGPWKAR	NAYDWTVEST	VYVSHRHQRL
PAT ( <i>pat</i> )	101	GLGSTLYTHL	LKSMEAQGFK	SVVAVIGLPN	DPSVRLHEAL	GYTARGTLRA
PAT ( <i>mo-pat</i> )	101	GLGSTLYTHL	LKSMEAQGFK	SVVAVIGLPN	DPSVRLHEAL	GYTARGTLRA
PAT ( <i>pat</i> )	151	AGYKHGGWHD	VGFWQRDFEL	PAPPRPVRPV	TQI*	
PAT ( <i>mo-pat</i> )	151	AGYKHGGWHD	VGFWQRDFEL	PAPPRPVRPV	TQI*	

**Figure 35. Alignment of the Deduced Amino Acid Sequence of PAT Protein Encoded by *pat* and *mo-pat* Genes**

Deduced amino acid sequence alignment, where PAT (*pat*) represents the deduced amino acid sequence from the translation of the *pat* gene that is found in a number of authorized events across several different crops that are currently commercialized and have a history of safe use ([Hérouet et al., 2005](#); [USDA-APHIS, 2001](#); [USDA-APHIS, 2005](#); [USDA-APHIS, 2013](#)). The PAT (*mo-pat*) sequence represents the deduced amino acid sequence from translation of the *mo-pat* gene. The asterisk (\*) indicates the translational stop codon.

As shown in Figure 35, the deduced amino acid sequence from translation of the *mo-pat* gene is identical to that of the already-deregulated PAT protein from translation of the *pat* gene, for which safety has been confirmed ([Hérouet et al., 2005](#)) in a number of approved events across several different crops that are currently in commercial use.

### Function and Activity of the PAT Protein

The mode of action of the PAT protein has been previously characterized and described ([CERA - ILSI Research Foundation, 2011](#); [Hérouet et al., 2005](#)). The PAT protein confers tolerance to the herbicidal active ingredient glufosinate-ammonium, the active ingredient in phosphinothricin herbicides. Glufosinate chemically resembles the amino acid glutamate and acts to inhibit an enzyme called glutamine synthetase, which is involved in the synthesis of glutamine. Glutamine synthetase is also involved in ammonia detoxification. Due to its similarity to glutamate, glufosinate blocks the activity of glutamine synthetase, resulting in reduced glutamine levels and a corresponding increase in concentrations of ammonia in plant tissues, leading to cell membrane disruption and cessation of photosynthesis resulting in plant death. The PAT protein confers tolerance to glufosinate-ammonium herbicides by acetylating phosphinothricin, an isomer of glufosinate-ammonium, thus detoxifying the herbicide ([CERA - ILSI Research Foundation, 2011](#); [Hérouet et al., 2005](#)).

### Characterization of the PAT Protein from DP915635

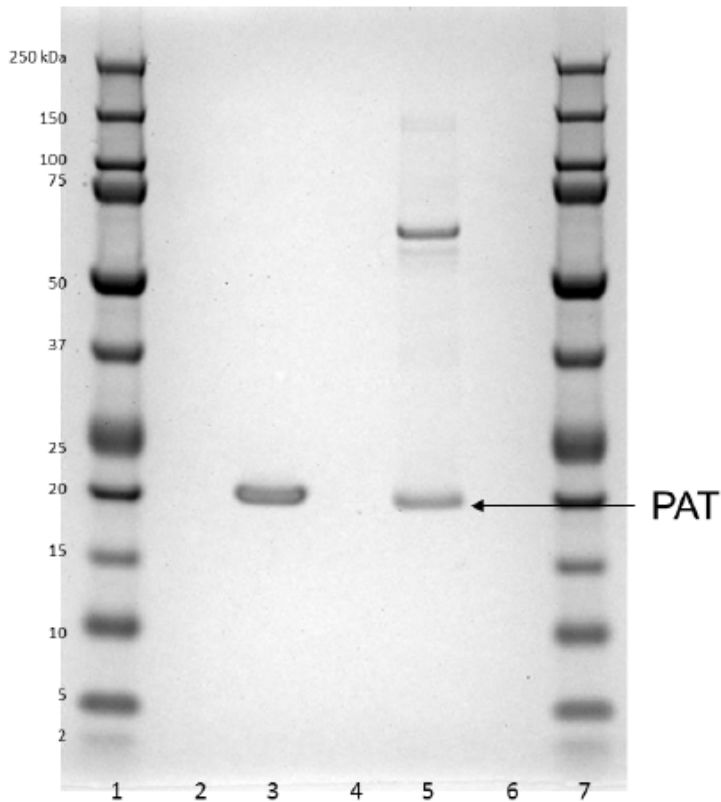
The DP915635 maize-expressed PAT protein was characterized using SDS-PAGE, western blot, glycosylation, mass spectrometry peptide mapping, and N-terminal amino acid sequence analyses. The results demonstrated that the PAT protein derived from DP915635 maize is of the expected molecular weight, immunoreactivity, lack of glycosylation, and amino acid sequence.

#### SDS-PAGE Analysis

Samples of PAT protein purified from DP915635 leaf tissue were analyzed by SDS-PAGE. As expected, the DP915635 maize derived PAT protein migrated as a band consistent with the expected molecular weight of approximately 21 kDa (Figure 36).

Additional details regarding SDS-PAGE analytical methods are provided in Appendix F.

Detailed methods and results are provided in the [PHI-2020-147 study](#).



Lane	Sample Identification
1	Pre-stained Protein Molecular Weight Marker <sup>a</sup>
2	1X LDS/DTT Sample Buffer Blank
3	Microbially derived PAT Protein <sup>b</sup>

4	1X LDS/DTT Sample Buffer Blank
5	DP915635 Maize-Derived PAT Protein <sup>c</sup>
6	1X LDS/DTT Sample Buffer Blank
7	Pre-stained Protein Molecular Weight Marker <sup>a</sup>

Note: kilodalton (kDa)

<sup>a</sup> Molecular weight markers were included to provide a visual estimate that migration was within the expected range of the predicted molecular weight.

<sup>b</sup> Protein Lot PCF-0038; Diluted to 1 µg per lane.

<sup>c</sup> After 1:2 dilution.

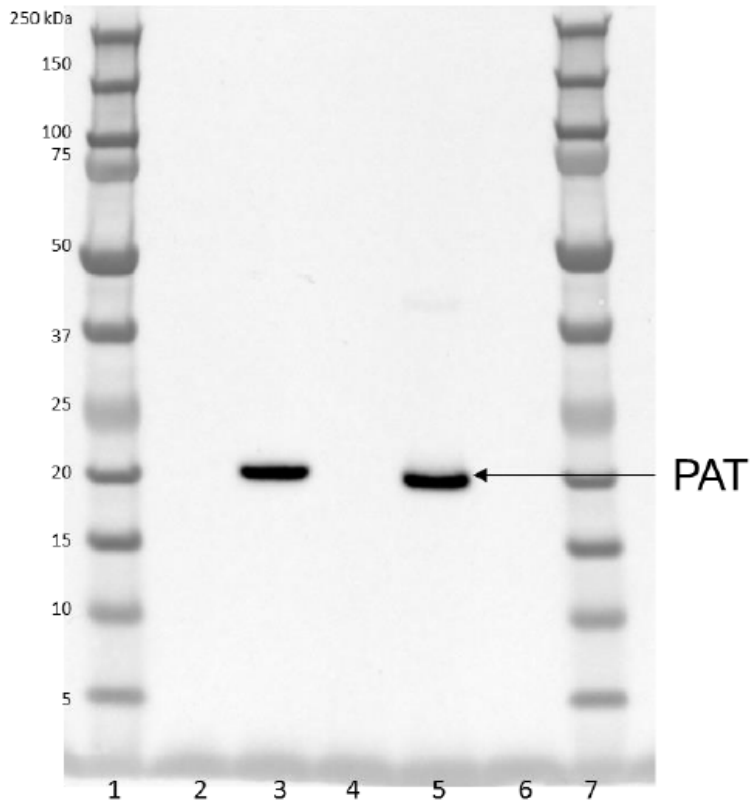
**Figure 36. SDS-PAGE Analysis of DP915635 Maize-Derived PAT Protein**

*Western Blot Analysis*

Samples of PAT protein purified from DP915635 maize leaf tissue were analyzed by Western blot. As expected, both the DP915635 maize derived PAT and a microbially derived PAT proteins were immunoreactive to a PAT monoclonal antibody and visible as a band consistent with the expected molecular weight of approximately 21 kDa. (Figure 37).

Additional details regarding western blot analytical methods are provided in Appendix F.

Detailed methods and results are provided in the [PHI-2020-147 study](#).



Lane	Sample Identification
1	Pre-stained Protein Molecular Weight Marker <sup>a</sup>
2	1X LDS/DTT Sample Buffer Blank
3	Microbially derived PAT Protein <sup>b</sup>
4	1X LDS/DTT Sample Buffer Blank
5	DP915635 Maize-Derived PAT Protein <sup>c</sup>
6	1X LDS/DTT Sample Buffer Blank
7	Pre-stained Protein Molecular Weight Marker <sup>a</sup>

Note: kilodalton (kDa)

<sup>a</sup> Molecular weight markers were included to provide a visual estimate that migration was within the expected range of the predicted molecular weight.

<sup>b</sup> Protein Lot PCF-0038; Diluted to 10 ng per lane.

<sup>c</sup> After 1:80 dilution.

**Figure 37. Western Blot Analysis of PAT Protein**

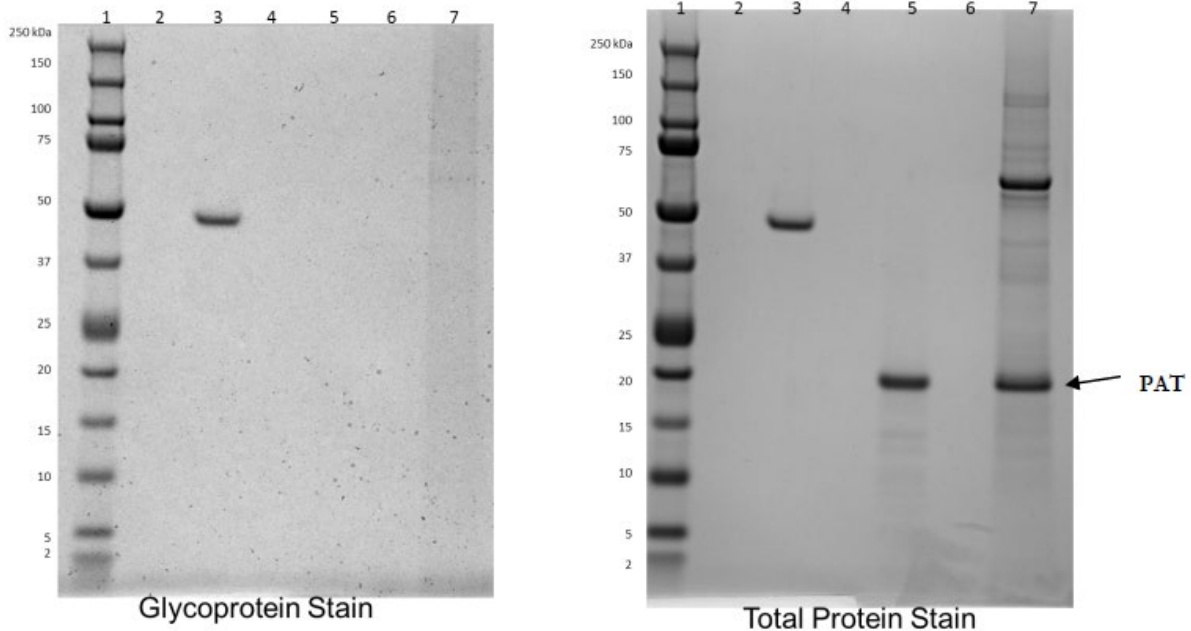
### Protein Glycosylation Analysis

The PAT protein purified from DP915635 maize leaf tissue was analyzed by SDS-PAGE. The gel also included a positive control (horseradish peroxidase) and negative control (soybean trypsin inhibitor). The gel was stained using a Pierce Glycoprotein Staining Kit to visualize any glycoproteins. The gel was imaged and then stained with GelCode Blue stain reagent to visualize all protein bands.

Glycosylation was not detected for the PAT protein (Figure 38). The horseradish peroxidase positive control was stained and clearly visible as a magenta-colored band. The soybean trypsin inhibitor negative control was not stained by the glycoprotein stain.

Additional details regarding glycosylation analytical methods are provided in Appendix F.

Detailed methods and results are provided in the [PHI-2020-147 study](#).



Lane	Sample Identification
1	Pre-stained Protein Molecular Weight Marker <sup>a</sup>
2	1X LDS/DTT Sample Buffer Blank
3	Horseradish Peroxidase (1.0 µg)
4	1X LDS/DTT Sample Buffer Blank
5	Soybean Trypsin Inhibitor (1.0 µg)
6	1X LDS/DTT Sample Buffer Blank
7	DP915635 Maize-Derived PAT Protein <sup>b</sup>

Note: The glycoprotein gel was stained with glycoprotein staining reagent. The total protein stain gel was stained with glycoprotein staining reagent followed by staining with Coomassie Blue Reagent for total proteins. Kilodalton (kDa) and microgram ( $\mu\text{g}$ ).

<sup>a</sup> Molecular weight markers were included to provide a visual estimate that migration was within the expected range of the predicted molecular weight.

<sup>b</sup> Undiluted sample.

**Figure 38. Glycosylation Analysis of the DP915635 Maize-Derived PAT Protein**

*Mass Spectrometry Peptide Mapping Analysis*

Samples of PAT protein purified from DP915635 maize leaf tissue were analyzed by SDS-PAGE. Protein bands were stained with Coomassie stain reagent, and the band containing PAT protein was excised for each sample. The excised PAT protein bands were digested with trypsin or chymotrypsin. Digested samples were analyzed using LC-MS, and an MS/MS ion search was used to match the detected peaks to peptides from the expected PAT protein sequence.

The identified tryptic and chymotryptic peptides for DP915635 maize-derived PAT protein are shown in Table 22. The combined sequence coverage was 75.3% (137/182) of the expected PAT amino acid sequence (Table 23 and Figure 39).

Additional details regarding peptide mapping analytical methods are provided in Appendix F.

Detailed methods and results are provided in the [PHI-2020-147 study](#).

**Table 22. Identified Tryptic and Chymotryptic Peptides of DP915635 Maize-Derived PAT Protein Using LC-MS Analysis**

Matched Residue Position	Experimental Mass <sup>a</sup>	Theoretical Mass <sup>b</sup>	Identified Peptide Sequence
<b>Tryptic Peptides</b>			
37–51	1855.8505	1855.8588	TEPQTPQEWIDDLER
99–111	1414.8149	1414.8184	LGLGSTLYTHLLK
112–119	896.4023	896.4062	SMEAQGFK
120–134	1521.8457	1521.8515	SVVAVIGLPNDPSVR
135–144	1129.5812	1129.588	LHEALGYTAR
166–182	1931.0565	1931.0629	DFELPAPPRPVRPVTQI
<b>Chymotryptic Peptides</b>			
28–35	909.4424	909.4444	IETSTVNF
36–45	1270.5888	1270.5942	RTEPQTPQEW
46–52	872.4582	872.4603	IDDLERL
46–58	1717.8361	1717.8424	IDDLERLQDRYPW
59–72	1388.7488	1388.7551	LVAEVEGVVAGIAY
77–82	721.3859	721.3871	KARNAY
83–91	1098.4833	1098.487	DWTVESTVY
107–118	1360.6785	1360.6809	THLLKSMEAQGF
110–118	1009.4855	1009.4902	LKSMEAQGF
111–118	896.4031	896.4062	KSMEAQGF
142–147	617.3489	617.3497	TARGTL
153–163	1324.608	1324.6102	KHGGWHDVGFW
158–163	759.3324	759.334	HDVGFW
168–182	1668.9632	1668.9675	ELPAPPRPVRPVTQI

<sup>a</sup> The experimental mass is the uncharged mass calculated from the mass to charge ratio of the observed ion.

<sup>b</sup> The theoretical mass is the in silico generated mass that matches closest to the experimental mass.

**Table 23. Combined Sequence Coverage of Identified Tryptic and Chymotryptic Peptides of DP915635 Maize-Derived PAT Protein Using LC-MS Analysis**

Protease	% Coverage	Combined % Coverage
Trypsin	42	75.3
Chymotrypsin	57	

1 SPERRPVEIR PATAADMAAV CDIVNHYIET STVNFRTPEQ TPQEWIDDLE  
 51 RLQDRYPWLIV AEVEGVVAGI AYAGPWKARN AYDWTVESTV YVSHRHQRLG  
 101 LGSTLYTHLL KSMEAQGFKS VVAVIGLPND PSVRLHEALG YTARGTLRAA  
 151 GYKHGGWHDV GFWQRDFELP APPRPVRPVT QI

Gray shading	Gray-shaded type indicates DP915635 maize-derived PAT peptides identified using LC-MS analysis.
Amino acid residue abbreviations	A (alanine), D (aspartic acid), E (glutamic acid), F (phenylalanine), G (glycine), H (histidine), I (isoleucine), K (lysine), L (leucine), M (methionine), N (asparagine), P (proline), Q (glutamine), R (arginine), S (serine), T (threonine), W (tryptophan), Y (tyrosine), and V (valine).

**Figure 39. Identified Tryptic and Chymotryptic Peptide Amino Acid Sequence of DP915635 Maize-Derived PAT Protein Using LC-MS Analysis**

#### *N-Terminal Amino Acid Sequence Analysis*

Samples of PAT protein purified from DP915635 maize leaf tissue were analyzed by SDS-PAGE, followed by electrophoretic protein transfer to a polyvinylidene difluoride (PVDF) membrane. The membrane was stained using GelCode Blue stain reagent to visualize the proteins, and the band containing PAT protein was excised. The excised band was analyzed using Edman degradation (Edman sequencing) to determine the N-terminal amino acid sequence.

The analysis identified a sequence (SPERRPVEIR) matching amino acid residues 1-10 of the expected PAT protein sequence (Table 24), indicating the N-terminal methionine was absent as expected ([Dummitt et al., 2003](#); [Sherman et al., 1985](#)).

Additional details regarding N-terminal amino acid sequence analytical methods are provided in Appendix F.

Detailed methods and results are provided in the [PHI-2020-147 study](#).

**Table 24. N-Terminal Amino Acid Sequence Analysis of DP915635 Maize-Derived PAT Protein**

<b>Expected PAT Sequence</b>	S – P – E – R – R – P – V – E – I – R
<b>Detected Primary Sequence</b>	S – P – E – R – R – P – V – E – I – R

Note: The expected PAT sequence does not include the N-terminal methionine as it is anticipated to be absent for Edman sequencing.

## Allergenicity and Toxicity of the PAT Protein

The PAT protein present in DP915635 maize is found in several approved events that are currently in commercial use. Therefore, in accordance with the FSANZ Application Handbook, only the updated bioinformatics analysis is provided in this dossier for safety assessment.

### *Bioinformatic Analysis of PAT Protein Homology to Known or Putative Allergens (PHI-2020-104/201 study)*

Assessing newly expressed proteins for potential cross-reactivity with known or putative allergens is a critical part of the weight-of-evidence approach used to evaluate the safety of these proteins in genetically-modified plant products ([Codex Alimentarius Commission, 2003](#)). In this study, a bioinformatic assessment of the PAT protein sequence for potential cross-reactivity with known or putative allergens was conducted according to relevant guidelines ([Codex Alimentarius Commission, 2003](#); [FAO/WHO, 2001](#)).

Two separate searches for the PAT protein sequence were performed using the Comprehensive Protein Allergen Resource (COMPARE) 2020 database (January 2020) available at <http://comparedatabase.org>. This peer-reviewed database is a collaborative effort of the Health and Environmental Sciences Institute (HESI) Protein Allergens, Toxins, and Bioinformatics (PATB) Committee and is comprised of 2,248 sequences.

Two separate searches for the PAT protein sequence were performed using the comprehensive protein allergen resources (COMPARE) 2020 database (January 2020) available at <http://comparedatabase.org>. This peer reviewed database is a collaborative effort of the Health and Environment Sciences Institute (HESI) Protein Allergens, Toxins, and Bioinformatics (PATB) Committee and is comprised of 2,248 sequences. The first search used the PAT protein sequence as the query in FASTA v25.4.4 ([Pearson and Lipman, 1988](#)) search against the allergen sequences. The search was conducted using default parameters, except the *e-score* threshold was set to  $10^{-4}$ . An *E-score* threshold of  $10^{-4}$  has been shown to be an appropriate value for allergenicity searches ([Mirsky et al, 2013](#)). The generated alignments were examined to identify any that are a length of 80 or greater and possess a sequence identity of  $\geq 35\%$ . The second search used the FUZZPROD program (Emboss Package v6.4.0) to identify any contiguous 8 residue identical matches between the PAT protein sequence and the allergen sequences.

Result of the search of the PAT protein sequence against the COMPARE database of known and putative allergen sequences found no alignments that were a length of 80 or greater with a sequence identity  $\geq 35\%$ . No contiguous 8 residue matches between the PAT protein sequence and the allergen sequences were identified in the second search.

Collectively, these data indicate that no allergenicity concern arose from the bioinformatics assessment of the PAT protein.

### *Bioinformatic Analysis of PAT Protein Homology to Known or Putative Toxins (PHI-2020-103/211 study)*

Assessing newly expressed proteins for potential toxicity is a critical part of the weight-of-evidence approach used to evaluate the safety of these proteins in genetically modified plant products ([Codex Alimentarius Commission, 2003](#)). The potential toxicity of the PAT protein was assessed by comparison of its sequence to the sequences in an internal toxin database. The internal toxin database is a subset of sequences found in UniProtKB/Swiss-Prot (<https://www.uniprot.org/>). To produce the internal toxin database, the proteins in UniProtKB/Swiss-Prot are filtered for molecular function by keywords that could imply toxicity or adverse health effects (e.g., toxin, hemagglutinin, vasoactive, etc.). The internal toxin database is updated annually.

The search between the PAT protein sequence and protein sequences in the internal toxin database was conducted with BLASTP using default parameters, except that low complexity filtering was turned off, the *E*-value threshold was set to  $10^{-4}$ , and unlimited alignments were returned.

No alignments with an *E*-value  $\leq 10^{-4}$  were returned between the PAT protein sequence and any protein sequence in the internal toxin database. Therefore, no toxicity concern arose from the bioinformatics assessment of the PAT protein.

#### **Conclusions on the Safety of PAT Protein in DP915635 Maize**

The amino acid sequence of the PAT protein present in DP915635 maize was demonstrated to be identical to the corresponding protein found in a number of authorized GM events across several different crops that are currently commercialized and have a history of safe use.

Therefore, in accordance with the FSANZ Application Handbook, only the updated bioinformatics analysis is provided in this dossier for safety assessment. This along with the history of safe use of the PAT protein expressed in DP915635 maize supports a weight of evidence that the PAT protein is unlikely to present significant risks to the environment, human, or animal health.

## PMI protein

### Amino Acid Sequence of the PMI Protein

The gene encoding the PMI protein in DP915635 maize, referred to as the *pmi* gene, was isolated from *Escherichia coli*. PMI served as a selectable marker during transformation which allowed for tissue growth using mannose as the carbon source. The deduced amino acid sequence from translation of the *pmi* gene is 391 amino acids in length and has a molecular weight of approximately 43 kDa (Figure 40).

```
1   MQKLINSVQN  YAWGSKTALT  ELYGMENPSS  QPMAELWMGA  HPKSSSRVQN
51  AAGDIVSLRD  VIESDKSTLL  GEAVAKRFG  LPFLFKVLCA  AQPLSIQVHP
101 NKHNSEIGFA  KENAAGIPMD  AAERNYKDPN  HKPELVFALT  PFLAMNAFRE
151 FSEIVSLLQP  VAGAHPAIAH  FLQQPDAERL  SELFASLLNM  QGEEKSRALA
201 ILKSALDSQQ  GEPWQTIRLI  SEFYPEDSGL  FSPLLLNVVK  LNPGEAMFLF
251 AETPHAYLQG  VALEVMANS  NVLRAGLTPK  YIDIPELVAN  VKFEAKPANQ
301 LLTQPVKQGA  ELDFPIPVDD  FAFSLHDLS  KETTISQQSA  AILFCVEGDA
351 TLWKGSQQLQ  LKPGESAFIA  ANESPVTVKG  HGRLARVYNK  L*
```

**Figure 40. Deduced Amino Acid Sequence of the PMI Protein**

The deduced amino acid sequence from the translation of the *pmi* gene from plasmid PHP83175. The asterisk (\*) indicates the translational stop codon. The full-length protein is 391 amino acids in length and has a molecular weight of approximately 43 kDa.

### Function and Activity of the PMI Protein

The mode of action of PMI has been previously characterized and described ([Negrotto et al., 2000](#); [Privalle, 2002](#); [Reed et al., 2001](#); [Weisser et al., 1996](#)). PMI is widely present in nature and is expressed in fungi, insects, plants, and mammals ([Slein, 1950](#); [US-EPA, 2004](#)). The United States EPA has granted an exemption from the requirement of a tolerance for the PMI protein as an inert ingredient in plants ([US-EPA, 2004](#)). The PMI protein catalyzes the reversible interconversion between mannose-6-phosphate and fructose-6-phosphate. Mannose is phosphorylated by hexokinase to mannose-6-phosphate and in the presence of PMI enters the glycolytic pathway after isomerization to fructose 6-phosphate. In the absence of PMI, mannose-6-phosphate accumulates in the plant cells and inhibits glycolysis; additionally, high levels of mannose can lead to other impacts on photosynthesis and ATP production ([Negrotto et al., 2000](#); [Privalle, 2002](#)). However, in the presence of PMI, plant cells may survive on media containing mannose as a carbon source, thus allowing PMI to be utilized as a selectable marker ([Negrotto et al., 2000](#); [Reed et al., 2001](#)).

### Characterization of the PMI Protein Derived from DP915635 Maize

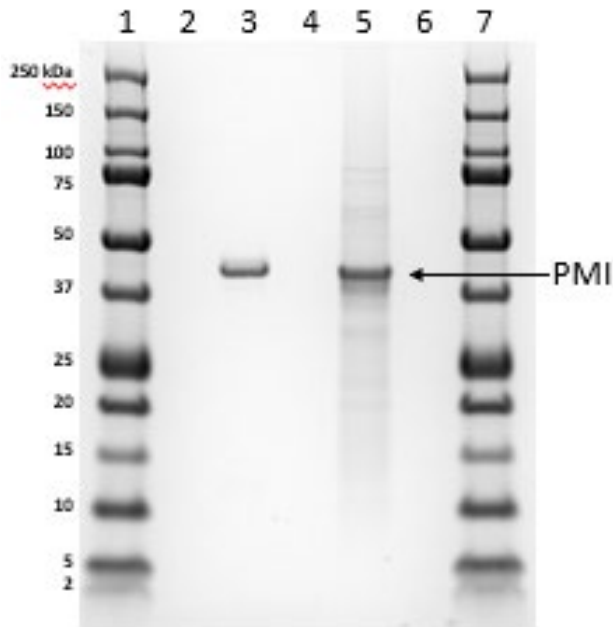
The DP915635 maize-expressed PMI protein was characterized using SDS-PAGE, western blot, glycosylation, mass spectrometry peptide mapping, and N-terminal amino acid sequence. The results demonstrated that the PMI protein derived from DP915635 maize is of the expected molecular weight, immunoreactivity, lack of glycosylation, and amino acid sequence.

### SDS-PAGE Analysis

Samples of PMI protein purified from DP915635 root tissue were analyzed by SDS-PAGE. As expected, the PMI protein derived from DP915635 maize migrated as a band consistent with the expected molecular weight of approximately 43 kDa and with a microbially derived PMI protein reference substance (Figure 41).

Additional details regarding SDS-PAGE analytical methods are provided in Appendix G.

Detailed methods and results are provided in the [PHI-2020-166 study](#).



Lane	Sample Identification
1	Pre-stained Protein Molecular Weight Marker <sup>a</sup>
2	1X LDS/DTT Sample Buffer Blank
3	PMI Reference Standard (1 µg)
4	1X LDS/DTT Sample Buffer Blank
5	DP915635 Maize-Derived PMI Protein
6	1X LDS/DTT Sample Buffer Blank
7	Pre-stained Protein Molecular Weight Marker

Note: kilodalton (kDa) and microgram (µg).

<sup>a</sup> Molecular weight markers were included to provide a visual estimate that migration was within the expected range of the predicted molecular weight.

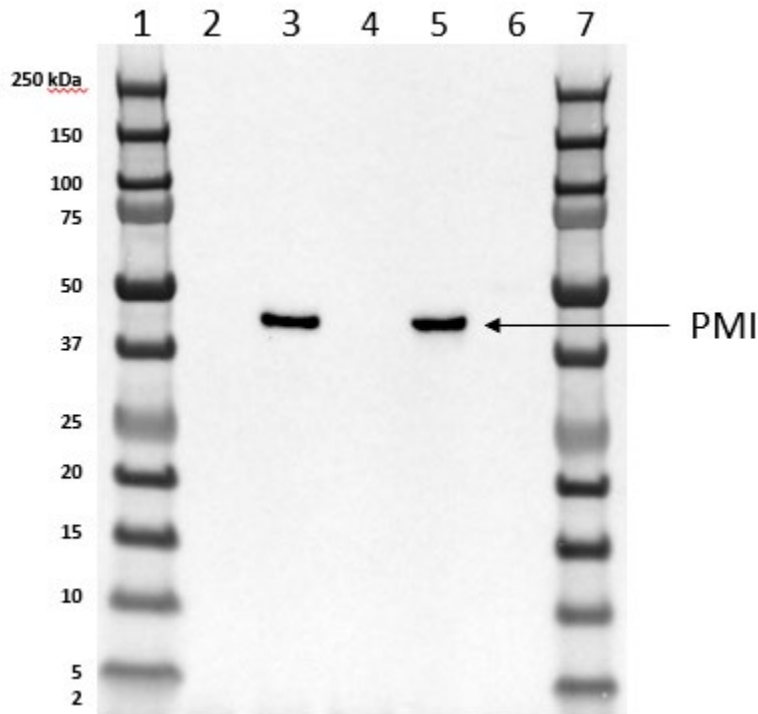
**Figure 41. SDS-PAGE Analysis of DP915635 Maize-Derived PMI Protein**

### Western Blot Analysis

Samples of PMI protein purified from DP915635 maize root tissue were analyzed by Western blot. As expected, the PMI protein derived from DP915635 maize was immunoreactive to a PMI monoclonal antibody and visible as a band consistent with the expected molecular weight of approximately 43 kDa and with a microbially derived PMI protein reference substance (Figure 42).

Additional details regarding western blot analytical methods are provided in Appendix G.

Detailed methods and results are provided in the [PHI-2020-166 study](#).



Lane	Sample Identification
1	Pre-stained Protein Molecular Weight Marker <sup>a</sup>
2	1X LDS/DTT Sample Buffer Blank
3	PMI Reference Standard (10 ng)
4	1X LDS/DTT Sample Buffer Blank
5	DP915635 Maize-Derived PMI Protein <sup>b</sup>
6	1X LDS/DTT Sample Buffer Blank

7	Pre-stained Protein Molecular Weight Marker
---	---

Note: kilodalton (kDa) and nanogram (ng).

<sup>a</sup> Molecular weight markers were included to provide a visual estimate that migration was within the expected range of the predicted molecular weight.

<sup>b</sup> Diluted 1:300.

**Figure 42. Western Blot Analysis of DP915635 Maize-Derived PMI Protein**

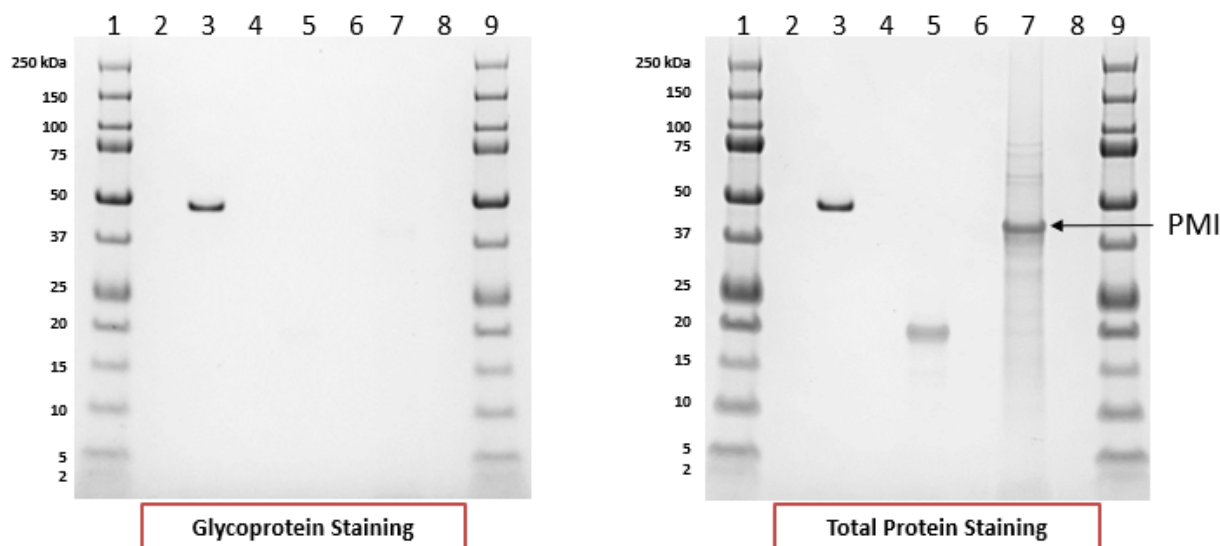
*Glycosylation Analysis*

The of PMI protein purified from DP915635 maize root tissue was analyzed by SDS-PAGE. The gel also included a positive control (horseradish peroxidase) and negative control (soybean trypsin inhibitor). The gel was stained using a Pierce Glycoprotein Staining Kit to visualize any glycoproteins. The gel was imaged and then stained with GelCode Blue stain reagent to visualize all protein bands.

Glycosylation was not detected for the PMI protein (Figure 43). The horseradish peroxidase positive control was stained and clearly visible as a magenta-colored band. The soybean trypsin inhibitor negative control was not stained by the glycoprotein stain.

Additional details regarding glycosylation analytical methods are provided in Appendix G.

Detailed methods and results are provided in the [PHI-2020-166 study](#).



Lane	Sample Identification
1	Pre-stained Protein Molecular Weight Marker <sup>a</sup>
2	1X LDS/DTT Sample Buffer Blank
3	Horseradish Peroxidase (1.0 µg)

4	1X LDS/DTT Sample Buffer Blank
5	Soybean Trypsin Inhibitor (1.0 µg)
6	1X LDS/DTT Sample Buffer Blank
7	DP915635 Maize-Derived PMI Protein
8	1X LDS/DTT Sample Buffer Blank
9	Pre-stained Protein Molecular Weight Marker

Note: kilodalton (kDa) and microgram (µg). The gel on the left was stained with glycoprotein staining reagent. The gel on the right was stained with glycoprotein staining reagent followed by staining with Coomassie Blue Reagent for total proteins.

<sup>a</sup> Molecular weight markers were included to provide a visual estimate that migration was within the expected range of the predicted molecular weight.

### Figure 43. Glycosylation Analysis of DP915635 Maize-Derived PMI Protein

#### LC-MS Peptide Mapping and N-Terminal Amino Acid Sequencing Analyses

Samples of PMI protein purified from DP915635 maize root tissue were analyzed by SDS-PAGE. Protein bands were stained with Coomassie stain reagent, and the band containing PMI protein was excised for each sample. The excised PMI protein bands were digested with trypsin or chymotrypsin. Digested samples were analyzed using LC-MS, and an MS/MS ion search was used to match the detected peaks to peptides from the expected PMI protein sequence.

The identified tryptic and chymotryptic peptides for DP915635 maize-derived PMI protein are shown in Table 25 and Table 26, respectively, and together accounted for 91.8% (359/391) of the expected PMI amino acid sequence (Table 27 and Figure 44).

The N-terminal peptide was identified as MQKLINSVQNY from the chymotryptic digestion and the sequence matched amino acid residues 1-11 of the expected protein sequence). The results also indicated the N-terminal methionine residue of the protein was acetylated.

Additional details regarding peptide mapping and N-terminal amino acid sequencing analytical methods are provided in Appendix G.

Detailed methods and results are provided in the [PHI-2020-166 study](#).

**Table 25. Identified Tryptic Peptides of DP915635 Maize-Derived PMI Protein Using LC-MS Analysis**

Matched Residue Position	Experimental Mass <sup>a</sup>	Theoretical Mass <sup>b</sup>	Identified Peptide Sequence
4 – 16	1478.7504	1478.7518	LINSVQNYAWGSK
48 – 59	1241.6724	1241.6728	VQNAAGDIVSLR
48 – 66	2028.0496	2028.0487	VQNAAGDIVSLRDVIESDK
60 – 66	804.3846	804.3865	DVIESDK
60 – 76	1773.9356	1773.936	DVIESDKSTLLGEAVAK
67 – 76	987.5587	987.56	STLLGEAVAK
78 – 86	1096.5945	1096.5957	FGELPFLFK
87 – 102	1773.9552	1773.956	VLCAAQPLSIQVHPNK

103 – 111	1001.4921	1001.493	HNSEIGFAK
112 – 124	1343.6129	1343.6139	ENAAGIPMDAAER
180 – 195	1807.9072	1807.9026	LSELFASLLNMQGEEK
198 – 203	627.4306	627.4319	ALAILK
204 – 218	1714.8317	1714.8275	SALDSQQGEPWQTIR
281 – 292	1372.7605	1372.7602	YIDIPELVANVK
293 – 307	1682.9349	1682.9355	FEAKPANQLLTQPVK
355 – 379	2598.3632	2598.3653	GSQQLQLKPGESAFIAANESPVTVK

<sup>a</sup> The experimental mass is the uncharged mass calculated from the mass to charge ratio of the observed ion.

<sup>b</sup> The theoretical mass is the *in silico* generated mass that matches closest to the experimental mass.

**Table 26. Identified Chymotryptic Peptides of DP915635 Maize-Derived PMI Protein Using LC-MS Analysis**

Matched Residue Position	Experimental Mass <sup>a</sup>	Theoretical Mass <sup>b</sup>	Identified Peptide Sequence
1 – 11	1394.6913	1394.6864	MQKLINSVQNY <sup>c,d</sup>
5 – 11	836.4013	836.4028	INSVQNY
12 – 19	832.4437	832.4443	AWGSKTAL
12 – 22	1175.6201	1175.6186	AWGSKTALTEL
14 – 23	1081.5679	1081.5655	GSKTALTELY
24 – 36	1389.5955	1389.5904	GMENPSSQPMAEL
24 – 37	1575.6766	1575.6697	GMENPSSQPMAELW
59 – 69	1261.6521	1261.6514	RDVIESDKSTL
59 – 70	1374.737	1374.7354	RDVIESDKSTLL
70 – 78	989.5654	989.5658	LGEAVAKRF
71 – 78	876.4815	876.4817	GEAVAKRF
95 – 109	1705.8601	1705.8536	SIQVHPNKHNSEIGF
110 – 126	1819.8573	1819.8522	AKENAAGIPMDAAERNY
127 – 137	1322.6995	1322.6983	KDPNHKPELVF
143 – 151	1113.5287	1113.5277	LAMNAFREF <sup>d</sup>
144 – 151	984.4503	984.4487	AMNAFREF
149 – 157	1078.5676	1078.5659	REFSEIVSL
149 – 158	1191.653	1191.6499	REFSEIVSLL
158 – 171	1427.7705	1427.7674	LQPVAGAHPAIAHF
159 – 171	1314.6833	1314.6833	QPVAGAHPAIAHF
172 – 180	1068.5578	1068.5564	LQQPDAERL
172 – 183	1397.7207	1397.715	LQQPDAERLSEL
173 – 184	1431.7059	1431.6994	QQPDAERLSELF
188 – 199	1374.6932	1374.6925	LNMQGEEKSRAL
189–199	1261.6083	1261.6084	NMQGEEKSRAL
200 – 206	714.4618	714.4639	AILKSAL
200 – 214	1641.8461	1641.8362	AILKSALDSQQGEPW
203 – 214	1344.636	1344.631	KSALDSQQGEPW
207 – 214	945.3835	945.3828	DSQQGEPW
215 – 219	629.3852	629.386	QTIRL
215 – 223	1105.615	1105.6131	QTIRLISEF
220 – 231	1402.6347	1402.6293	ISEFYPEDSGLF
235 – 241	797.5359	797.5375	LLNVVKL
237 – 248	1317.6773	1317.6751	NVVKLNPGEAMF
237 – 249	1430.764	1430.7592	NVVKLNPGEAMFL

Matched Residue Position	Experimental Mass <sup>a</sup>	Theoretical Mass <sup>b</sup>	Identified Peptide Sequence
249 – 257	1047.5032	1047.5025	LFAETPHAY
250 – 257	934.4197	934.4185	FAETPHAY
250 – 258	1047.5032	1047.5025	FAETPHAYL
251 – 257	787.3484	787.3501	AETPHAY
258 – 273	1671.8611	1671.8502	LQGVALEVMANS DNVL
259 – 273	1558.7725	1558.7661	QGVALEVMANS DNVL
264 – 273	1090.4971	1090.4965	EVMANS DNVL
294 – 301	869.4606	869.4606	EAKPANQL
294 – 302	982.5473	982.5447	EAKPANQLL
302 – 312	1182.6649	1182.6608	LTQPVKQGAEL
303 – 312	1069.5769	1069.5768	TQPVKQGAEL
303 – 321	2115.0681	2115.0525	TQPVKQGAELDFPIPVDDF
303 – 323	2333.1706	2333.158	TQPVKQGAELDFPIPVDDFAF
313 – 321	1063.4882	1063.4863	DFPIPVDDF
324 – 343	2156.108	2156.0961	SLHDLSDKETTISQQAAIL
344 – 353	1196.5188	1196.5172	FCVEGDATLW
345 – 353	1049.45	1049.4488	CVEGDATLW
354 – 359	659.3586	659.3602	KGSQQL
354 – 361	900.5021	900.5029	KGSQQLQL
360 – 368	975.5036	975.5025	QLKPGESAF
369 – 384	1647.9078	1647.9056	IAANESPVTVKGGHRL

<sup>a</sup> The experimental mass is the uncharged mass calculated from the mass to charge ratio of the observed ion.

<sup>b</sup> The theoretical mass is the *in silico* generated mass that matches closest to the experimental mass.

<sup>c</sup> The N-terminus was acetylated.

<sup>d</sup> This peptide was modified by methionine oxidation (Oxidation-M).

**Table 27. Combined Sequence Coverage of Identified Tryptic and Chymotryptic Peptides of DP915635 Maize-Derived PMI Protein Using LC-MS Analysis**

Protease	% Coverage	Combined % Coverage
Trypsin	45	91.8
Chymotrypsin	80	

1 MQKLINSVQN YAWGSKTALT ELYGMENPSS QPMAELWMGA HPKSSSRVQN  
 51 AAGDIVSLRD VIESDKSTLL GEAVAKRFGE LPFLFKVLCA AQPLSIQVHP  
 101 NKHNSEIGFA KENAAGIPMD AAERNYKDPN HKPELVFALT PFLAMNAFRE  
 151 FSEIVSLLQP VAGAHPAIAH FLOQPAERL SELFASLLNM QGEEKSRALA  
 201 ILKSALDSQQ GEPWQTIRLI SEFYPEDSGL FSPLLLNVVK LNPGEAMFLF  
 251 AETPHAYLQG VALEVMANS NVLRAGLTPK YIDIPELVAN VKFEAKPANQ  
 301 LLTQPVKQGA ELDFPIPVDD FAFSLHDLSD KETTISQQA AILFCVEGDA  
 351 TLWKGSQQLQ LKPGESAFIA ANESPVTVKG HGRLARVYNK L

Gray shading	Gray-shaded type indicates maize-derived PMI peptides identified using LC-MS analysis.
Amino acid residue abbreviations	alanine (A), cysteine (C), aspartic acid (D), glutamic acid (E), phenylalanine (F), glycine (G), histidine (H), isoleucine (I), lysine (K), leucine (L), methionine (M), asparagine (N), proline (P), glutamine (Q), arginine (R), serine (S), threonine (T), tryptophan (W), tyrosine (Y), and valine (V).

**Figure 44. Amino Acid Sequence of DP915635 Maize-Derived PMI Protein Indicating the Identified Tryptic and Chymotryptic Peptide Using LC-MS Analysis**

### Allergenicity and Toxicity of the PMI Protein

The PMI protein present in DP915635 maize is found in several approved events that are currently in commercial use. Therefore, in accordance with the FSANZ Application Handbook, only the updated bioinformatics analysis is provided in this dossier for safety assessment.

#### *Bioinformatic Analysis of PMI Protein Homology to Known or Putative Allergens (2020-205/201 study)*

Assessing newly expressed proteins for potential cross-reactivity with known or putative allergens is an important part of the weight-of-evidence approach used to evaluate the safety of these proteins in genetically-modified plant products ([Codex Alimentarius Commission, 2003](#)). In this study, a bioinformatic assessment of the PMI protein sequence for potential cross-reactivity with known or putative allergens was conducted according to relevant guidelines ([Codex Alimentarius Commission, 2003](#); [FAO/WHO, 2001](#)).

Two separate searches for the PMI protein sequence were performed using the Comprehensive Protein Allergen Resource (COMPARE) 2020 database (January 2020) available at <http://comparedatabase.org>. This peer-reviewed database is a collaborative effort of the Health and Environmental Sciences Institute (HESI) Protein Allergens, Toxins, and Bioinformatics (PATB) Committee and is comprised of 2,248 sequences.

The first search used the PMI protein sequence as the query in a FASTA v35.4.4 ([Pearson and Lipman, 1988](#)) search against the allergen sequences. The search was conducted using default parameters, except the *E*-score threshold was set to  $10^{-4}$ . An *E*-score threshold of  $10^{-4}$  has been shown to be an appropriate value for allergenicity searches ([Mirsky et al., 2013](#)). The generated alignments were examined to identify any that are a length of 80 or greater and possess a sequence identity of  $\geq 35\%$ . The second search used the FUZZPRO program (Emboss Package v6.4.0) to identify any contiguous 8-residue identical matches between the PMI protein sequence and the allergen sequences.

Results of the search of the PMI protein sequence against the COMPARE database of known and putative allergen sequences found no alignments that were a length of 80 or greater with a sequence identity of  $\geq 35\%$ . One contiguous 8-residue amino acid match (DLSDKETT) was found between the PMI protein sequence and the sequence of an allergen (a putative alpha-parvalbumin from frog, GenBank Accession CAC83047.1; [Hilger et al., 2002](#)). Comprehensive analysis of this match strongly indicates that this is a false positive and is unlikely to represent a cross-reactive risk.

Collectively, these data indicate that no allergenicity concern arose from the bioinformatics assessment of the PMI protein.

*Bioinformatic Analysis of PMI Protein Homology to Known or Putative Toxins (PHI-2020-206/211 study)*

Assessing newly expressed proteins for potential toxicity is an important part of the weight-of-evidence approach used to evaluate the safety of these proteins in genetically modified plant products ([Codex Alimentarius Commission, 2003](#)). The potential toxicity of the PMI protein was assessed by comparison of its sequence to the sequences in an internal toxin database. The internal toxin database is a subset of sequences found in UniProtKB/Swiss-Prot (<https://www.uniprot.org/>). To produce the internal toxin database, the proteins in UniProtKB/Swiss-Prot are filtered for molecular function by keywords that could imply toxicity or adverse health effects (e.g., toxin, hemagglutinin, vasoactive, etc.). The internal toxin database is updated annually.

The search between the PMI protein sequence and protein sequences in the internal toxin database was conducted with BLASTP using default parameters, except that low complexity filtering was turned off, the *E*-value threshold was set to  $10^{-4}$ , and unlimited alignments were returned.

No alignments with an *E*-value  $\leq 10^{-4}$  were returned between the PMI protein sequence and any protein sequence in the internal toxin database.

Based on these data, no toxicity concerns arose from the bioinformatics assessment of the PMI protein.

#### **Conclusions on the Safety of PMI Protein in DP915635 Maize**

The amino acid sequence of the PMI protein present in DP915635 maize was demonstrated to be identical to the corresponding protein found in a number of authorized GM events across several different crops that are currently commercialized and have a history of safe use.

Therefore, in accordance with the FSANZ Application Handbook, only the updated bioinformatics analysis is provided in this dossier for safety assessment. This along with the history of safe use of the PAT protein expressed in DP915635 maize supports a weight of evidence that the PMI protein is unlikely to present significant risks to the environment, human, or animal health.

### B.3 OTHER (NON-PROTEIN) NEW SUBSTANCES

There are no other new substances associated with DP915635 maize.

### B.4 NOVEL HERBICIDE METABOLITES IN GM HERBICIDE-TOLERANT PLANTS

There are no novel herbicide metabolites associated with DP915635 maize.

### B.5 COMPOSITIONAL ANALYSES OF THE FOOD PRODUCED USING GENE TECHNOLOGY

#### Trait Expression Assessment ([PHI-2019-015 study](#))

The expression levels of the IPD079Ea, PAT, and PMI proteins were evaluated in DP915635 maize.

Tissue samples were collected during the 2019 growing season at six sites in commercial maize-growing regions of the United States and Canada. A randomized complete block design with four blocks was utilized at each site. The following tissue samples were collected: root (V6, V9, R1, and R4 growth stages), leaf (V9, R1, and R4 growth stages), pollen (R1 growth stage), forage (R4 growth stage), and grain (R6 growth stage). During sample processing, a lyophilizer issue occurred which affected all of the root R1 samples as well as some of the leaf R1 and root R4 samples; data for the affected samples will not be reported. The concentrations of the IPD079Ea, PAT, and PMI proteins were determined using quantitative enzyme-linked immunosorbent assays (ELISAs).

Concentration results (means, ranges, and standard deviations) are summarized across sites in Table 28 - Table 30 for IPD079Ea protein, PAT protein, and PMI protein, respectively. Individual sample results below the LLOQ were assigned a value equal to half of the LLOQ for calculation purposes.

Additional details regarding methods for trait expression analysis are provided in Appendix H.

Detailed methods and results are provided in the [PHI-2019-015 study](#).

**Table 28. Across-Sites Summary of IPD079Ea Protein Concentrations in DP915635 Maize**

Tissue (Growth Stage)	ng IPD079Ea/mg Tissue Dry Weight				Number of Samples <LLOQ/ Number of Samples Reported
	Mean	Range	Standard Deviation	Sample LLOQ	
Root (V6)	18	5.7 - 25	4.1	0.069	0/24
Root (V9)	10	0.63 - 33	6.5	0.069	0/24
Root (R4)	1.1	0.36 - 2.0	0.52	0.069	0/24
Leaf (V9)	0.82	0.45 - 2.6	0.46	0.14	0/24
Leaf (R1)	0.080 <sup>a</sup>	<0.14 - 0.16	0.027 <sup>a</sup>	0.14	21/24
Leaf (R4)	<0.14	<0.14	ND	0.14	24/24
Pollen (R1)	0.88	0.62 - 1.3	0.20	0.28	0/24
Forage (R4)	0.24	0.12 - 0.40	0.072	0.046	0/24
Grain (R6)	0.16 <sup>a</sup>	<0.069 - 0.30	0.068 <sup>a</sup>	0.069	2/24

Note: Growth stages ([Abendroth et al. 2011](#)). Lower limit of quantification (LLOQ) in ng/mg tissue dry weight. Not determined (ND); all samples were below the LLOQ. An additional tissue set was collected (root at R1 growth stage); however, sample integrity was compromised during lyophilization and therefore these samples were not reported.

<sup>a</sup> Some, but not all, sample results were below the LLOQ. A value equal to half the LLOQ value was assigned to those samples to calculate the mean and standard deviation.

**Table 29. Across-Sites Summary of PAT Protein Concentrations in DP915635 Maize.**

Tissue (Growth Stage)	ng PAT/mg Tissue Dry Weight				Number of Samples <LLOQ/ Number of Samples Reported
	Mean	Range	Standard Deviation	Sample LLOQ	
Root (V6)	13	6.6 - 17	2.6	0.054	0/24
Root (V9)	8.6	2.6 - 19	4.3	0.054	0/24
Root (R4)	1.7	0.54 - 3.3	0.66	0.054	0/24
Leaf (V9)	5.0	2.9 - 10	1.7	0.11	0/24
Leaf (R1)	7.0	5.5 - 9.6	1.0	0.11	0/24
Leaf (R4)	3.8	1.9 - 5.0	0.85	0.11	0/24
Pollen (R1)	79	64 - 98	10	0.22	0/24
Forage (R4)	9.2	4.0 - 16	2.3	0.036	0/24
Grain (R6)	7.3	1.6 - 13	2.9	0.054	0/24

Note: Growth stages ([Abendroth et al., 2011](#)). Lower limit of quantification (LLOQ) in ng/mg tissue dry weight. Not determined (ND); all samples were below the LLOQ. An additional tissue set was collected (root at R1 growth stage); however, sample integrity was compromised during lyophilization and therefore these samples were not reported.

**Table 30. Across-Sites Summary of PMI Protein Concentrations in DP915635 Maize**

Tissue (Growth Stage)	ng PMI/mg Tissue Dry Weight				Number of Samples <LLOQ/ Number of Samples Reported
	Mean	Range	Standard Deviation	Sample LLOQ	
Root (V6)	6.4	4.2 - 11	1.6	0.27	0/24
Root (V9)	5.1	2.1 - 8.4	1.8	0.27	0/24
Root (R4)	2.5	1.5 - 3.9	0.72	0.27	0/24
Leaf (V9)	6.6	3.8 - 11	2.0	0.54	0/24
Leaf (R1)	14	9.0 - 28	3.9	0.54	0/24
Leaf (R4)	28	20 - 34	3.1	0.54	0/24
Pollen (R1)	22	17 - 26	2.4	1.1	0/24
Forage (R4)	8.9	5.4 - 11	1.3	1.8	0/24
Grain (R6)	4.0	1.4 - 8.4	1.8	0.27	0/24

Note: Growth stages ([Abendroth et al., 2011](#)). Lower limit of quantification (LLOQ) in ng/mg tissue dry weight. An additional tissue set was collected (root at R1 growth stage); however, sample integrity was compromised during lyophilization and therefore these samples were not reported.

### Nutrient Composition Assessment ([PHI-2019-016/021 study](#))

An assessment of the compositional comparability of a GM product compared to that of a conventional non-GM comparator with a history of safe use in food and feed is an important part of the weight-of-evidence approach used to evaluate the safety of genetically modified plant products ([Codex Alimentarius Commission, 2008](#); [OECD, 1993](#)). Compositional assessments of DP915635 maize were evaluated in comparison to concurrently grown non-GM, near-isoline maize (referred to as control maize) to identify statistical differences, and subsequently were evaluated in the context of biological variation established from multiple sources of non-GM, commercial maize data.

Forage (R4 growth stage) and grain (R6 growth stage) samples were collected during the 2019 growing season at eight sites in commercial maize-growing regions of the United States and Canada. A randomized complete block design with four blocks was utilized at each site. Each block included DP915635 maize, non-GM near-isoline control maize, and four non-GM commercial maize reference lines. An herbicide treatment of glufosinate was applied to DP915635 maize.

The samples were assessed for key nutritional components. Proximate, fiber, and mineral analytes were assessed in the forage samples (9 analytes total), and the grain sample assessment included proximate, fiber, fatty acid, amino acid, mineral, vitamin, secondary metabolite, and anti-nutrient analytes (69 analytes total). The analytes included in the compositional assessment were selected based on the OECD consensus document on compositional considerations for new varieties of maize ([OECD, 2002](#)). Procedures and methods for nutrient composition analyses of maize forage and grain were conducted in accordance with the requirements for the U.S. EPA Good Laboratory Practice (GLP) Standards, 40 CFR Part 160. The analytical procedures used were validated methods, with the majority based on methods published by AOAC International, AACC (American Association of Cereal Chemists), and AOCS (American Oil Chemists' Society).

Statistical analyses were conducted to evaluate and compare the nutrient composition of DP915635 maize and the control maize. Across-sites comparisons were conducted for a total of 72 analytes, where 69 analytes were analyzed using mixed model analysis and 2 analytes did not meet criteria for sufficient quantities of observations above the LLOQ and were therefore subjected to Fisher's exact test. No statistical analysis was conducted on the remaining 7 analytes as all data values were below the LLOQ. For a given analyte in the mixed model analysis, if a statistical difference ( $P$ -value  $< 0.05$ ) was observed between DP915635 maize and the control maize, the False Discovery Rate (FDR)-adjusted  $P$ -value was examined. In cases where a raw  $P$ -value indicated a significant difference but the FDR-adjusted  $P$ -value was non-significant, it was concluded that the difference was likely a false positive. Additionally, three reference ranges representing the non-GM maize population with a history of safe use (i.e., tolerance interval, literature range, and in-study reference range) were utilized to evaluate statistical differences in the context of biological variation. If the measured values of DP915635 maize for that analyte fell within at least one of the reference ranges, then this analyte would be considered comparable to conventional maize.

The outcome of the nutrient composition assessment is provided in Table 31. Nutrient composition analysis results are provided in Table 32 to Table 42. No statistically significant differences were observed between DP915635 maize and the control maize for 66 of the analytes that went through across-site analysis via either mixed model analysis or Fisher's exact test. A statistically significant difference, before FDR adjustment, was observed in the across-site analysis between DP915635 maize and the control maize for 4 grain analytes: palmitoleic acid (C16:1), lignoceric acid (C24:0), iron, and *p*-coumaric acid. After FDR adjustment of  $P$ -values, the FDR-adjusted  $P$ -value was not significant for all 4 analytes, indicating that the observed differences were likely false positives. The two fatty acids were within the tolerance interval, while iron and *p*-coumaric acid exceeded the tolerance interval but were within the literature range. All individual values for these analytes were within the literature range, and/or in-study reference range, indicating DP915635 maize is within the range of biological variation for these analytes and the statistical differences are not biologically meaningful.

The results of the nutrient composition assessment demonstrated that nutrient composition of forage and grain derived from DP915635 maize was comparable to that of conventional maize represented by non-GM near-isoline control maize and non-GM commercial maize.

Additional details regarding methods for nutrient composition and statistical analyses are provided in Appendix I.

Detailed methods and results are provided in the [PHI-2019-016/021 study](#).

**Table 31. Outcome of the Nutrient Composition Assessment for DP915635 Maize**

Subgroup	No Statistical Difference Identified	Statistical Difference Identified				Adjusted P-Value<0.05	Not Included in Statistical Analysis (All Data Values Below the Lower Limit of Quantification)	
		All Data Values Within Tolerance Interval	One or More Data Values Outside Tolerance Interval, or Tolerance Interval Not Available		One or More Data Values Outside Literature Range			
			All Data Values Within Literature Range	One or More Data Values Outside Reference Data Range				
				All Data Values Within Reference Data Range				One or More Data Values Outside Reference Data Range
<b>Forage (R4 Growth Stage)</b>								
Proximate, Fiber, and Mineral Composition	Crude Protein Crude Fat Crude Fiber ADF NDF Ash Carbohydrates Calcium Phosphorus	--	--	--	--	--	--	
<b>Grain (R6 Growth Stage)</b>								
Proximate and Fiber Composition	Moisture Crude Protein Crude Fat Crude Fiber ADF NDF Total Dietary Fiber Ash Carbohydrates	--	--	--	--	--	--	
Fatty Acid Composition	Palmitic Acid (C16:0) Heptadecanoic Acid (C17:0) Stearic Acid (C18:0) Oleic Acid (C18:1) Linoleic Acid (C18:2) α-Linolenic Acid (C18:3) Arachidic Acid (C20:0) Eicosenoic Acid (C20:1) Behenic Acid (C22:0)	Palmitoleic Acid (C16:1) Lignoceric Acid (C24:0)	--	--	--	--	Lauric Acid (C12:0) Myristic Acid (C14:0) Heptadecenoic Acid (C17:1) Eicosadienoic Acid (C20:2)	

**Table 31. Outcome of Nutrient Composition Assessment Across Sites (continued)**

Subgroup	No Statistical Difference Identified	Statistical Difference Identified				Adjusted P-Value<0.05	Not Included in Statistical Analysis (All Data Values Below the Lower Limit of Quantification)	
		All Data Values Within Tolerance Interval	One or More Data Values Outside Tolerance Interval, or Tolerance Interval Not Available		One or More Data Values Outside Literature Range			
			All Data Values Within Literature Range	All Data Values Within Reference Data Range				
				All Data Values Within Reference Data Range				One or More Data Values Outside Reference Data Range
<b>Grain (R6 Growth Stage)</b>								
Amino Acid Composition	Alanine Arginine Aspartic Acid Cystine Glutamic Acid Glycine Histidine Isoleucine Leucine Lysine Methionine Phenylalanine Proline Serine Threonine Tryptophan Tyrosine Valine	--	--	--	--	--	--	

**Table 31. Outcome of Nutrient Composition Assessment Across Sites (continued)**

Subgroup	No Statistical Difference Identified	Statistical Difference Identified				Adjusted P-Value<0.05	Not Included in Statistical Analysis (All Data Values Below the Lower Limit of Quantification)	
		All Data Values Within Tolerance Interval	One or More Data Values Outside Tolerance Interval, or Tolerance Interval Not Available		One or More Data Values Outside Literature Range			
			All Data Values Within Literature Range	One or More Data Values Outside Literature Range				
				All Data Values Within Reference Data Range				One or More Data Values Outside Reference Data Range
<b>Grain (R6 Growth Stage)</b>								
Mineral Composition	Calcium Copper Magnesium Manganese Phosphorus Potassium Sodium Zinc	--	Iron	--	--	--	--	
Vitamin Composition	$\beta$ -Carotene Vitamin B1 (Thiamine) Vitamin B3 (Niacin) Vitamin B5 (Pantothenic Acid) Vitamin B6 (Pyridoxine) Vitamin B9 (Folic Acid) $\alpha$ -Tocopherol $\gamma$ -Tocopherol $\delta$ -Tocopherol Total Tocopherols	--	--	--	--	--	Vitamin B2 (Riboflavin) $\beta$ -Tocopherol	
Secondary Metabolite and Anti-Nutrient Composition	Ferulic Acid Inositol Phytic Acid Raffinose Trypsin Inhibitor	--	<i>p</i> -Coumaric Acid	--	--	--	Furfural	

Note: Growth stages ([Abendroth et al., 2011](#)).

*Proximate, Fiber, and Mineral Assessment of DP915635 Maize Forage*

Proximate, fiber, and mineral assessments were conducted on forage derived from DP915635 maize and control maize. Results are shown in Table 32. No statistically significant differences (P-value < 0.05) were observed between DP915635 maize and control maize.

The results of proximate, fiber, and mineral analysis in maize forage demonstrate that DP915635 maize is comparable to conventional maize represented by non-GM near-isoline control maize and non-GM commercial maize.

**Table 32. Proximate, Fiber, and Mineral Results for DP915635 Maize Forage**

Analyte	Reported Statistics	Control Maize	DP915635 Maize	Tolerance Interval	Literature Range	Reference Data Range
Crude Protein	Mean	7.22	6.83			
	Range	3.55 - 9.43	4.84 - 8.74			
	Confidence Interval	6.24 - 8.19	5.85 - 7.81	3.64 - 12.3	2.37 - 16.32	3.91 - 10.4
	Adjusted P-Value	--	0.737			
	P-Value	--	0.107			
Crude Fat	Mean	3.65	3.76			
	Range	2.00 - 6.08	2.43 - 5.83			
	Confidence Interval	3.25 - 4.06	3.35 - 4.17	0.822 - 6.42	NQ - 6.755	2.11 - 5.43
	Adjusted P-Value	--	0.830			
	P-Value	--	0.483			
Crude Fiber	Mean	23.1	23.0			
	Range	18.3 - 30.4	16.4 - 29.1			
	Confidence Interval	21.1 - 25.2	21.0 - 25.1	13.8 - 31.0	12.5 - 42	12.6 - 28.8
	Adjusted P-Value	--	0.961			
	P-Value	--	0.892			
ADF	Mean	28.0	28.0			
	Range	20.1 - 35.8	19.7 - 37.4			
	Confidence Interval	25.3 - 30.7	25.3 - 30.6	15.7 - 39.9	5.13 - 47.39	11.4 - 35.8
	Adjusted P-Value	--	0.996			
	P-Value	--	0.961			
NDF	Mean	45.6	46.3			
	Range	33.2 - 55.2	26.1 - 58.2			
	Confidence Interval	41.9 - 49.2	42.6 - 50.0	28.6 - 63.2	18.30 - 67.80	26.8 - 57.1
	Adjusted P-Value	--	0.830			
	P-Value	--	0.495			
Ash	Mean	4.21	4.10			
	Range	3.03 - 5.88	3.01 - 5.68			
	Confidence Interval	3.68 - 4.74	3.58 - 4.63	2.43 - 9.36	0.66 - 13.20	2.55 - 7.24
	Adjusted P-Value	--	0.803			
	P-Value	--	0.416			
Carbohydrates	Mean	84.9	85.3			
	Range	80.8 - 91.2	81.7 - 89.1			
	Confidence Interval	83.4 - 86.4	83.8 - 86.8	76.8 - 91.3	73.3 - 92.9	78.7 - 89.0
	Adjusted P-Value	--	0.803			
	P-Value	--	0.325			
Calcium	Mean	0.203	0.197			
	Range	0.0677 - 0.354	0.114 - 0.368			
	Confidence Interval	0.165 - 0.242	0.159 - 0.235	0.0755 - 0.530	0.04 - 0.58	0.0848 - 0.358
	Adjusted P-Value	--	0.913			
	P-Value	--	0.694			
Phosphorus	Mean	0.244	0.244			
	Range	0.149 - 0.376	0.138 - 0.353	0.0899 - 0.433	0.07 - 0.55	0.111 - 0.385
	Confidence Interval	0.210 - 0.278	0.210 - 0.278			

Analyte	Reported Statistics	Control Maize	DP915635 Maize	Tolerance Interval	Literature Range	Reference Data Range
	Adjusted P-Value	--	0.996			
	P-Value	--	0.996			

Note: Proximate, fiber, and mineral unit of measure is % dry weight. Not quantified (NQ); one or more assay values in the published literature references were below the lower limit of quantification (LLOQ) and were not quantified.

### Proximate and Fiber Assessment of DP915635 Maize Grain

Proximate and fiber assessments were conducted on grain derived from DP915635 maize and near-isoline control maize. Results are shown in Table 33. No statistically significant differences (P-value < 0.05) were observed between DP915635 maize and control maize.

The results of proximate and fiber analysis in maize grain demonstrate that DP915635 maize is comparable to conventional maize represented by non-GM near-isoline control maize and non-GM commercial maize.

**Table 33. Proximate and Fiber Results for DP915635 Maize Grain**

Analyte	Reported Statistics	Control Maize	DP915635 Maize	Tolerance Interval	Literature Range	Reference Data Range
Moisture	Mean	21.5	21.8			
	Range	10.6 - 31.9	10.0 - 33.8			
	Confidence Interval	17.0 - 26.0	17.3 - 26.3	3.92 - 37.8	5.1 - 40.7	9.89 - 32.4
	Adjusted P-Value	--	0.737			
	P-Value	--	0.167			
Crude Protein	Mean	9.71	9.78			
	Range	7.77 - 11.5	8.23 - 12.2			
	Confidence Interval	8.99 - 10.4	9.05 - 10.5	6.63 - 13.2	5.72 - 17.26	7.05 - 11.0
	Adjusted P-Value	--	0.897			
	P-Value	--	0.650			
Crude Fat	Mean	3.60	3.67			
	Range	2.92 - 5.07	2.38 - 4.49			
	Confidence Interval	3.40 - 3.79	3.47 - 3.86	2.38 - 5.91	1.363 - 7.830	1.95 - 5.31
	Adjusted P-Value	--	0.869			
	P-Value	--	0.577			
Crude Fiber	Mean	2.42	2.45			
	Range	2.08 - 2.78	2.01 - 2.97			
	Confidence Interval	2.31 - 2.53	2.34 - 2.56	1.58 - 3.54	0.49 - 5.5	1.94 - 3.08
	Adjusted P-Value	--	0.861			
	P-Value	--	0.549			
ADF	Mean	4.19	4.23			
	Range	3.47 - 4.90	3.40 - 5.39			
	Confidence Interval	3.91 - 4.47	3.95 - 4.50	2.67 - 6.15	1.41 - 11.34	2.53 - 5.69
	Adjusted P-Value	--	0.943			
	P-Value	--	0.747			
NDF	Mean	10.8	11.1			
	Range	8.83 - 15.7	8.82 - 18.5			
	Confidence Interval	9.60 - 12.1	9.88 - 12.3	7.57 - 18.1	4.28 - 24.30	7.98 - 17.9
	Adjusted P-Value	--	0.803			
	P-Value	--	0.416			
Total Dietary Fiber	Mean	8.73	8.83			
	Range	7.63 - 10.3	7.62 - 10.5			
	Confidence Interval	8.41 - 9.05	8.51 - 9.15	3.14 - 20.6	5.78 - 35.31	6.99 - 12.1
	Adjusted P-Value	--	0.803			
	P-Value	--	0.401			
Ash	Mean	1.34	1.36			
	Range	0.861 - 1.63	1.02 - 1.60	0.959 - 1.78	0.616 - 6.282	0.916 - 1.48

Analyte	Reported Statistics	Control Maize	DP915635 Maize	Tolerance Interval	Literature Range	Reference Data Range
Carbohydrates	Confidence Interval	1.23 - 1.46	1.24 - 1.47			
	Adjusted P-Value	--	0.818			
	P-Value	--	0.448			
	Mean	85.2	85.3			
	Range	82.9 - 87.8	82.4 - 87.0			
	Confidence Interval	84.3 - 86.1	84.4 - 86.2	80.6 - 88.5	77.4 - 89.7	82.4 - 88.8
	Adjusted P-Value	--	0.803			
	P-Value	--	0.419			

Note: Proximate and fiber unit of measure is % dry weight, with the exception of moisture (%).

#### Fatty Acid Assessment of DP915635 Maize Grain

A fatty acid assessment was conducted on grain derived from DP915635 maize and near-isoline control maize. Results are shown in Table 34 and Table 35.

A statistically significant difference (P-value < 0.05) was observed between DP915635 maize and control maize for two analytes: palmitoleic acid (C16:1) and lignoceric acid (C24:0). All individual values for these analytes were within the tolerance interval, indicating DP915635 maize is within the range of biological variation for these analytes and the statistical differences are not biologically meaningful. Additionally, the non-significant FDR-adjusted P-values for these analytes indicate that these differences were likely false positives.

The results of the analysis of fatty acids in maize grain demonstrate that DP915635 maize is comparable to conventional maize represented by non-GM near-isoline control maize and non-GM commercial maize.

**Table 34. Fatty Acid Results for DP915635 Maize Grain**

Analyte	Reported Statistics	Control Maize	DP915635 Maize	Tolerance Interval	Literature Range	Reference Data Range
Lauric Acid (C12:0)	Mean	<LLOQ <sup>a</sup>	<LLOQ <sup>a</sup>			
	Range	<LLOQ <sup>a</sup>	<LLOQ <sup>a</sup>			
	Confidence Interval	NA	NA	0 - 0.423 <sup>f</sup>	NQ - 0.698	<LLOQ <sup>a</sup>
	Adjusted P-Value	--	NA			
	P-Value	--	NA			
Myristic Acid (C14:0)	Mean	<LLOQ <sup>a</sup>	<LLOQ <sup>a</sup>			
	Range	<LLOQ <sup>a</sup>	<LLOQ <sup>a</sup>			
	Confidence Interval	NA	NA	0 - 0.267 <sup>f</sup>	NQ - 0.288	0.0319 - 0.0994
	Adjusted P-Value	--	NA			
	P-Value	--	NA			
Palmitic Acid (C16:0)	Mean	11.8	11.8			
	Range	11.3 - 13.0	11.2 - 12.8			
	Confidence Interval	11.4 - 12.1	11.4 - 12.1	9.45 - 24.5	6.81 - 39.0	10.8 - 14.7
	Adjusted P-Value	--	0.869			
	P-Value	--	0.586			
Palmitoleic Acid (C16:1)	Mean	0.119	0.123			
	Range	0.0940 - 0.145	0.101 - 0.139			
	Confidence Interval	0.111 - 0.127	0.115 - 0.131	0 - 0.435	NQ - 0.67	0.0911 - 0.184
	Adjusted P-Value	--	0.230			
	P-Value	--	0.0100 <sup>*</sup>			
Heptadecanoic Acid (C17:0)	Mean	0.0954	0.0945			
	Range	0.0393 - 0.116	0.0402 - 0.116	0 - 0.225	NQ - 0.203	0.0361 - 0.156
	Confidence Interval	0.0853 - 0.106	0.0844 - 0.105			

	Adjusted P-Value	--	0.803			
	P-Value	--	0.408			
Heptadecenoic Acid (C17:1)	Mean	<LLOQ <sup>a</sup>	<LLOQ <sup>a</sup>			
	Range	<LLOQ <sup>a</sup>	<LLOQ <sup>a</sup>			
	Confidence Interval	NA	NA	0 - 0.135 <sup>r</sup>	NQ - 0.131	0.0323 - 0.0990
	Adjusted P-Value	--	NA			
	P-Value	--	NA			
Stearic Acid (C18:0)	Mean	1.98	2.02			
	Range	1.74 - 2.44	1.75 - 2.51			
	Confidence Interval	1.80 - 2.16	1.84 - 2.20	1.32 - 3.69	NQ - 4.9	1.73 - 2.92
	Adjusted P-Value	--	0.566			
	P-Value	--	0.0652			
Oleic Acid (C18:1)	Mean	24.1	23.9			
	Range	22.2 - 25.6	22.7 - 25.1			
	Confidence Interval	23.6 - 24.5	23.4 - 24.4	16.9 - 38.4	16.38 - 42.81	21.0 - 32.2
	Adjusted P-Value	--	0.737			
	P-Value	--	0.171			
Linoleic Acid (C18:2)	Mean	58.8	59.0			
	Range	56.6 - 61.4	57.3 - 60.5			
	Confidence Interval	58.0 - 59.7	58.1 - 59.8	31.9 - 65.3	13.1 - 67.68	49.2 - 61.5
	Adjusted P-Value	--	0.803			
	P-Value	--	0.396			
$\alpha$ -Linolenic Acid (C18:3)	Mean	1.74	1.73			
	Range	1.55 - 1.89	1.58 - 1.89			
	Confidence Interval	1.68 - 1.81	1.67 - 1.80	0 - 2.06	NQ - 2.33	1.46 - 2.31
	Adjusted P-Value	--	0.855			
	P-Value	--	0.533			
Arachidic Acid (C20:0)	Mean	0.372	0.372			
	Range	0.329 - 0.458	0.338 - 0.453			
	Confidence Interval	0.341 - 0.403	0.341 - 0.403	0.296 - 0.850	0.267 - 1.2	0.328 - 0.510
	Adjusted P-Value	--	0.961			
	P-Value	--	0.847			
Eicosenoic Acid (C20:1)	Mean	0.319	0.316			
	Range	0.278 - 0.423	0.274 - 0.397			
	Confidence Interval	0.308 - 0.331	0.304 - 0.327	0 - 0.581	NQ - 1.952	0.247 - 0.433
	Adjusted P-Value	--	0.762			
	P-Value	--	0.221			
Eicosadienoic Acid (C20:2)	Mean	<LLOQ <sup>a</sup>	<LLOQ <sup>a</sup>			
	Range	<LLOQ <sup>a</sup>	<LLOQ <sup>a</sup>			
	Confidence Interval	NA	NA	0 - 0.825 <sup>r</sup>	NQ - 2.551	<LLOQ <sup>a</sup>
	Adjusted P-Value	--	NA			
	P-Value	--	NA			
Behenic Acid (C22:0)	Mean	0.232	0.228			
	Range	0.171 - 0.299	0.177 - 0.284			
	Confidence Interval	0.210 - 0.254	0.205 - 0.250	0 - 0.430	NQ - 0.5	0.168 - 0.330
	Adjusted P-Value	--	0.737			
	P-Value	--	0.148			
Lignoceric Acid (C24:0)	Mean	0.301	0.295			
	Range	0.270 - 0.376	0.259 - 0.363			
	Confidence Interval	0.276 - 0.325	0.270 - 0.319	0 - 0.622	NQ - 0.91	0.250 - 0.451
	Adjusted P-Value	--	0.566			
	P-Value	--	0.0370 <sup>*</sup>			

Note: Fatty acid unit of measure is % total fatty acids. Not applicable (NA); mixed model analysis was not performed or confidence interval was not determined. Not quantified (NQ); one or more assay values in the published literature references were below the LLOQ and were not quantified.

<sup>a</sup> < LLOQ, all fatty acid sample values in the current study were below the assay LLOQ. Statistical analysis was not performed for those analytes.

<sup>r</sup> A historical reference data range was provided as tolerance interval was not calculated since the data did not meet the assumptions of any tolerance interval calculation method.

<sup>\*</sup> A statistically significant difference (P-Value < 0.05) was observed.

**Table 35. Number of Fatty Acid Sample Values Below the Lower Limit of Quantification for DP915635 Maize Grain**

Analyte	Number of Samples Below the LLOQ	
	Control Maize (n=32)	DP915635 Maize (n=32)
Lauric Acid (C12:0)	32	32
Myristic Acid (C14:0)	32	32
Heptadecanoic Acid (C17:0) <sup>a</sup>	1	2
Heptadecenoic Acid (C17:1)	32	32
Eicosadienoic Acid (C20:2)	32	32

<sup>a</sup> This analyte had < 50% below-LLOQ sample values in both maize lines and was subjected to the mixed model analyses.

*Amino Acid Assessment of DP915635 Maize Grain*

An amino acid assessment was conducted on grain derived from DP915635 maize and near-isoline control maize. Results are shown in Table 36. No statistically significant differences (P-value < 0.05) were observed between DP915635 maize and control maize.

The results of the analysis of amino acids in maize grain demonstrate that DP915635 maize is comparable to conventional maize represented by non-GM near-isoline control maize and non-GM commercial maize.

**Table 36. Amino Acid Results for DP915635 Maize Grain**

Analyte	Reported Statistics	Control Maize	DP915635 Maize	Tolerance Interval	Literature Range	Reference Data Range
Alanine	Mean	0.720	0.717			
	Range	0.550 - 0.887	0.556 - 0.907			
	Confidence Interval	0.658 - 0.782	0.655 - 0.779	0.453 - 1.07	0.40 - 1.48	0.465 - 0.865
	Adjusted P-Value	--	0.961			
	P-Value	--	0.846			
Arginine	Mean	0.406	0.407			
	Range	0.339 - 0.469	0.319 - 0.471			
	Confidence Interval	0.384 - 0.428	0.385 - 0.429	0.305 - 0.592	0.12 - 0.71	0.302 - 0.481
	Adjusted P-Value	--	0.977			
	P-Value	--	0.921			
Aspartic Acid	Mean	0.610	0.615			
	Range	0.493 - 0.723	0.448 - 0.728			
	Confidence Interval	0.560 - 0.660	0.565 - 0.665	0.415 - 0.895	0.30 - 1.21	0.412 - 0.758
	Adjusted P-Value	--	0.913			
	P-Value	--	0.702			
Cystine	Mean	0.234	0.229			
	Range	0.165 - 0.302	0.182 - 0.286			
	Confidence Interval	0.220 - 0.247	0.216 - 0.243	0.129 - 0.294	0.12 - 0.51	0.152 - 0.289
	Adjusted P-Value	--	0.818			
	P-Value	--	0.462			
Glutamic Acid	Mean	1.85	1.85			
	Range	1.29 - 2.33	1.43 - 2.39			
	Confidence Interval	1.67 - 2.03	1.67 - 2.03	1.11 - 2.76	0.83 - 3.54	1.17 - 2.21
	Adjusted P-Value	--	0.961			
	P-Value	--	0.892			
Glycine	Mean	0.364	0.370			
	Range	0.295 - 0.428	0.313 - 0.423			
	Confidence Interval	0.342 - 0.386	0.348 - 0.393	0.286 - 0.483	0.184 - 0.685	0.245 - 0.457
	Adjusted P-Value	--	0.803			
	P-Value	--	0.387			

Analyte	Reported Statistics	Control Maize	DP915635 Maize	Tolerance Interval	Literature Range	Reference Data Range
Histidine	Mean	0.297	0.302			
	Range	0.239 - 0.356	0.238 - 0.347			
	Confidence Interval	0.279 - 0.316	0.284 - 0.320	0.191 - 0.380	0.14 - 0.46	0.202 - 0.345
	Adjusted P-Value	--	0.818			
	P-Value	--	0.455			
Isoleucine	Mean	0.342	0.344			
	Range	0.267 - 0.414	0.272 - 0.434			
	Confidence Interval	0.316 - 0.369	0.318 - 0.371	0.212 - 0.494	0.18 - 0.69	0.226 - 0.404
	Adjusted P-Value	--	0.899			
	P-Value	--	0.664			
Leucine	Mean	1.22	1.22			
	Range	0.908 - 1.54	0.962 - 1.61			
	Confidence Interval	1.10 - 1.34	1.10 - 1.34	0.687 - 1.83	0.60 - 2.49	0.695 - 1.51
	Adjusted P-Value	--	0.961			
	P-Value	--	0.889			
Lysine	Mean	0.266	0.271			
	Range	0.210 - 0.333	0.195 - 0.328			
	Confidence Interval	0.242 - 0.291	0.247 - 0.295	0.180 - 0.399	0.129 - 0.668	0.188 - 0.348
	Adjusted P-Value	--	0.803			
	P-Value	--	0.273			
Methionine	Mean	0.214	0.204			
	Range	0.165 - 0.292	0.152 - 0.249			
	Confidence Interval	0.198 - 0.230	0.188 - 0.219	0.106 - 0.315	0.10 - 0.47	0.151 - 0.255
	Adjusted P-Value	--	0.737			
	P-Value	--	0.0982			
Phenylalanine	Mean	0.496	0.502			
	Range	0.376 - 0.601	0.387 - 0.621			
	Confidence Interval	0.455 - 0.538	0.460 - 0.543	0.302 - 0.735	0.24 - 0.93	0.299 - 0.612
	Adjusted P-Value	--	0.869			
	P-Value	--	0.592			
Proline	Mean	0.900	0.903			
	Range	0.701 - 1.10	0.726 - 1.14			
	Confidence Interval	0.825 - 0.975	0.828 - 0.979	0.558 - 1.25	0.46 - 1.75	0.549 - 0.989
	Adjusted P-Value	--	0.943			
	P-Value	--	0.757			
Serine	Mean	0.470	0.485			
	Range	0.320 - 0.593	0.350 - 0.603			
	Confidence Interval	0.432 - 0.509	0.447 - 0.524	0.310 - 0.681	0.15 - 0.91	0.303 - 0.579
	Adjusted P-Value	--	0.803			
	P-Value	--	0.366			
Threonine	Mean	0.364	0.373			
	Range	0.290 - 0.449	0.303 - 0.447			
	Confidence Interval	0.339 - 0.390	0.347 - 0.399	0.248 - 0.487	0.17 - 0.67	0.263 - 0.441
	Adjusted P-Value	--	0.786			
	P-Value	--	0.239			
Tryptophan	Mean	0.0572	0.0574			
	Range	0.0456 - 0.0706	0.0444 - 0.0740			
	Confidence Interval	0.0545 - 0.0598	0.0548 - 0.0601	0.0376 - 0.0990	0.027 - 0.215	0.0419 - 0.0723
	Adjusted P-Value	--	0.961			
	P-Value	--	0.830			
Tyrosine	Mean	0.256	0.242			
	Range	0.128 - 0.357	0.157 - 0.307			
	Confidence Interval	0.235 - 0.277	0.221 - 0.263	0.154 - 0.513	0.10 - 0.73	0.140 - 0.356
	Adjusted P-Value	--	0.759			
	P-Value	--	0.198			
Valine	Mean	0.454	0.457	0.306 - 0.629	0.21 - 0.86	0.329 - 0.519

Analyte	Reported Statistics	Control Maize	DP915635 Maize	Tolerance Interval	Literature Range	Reference Data Range
	Range	0.366 - 0.530	0.379 - 0.561			
	Confidence Interval	0.423 - 0.484	0.427 - 0.488			
	Adjusted P-Value	--	0.830			
	P-Value	--	0.505			

Note: Amino acid unit of measure is % dry weight.

### Mineral Assessment of DP915635 Maize Grain

A mineral assessment was conducted on grain derived from DP915635 maize and near-isoline control maize. Results are shown in Table 37 and Table 38.

A statistically significant difference (P-value < 0.05) was observed between DP915635 maize and control maize for one analyte (iron). As all values for this analyte were within one or more of the reference ranges, DP915635 maize is within the range of biological variation for this analyte and the statistical difference is not biologically meaningful. Additionally, the non-significant FDR-adjusted P-value for iron indicates that this difference was likely a false positive.

The results of the analysis of minerals in maize grain demonstrate that DP915635 maize is comparable to conventional maize represented by non-GM near-isoline control maize and non-GM commercial maize.

**Table 37. Mineral Results for DP915635 Maize Grain**

Analyte	Reported Statistics	Control Maize	DP915635 Maize	Tolerance Interval	Literature Range	Reference Data Range
Calcium	Mean	0.00288	0.00300			
	Range	0.00175 - 0.00468	0.00196 - 0.00475			
	Confidence Interval	0.00232 - 0.00343	0.00245 - 0.00355	0.00144 - 0.00737	NQ - 0.101	0.00178 - 0.00685
	Adjusted P-Value	--	0.759			
	P-Value	--	0.189			
Copper	Mean	0.0000912	0.0000785			
	Range	<0.0000625 <sup>a</sup> - 0.000176	<0.0000625 <sup>a</sup> - 0.000167	<0.0000625 <sup>a</sup> - 0.000345	NQ - 0.0021	<0.0000625 <sup>a</sup> - 0.000242
	Confidence Interval	0.0000573 - 0.000125	NA			
	Adjusted P-Value	--	NA			
	P-Value	--	NA			
Iron	Mean	0.00146	0.00156			
	Range	0.00112 - 0.00181	0.00114 - 0.00222			
	Confidence Interval	0.00135 - 0.00157	0.00145 - 0.00167	0.00116 - 0.00332	0.0000712 - 0.0191	0.00104 - 0.00221
	Adjusted P-Value	--	0.124			
	P-Value	--	0.00359*			
Magnesium	Mean	0.112	0.111			
	Range	0.0901 - 0.139	0.0833 - 0.144			
	Confidence Interval	0.101 - 0.122	0.101 - 0.122	0.0800 - 0.157	0.0035 - 1.000	0.0723 - 0.140
	Adjusted P-Value	--	0.961			
	P-Value	--	0.864			
Manganese	Mean	0.000570	0.000594			
	Range	0.000421 - 0.000756	0.000481 - 0.000812			
	Confidence Interval	0.000513 - 0.000628	0.000536 - 0.000651	0.000325 - 0.00121	0.0000312 - 0.0054	0.000302 - 0.000991
	Adjusted P-Value	--	0.566			
	P-Value	--	0.0524			
Phosphorus	Mean	0.318	0.323			
	Range	0.222 - 0.411	0.256 - 0.414	0.211 - 0.413	0.010 - 0.750	0.201 - 0.374
	Confidence Interval	0.286 - 0.350	0.291 - 0.356			

Analyte	Reported Statistics	Control Maize	DP915635 Maize	Tolerance Interval	Literature Range	Reference Data Range
Potassium	Adjusted P-Value	--	0.803			
	P-Value	--	0.367			
	Mean	0.342	0.348			
	Range	0.273 - 0.444	0.298 - 0.418			
	Confidence Interval	0.319 - 0.366	0.325 - 0.372	0.258 - 0.527	0.020 - 0.720	0.241 - 0.437
Sodium	Adjusted P-Value	--	0.803			
	P-Value	--	0.394			
	Mean	0.000208	0.000264			
	Range	<0.0000625 <sup>a</sup> - 0.00216	<0.0000625 <sup>a</sup> - 0.00791			
	Confidence Interval	0.0000971 - 0.000446	0.000123 - 0.000566	<LLOQ <sup>a</sup> - 0.0141	NQ - 0.15	<0.0000625 <sup>a</sup> - 0.00382
Zinc	Adjusted P-Value	--	0.883			
	P-Value	--	0.627			
	Mean	0.00183	0.00179			
	Range	0.00136 - 0.00236	0.00149 - 0.00234			
	Confidence Interval	0.00172 - 0.00195	0.00168 - 0.00191	0.00135 - 0.00343	0.0000283 - 0.0043	0.00123 - 0.00252
	Adjusted P-Value	--	0.803			
	P-Value	--	0.279			

Note: Mineral unit of measure is % dry weight. Not quantified (NQ); one or more assay values in the published literature references were below the LLOQ and were not quantified.

<sup>a</sup> < LLOQ; one or more sample values were below the assay LLOQ.

\* A statistically significant difference (P-Value < 0.05) was observed.

**Table 38. Number of Mineral Sample Values Below the Lower Limit of Quantification for DP915635 Maize Grain**

Analyte	Number of Samples Below the LLOQ		Fisher's Exact Test P-Value
	Control Maize (n=32)	DP915635 Maize (n=32)	
Copper	9	16	0.123
Sodium <sup>a</sup>	8	11	--

<sup>a</sup> This analyte had < 50% below-LLOQ sample values in both maize lines and was subjected to the mixed model analyses.

#### *Vitamin Assessment of DP915635 Maize Grain*

A vitamin assessment was conducted on grain derived from DP915635 maize and near-isoline control maize. Results are shown in Table 39 and Table 40. No statistically significant differences (P-value < 0.05) were observed between DP915635 maize and control maize.

The results of the analysis of vitamins in maize grain demonstrate that DP915635 maize is comparable to conventional maize represented by non-GM near-isoline control maize and non-GM commercial maize.

**Table 39. Vitamin Results for DP915635 Maize Grain**

Analyte	Reported Statistics	Control Maize	DP915635 Maize	Tolerance Interval	Literature Range	Reference Data Range
β-Carotene	Mean	0.167	0.178			
	Range	<0.0500 <sup>a</sup> - 0.340	<0.0500 <sup>a</sup> - 0.331			
	Confidence Interval	0.100 - 0.234	0.110 - 0.245	0.00197 - 3.68	0.3 - 5.4	<0.0500 <sup>a</sup> - 0.710
	Adjusted P-Value	--	0.803			
	P-Value	--	0.393			
Vitamin B1 (Thiamine)	Mean	2.90	2.89			
	Range	2.18 - 3.68	2.24 - 3.69			
	Confidence Interval	2.64 - 3.15	2.64 - 3.15	1.11 - 4.93	NQ - 40.00	1.89 - 3.91
	Adjusted P-Value	--	0.996			
	P-Value	--	0.979			
Vitamin B2 (Riboflavin)	Mean	<0.900 <sup>a</sup>	<0.900 <sup>a</sup>			
	Range	<0.900 <sup>a</sup>	<0.900 <sup>a</sup>			
	Confidence Interval	NA	NA	<0.900 <sup>a</sup> - 2.27 <sup>r</sup>	NQ - 7.35	<0.900 <sup>a</sup>
	Adjusted P-Value	--	NA			
	P-Value	--	NA			
Vitamin B3 (Niacin)	Mean	14.6	14.7			
	Range	12.0 - 19.5	12.3 - 21.2			
	Confidence Interval	12.8 - 16.4	12.9 - 16.5	7.66 - 31.3	NQ - 70	10.9 - 18.1
	Adjusted P-Value	--	0.876			
	P-Value	--	0.609			
Vitamin B5 (Pantothenic Acid)	Mean	5.68	5.74			
	Range	4.84 - 7.14	4.93 - 6.64			
	Confidence Interval	5.39 - 5.97	5.45 - 6.03	2.49 - 7.52	3.01 - 14	4.68 - 7.04
	Adjusted P-Value	--	0.737			
	P-Value	--	0.124			
Vitamin B6 (Pyridoxine)	Mean	4.92	4.41			
	Range	2.39 - 10.7	1.75 - 8.09			
	Confidence Interval	3.93 - 6.15	3.53 - 5.52	0.964 - 9.01	NQ - 12.14	1.76 - 10.2
	Adjusted P-Value	--	0.737			
	P-Value	--	0.171			
Vitamin B9 (Folic Acid)	Mean	1.91	1.60			
	Range	0.602 - 4.80	0.430 - 7.56			
	Confidence Interval	1.46 - 2.52	1.21 - 2.10	0.103 - 2.87	NQ - 3.50	0.290 - 6.98
	Adjusted P-Value	--	0.803			
	P-Value	--	0.297			
α-Tocopherol	Mean	3.67	3.84			
	Range	<0.500 <sup>a</sup> - 9.83	<0.500 <sup>a</sup> - 9.71			
	Confidence Interval	1.48 - 5.87	1.65 - 6.04	0 - 22.9	NQ - 68.67	<0.500 <sup>a</sup> - 25.2
	Adjusted P-Value	--	0.566			
	P-Value	--	0.0583			
β-Tocopherol	Mean	<0.500 <sup>a</sup>	<0.500 <sup>a</sup>			
	Range	<0.500 <sup>a</sup>	<0.500 <sup>a</sup>			
	Confidence Interval	NA	NA	<0.500 <sup>a</sup> - 1.10 <sup>r</sup>	NQ - 19.80	<0.500 <sup>a</sup> - 0.694
	Adjusted P-Value	--	NA			
	P-Value	--	NA			
γ-Tocopherol	Mean	21.4	21.3			
	Range	3.91 - 33.4	3.92 - 34.8			
	Confidence Interval	15.5 - 27.3	15.4 - 27.2	0.0611 - 55.4	NQ - 58.61	2.14 - 29.8
	Adjusted P-Value	--	0.961			
	P-Value	--	0.873			
δ-Tocopherol	Mean	0.303	0.319			
	Range	<0.500 <sup>a</sup> - 0.881	<0.500 <sup>a</sup> - 0.967			
	Confidence Interval	NA	NA	<0.500 <sup>a</sup> - 2.61 <sup>r</sup>	NQ - 14.61	<0.500 <sup>a</sup> - 0.707
	Adjusted P-Value	--	NA			
	P-Value	--	NA			
Total Tocopherols	Mean	25.7	25.7			
	Range	4.66 - 39.5	4.67 - 39.0	0 - 58.8	NQ - 89.91	5.52 - 39.0

Analyte	Reported Statistics	Control Maize	DP915635 Maize	Tolerance Interval	Literature Range	Reference Data Range
	Confidence Interval	18.2 - 33.2	18.2 - 33.2			
	Adjusted P-Value	--	0.996			
	P-Value	--	0.985			

Note: Vitamin unit of measure is mg/kg dry weight. Not quantified (NQ); one or more assay values in the published literature references were below the LLOQ and were not quantified. Not applicable (NA); mixed model analysis was not performed or confidence interval was not determined.

<sup>a</sup> < LLOQ; one or more sample values were below the assay LLOQ.

<sup>r</sup> Historical reference data range was provided as tolerance interval was not calculated since the data did not meet the assumptions of any tolerance interval calculation method.

**Table 40. Number of Vitamin Sample Values Below the Lower Limit of Quantification for DP915635 Maize Grain**

Analyte	Number of Samples Below the LLOQ		Fisher's Exact Test P-Value
	Control Maize (n=32)	DP915635 Maize (n=32)	
$\beta$ -Carotene <sup>a</sup>	9	7	--
Vitamin B2 (Riboflavin)	32	32	--
$\alpha$ -Tocopherol <sup>a</sup>	4	4	--
$\beta$ -Tocopherol	32	32	--
$\delta$ -Tocopherol	28	28	1.00

<sup>a</sup> This analyte had < 50% below-LLOQ sample values in both maize lines and was subjected to the mixed model analyses.

#### Secondary Metabolite and Anti-Nutrient Assessment of DP915635 Maize Grain

Secondary metabolite and anti-nutrient assessments were conducted on grain derived from DP915635 maize and near-isoline control maize. Results are shown in Table 41 and Table 42.

A statistically significant difference (P-value < 0.05) was observed between DP915635 maize and control maize for one analyte (*p*-coumaric acid). As all values for this analyte were within one or more of the reference ranges, DP915635 maize is within the range of biological variation for this analyte and the statistical difference is not biologically meaningful. Additionally, the non-significant FDR-adjusted P-value for *p*-coumaric acid indicates that this difference was likely a false positive.

The results of the analysis of secondary metabolites and anti-nutrients in maize grain demonstrate that DP915635 maize is comparable to conventional maize represented by non-GM near-isoline control maize and non-GM commercial maize.

**Table 41. Secondary Metabolite and Anti-Nutrient Results for DP915635 Maize Grain**

Analyte	Reported Statistics	Control Maize	DP915635 Maize	Tolerance Interval	Literature Range	Reference Data Range
<i>p</i> -Coumaric Acid	Mean	0.0258	0.0275			
	Range	0.0181 - 0.0441	0.0211 - 0.0539			
	Confidence Interval	0.0203 - 0.0313	0.0221 - 0.0330	0.00773 - 0.0485	NQ - 0.08	0.0126 - 0.0504
	Adjusted P-Value	--	0.124			
	P-Value	--	0.00187 <sup>*</sup>			
Ferulic Acid	Mean	0.238	0.245			
	Range	0.191 - 0.285	0.211 - 0.290			
	Confidence Interval	0.224 - 0.253	0.231 - 0.260	0.128 - 0.345	0.02 - 0.44	0.183 - 0.336
	Adjusted P-Value	--	0.762			
	P-Value	--	0.214			

Analyte	Reported Statistics	Control Maize	DP915635 Maize	Tolerance Interval	Literature Range	Reference Data Range
Furfural	Mean	<0.000100 <sup>a</sup>	<0.000100 <sup>a</sup>			
	Range	<0.000100 <sup>a</sup>	<0.000100 <sup>a</sup>			
	Confidence Interval	NA	NA	<0.0000500 <sup>a</sup>	NQ	<0.000100 <sup>a</sup>
	Adjusted P-Value	--	NA			
	P-Value	--	NA			
Inositol	Mean	0.0257	0.0272			
	Range	0.0185 - 0.0372	0.0182 - 0.0423			
	Confidence Interval	0.0218 - 0.0296	0.0232 - 0.0311	0.00731 - 0.0481	0.00613 - 0.257	0.0153 - 0.0523
	Adjusted P-Value	--	0.566			
	P-Value	--	0.0656			
Phytic Acid	Mean	0.970	0.979			
	Range	0.498 - 1.28	0.718 - 1.26			
	Confidence Interval	0.891 - 1.05	0.900 - 1.06	0.504 - 1.33	NQ - 1.940	0.538 - 1.13
	Adjusted P-Value	--	0.943			
	P-Value	--	0.765			
Raffinose	Mean	0.108	0.0837			
	Range	<0.0800 <sup>a</sup> - 0.216	<0.0800 <sup>a</sup> - 0.169			
	Confidence Interval	0.0712 - 0.145	NA	0 - 0.389	NQ - 0.466	<0.0800 <sup>a</sup> - 0.228
	Adjusted P-Value	--	NA			
	P-Value	--	NA			
Trypsin Inhibitor	Mean	2.25	2.36			
	Range	1.52 - 3.34	1.39 - 3.19			
	Confidence Interval	1.89 - 2.61	2.00 - 2.72	1.05 - 8.34	NQ - 8.42	1.25 - 3.82
	Adjusted P-Value	--	0.737			
	P-Value	--	0.162			

Note: Secondary metabolite and anti-nutrient unit of measure is % dry weight or as indicated. Trypsin inhibitors unit of measure is trypsin inhibitor units per milligram dry weight (TIU/mg DW). Not quantified (NQ); one or more assay values in the published literature references were below the lower limit of quantification (LLOQ) and were not quantified. Not applicable (NA); mixed model analysis was not performed or confidence interval was not determined

<sup>a</sup> < LLOQ, one or more sample values were below the assay LLOQ.

\* A statistically significant difference (P-Value < 0.05) was observed.

**Table 42. Number of Secondary Metabolite and Anti-Nutrient Sample Values Below the Lower Limit of Quantification for DP915635 Maize Grain**

Analyte	Number of Samples Below the LLOQ		Fisher's Exact Test P-Value
	Control Maize (n=32)	DP915635 Maize (n=32)	
Furfural	32	32	--
Raffinose	12	18	0.210

## **C. INFORMATION RELATED TO THE NUTRITIONAL IMPACT OF THE FOOD**

As seen in above Section B5, the compositional analysis did not indicate any biologically relevant changes to the levels of nutrients in the forage and grain derived from DP915635 maize compared to the non-GM counterpart. The results demonstrated that nutrient composition of forage and grain derived from DP915635 maize was comparable to that of conventional maize represented by non-GM near-isoline maize and non-GM commercial maize. Therefore, no nutritional impact of DP915635 is expected.

## **D. OTHER INFORMATION**

### **OVERALL RISK ASSESSMENT CONCLUSIONS FOR DP915635 MAIZE**

This application presents information supporting the safety and nutritional comparability of DP915635 maize. The molecular characterization analyses conducted on DP915635 maize demonstrated that the introduced genes are integrated at a single locus, stably inherited across multiple generations, and segregate according to Mendel's law of genetics. The allergenic and toxic potential of the IPD079Ea, PAT, and PMI proteins were evaluated and found unlikely to be allergenic or toxic to humans or animals. Based on the weight of evidence, consumption of the IPD079Ea, PAT, and PMI proteins is unlikely to cause an adverse effect on humans or animals. A compositional comparability assessment demonstrated that the nutrient composition of DP915635 maize forage and grain is comparable to that of conventional maize, represented by non-genetically modified (non-GM) near-isoline maize and non-GM commercial maize.

Overall, data and information contained herein support the conclusion that DP915635 maize containing the IPD079Ea, PAT, and PMI proteins is as safe and nutritious as non-GM maize for food and feed uses.

## REFERENCES

- Abbitt SE, inventor, Aug. 8, 2017. SB-UBI terminator sequence for gene expression in plants. United States Patent, Patent No. US 9,725,731 B2
- Abbitt SE, Klein K, Selinger D, inventors. 07 June 2018. Transcriptional Terminators for Gene Expression in Plants. World Intellectual Property Organization, Patent No. WO 2018/102131 A1
- Abbitt SE, Shen B, inventors. 7 July 2016. Maize and sorghum s-adenosyl-homocysteine hydrolase promoters. World Intellectual Property Organization, Patent No. WO 2016/109157 A1
- Abendroth LJ, Elmore RW, Boyer MJ, Marlay SK (2011) Corn Growth and Development. Iowa State University Extension, PMR 1009
- AFSI (2019) Crop Composition Database, Version 7.0. Agriculture & Food Systems Institute, <http://www.cropcomposition.org/>
- Allen SM, Barry J, Crane V, English J, Fengler K, Schepers E, Udranszky I, inventors. 9 February 2017. Plant Derived Insecticidal Proteins and Methods for Their Use. World Intellectual Property Organization, Patent No. WO 2017/023486 A1
- An G, Mitra A, Choi HK, Costa MA, An K, Thornburg RW, Ryan CA (1989) Functional Analysis of the 3' Control Region of the Potato Wound-Inducible Proteinase Inhibitor II Gene. *The Plant Cell* 1: 115-122
- Anand A, Wu E, Li Z, TeRonde S, Arling M, Lenderts B, Mutti JS, Gordon-Kamm W, Jones TJ, Chilcoat ND (2019) High efficiency *Agrobacterium*-mediated site-specific gene integration in maize utilizing the FLP-*FRT* recombination system. *Plant Biotechnology Journal* 17: 1636-1645
- Anderluh G, Kisovec M, Kraševc N, Gilbert RJC (2014) Distribution of MACPF/CDC Proteins. In G Anderluh, R Gilbert, eds, *MACPF/CDC Proteins - Agents of Defence, Attack and Invasion*. Springer Netherlands, Dordrecht, pp 7-30
- Benjamini Y, Hochberg Y (1995) Controlling the False Discovery Rate: a Practical and Powerful Approach to Multiple Testing. *Journal of the Royal Statistical Society B* 57: 289-300
- Boeckman CJ, Ballou S, Gunderson T, Huang E, Linderblood C, Olson T, Stolte B, LeRoy K, Walker C, Wang Y, Woods R, Zhang J. Characterization of the Spectrum of Activity of IPD079Ea: A Protein Derived From *Ophioglossum pendulum* (Ophioglossales: Ophioglossaceae) With Activity Against Western Corn Rootworm [*Diabrotica virgifera virgifera* (Coleoptera: Chrysomelidae)]. *J Econ Entomol.* 2022 Oct 12;115(5):1531-1538
- ██████████ (2000) PAT Microbial protein (FL): Acute Oral-Toxicity Study in CD-1 Mice. Dow AgroSciences LLC, Study No. 991249
- Carlson AB, Mathesius CA, Ballou S, Fallers MN, Gunderson TA, Hession A, Mirsky H, Stolte B, Zhang J, Woods RM, Herman RA, Roper JM. Safety assessment of the insecticidal protein IPD079Ea from the fern, *Ophioglossum pendulum*. *Food Chem Toxicol.* 2022 Aug;166:113187. doi: 10.1016/j.fct.2022.113187
- Callis J, Carpenter T, Sun CW, Vierstra RD (1995) Structure and Evolution of Genes Encoding Polyubiquitin and Ubiquitin-Like Proteins in *Arabidopsis thaliana* Ecotype Columbia. *Genetics* 139: 921-939
- CERA - ILSI Research Foundation (2011) A Review of the Environmental Safety of the PAT Protein. International Life Sciences Institute, Center for Environmental Risk Assessment

- CERA - ILSI Research Foundation (2016) A Review of the Food and Feed Safety of the PAT Protein. International Life Sciences Institute, Center for Environmental Risk Assessment
- Cheo DL, Titus SA, Byrd DRN, Hartley JL, Temple GF, Brasch MA (2004) Concerted Assembly and Cloning of Multiple DNA Segments Using In Vitro Site-Specific Recombination: Functional Analysis of Multi-Segment Expression Clones. *Genome Research* 14: 2111-2120
- Christensen AH, Sharrock RA, Quail PH (1992) Maize polyubiquitin genes: structure, thermal perturbation of expression and transcript splicing, and promoter activity following transfer to protoplasts by electroporation. *Plant Molecular Biology* 18: 675-689
- Codex Alimentarius Commission (2003) Alinorm 03/34: Appendix III: Draft guideline for the conduct of food safety assessment of foods derived from recombinant-DNA plants, and Appendix IV: Proposed Draft Annex of the Assessment of Possible Allergenicity. Food and Agriculture Organization of the United Nations, World Health Organization, Rome, pp 47-60
- Codex Alimentarius Commission (2008) Guideline for the Conduct of Food Safety Assessment of Foods Derived from Recombinant-DNA Plants. Codex Alimentarius, CAC/GL 45-2003
- Codex Alimentarius Commission (2019) Codex Standard for Named Vegetable Oils. Codex Alimentarius, CXS 210-1999
- Cong B, Maxwell C, Luck S, Vespestad D, Richard K, Mickelson J, Zhong C (2015) Genotypic and Environmental Impact on Natural Variation of Nutrient Composition in 50 Non Genetically Modified Commercial Maize Hybrids in North America. *Journal of Agricultural and Food Chemistry* 63: 5321-5334
- Crow A, Diehn S, Sims L, inventors. 28 December 2017. Plant regulatory elements and methods of use thereof. World Intellectual Property Organization, Patent No. WO 2017/222821 A2
- Cullen EM, Gray ME, Gassmann AJ, Hibbard BE (2013) Resistance to Bt Corn by Western Corn Rootworm (Coleoptera: Chrysomelidae) in the U.S. Corn Belt. *Journal of Integrated Pest Management* 4: D1-D6
- Dale EC, Ow DW (1990) Intra- and intramolecular site-specific recombination in plant cells mediated by bacteriophage P1 recombinase. *Gene* 91: 79-85
- Das OP, Ward K, Ray S, Messing J (1991) Sequence Variation between Alleles Reveals Two Types of Copy Correction at the 27-kDa Zein Locus of Maize. *Genomics* 11: 849-856
- de Freitas FA, Yunes JA, da Silva MJ, Arruda P, Leite A (1994) Structural characterization and promoter activity analysis of the  $\gamma$ -kafirin gene from sorghum. *Molecular and General Genetics* 245: 177-186
- Diehn S, Peterson-Burch B, inventors. 23 August 2012. Root-Preferred Promoter and Methods of Use. World Intellectual Property Organization, Patent No. WO 2012/112411 A1
- Dong J, Feng Y, Kumar D, Zhang W, Zhu T, Luo M-C, Messing J (2016) Analysis of tandem gene copies in maize chromosomal regions reconstructed from long sequence reads. *Proceedings of the National Academy of Sciences* 113: 7949-7956
- Dummitt B, Micka WS, Chang Y-H (2003) N-Terminal Methionine Removal and Methionine Metabolism in *Saccharomyces cerevisiae*. *Journal of Cellular Biochemistry* 89: 964-974
- Dymecki SM (1996) A modular set of *Flp*, FRT and *lacZ* fusion vectors for manipulating genes by site-specific recombination. *Gene* 171: 197-201

- Eckes P, Rosahl S, Schell J, Willmitzer L (1986) Isolation and characterization of a light-inducible, organ-specific gene from potato and analysis of its expression after tagging and transfer into tobacco and potato shoots. *Molecular and General Genetics* 205: 14-22
- Ewing B, Green P (1998) Base-Calling of Automated Sequencer Traces Using *Phred*. II. Error Probabilities. *Genome Research* 8: 186-194
- Ewing B, Hillier L, Wendl MC, Green P (1998) Base-Calling of Automated Sequencer Traces Using *Phred*. I. Accuracy Assessment. *Genome Research* 8: 175-185
- FAO/WHO (2001) Evaluation of Allergenicity of Genetically Modified Foods: Report of a Joint FAO/WHO Expert Consultation on Allergenicity of Foods Derived from Biotechnology, 22 - 25 January 2001. Food and Agriculture Organization of the United Nations, Rome
- Fernández H (2011) Chapter 1 Introduction. In H Fernández, A Kumar, A Revilla, eds, *Working with Ferns Issues and Applications*. Springer-Verlag New York, pp 1-8
- Fling ME, Kopf J, Richards C (1985) Nucleotide sequence of the transposon Tn7 gene encoding an aminoglycoside-modifying enzyme, 3' (9)-O-nucleotidyltransferase. *Nucleic Acids Research* 13: 7095-7106
- Franck A, Guilley H, Jonard G, Richards K, Hirth L (1980) Nucleotide sequence of cauliflower mosaic virus DNA. *Cell* 21: 285-294
- Gao H, Mutti J, Young JK, Yang M, Schroder M, Lenderts B, Wang L, Peterson D, St. Clair G, Jones S, Feigenbutz L, Marsh W, Zeng M, Wagner S, Farrell J, Snopek K, Scelonge C, Sopko X, Sander JD, Betts S, Cigan AM, Chilcoat ND (2020) Complex Trait Loci in Maize Enabled by CRISPR-Cas9 Mediated Gene Insertion. *Frontiers in Plant Science* 11: 535
- Gassmann AJ, Shrestha RB, Jakka SR, Dunbar MW, Clifton EH, Paolino AR, Ingber DA, French BW, Masloski KE, Dounda JW, St Clair CR (2016) Evidence of Resistance to Cry34/35Ab1 Corn by Western Corn Rootworm (Coleoptera: Chrysomelidae): Root Injury in the Field and Larval Survival in Plant-Based Bioassays. *Journal of Economic Entomology* 109: 1872-1880
- Greger IH, Demarchi F, Giacca M, Proudfoot NJ (1998) Transcriptional interference perturbs the binding of Sp1 to the HIV-1 promoter. *Nucleic Acids Research* 26: 1294-1300
- Guilley H, Dudley RK, Jonard G, Balázs E, Richards KE (1982) Transcription of cauliflower mosaic virus DNA: detection of promoter sequences, and characterization of transcripts. *Cell* 30: 763-773
- Hartley JL, Temple GF, Brasch MA (2000) DNA Cloning Using In Vitro Site-Specific Recombination. *Genome Research* 10: 1788-1795
- Hérouet C, Esdaile DJ, Mallyon BA, Debruyne E, Schulz A, Currier T, Hendrickx K, van der Klis R-J, Rouan D (2005) Safety evaluation of the phosphinothricin acetyltransferase proteins encoded by the *pat* and *bar* sequences that confer tolerance to glufosinate-ammonium herbicide in transgenic plants. *Regulatory Toxicology and Pharmacology* 41: 134-149
- Hershey HP, Stoner TD (1991) Isolation and characterization of cDNA clones for RNA species induced by substituted benzenesulfonamides in corn. *Plant Molecular Biology* 17: 679-690
- Hilger C, Grigioni F, Thill L, Mertens L, Hentges F (2002) Severe IgE-mediated anaphylaxis following consumption of fried frog legs: Definition of alpha-parvalbumin as the allergen in cause. *Allergy* 57:1053-1058

- Hong B, Fisher TL, Sult TS, Maxwell CA, Mickelson JA, Kishino H, Locke MEH (2014) Model-Based Tolerance Intervals Derived from Cumulative Historical Composition Data: Application for Substantial Equivalence Assessment of a Genetically Modified Crop. *Journal of Agricultural and Food Chemistry* 62: 9916-9926
- ISAAA (2020) Gene: pmi (events list). International Service for the Acquisition of Agribiotech Applications, <https://www.isaaa.org/gmapprovaldatabase/gene/default.asp?GeneID=37&Gene=pmi>
- Jakka SRK, Shrestha RB, Gassmann AJ (2016) Broad-spectrum resistance to *Bacillus thuringiensis* toxins by western corn rootworm (*Diabrotica virgifera virgifera*). *Scientific Reports* 6: 27860
- Katzen F (2007) Gateway<sup>®</sup> recombinational cloning: a biological operating system. *Expert Opinion on Drug Discovery* 2: 571-589
- Keil M, Sanchez-Serrano J, Schell J, Willmitzer L (1986) Primary structure of a proteinase inhibitor II gene from potato (*Solanum tuberosum*). *Nucleic Acids Research* 14: 5641-5650
- Kenward MG, Roger JH (2009) An improved approximation to the precision of fixed effects from restricted maximum likelihood. *Computational Statistics & Data Analysis* 53: 2583-2595
- Kew Science (2020a) *Ophioglossum* L. Plants of the World online, <http://www.plantsoftheworldonline.org/taxon/urn:lsid:ipni.org:names:17408900-1#distribution-map>
- Kew Science (2020b) *Ophioglossum pendulum* L. Plants of the World online, <http://www.plantsoftheworldonline.org/taxon/urn:lsid:ipni.org:names:17167860-1>
- Komari T, Hiei Y, Saito Y, Murai N, Kumashiro T (1996) Vectors carrying two separate T-DNAs for co-transformation of higher plants mediated by *Agrobacterium tumefaciens* and segregation of transformants free from selection markers. *The Plant Journal* 10: 165-174
- La Paz JL, Pla M, Papazova N, Puigdomenech P, Vicient CM (2010) Stability of the MON 810 transgene in maize. *Plant Molecular Biology* 74: 563-571
- Liu H, Shi J, Sun C, Gong H, Fan X, Qiu F, Huang X, Feng Q, Zheng X, Yuan N, Li C, Zhang Z, Deng Y, Wang J, Pan G, Han B, Lai J, Wu Y (2016) Gene duplication confers enhanced expression of 27-kDa  $\gamma$ -zein for endosperm modification in quality protein maize. *Proceedings of the National Academy of Sciences* 113: 4964-4969
- Lowe K, Wu E, Wang N, Hoerster G, Hastings C, Cho M-J, Scelonge C, Lenderts B, Chamberlin M, Cushatt J, Wang L, Ryan L, Khan T, Chow-Yiu J, Hua W, Yu M, Banh J, Bao Z, Brink K, Igo E, Rudrappa B, Shamseer P, Bruce W, Newman L, Shen B, Zheng P, Bidney D, Falco C, Register J, Zhao Z-Y, Xu D, Jones T, Gordan-Kamm W (2016) Morphogenic Regulators *Baby boom* and *Wuschel* Improve Monocot Transformation. *The Plant Cell* 28: 1998-2015
- Lundry DR, Burns JA, Nemeth MA, Riordan SG (2013) Composition of Grain and Forage from Insect-Protected and Herbicide-Tolerant Corn, MON 89034 x TC1507 x MON 88017 x DAS-59122-7 (SmartStax), Is Equivalent to That of Conventional Corn (*Zea mays* L.). *Journal of Agricultural and Food Chemistry* 61: 1991-1998
- Marçais G, Kingsford C (2011) A fast, lock-free approach for efficient parallel counting of occurrences of  $k$ -mers. *Bioinformatics* 27: 764-770
- Mayer KFX, Schoof H, Haecker A, Lenhard M, Jürgens G, Laux T (1998) Role of *WUSCHEL* in Regulating Stem Cell Fate in the *Arabidopsis* Shoot Meristem. *Cell* 95: 805-815

- Metcalfe RL (1986) Foreward. In JL Krysan, TA Miller, eds, *Methods for the Study of Pest Diabrotica*. Springer-Verlag, New York, pp vii-xv
- Mirsky HP, Cressman RF, Jr., Ladics GS (2013) Comparative assessment of multiple criteria for the in silico prediction of cross-reactivity of proteins to known allergens. *Regulatory Toxicology and Pharmacology* 67: 232-239
- NCGA (2020) World of Corn 2020. National Corn Growers Association, <http://www.worldofcorn.com/#/>
- Negrotto D, Jolley M, Beer S, Wenck AR, Hansen G (2000) The use of phosphomannose-isomerase as a selectable marker to recover transgenic maize plants (*Zea mays* L.) via *Agrobacterium* transformation. *Plant Cell Reports* 19: 798-803
- Niu X, Kassa A, Hu X, Robeson J, McMahon M, Richtman NM, Steimel JP, Kernodle BM, Crane VC, Sandahl G, Ritland JL, Presnail JK, Lu AL, Wu G (2017) Control of Western Corn Rootworm (*Diabrotica virgifera virgifera*) Reproduction through Plant-Mediated RNA Interference. *Scientific Reports* 7: 12591
- OECD (1993) Safety Evaluation of Foods Derived by Modern Biotechnology: Concepts and Principles. Organisation for Economic Cooperation and Development
- OECD (1999) Consensus document on general information concerning the genes and their enzymes that confer tolerance to phosphinothricin herbicide. Organisation for Economic Co-operation and Development, ENV/JM/MONO(99)13
- OECD (2002) Consensus Document on Compositional Considerations for New Varieties of Maize (*Zea Mays*): Key Food and Feed Nutrients, Anti-Nutrients and Secondary Plant Metabolites. Organisation for Economic Co-operation and Development, ENV/JM/MONO(2002)25
- Pawitan Y, Michiels S, Koscielny S, Gusnanto A, Ploner A (2005) False discovery rate, sensitivity and sample size for microarray studies. *Bioinformatics* 21: 3017-3024
- Pearson WR, Lipman DJ (1988) Improved tools for biological sequence comparison. *Proceedings of the National Academy of Sciences* 85: 2444-2448
- Perkins DN, Pappin DJC, Creasy DM, Cottrell JS (1999) Probability-based protein identification by searching sequence databases using mass spectrometry data. *Electrophoresis* 20: 3551-3567
- PHI (2010) CropFocus: Corn Rootworm. Pioneer Hi-Bred International, Inc, [https://www.pioneer.com/CMRoot/Pioneer/US/Non\\_Searchable/agronomy/cropfocus\\_pdf/corn\\_rootworm.pdf](https://www.pioneer.com/CMRoot/Pioneer/US/Non_Searchable/agronomy/cropfocus_pdf/corn_rootworm.pdf)
- Privalle LS (2002) Phosphomannose Isomerase, a Novel Plant Selection System. *Annals of the New York Academy of Sciences* 964: 129-138
- Proteau G, Sidenberg D, Sadowski P (1986) The minimal duplex DNA sequence required for site-specific recombination promoted by the FLP protein of yeast *in vitro*. *Nucleic Acids Research* 14: 4787-4802
- Reed J, Privalle L, Powell ML, Meghji M, Dawson J, Dunder E, Sutthe J, Wenck A, Launis K, Kramer C, Chang Y-F, Hansen G, Wright M (2001) Phosphomannose isomerase: An efficient selectable marker for plant transformation. *In Vitro Cellular & Developmental Biology - Plant* 37: 127-132
- Rosado CJ, Kondos S, Bull TE, Kuiper MJ, Law RHP, Buckle AM, Voskoboinik I, Bird PI, Trapani JA, Whisstock JC, Dunstone MA (2008) The MACPF/CDC family of pore-forming toxins. *Cellular Microbiology* 10: 1765-1774

- Shearwin KE, Callen BP, Egan JB (2005) Transcriptional interference – a crash course. *Trends in Genetics* 21: 339-345
- Sherman F, Stewart JW, Tsunasawa S (1985) Methionine or Not Methionine at the Beginning of a Protein. *Bioessays* 3: 27-31
- Shrestha RB, Dunbar MW, French BW, Gassmann AJ (2018) Effects of field history on resistance to Bt maize by western corn rootworm, *Diabrotica virgifera virgifera* LeConte (Coleoptera: Chrysomelidae). *PLoS ONE* 13: e0200156
- Slein MW (1950) Phosphomannose Isomerase. *Journal of Biological Chemistry* 186: 753-761
- Spelman RJ, Bovenhuis H (1998) Moving from QTL experimental results to the utilization of QTL in breeding programmes. *Animal Genetics* 29: 77-84
- Tomizawa J-I, Ohmori H, Bird RE (1977) Origin of replication of colicin E1 plasmid DNA. *Proceedings of the National Academy of Sciences* 74: 1865-1869
- US-EPA (1997) *Escherichia coli* K-12 Derivatives Final Risk Assessment. United States Environmental Protection Agency, [http://epa.gov/biotech\\_rule/pubs/fra/fra004.htm](http://epa.gov/biotech_rule/pubs/fra/fra004.htm)
- US-EPA (2004) Phosphomannose Isomerase and the Genetic Material Necessary for Its Production in All Plants; Exemption from the Requirement of a Tolerance. *Federal Register* 69: 26770-26775
- USDA-APHIS (2001) Approval of Mycogen Seeds c/o Dow AgroSciences LLC and Pioneer Hi-Bred International, Inc., Request (00-136-01p) Seeking a Determination of Non-regulated Status for Bt Cry1F Insect Resistant, Glufosinate Tolerant Corn Line 1507: Environmental Assessment and Finding of No Significant Impact. United States Department of Agriculture, Animal and Plant Health Inspection Service
- USDA-APHIS (2005) Mycogen Seeds/Dow AgroSciences LLC and Pioneer Hi-Bred International Inc.; Availability of Determination of Nonregulated Status for Genetically Engineered Corn: Environmental Assessment and Finding of No Significant Impact. United States Department of Agriculture, Animal and Plant Health Inspection Service
- USDA-APHIS (2013) Determination of nonregulated status for Pioneer Event DP-ØØ4114-3 corn. United States Department of Agriculture, Animal and Plant Health Inspection Service, [https://www.aphis.usda.gov/brs/aphisdocs/11\\_24401p\\_det.pdf](https://www.aphis.usda.gov/brs/aphisdocs/11_24401p_det.pdf)
- USDA-NASS (2020) National Statistics for Corn: Corn - Acres Planted. United States Department of Agriculture, National Agricultural Statistics Service, [https://www.nass.usda.gov/Statistics\\_by\\_Subject/result.php?12C29E97-8879-372A-B4F1-1BDFF54F7196&sector=CROPS&group=FIELD%20CROPS&comm=CORN](https://www.nass.usda.gov/Statistics_by_Subject/result.php?12C29E97-8879-372A-B4F1-1BDFF54F7196&sector=CROPS&group=FIELD%20CROPS&comm=CORN)
- USDA-NRCS (2020) Classification for Kingdom Plantae Down to Family *Ophioglossaceae*. United States Department of Agriculture - Natural Resources Conservation Service, <https://plants.usda.gov/java/ClassificationServlet?source=display&classid=Ophioglossaceae>
- Waigmann E, Gomes A, Lanzoni A, Perry JN (2013) Editorial: New Commission Implementing Regulation on Risk Assessment of GM plant applications: novel elements and challenges. *The EFSA Journal* 11: e11121
- Watson SA (1982) Corn: Amazing Maize. General Properties. In IA Wolff, ed, *CRC Handbook of Processing and Utilization in Agriculture*, Vol 2. CRC Press, Boca Raton, pp 3-29

- Weber N, Halpin C, Hannah LC, Jez JM, Kough J, Parrott W (2012) Editor's Choice: Crop Genome Plasticity and Its Relevance to Food and Feed Safety of Genetically Engineered Breeding Stacks. *Plant Physiology* 160: 1842-1853
- Weisser P, Krämer R, Sprenger GA (1996) Expression of the *Escherichia coli pmi* gene, encoding phosphomannose-isomerase in *Zymomonas mobilis*, leads to utilization of mannose as a novel growth substrate, which can be used as a selective marker. *Applied and Environmental Microbiology* 62: 4155-4161
- Westfall PH, Tobias RD, Rom D, Wolfinger RD, Hochberg Y (1999) Concepts and Basic Methods for Multiple Comparisons and Tests. In *Multiple Comparisons and Multiple Tests: Using SAS*. SAS Institute Inc., Cary, NC, pp 13-40
- Wohlleben W, Arnold W, Broer I, Hillemann D, Strauch E, Punier A (1988) Nucleotide sequence of the phosphinothricin *N*-acetyltransferase gene from *Streptomyces viridochromogenes* Tü494 and its expression in *Nicotiana tabacum*. *Gene* 70: 25-37
- Yu L, Liu D, Chen S, Dai Y, Guo W, Zhang X, Wang L, Ma S, Xiao M, Qi H, Xiao S, Chen Q (2020) Evolution and Expression of the Membrane Attack Complex and Perforin Gene Family in the Poaceae. *International Journal of Molecular Sciences* 21: 5736
- Zastrow-Hayes GM, Lin H, Sigmund AL, Hoffman JL, Alarcon CM, Hayes KR, Richmond TA, Jeddloh JA, May GD, Beatty MK (2015) Southern-by-Sequencing: A Robust Screening Approach for Molecular Characterization of Genetically Modified Crops. *The Plant Genome* 8: 1-15

## STUDY INDEX

- ██████████ (2020) "Characterization of DP-915635-4 Maize for Insertion Stability in Five Generations Using Southern Blot Analysis" Corteva Agriscience study ID: PHI-2020-114
- ██████████████████████████████ (2020) "Characterization of IPD079Ea Following In Vitro Pepsin and Sequential Pancreatin Digestion Using SDS-PAGE Analysis" Corteva Agriscience study ID: PHI-2020-174
- ██████████████████████████████ (2020) "Characterization of the In Vitro Pancreatin Resistance of IPD079Ea Using SDS-PAGE and Western Blot Analysis" Corteva Agriscience study ID: PHI-2020-175
- ██████████████████████████████ (2020) "Characterization of the In Vitro Pepsin Resistance of IPD079Ea Using SDS-PAGE and Western Blot Analysis" Corteva Agriscience study ID: PHI-2020-165
- ██████████ et al. (2020) "Vector maps for helper plasmids and DP915635 insertion, SbS for copy number, intactness and absence of backbone - full coverage at T1" Corteva Agriscience study ID: PHI-2020-044
- ██████████. (2021) "IPD079Ea Protein: Acute Oral Toxicity Study in Mice" Corteva Agriscience study ID: PHI-2019-224
- ██████████. (2020) "Characterization of PAT Protein Derived from DP-915635-4 Maize" Corteva Agriscience study ID: PHI-2020-147
- ██████████. et al. (2020) "Characterization of IPD079Ea Protein Derived from DP-915635-4 Maize" Corteva Agriscience study ID: PHI-2020-146
- ██████████ et al. (2020) "Determination of the Biological Activity of Heat-Treated IPD079Ea Protein Incorporated in an Artificial Diet and Fed to *Diabrotica virgifera virgifera*" Corteva Agriscience study ID: PHI-2020-030
- ██████████████████████████████., (2020) "Sequence Characterization of Insert and Flanking Genomic Regions of DP-915635-4 Maize" Corteva Agriscience study ID: PHI-2019-245
- ██████████ et al. (2020) "Segregation Analysis and Tissue Production of Multiple Maize Generations Containing Event DP-915635-4" Corteva Agriscience study ID: PHI-2019-127
- ██████████ (2020) "Comparison of the Amino Acid Sequence of the IPD079Ea Protein to the Amino Acid Sequences of Known and Putative Protein Allergens" Corteva Agriscience study ID: PHI-2020-106/201
- ██████████ (2020) "Comparison of the Amino Acid Sequence of the PAT Protein to the Amino Acid Sequences of Known and Putative Protein Allergens" Corteva Agriscience study ID: PHI-2020-104/201
- ██████████ (2020) "Comparison of the Amino Acid Sequence of the PMI Protein to the Amino Acid Sequences of Known and Putative Protein Allergens" Corteva Agriscience study ID: PHI-2020-205/201
- ██████████ (2020) "Comparison of the Cry1F Protein Sequence to the Protein Sequences in the Internal Toxin Database" Corteva Agriscience study ID: PHI-2020-103/211
- ██████████ (2020) "Comparison of the IPD079Ea Protein Sequence to the Protein Sequences in the Internal Toxin Database" Corteva Agriscience study ID: PHI-2020-105/211
- ██████████ (2020) "Comparison of the PMI Protein Sequence to the Protein Sequences in the Internal Toxin Database" Corteva Agriscience study ID: PHI-2020-206/211

- ██████████. (2020) "Reading Frame Analysis at the Insertion Site of Maize Event DP-915635-4" Corteva Agriscience study ID: PHI-2020-213/222
- ██████████. (2019) "Agronomic Characteristics and Nutrient Composition of a Maize Line Containing Event DP-915635-4: U.S. and Canada Test Sites" Corteva Agriscience study ID: PHI-2019-016/021
- ██████████ (2019) "Expressed Trait Protein Concentrations of a Maize Line Containing Event DP-915635-4: U.S. and Canada Test Sites" Corteva Agriscience study ID: PHI-2019-015
- ██████████ (2020) "Development and Validation of an Event-Specific Quantitative Real-Time PCR (qPCR) Detection Method for Maize Event DP-915635-4" Corteva Agriscience study ID: PHI-2020-154
- ██████████ et al. (2020) "Characterization of IPD079Ea Protein Derived from a Microbial Expression System" Corteva Agriscience study ID: PHI-2019-187
- ██████████ (2020) "Characterization of PMI Protein Derived from DP-915635-4 Maize" Corteva Agriscience study ID: PHI-2020-166

## APPENDIX A. METHODS FOR SOUTHERN-BY-SEQUENCING ANALYSIS

### [PHI-2020-044 study](#)

#### Test, Control and Reference Substances

The test substance in the study was defined as seeds from the T1 generation of DP915635 maize. The control substance was defined as seed from a maize line (PHR03) that was not transformed. PHR03 maize has a similar genetic background to the test substance; however, it does not contain the DP915635 maize insertion.

#### DNA Extraction and Quantitation

Genomic DNA was separately extracted from leaf tissue of ten individual DP915635 maize plants and one control maize plants. The tissue was pulverized in tubes containing grinding beads using a Geno/Grinder™ (SPEX CertiPrep) and the genomic DNA was isolated using a standard Urea Extraction Buffer procedure. Following extraction, the DNA was quantified on a spectrofluorometer using the Quant-iT™ PicoGreen® dsDNA Assay Kit (Invitrogen) and visualized on an agarose gel to determine the DNA quality.

#### Southern-by-Sequencing

SbS was performed by Pioneer Hi-Bred International, Inc. Genomics Technologies. SbS analysis utilizes probe-based sequence capture, Next Generation Sequencing (NGS) techniques, and bioinformatics procedures to capture, sequence, and identify inserted DNA within the maize genome ([Zastrow-Hayes et al., 2015](#)). By compiling a large number of unique sequencing reads and mapping them against the linearized transformation plasmid map and control maize genome, unique junctions due to inserted DNA are identified in the bioinformatics analysis. This information is used to determine the number of insertions within the plant genome, verify insertion intactness, and confirm the absence of plasmid backbone sequences. Genomic DNA isolated from the T1 generation of DP915635 maize was analyzed by SbS to determine the insertion copy number and intactness. SbS was also performed on control maize DNA and positive control samples (control maize DNA spiked with PHP83175, PHP73878, PHP70605, PHP21139, or PHP21875 plasmid DNA at a level corresponding to one copy of plasmid per copy of the maize genome) to confirm that the assay could reliably detect plasmid fragments within the genomic DNA.

The following processes were performed by Pioneer Hi-Bred International, Inc. Genomics Technologies using standard methods and were based on the procedures described in [Zastrow-Hayes et al. \(2015\)](#).

#### Capture Probe Design and Synthesis

Biotinylated capture probes used to select plasmid sequences were designed and synthesized by Roche NimbleGen, Inc. The probe set was designed to target all sequences within the PHP83175, PHP73878, PHP70605, PHP21139, and PHP21875 plasmids (Figure 9, Step 2).

### Sequencing Library Construction

NGS libraries were constructed for DNA samples from individual maize plants, including DP915635 maize plants, a control maize plant, and the positive control samples. Genomic DNA purified as described above was sheared to an average fragment size of 400 bp using an ultrasonicator. Sheared DNA was end-repaired, A-tailed, and ligated to NEXTflex-HT™ Barcode adaptors (Bioo Scientific Corp.) following the kit protocol so that samples would be indexed to enable identification after sequencing. The DNA fragment libraries were amplified by PCR for eight cycles prior to the capture process. Amplified libraries were analyzed using a fragment analyzer and diluted to 5 ng/μl with nuclease-free water (Figure 9, Step 3).

### Probe Hybridization and Sequence Enrichment

A double capture procedure was used to capture and enrich DNA fragments that contained sequences homologous to the capture probes. The genomic DNA libraries described above were mixed with hybridization buffer and blocking oligonucleotides corresponding to the adapter sequences and denatured. Following denaturation, the biotinylated probes were added to the genomic DNA library and incubated at 47 °C for 16 hours. Streptavidin beads were added to the hybridization mix to bind DNA fragments that were associated with the probes. Bound fragments were washed and eluted, PCR-amplified for five cycles, and purified using spin columns. The enriched DNA libraries underwent a second capture reaction using the same conditions to further enrich the sequences targeted by the probes. This was followed by PCR amplification for 16 cycles and purification as described above. The final double-enriched libraries were quantified and diluted to 2 nM for sequencing (Figure 9, Step 4).

### Next Generation Sequencing on Illumina Platform

Following sequence capture, the libraries were submitted for NGS to a depth of 100x for the captured sequences. The sequence reads were trimmed for quality below Q20 ([Ewing and Green, 1998](#); [Ewing et al., 1998](#)) and assigned to the corresponding individual plant based on the indexing adapters. A complete sequence set from each plant is referred to as “AllReads” for bioinformatics analysis of that plant (Figure 9, Step 5).

### Quality Assurance of Sequencing Reads

The adapter sequences were trimmed from the NGS sequence reads using cutadapt, v1.9.1 (Martin, 2011). Further analysis to eliminate sequencing errors used JELLYFISH, version 1.1.4 ([Marçais and Kingsford, 2011](#)), to exclude any 31 bp sequence that occurred less than twice within “AllReads” as described in [Zastrow-Hayes et al. \(2015\)](#). This set of sequences was used for further bioinformatics analysis and is referred to as “CleanReads”. Identical sequence reads were combined into non-redundant read groups (referred to as “Non-redundantReads”) while retaining abundance information for each group and were used for further analysis, as described in [Zastrow-Hayes et al. \(2015\)](#) (Figure 9, Step 6).

### Aligning Reads

Each set of “Non-redundantReads” was aligned to the maize reference genome using Bowtie, version 2.3.4.2 (Langmead and Salzberg, 2012) with up to two mismatches allowed. The “Non-redundantReads” not matching the

maize reference genome were then compared to the plasmid sequences using Bowtie with zero mismatches allowed. Any “Non-redundantReads” that were not wholly derived from either maize or plasmid sequences were aligned to the plasmid backbone sequences with Bowtie 2, version 2.1.0, allowing zero mismatches (Figure 9, Step 7).

### Junction Detection

Following removal of “Non-redundantReads” with alignments wholly to the maize reference genome or plasmid sequence identified during the quality assurance phase, the remaining “Non-redundantReads” were aligned to the full plasmid sequence using Bowtie2, version 2.3.4.2, with the soft-trimming feature enabled. Chimeric reads contain sequence that is non-contiguous with the plasmid sequence from the alignment, such as genome-plasmid junctions or rearrangements of the plasmid. These chimeric reads are referred to as junction reads or junctions. The individual reads defining a junction were condensed to a unique identifier to represent the junction. This identifier (referred to as a 30\_20 mer) includes 20 bp of sequence from PHP83175, PHP73878, PHP70605, PHP21139, or PHP21875, and 30 bp of sequence adjacent to the 20 bp from the plasmid. The adjacent 30 bp did not align to the plasmid contiguously to the known 20 bp. When the 20 bp from the plasmid and the adjacent 30 bp are combined into a 30\_20 mer, they indicate the junction shown by the chimeric read. Junction reads were condensed into a unique junction if their 30\_20 mers were identical, or if the 30\_20 mer junctions were within 2 bp. The total number of sequence reads (referred to as “TotalSupportingReads”) for each unique junction was retained for filtering. Junctions with fewer than 10 “TotalSupportingReads” for positions aligned to the plasmid, were filtered and removed from further analysis (Figure 9, Step 8).

### Junction Identification

Variations between the maize reference genome used in the SbS analysis and the control maize genome may result in identification of junctions that are due to these differences in the endogenous maize sequences. In order to detect these endogenous junctions, control maize genomic DNA libraries were captured and sequenced in the same manner. The 30\_20 mers of the endogenous junctions detected in this analysis were used to filter the same endogenous junctions in the DP915635 maize samples (Figure 9, Step 8), so that the only junctions remaining in the DP915635 samples are due to actual insertions derived from PHP83175, PHP73878, PHP70605, PHP21139, or PHP21875 (Figure 9, Step 9).

### Data QC

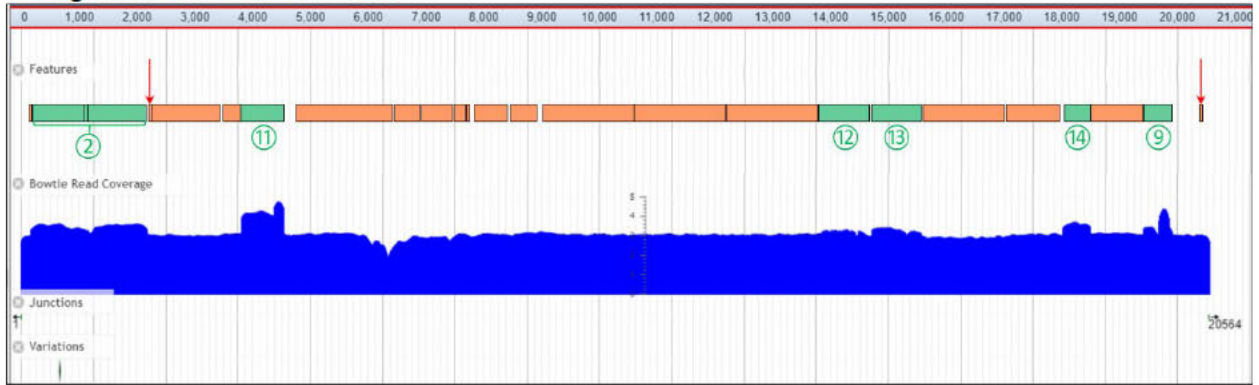
The ubiquitous presence of environmental bacteria, such as *Serratia marcescens*, provides an opportunity for their plasmid DNA to be sequenced along with plant genomic DNA. This resulted in low level detection of plasmid backbone sequences in the genomic DNA samples due to similarity with the plasmid backbone regions. The “Non-redundantReads” that aligned to the plasmid backbone sequence, but at a coverage depth below 35x across 50 bp, were deemed to be due to environmental bacteria. Due to the detection of these bacterial sequences, coverage levels of 35x or below were considered to be the background level of sequencing.

### SbS Results

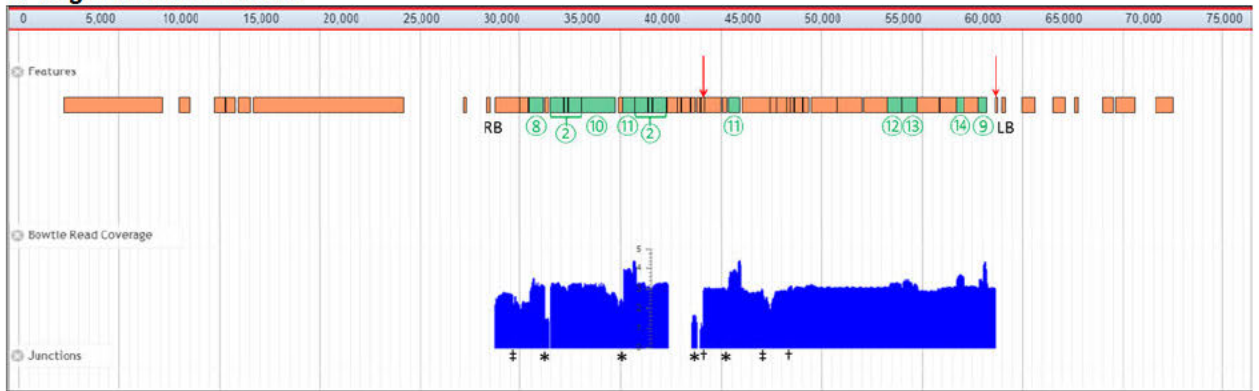
Results for the control maize, positive control, and one DP915635 maize plant (Plant ID 385269369) are presented in the main body of this document (A.3(c) Molecular characterisation).

Remaining plant results from SbS analysis are presented in Figures A1 to A4 (positive plants) and Figures A5 to A9 (negative plants) below:

### A. Alignment to Intended Insertion



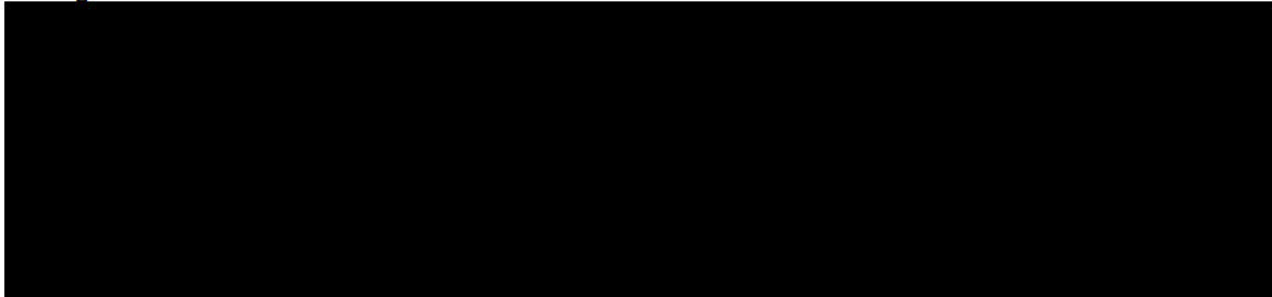
### B. Alignment to PHP83175



### C. Alignment to PHP73878



### D. Alignment to PHP70605



### E. Alignment to PHP21139



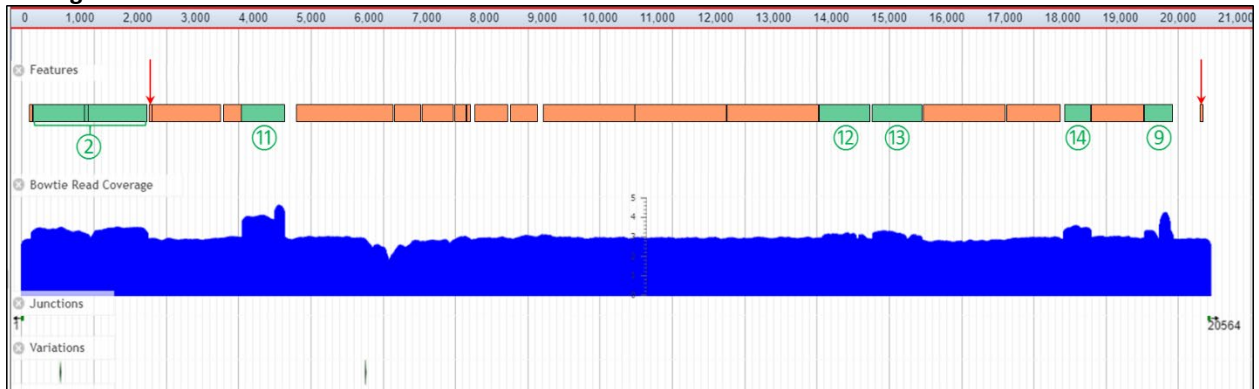
### F. Alignment to PHP21875



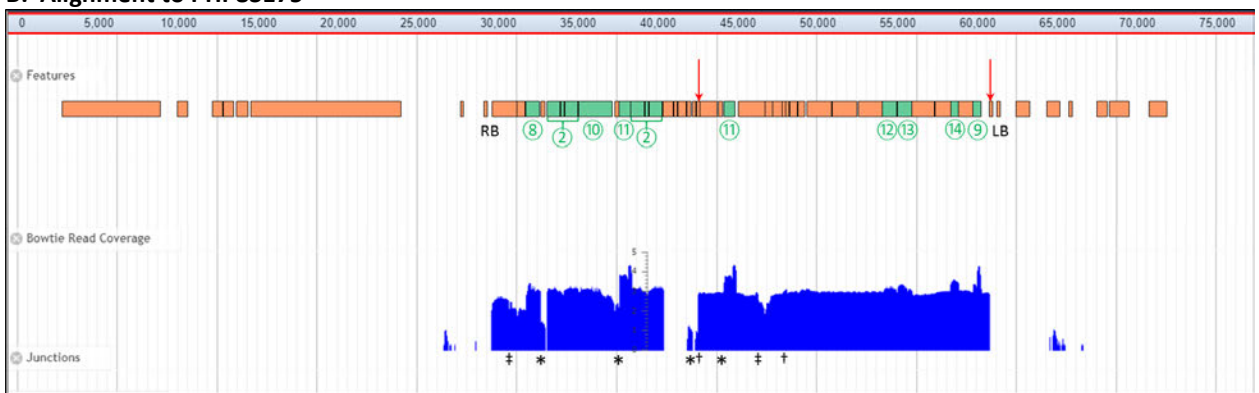
### Figure A.1. SbS Results for DP915635 Maize (Plant ID 385269371)

The blue coverage graph shows the number of individual NGS reads aligned at each point on the intended insertion or construct using a logarithmic scale at the middle of the graph. Green bars above the coverage graph indicate endogenous genetic elements in each plasmid derived from the maize genome (identified by numbers, Table 5), while tan bars indicate genetic elements derived from other sources. FRT sites are indicated by red arrows. **A)** SbS results aligned against the intended insertion (20,564 bp; Figure 8), indicating that this plant contains the intended insertion. Arrows below the graph indicate the two plasmid-to-genome sequence junctions identified by SbS; the numbers below the arrows refer to the bp location of the junction relative to the intended insertion (Figure 8). The presence of only two junctions demonstrates the presence of a single insertion in the DP915635 maize genome. The Variations panel indicates the location of a single nucleotide change identified in all plants containing the insertion. **B)** SbS results aligned against the plasmid PHP83175 sequence (74,997 bp; Figure 6). Coverage was obtained for the elements between FRT1 and FRT6 transferred into DP915635 maize (region between the red arrows at top of graph). Coverage was also obtained for the endogenous elements in the region between the RB and FRT1 that were not transferred into the DP915635 maize genome, and to the *pinII* terminator (\*), CaMV35S terminator (†), and *os*-actin promoter and intron (‡) elements outside of the FRT sites due to alignment of reads derived from identical elements in the final insertion to all copies of these elements in PHP83175. **C)** SbS results aligned against the plasmid PHP73878 sequence [REDACTED] bp; Figure 1). Coverage was obtained for *zm*-SEQ158, *zm*-SEQ159, and the elements found in the intended insertion (between *zm*-SEQ158 to FRT1 and between FRT6 to *zm*-SEQ159), along with the *pinII* terminator element (\*) in PHP73878 due to alignment of reads derived from the *pinII* terminator in the *pmi* cassette of the intended insertion to the copy of this element in PHP73878. **D)** SbS results aligned against the plasmid PHP70605 sequence [REDACTED] bp; Figure 3). Coverage was obtained only for the endogenous elements along with the *pinII* terminator element (\*). **E)** SbS results aligned against the plasmid PHP21139 sequence [REDACTED] bp; Figure 4). Coverage was obtained only for the endogenous elements. **F)** SbS results aligned against the plasmid PHP21875 sequence [REDACTED] bp; Figure 5). Coverage was obtained for the endogenous elements along with the *pinII* terminator element (\*). The absence of any junctions other than to the intended insertion indicates that there are no additional insertions or backbone sequence present in DP915635 maize.

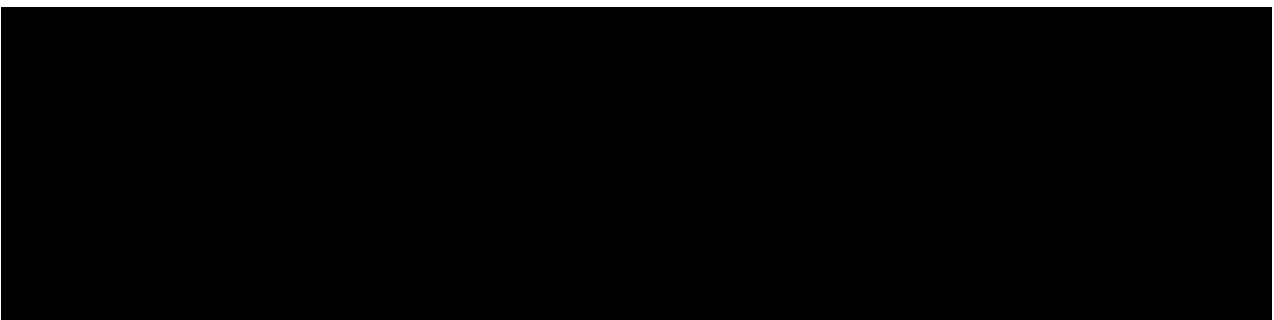
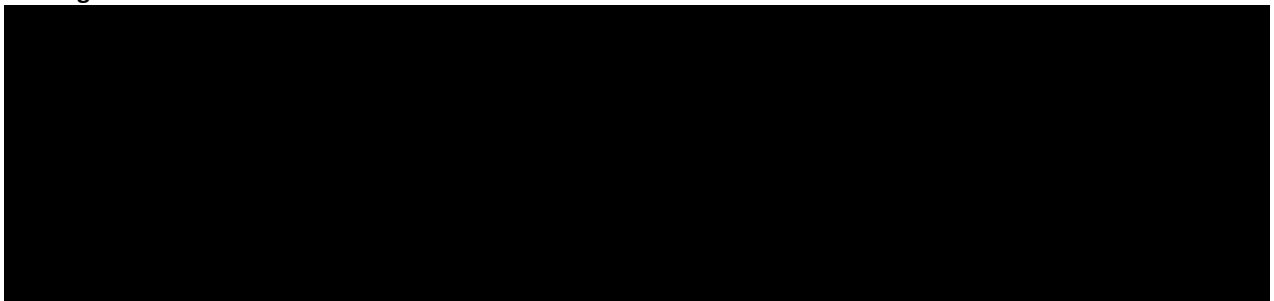
### A. Alignment to Intended Insertion



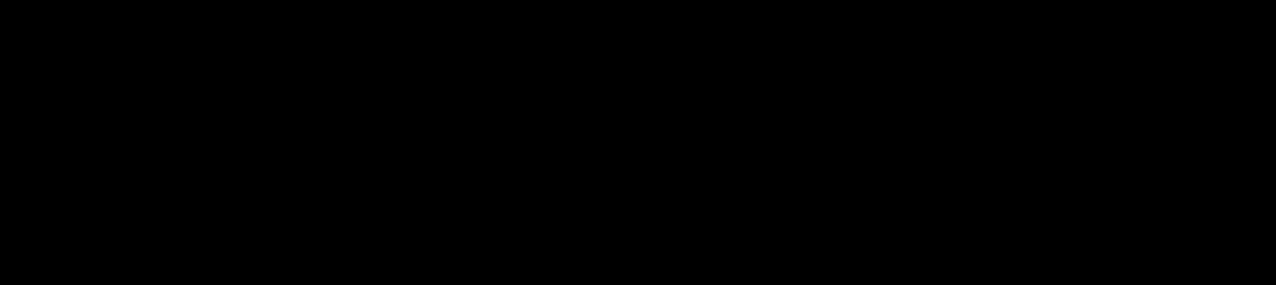
### B. Alignment to PHP83175



### C. Alignment to PHP73878



## E. Alignment to PHP21139



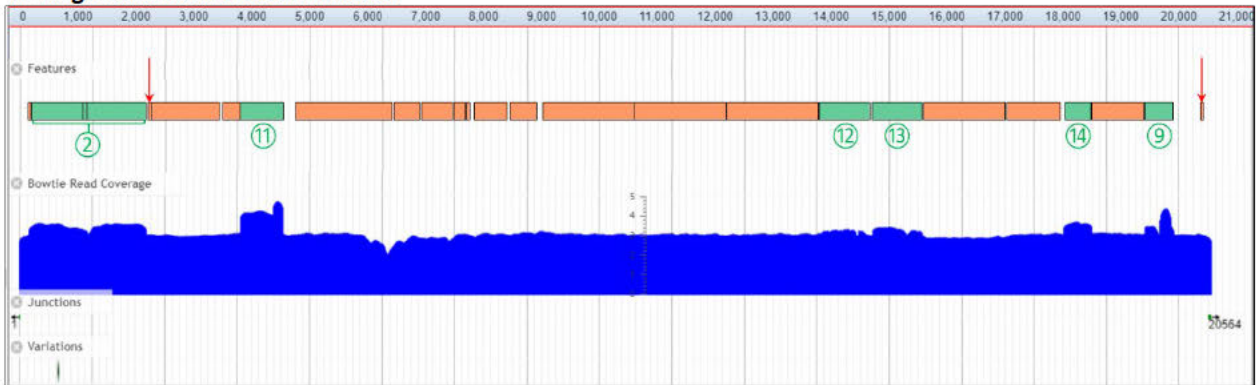
## F. Alignment to PHP21875



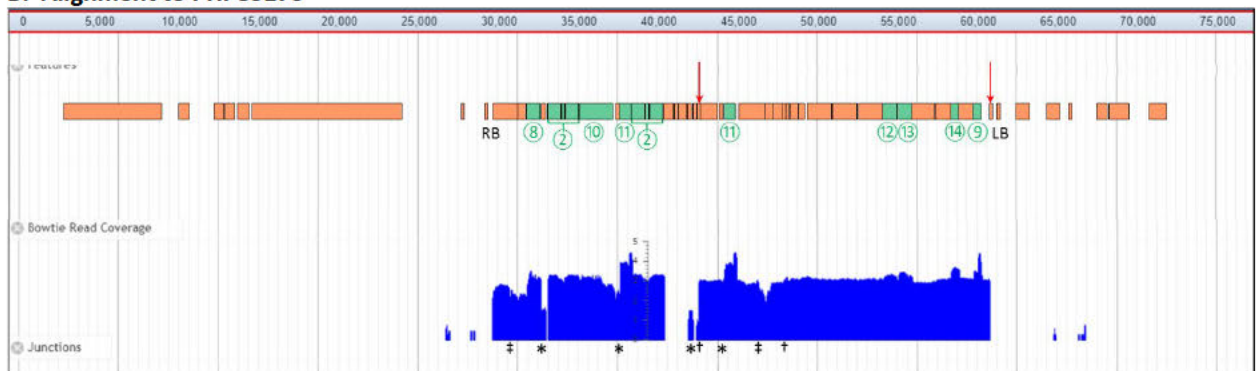
### Figure A.2. SbS Results for DP915635 Maize (Plant ID 385269372)

The blue coverage graph shows the number of individual NGS reads aligned at each point on the intended insertion or construct using a logarithmic scale at the middle of the graph. Green bars above the coverage graph indicate endogenous genetic elements in each plasmid derived from the maize genome (identified by numbers, Table 5), while tan bars indicate genetic elements derived from other sources. FRT sites are indicated by red arrows. **A)** SbS results aligned against the intended insertion (20,564 bp; Figure 8), indicating that this plant contains the intended insertion. Arrows below the graph indicate the two plasmid-to-genome sequence junctions identified by SbS; the numbers below the arrows refer to the bp location of the junction relative to the intended insertion (Figure 8). The presence of only two junctions demonstrates the presence of a single insertion in the DP915635 maize genome. The Variations panel indicates the location of a single nucleotide change identified in all plants containing the insertion. This plant also contains a single nucleotide change in the *os*-actin promoter element that is not present in the other plants containing the insertion. **B)** SbS results aligned against the plasmid PHP83175 sequence (74,997 bp; Figure 6). Coverage was obtained for the elements between FRT1 and FRT6 transferred into DP915635 maize (region between the red arrows at top of graph). Coverage was also obtained for the endogenous elements in the region between the RB and FRT1 that were not transferred into the DP915635 maize genome, and to the *pinII* terminator (\*), CaMV35S terminator (†), and *os*-actin promoter and intron (‡) elements outside of the FRT sites due to alignment of reads derived from identical elements in the final insertion to all copies of these elements in PHP83175. **C)** SbS results aligned against the plasmid PHP73878 sequence [REDACTED] bp; Figure 1). Coverage was obtained for *zm*-SEQ158, *zm*-SEQ159, and the elements found in the intended insertion (between *zm*-SEQ158 to FRT1 and between FRT6 to *zm*-SEQ159), along with the *pinII* terminator element (\*) in PHP73878 due to alignment of reads derived from the *pinII* terminator in the *pmi* cassette of the intended insertion to the copy of this element in PHP73878. **D)** SbS results aligned against the plasmid PHP70605 sequence [REDACTED] bp; Figure 3). Coverage was obtained only for the endogenous elements along with the *pinII* terminator element (\*). **E)** SbS results aligned against the plasmid PHP21139 sequence [REDACTED] bp; Figure 4). Coverage was obtained only for the endogenous elements. **F)** SbS results aligned against the plasmid PHP21875 sequence [REDACTED] bp; Figure 5). Coverage was obtained for the endogenous elements along with the *pinII* terminator element (\*). The absence of any junctions other than to the intended insertion indicates that there are no additional insertions or backbone sequence present in DP915635 maize.

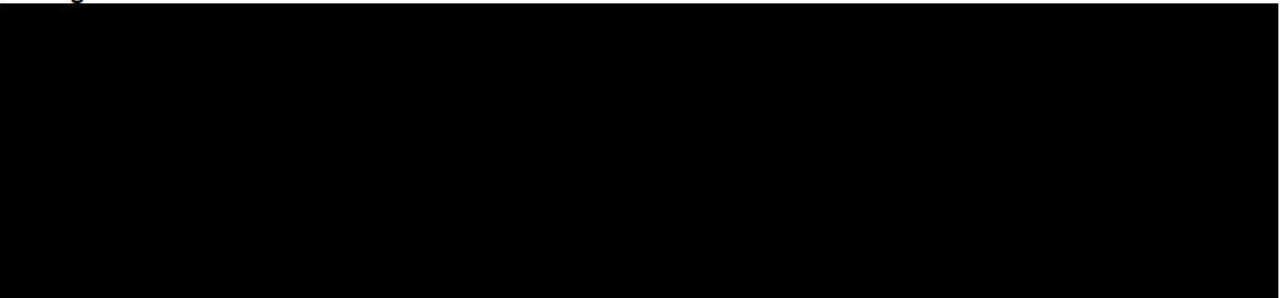
### A. Alignment to Intended Insertion



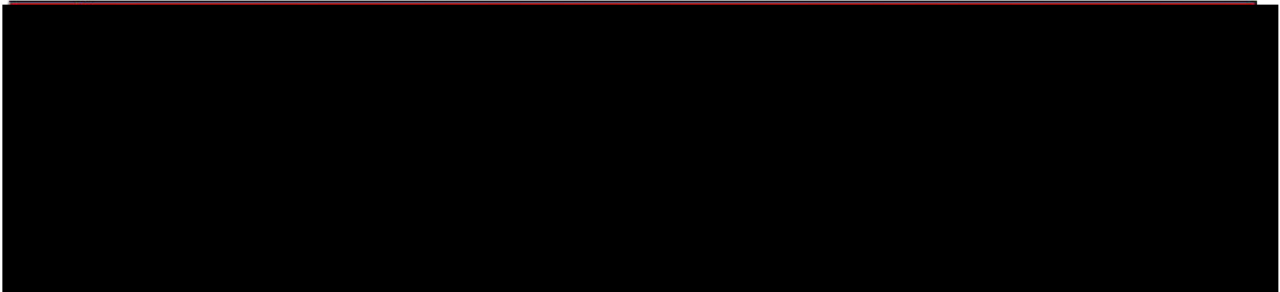
### B. Alignment to PHP83175



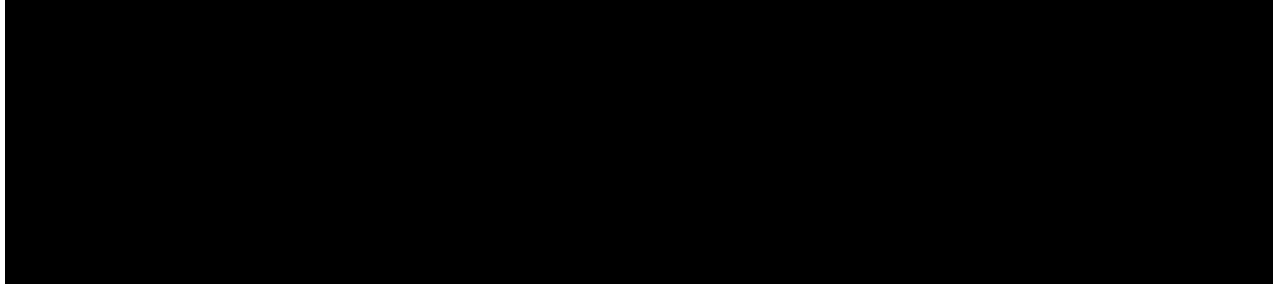
### C. Alignment to PHP73878



### D. Alignment to PHP70605



#### E. Alignment to PHP21139



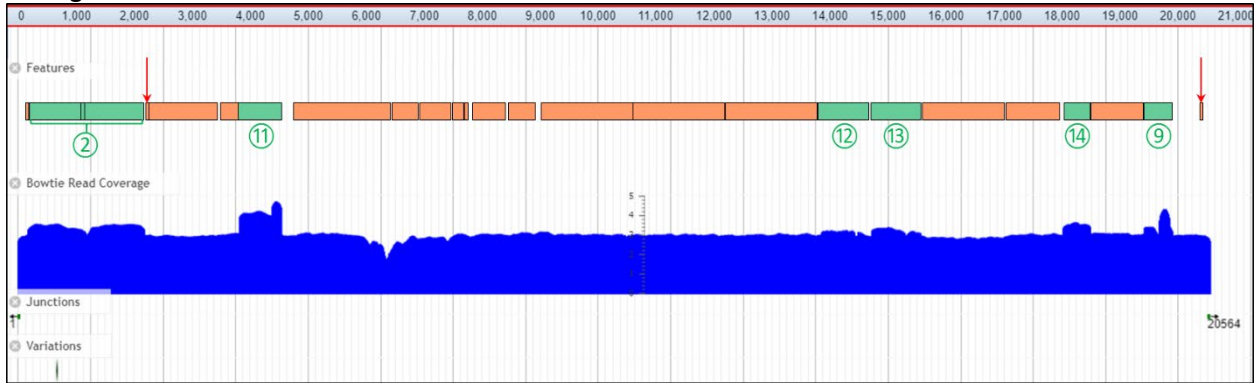
#### F. Alignment to PHP21875



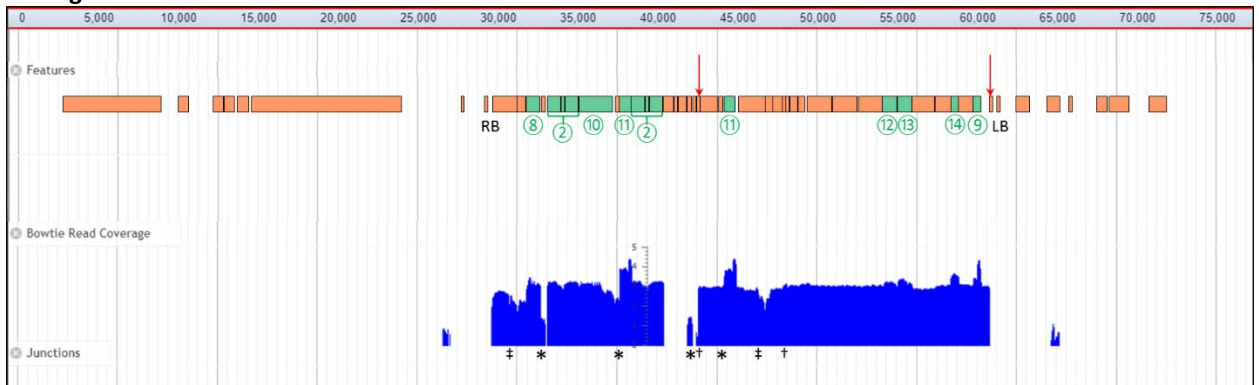
### Figure A.3. SbS Results for DP915635 Maize (Plant ID 385269373)

The blue coverage graph shows the number of individual NGS reads aligned at each point on the intended insertion or construct using a logarithmic scale at the middle of the graph. Green bars above the coverage graph indicate endogenous genetic elements in each plasmid derived from the maize genome (identified by numbers, Table 5), while tan bars indicate genetic elements derived from other sources. FRT sites are indicated by red arrows. **A)** SbS results aligned against the intended insertion (20,564 bp; Figure 8), indicating that this plant contains the intended insertion. Arrows below the graph indicate the two plasmid-to-genome sequence junctions identified by SbS; the numbers below the arrows refer to the bp location of the junction relative to the intended insertion (Figure 8). The presence of only two junctions demonstrates the presence of a single insertion in the DP915635 maize genome. The Variations panel indicates the location of a single nucleotide change identified in all plants containing the insertion. **B)** SbS results aligned against the plasmid PHP83175 sequence (74,997 bp; Figure 6). Coverage was obtained for the elements between FRT1 and FRT6 transferred into DP915635 maize (region between the red arrows at top of graph). Coverage was also obtained for the endogenous elements in the region between the RB and FRT1 that were not transferred into the DP915635 maize genome, and to the *pinII* terminator (\*), CaMV35S terminator (†), and *os*-actin promoter and intron (‡) elements outside of the FRT sites due to alignment of reads derived from identical elements in the final insertion to all copies of these elements in PHP83175. **C)** SbS results aligned against the plasmid PHP73878 sequence [REDACTED] bp; Figure 1). Coverage was obtained for *zm*-SEQ158, *zm*-SEQ159, and the elements found in the intended insertion (between *zm*-SEQ158 to FRT1 and between FRT6 to *zm*-SEQ159), along with the *pinII* terminator element (\*) in PHP73878 due to alignment of reads derived from the *pinII* terminator in the *pmi* cassette of the intended insertion to the copy of this element in PHP73878. **D)** SbS results aligned against the plasmid PHP70605 sequence [REDACTED] bp; Figure 3). Coverage was obtained only for the endogenous elements along with the *pinII* terminator element (\*). **E)** SbS results aligned against the plasmid PHP21139 sequence [REDACTED] bp; Figure 4). Coverage was obtained only for the endogenous elements. **F)** SbS results aligned against the plasmid PHP21875 sequence [REDACTED] bp; Figure 5). Coverage was obtained for the endogenous elements along with the *pinII* terminator element (\*). The absence of any junctions other than to the intended insertion indicates that there are no additional insertions or backbone sequence present in DP915635 maize.

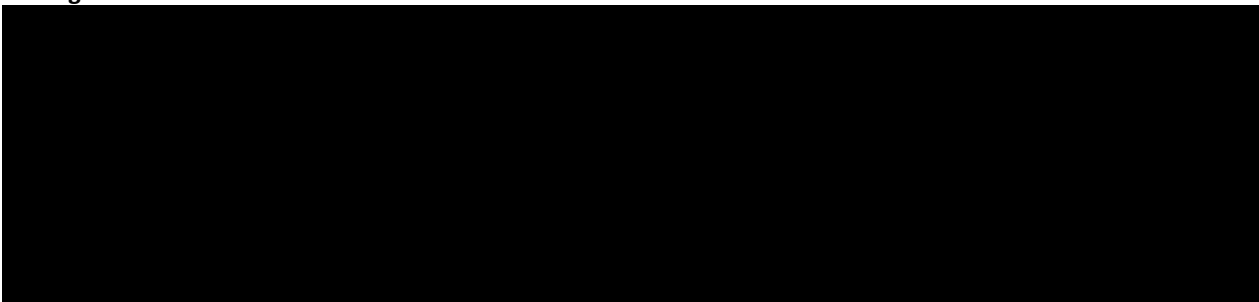
### A. Alignment to Intended Insertion



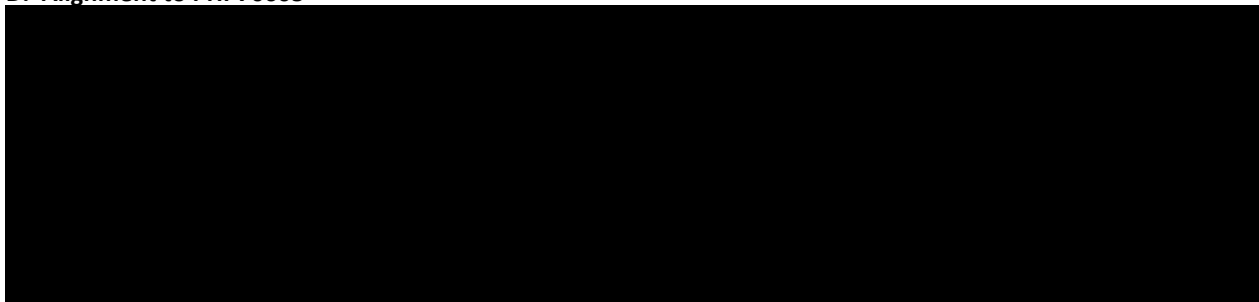
### B. Alignment to PHP83175



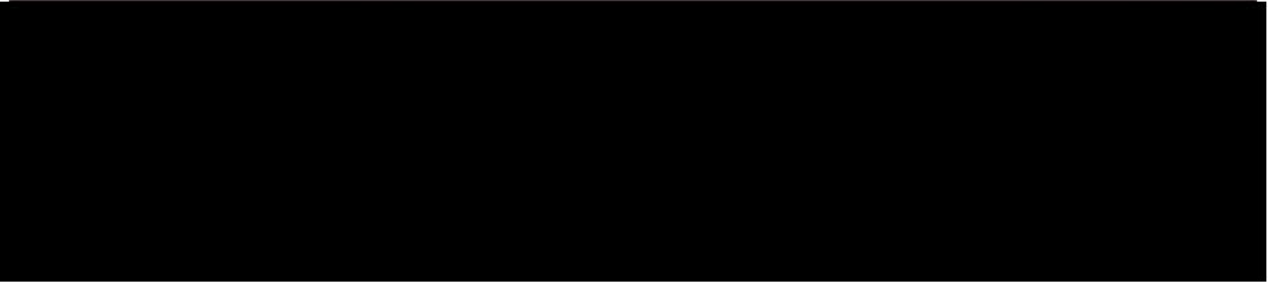
### C. Alignment to PHP73878



### D. Alignment to PHP70605



#### E. Alignment to PHP21139



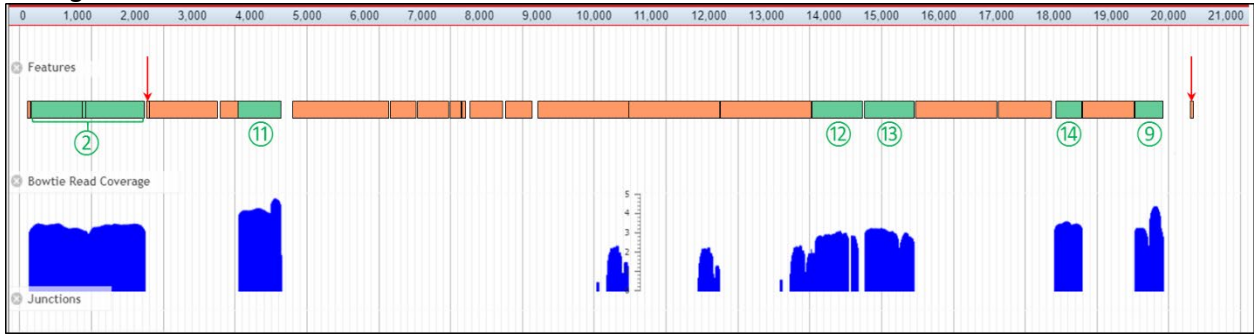
#### F. Alignment to PHP21875



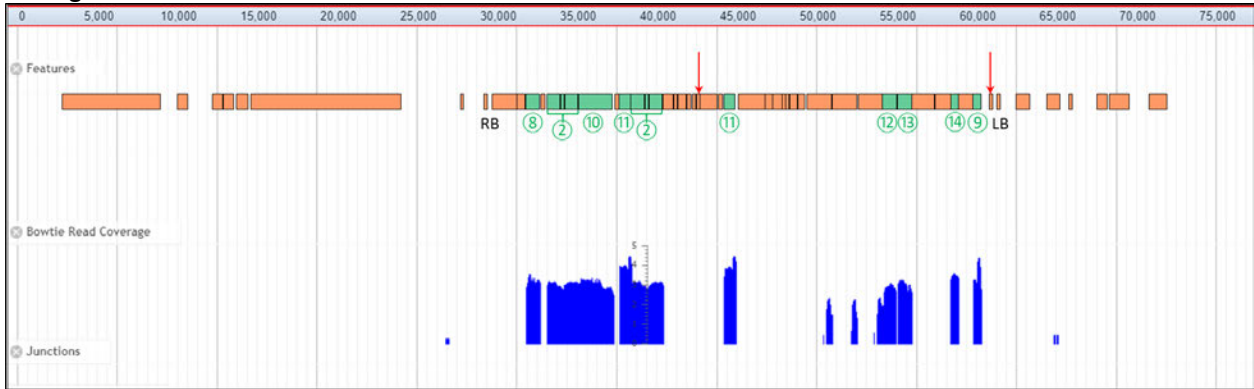
#### Figure A.4. SbS Results for DP915635 Maize (Plant ID 385269375)

The blue coverage graph shows the number of individual NGS reads aligned at each point on the intended insertion or construct using a logarithmic scale at the middle of the graph. Green bars above the coverage graph indicate endogenous genetic elements in each plasmid derived from the maize genome (identified by numbers, Table 5), while tan bars indicate genetic elements derived from other sources. FRT sites are indicated by red arrows. **A)** SbS results aligned against the intended insertion (20,564 bp; Figure 8), indicating that this plant contains the intended insertion. Arrows below the graph indicate the two plasmid-to-genome sequence junctions identified by SbS; the numbers below the arrows refer to the bp location of the junction relative to the intended insertion (Figure 8). The presence of only two junctions demonstrates the presence of a single insertion in the DP915635 maize genome. The Variations panel indicates the location of a single nucleotide change identified in all plants containing the insertion. **B)** SbS results aligned against the plasmid PHP83175 sequence (74,997 bp; Figure 6). Coverage was obtained for the elements between FRT1 and FRT6 transferred into DP915635 maize (region between the red arrows at top of graph). Coverage was also obtained for the endogenous elements in the region between the RB and FRT1 that were not transferred into the DP915635 maize genome, and to the *pinII* terminator (\*), CaMV35S terminator (†), and *os-actin* promoter and intron (‡) elements outside of the FRT sites due to alignment of reads derived from identical elements in the final insertion to all copies of these elements in PHP83175. **C)** SbS results aligned against the plasmid PHP73878 sequence [redacted] bp; Figure 1). Coverage was obtained for *zm*-SEQ158, *zm*-SEQ159, and the elements found in the intended insertion (between *zm*-SEQ158 to FRT1 and between FRT6 to *zm*-SEQ159), along with the *pinII* terminator element (\*) in PHP73878 due to alignment of reads derived from the *pinII* terminator in the *pmi* cassette of the intended insertion to the copy of this element in PHP73878. **D)** SbS results aligned against the plasmid PHP70605 sequence [redacted] bp; Figure 3). Coverage was obtained only for the endogenous elements along with the *pinII* terminator element (\*). **E)** SbS results aligned against the plasmid PHP21139 sequence [redacted] bp; Figure 4). Coverage was obtained only for the endogenous elements. **F)** SbS results aligned against the plasmid PHP21875 sequence [redacted] bp; Figure 5). Coverage was obtained for the endogenous elements along with the *pinII* terminator element (\*). The absence of any junctions other than to the intended insertion indicates that there are no additional insertions or backbone sequence present in DP915635 maize.

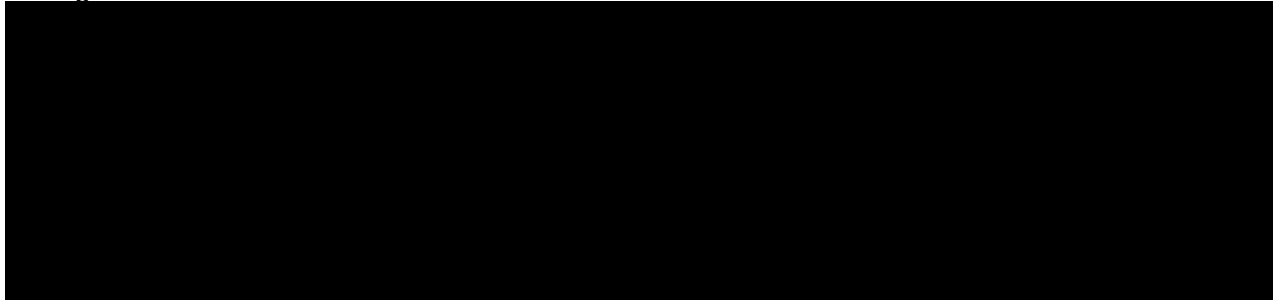
### A. Alignment to Intended Insertion



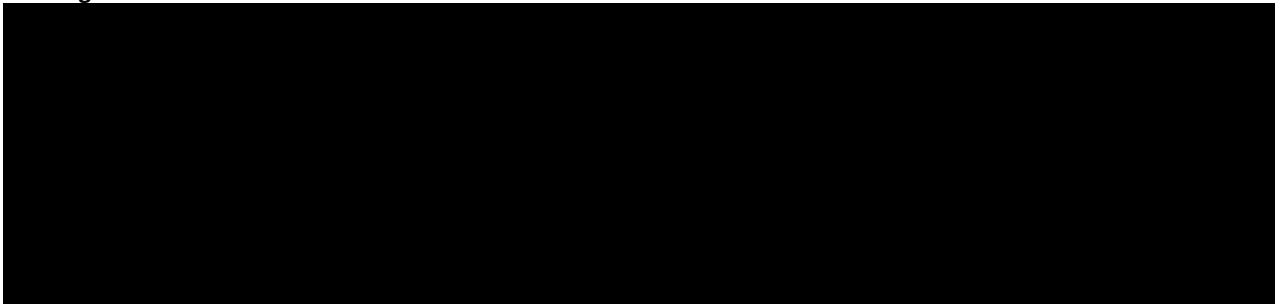
### B. Alignment to PHP83175



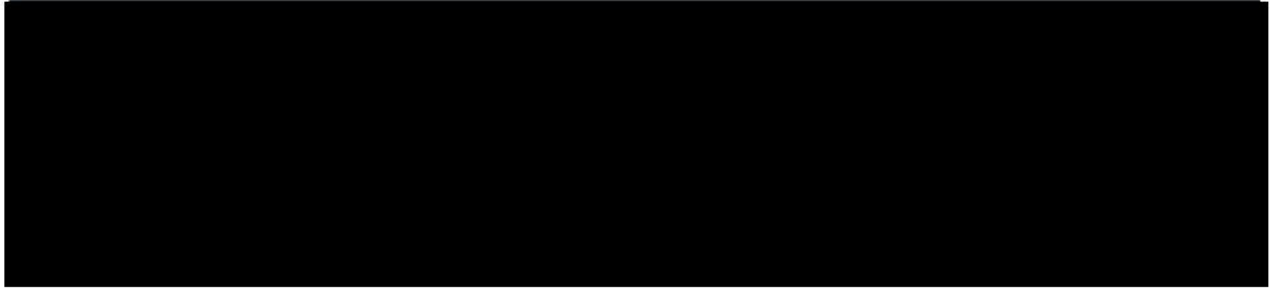
### C. Alignment to PHP73878



### D. Alignment to PHP70605



#### E. Alignment to PHP21139



#### F. Alignment to PHP21875

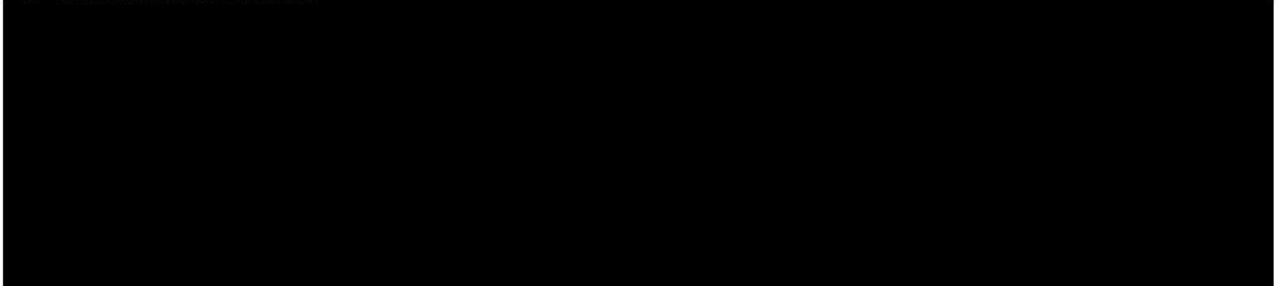
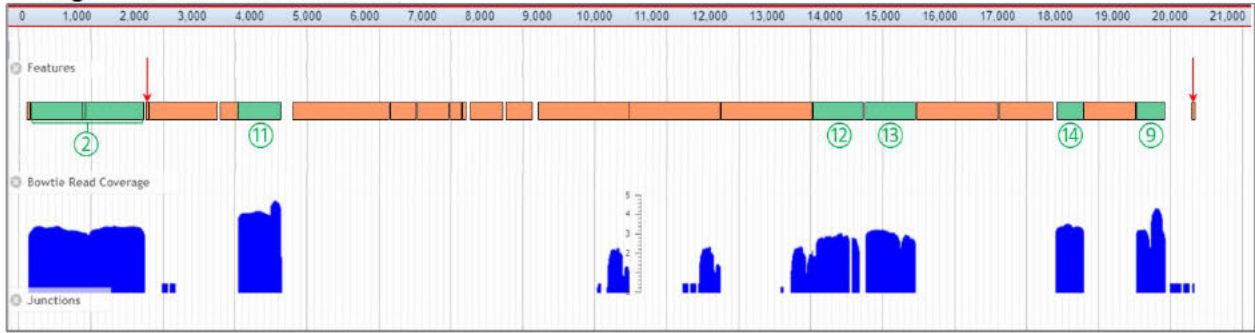


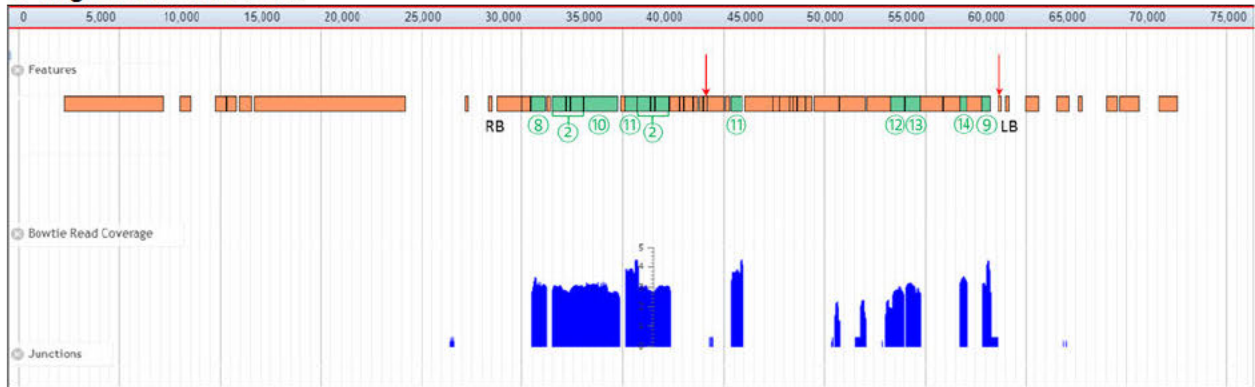
#### Figure A.5. SbS Results for DP915635 Maize (Plant ID 385269367)

The blue coverage graph shows the number of individual NGS reads aligned at each point on the intended insertion or construct using a logarithmic scale at the middle of the graph. Green bars above the coverage graph indicate endogenous genetic elements in each plasmid derived from the maize genome (identified by numbers, Table 5), while tan bars indicate genetic elements derived from other sources. FRT sites are indicated by red arrows. **A)** SbS results aligned against the intended insertion (20,564 bp; Figure 8), indicating that this plant does not contain the intended insertion. Coverage above background level (35x) was obtained only for regions derived from or showing homology to maize endogenous elements. Variation in coverage of the endogenous elements is due to some sequence variation between the genome of PHR03 maize and the source of the corresponding genetic elements. As no junctions were detected between plasmid sequences and the maize genome, there are no DNA insertions identified in this plant, and the sequence reads are solely due to the endogenous or homologous elements present in the PHR03 genome. **B)** SbS results aligned against the plasmid PHP83175 sequence (74,997 bp; Figure 6). Coverage was obtained only for the endogenous elements. **C)** SbS results aligned against the plasmid PHP73878 sequence [redacted] bp; Figure 1). Coverage was obtained only for the endogenous elements. **D)** SbS results aligned against the plasmid PHP70605 sequence [redacted] bp; Figure 3). Coverage was obtained only for the endogenous elements. **E)** SbS results aligned against the plasmid PHP21139 sequence [redacted] bp; Figure 4). Coverage was obtained only for the endogenous elements. **F)** SbS results aligned against the plasmid PHP21875 sequence [redacted] bp; Figure 5). Coverage was obtained only for the endogenous elements. The absence of any junctions between plasmid and genomic sequences indicates that there are no insertions or backbone sequence present in this plant from the T1 generation of DP915635 maize.

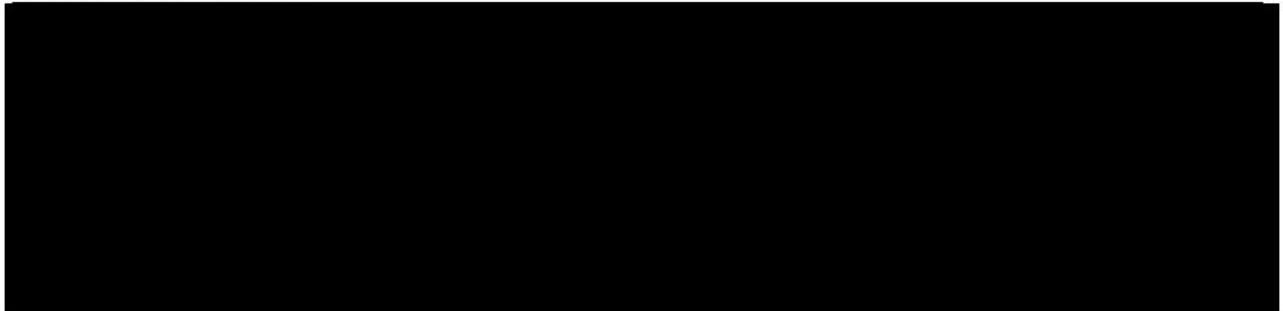
### A. Alignment to Intended Insertion



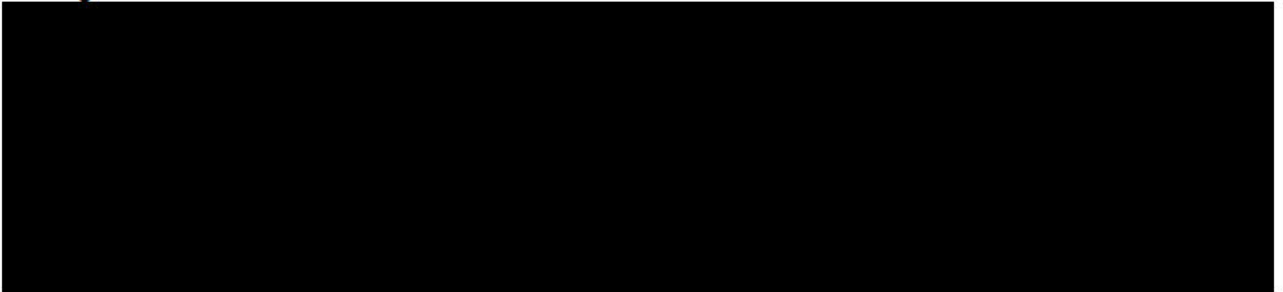
### B. Alignment to PHP83175



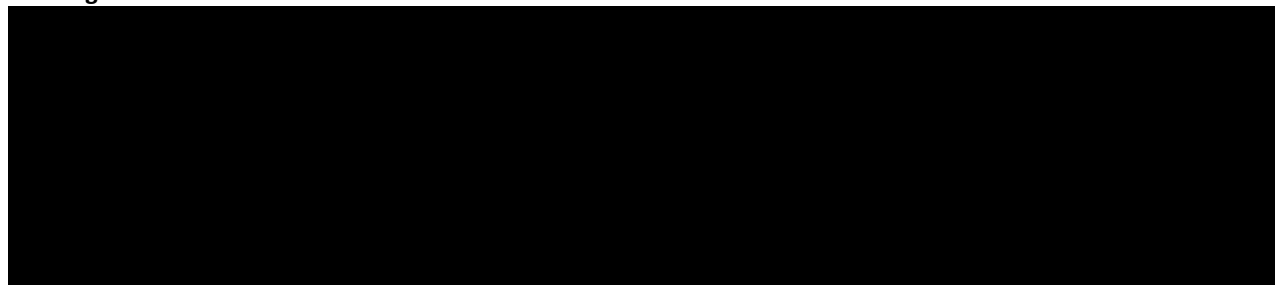
### C. Alignment to PHP73878



### D. Alignment to PHP70605



#### E. Alignment to PHP21139



#### F. Alignment to PHP21875

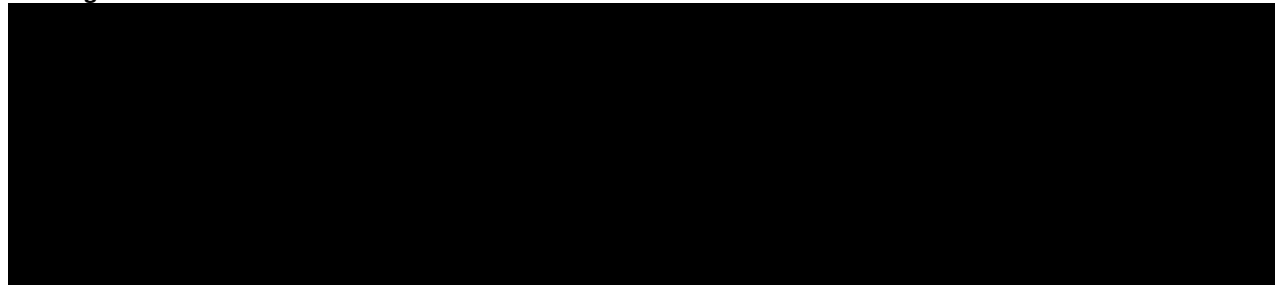
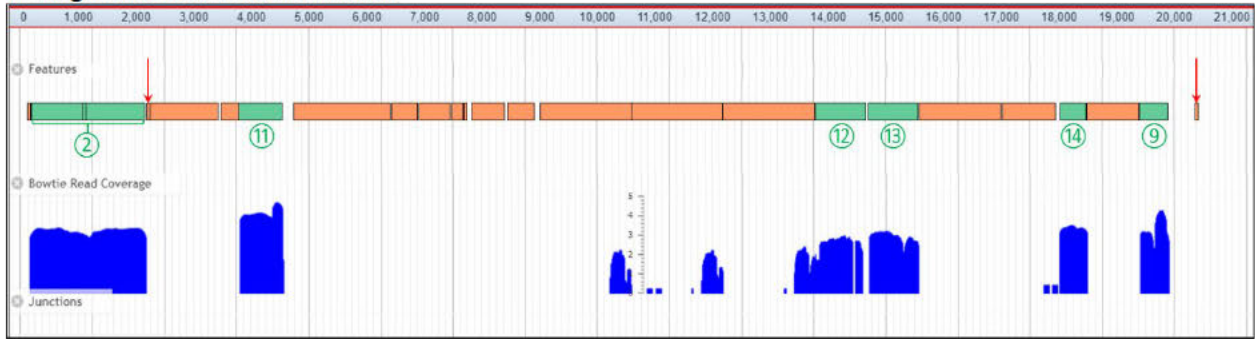


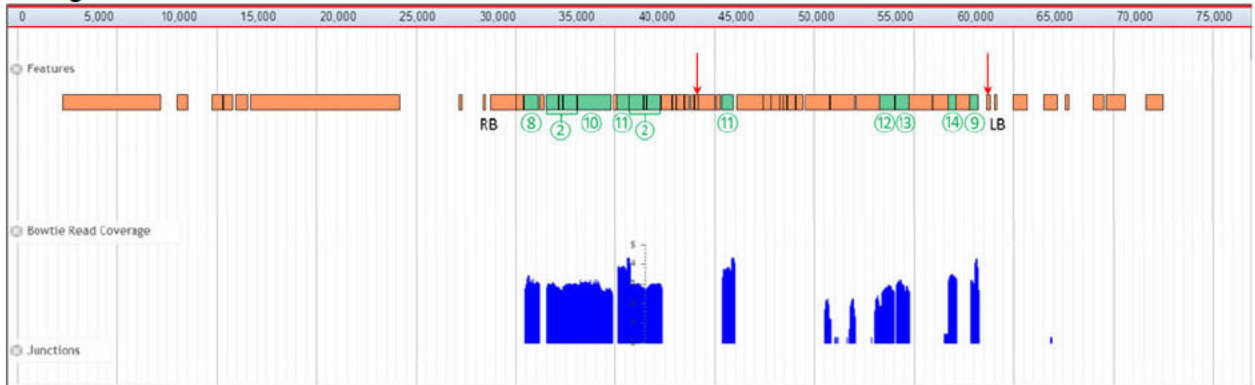
#### Figure A.6. SbS Results for DP915635 Maize (Plant ID 385269368)

The blue coverage graph shows the number of individual NGS reads aligned at each point on the intended insertion or construct using a logarithmic scale at the middle of the graph. Green bars above the coverage graph indicate endogenous genetic elements in each plasmid derived from the maize genome (identified by numbers, Table 5), while tan bars indicate genetic elements derived from other sources. FRT sites are indicated by red arrows. **A)** SbS results aligned against the intended insertion (20,564 bp; Figure 8), indicating that this plant does not contain the intended insertion. Coverage above background level (35x) was obtained only for regions derived from or showing homology to maize endogenous elements. Variation in coverage of the endogenous elements is due to some sequence variation between the genome of PHR03 maize and the source of the corresponding genetic elements. As no junctions were detected between plasmid sequences and the maize genome, there are no DNA insertions identified in this plant, and the sequence reads are solely due to the endogenous or homologous elements present in the PHR03 genome. **B)** SbS results aligned against the plasmid PHP83175 sequence (74,997 bp; Figure 6). Coverage was obtained only for the endogenous elements. **C)** SbS results aligned against the plasmid PHP73878 sequence [redacted] bp; Figure 1). Coverage was obtained only for the endogenous elements. **D)** SbS results aligned against the plasmid PHP70605 sequence [redacted] bp; Figure 3). Coverage was obtained only for the endogenous elements. **E)** SbS results aligned against the plasmid PHP21139 sequence [redacted] bp; Figure 4). Coverage was obtained only for the endogenous elements. **F)** SbS results aligned against the plasmid PHP21875 sequence [redacted] bp; Figure 5). Coverage was obtained only for the endogenous elements. The absence of any junctions between plasmid and genomic sequences indicates that there are no insertions or backbone sequence present in this plant from the T1 generation of DP915635 maize.

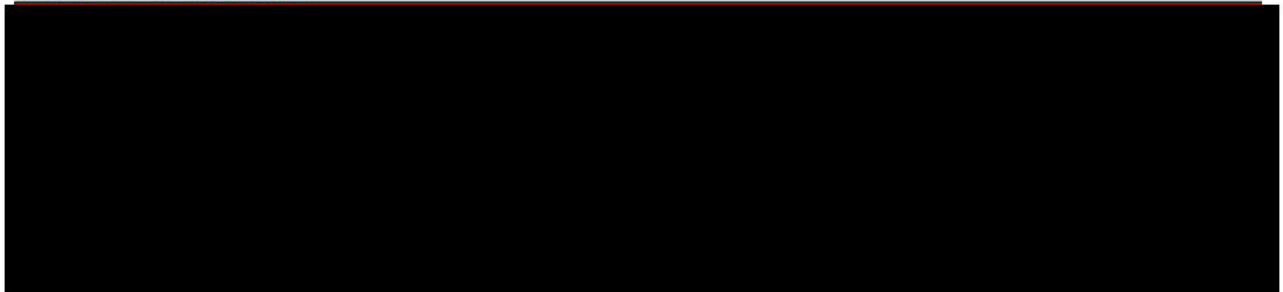
### A. Alignment to Intended Insertion



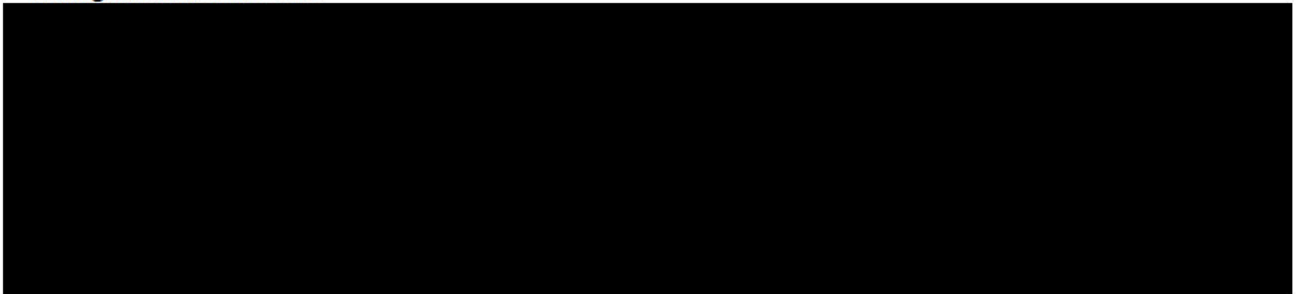
### B. Alignment to PHP83175



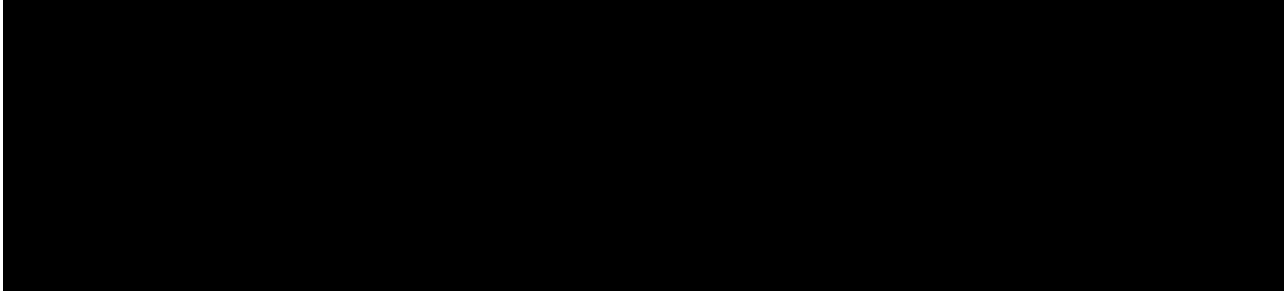
### C. Alignment to PHP73878



### D. Alignment to PHP70605



#### E. Alignment to PHP21139



#### F. Alignment to PHP21875

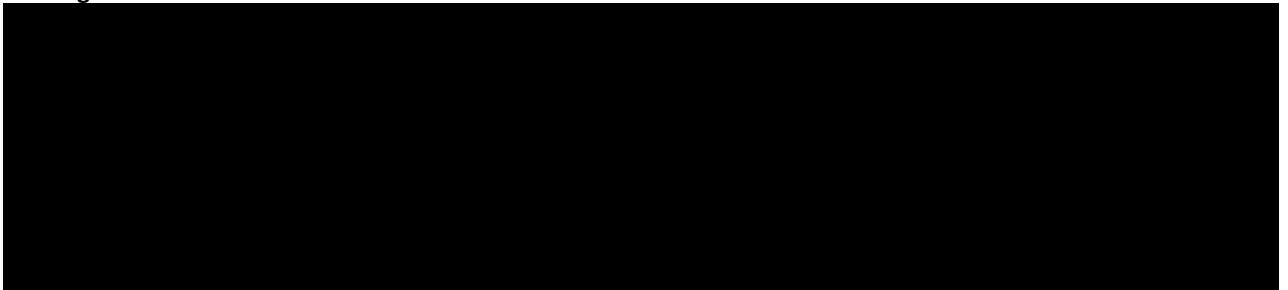
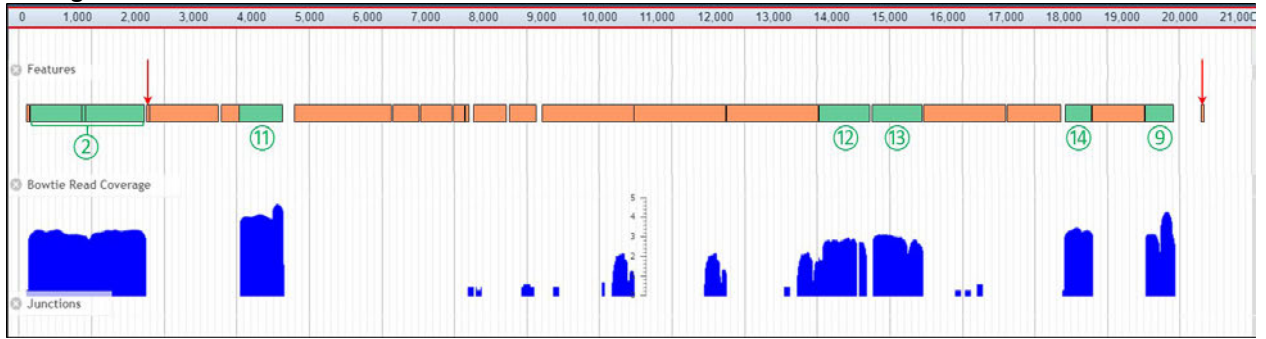


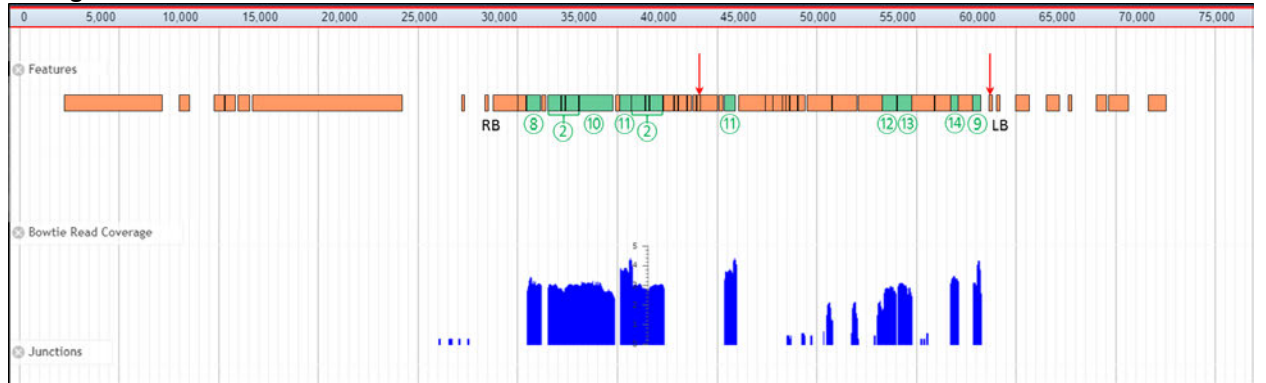
#### Figure A.7. Sbs Results for DP915635 Maize (Plant ID 385269370)

The blue coverage graph shows the number of individual NGS reads aligned at each point on the intended insertion or construct using a logarithmic scale at the middle of the graph. Green bars above the coverage graph indicate endogenous genetic elements in each plasmid derived from the maize genome (identified by numbers, Table 5), while tan bars indicate genetic elements derived from other sources. FRT sites are indicated by red arrows. **A)** Sbs results aligned against the intended insertion (20,564 bp; Figure 8), indicating that this plant does not contain the intended insertion. Coverage above background level (35x) was obtained only for regions derived from or showing homology to maize endogenous elements. Variation in coverage of the endogenous elements is due to some sequence variation between the genome of PHR03 maize and the source of the corresponding genetic elements. As no junctions were detected between plasmid sequences and the maize genome, there are no DNA insertions identified in this plant, and the sequence reads are solely due to the endogenous or homologous elements present in the PHR03 genome. **B)** Sbs results aligned against the plasmid PHP83175 sequence (74,997 bp; Figure 6). Coverage was obtained only for the endogenous elements. **C)** Sbs results aligned against the plasmid PHP73878 sequence [redacted] bp; Figure 1). Coverage was obtained only for the endogenous elements. **D)** Sbs results aligned against the plasmid PHP70605 sequence [redacted] bp; Figure 3). Coverage was obtained only for the endogenous elements. **E)** Sbs results aligned against the plasmid PHP21139 sequence [redacted] bp; Figure 4). Coverage was obtained only for the endogenous elements. **F)** Sbs results aligned against the plasmid PHP21875 sequence [redacted] bp; Figure 5). Coverage was obtained only for the endogenous elements. The absence of any junctions between plasmid and genomic sequences indicates that there are no insertions or backbone sequence present in this plant from the T1 generation of DP915635 maize.

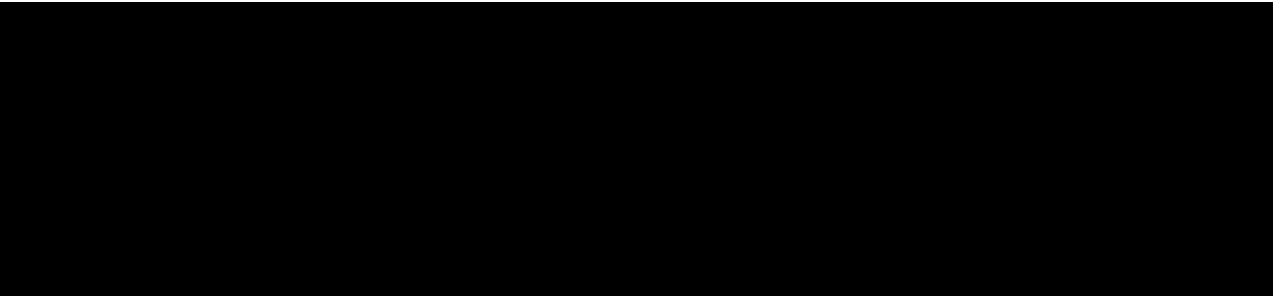
### A. Alignment to Intended Insertion



### B. Alignment to PHP83175



### C. Alignment to PHP73878



### D. Alignment to PHP70605



#### E. Alignment to PHP21139



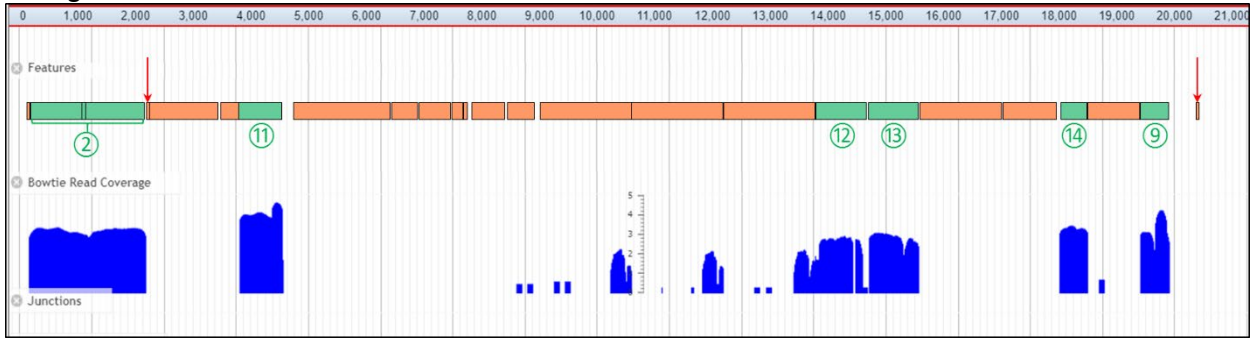
#### F. Alignment to PHP21875



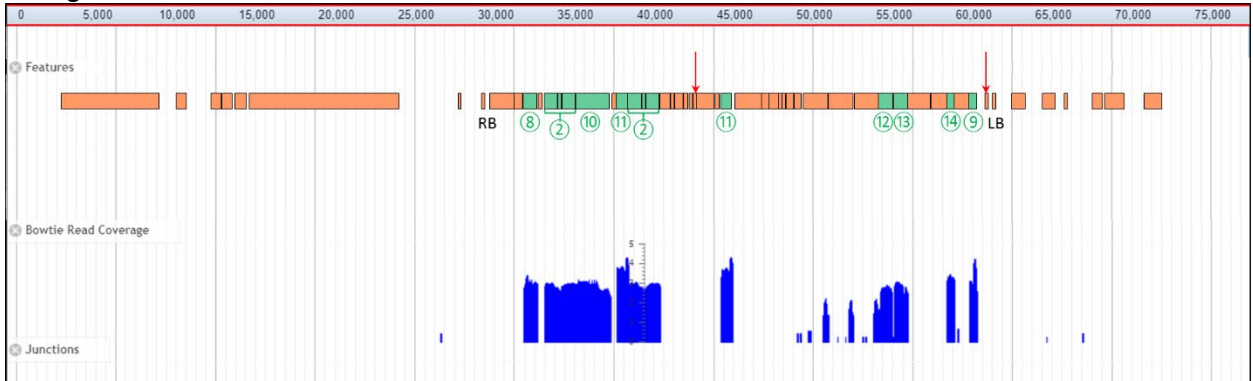
#### Figure A.8. SbS Results for DP915635 Maize (Plant ID 385269374)

The blue coverage graph shows the number of individual NGS reads aligned at each point on the intended insertion or construct using a logarithmic scale at the middle of the graph. Green bars above the coverage graph indicate endogenous genetic elements in each plasmid derived from the maize genome (identified by numbers, Table 5), while tan bars indicate genetic elements derived from other sources. FRT sites are indicated by red arrows. **A)** SbS results aligned against the intended insertion (20,564 bp; Figure 8), indicating that this plant does not contain the intended insertion. Coverage above background level (35x) was obtained only for regions derived from or showing homology to maize endogenous elements. Variation in coverage of the endogenous elements is due to some sequence variation between the genome of PHR03 maize and the source of the corresponding genetic elements. As no junctions were detected between plasmid sequences and the maize genome, there are no DNA insertions identified in this plant, and the sequence reads are solely due to the endogenous elements present in the maize genome. **B)** SbS results aligned against the plasmid PHP83175 sequence (74,997 bp; Figure 6). Coverage was obtained only for the endogenous elements. **C)** SbS results aligned against the plasmid PHP73878 sequence [REDACTED] bp; Figure 1). Coverage was obtained only for the endogenous elements. **D)** SbS results aligned against the plasmid PHP70605 sequence [REDACTED] bp; Figure 3). Coverage was obtained only for the endogenous elements. **E)** SbS results aligned against the plasmid PHP21139 sequence [REDACTED] bp; Figure 4). Coverage was obtained only for the endogenous elements. **F)** SbS results aligned against the plasmid PHP21875 sequence [REDACTED] bp; Figure 5). Coverage was obtained only for the endogenous elements. The absence of any junctions between plasmid and genomic sequences indicates that there are no insertions or backbone sequence present in this plant from the T1 generation of DP915635 maize.

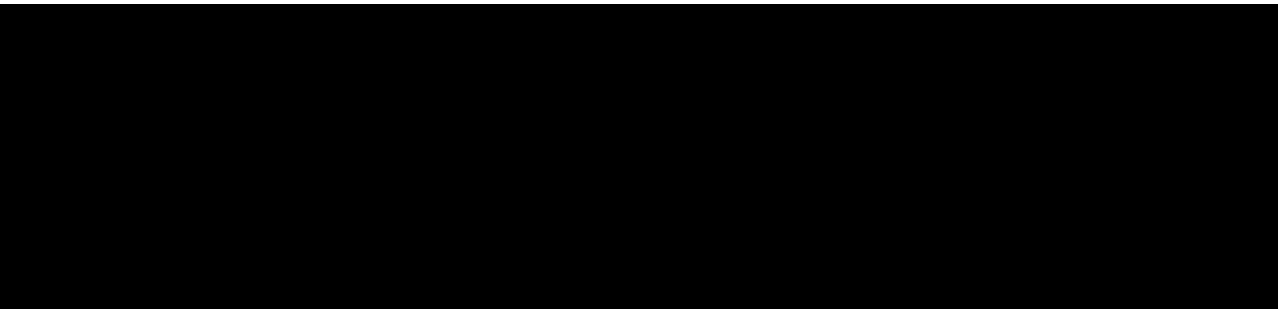
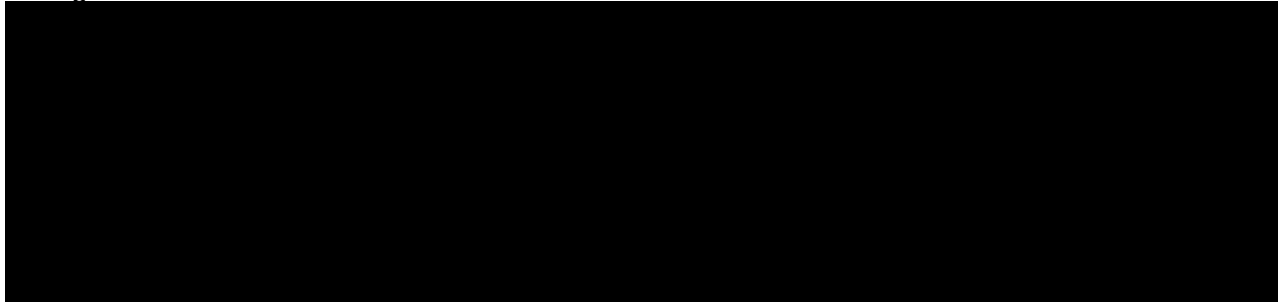
### A. Alignment to Intended Insertion



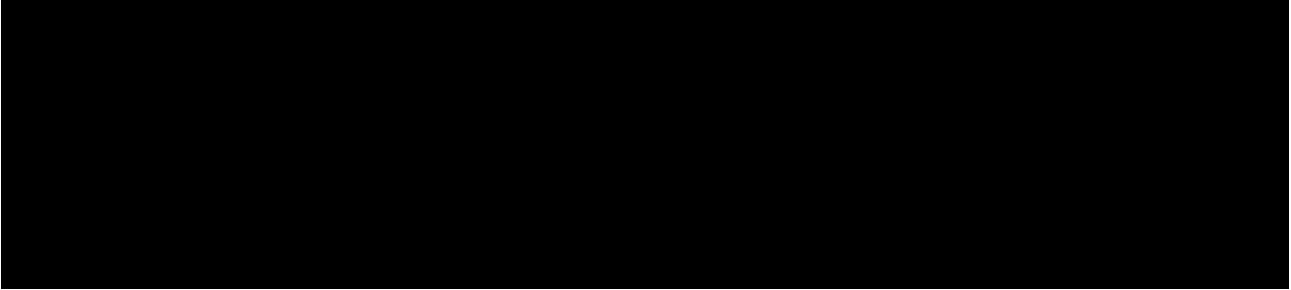
### B. Alignment to PHP83175



### C. Alignment to PHP73878



#### E. Alignment to PHP21139



#### F. Alignment to PHP21875

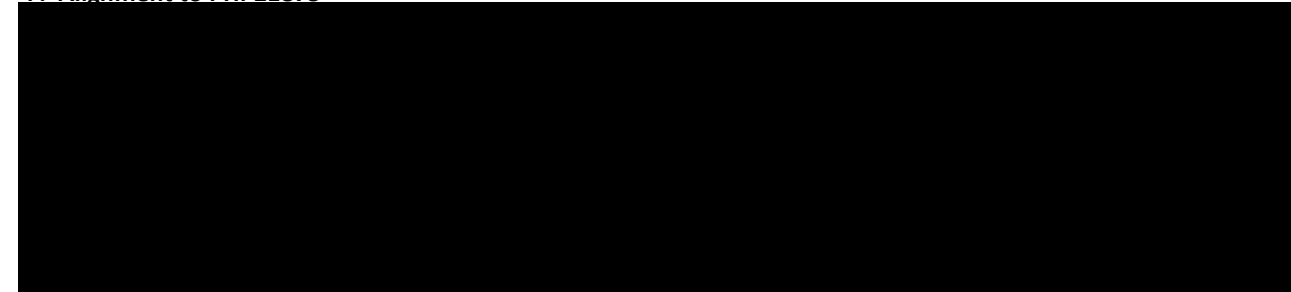


#### Figure A.9. SbS Results for DP915635 Maize (Plant ID 385269376)

The blue coverage graph shows the number of individual NGS reads aligned at each point on the intended insertion or construct using a logarithmic scale at the middle of the graph. Green bars above the coverage graph indicate endogenous genetic elements in each plasmid derived from the maize genome (identified by numbers, Table 5), while tan bars indicate genetic elements derived from other sources. FRT sites are indicated by red arrows. **A)** SbS results aligned against the intended insertion (20,564 bp; Figure 8), indicating that this plant does not contain the intended insertion. Coverage above background level (35x) was obtained only for regions derived from or showing homology to maize endogenous elements. Variation in coverage of the endogenous elements is due to some sequence variation between the genome of PHR03 maize and the source of the corresponding genetic elements. As no junctions were detected between plasmid sequences and the maize genome, there are no DNA insertions identified in this plant, and the sequence reads are solely due to the endogenous elements present in the maize genome. **B)** SbS results aligned against the plasmid PHP83175 sequence (74,997 bp; Figure 6). Coverage was obtained only for the endogenous elements. **C)** SbS results aligned against the plasmid PHP73878 sequence [redacted] bp; Figure 1). Coverage was obtained only for the endogenous elements. **D)** SbS results aligned against the plasmid PHP70605 sequence [redacted] bp; Figure 3). Coverage was obtained only for the endogenous elements. **E)** SbS results aligned against the plasmid PHP21139 sequence [redacted] bp; Figure 4). Coverage was obtained only for the endogenous elements. **F)** SbS results aligned against the plasmid PHP21875 sequence [redacted] bp; Figure 5). Coverage was obtained only for the endogenous elements. The absence of any junctions between plasmid and genomic sequences indicates that there are no insertions or backbone sequence present in this plant from the T1 generation of DP915635 maize.

## APPENDIX B. METHODS FOR SOUTHERN BLOT ANALYSIS

### [PHI-2020-114 study](#)

#### Test, Control and Reference Substances

The test substances in the study were defined as seeds from DP915635 maize of the T1, T2, T3, T4, and T5 generations. The control substance was defined as seed from a maize line (PHR03) that was not transformed. PHR03 maize has a similar genetic background to the test substance; however, it does not contain the DP915635 maize insertion.

Plasmid DNA of PHP83175 that was used for *Agrobacterium*-mediated transformation to produce DP915635 maize was defined as a reference substance. This plasmid was used as a positive control for Southern analysis to verify probe hybridization. The *ipd079Ea*, *mo-pat*, and *pmi* probes used in this analysis were derived from plasmid PHP83175.

DNA molecular weight markers for gel electrophoresis and Southern blot analysis were obtained from commercial vendors and were used as a reference to determine approximate molecular weights of DNA fragments. For Southern analysis, DNA Molecular Weight Marker III and VII, Digoxigenin (DIG)-labeled (Roche), were used as size standards for hybridizing fragments.

#### Sample Collection, Handling, Identification and Storage

Seed from each of the five generations of DP915635 maize and the control maize were planted in a controlled environment at Pioneer Hi-Bred International, Inc., Johnston, Iowa, USA. Fresh leaf tissue samples from test and control maize were harvested and then lyophilized. Lyophilized tissue samples were shipped to Regulatory Sciences, Multi Crop Research Center, Pioneer Hi-Bred Private Limited at Hyderabad, at ambient temperature. Upon arrival, samples were stored frozen (< -50°C freezer unit) until processing.

#### DNA Extraction and Quantification

Genomic DNA was isolated and analyzed from leaf tissue of one plant for each of the T1, T2, T3, T4, and T5 generations of DP915635 maize and one plant from the PHR03 control maize.

The lyophilized leaf samples were pulverized with steel beads in tubes using a paint shaker (AGS Transact Technology Ltd. Care was taken to ensure leaf samples were ground sufficiently for DNA isolation. Genomic DNA was isolated using a high salt extraction buffer (2.0 M Sodium chloride, 100 mM Tris-Hydrochloride pH-8.0, 50 mM Sodium salt of EDTA, 3%  $\beta$ -mercaptoethanol (v/v) and 100 mM Sodium metabisulphite) and sequentially precipitated using potassium acetate and isopropyl alcohol. DNA was treated with Ribonuclease A, purified and precipitated using sodium acetate and chilled ethanol. Following the extraction, DNA was quantified using PicoGreen<sup>®</sup> reagent (Molecular Probes, Invitrogen) and visualized on a 1% agarose gel to check the quality of the isolated DNA.

### Digestion of DNA and Electrophoretic Separation

Genomic DNA isolated from both test and control maize leaves was digested with the restriction enzyme *Pvu* II (Thermo Fisher Scientific). PHP83175 plasmid DNA was added to the control maize DNA samples at a level equivalent to one plasmid copy per genomic copy and digested in the same manner. Following digestion with the restriction enzyme, the fragments produced were electrophoretically separated according to their sizes using an agarose gel and documented by photographing the gel under UV illumination (BioRad Gel doc XR<sup>+</sup> System).

### Southern Transfer

The DNA fragments separated on the agarose gel were denatured *in situ*, transferred to a nylon membrane (GE Healthcare, LC) and fixed to the membrane by UV crosslinking (UV Stratalinker, UVP).

### Probe Labeling and Southern Blot Hybridization

The DNA fragments bound to the nylon membrane were detected as discrete bands when hybridized to a labeled probe. DNA probes specific to the *pmi*, *mo-pat* and *ipd079Ea* gene elements were labeled by incorporation of Digoxigenin (DIG) labeled nucleotide DIG-11-dUTP into the fragments.

Labeled probes were hybridized to the DNA on the nylon membrane for detection of the specific genomic DNA fragments. DNA Molecular Weight Marker III and VII, Digoxigenin (DIG) labeled (Roche) were used for visualization as the fragment size standards on the blot.

### Detection of Hybridized Probes

After stringent washes, DIG-labeled DNA standards and single stranded DIG-labeled probes hybridized to DNA bound to the nylon membrane were visualized using CDP-Star Chemiluminescent Nucleic Acid Detection System with DIG Wash and Block Buffer Set (Roche). Blots were exposed for one or more time points to detect hybridizing fragments and to visualize molecular weight standards. Images were captured by detection with the Syngene G-Box Chemi XT16 and XX6 (Syngene, Inc.). Detected bands were documented for each probe.

### Stripping of Probes and Subsequent Hybridization

Following hybridization and detection, membranes were stripped of DIG-labeled probe to prepare blot for subsequent re-hybridization to a different probe. Membranes were rinsed briefly in distilled and de-ionized water and then stripped in a solution of 0.2N NaOH and 0.1% SDS at 37°C with constant shaking. The membranes were then rinsed in 2x Saline sodium citrate and either used directly for subsequent hybridizations or stored for later use. The alkali-based stripping procedure effectively removed probes labeled with alkali-labile DIG used in these experiments.

## APPENDIX C. METHODS FOR MULTI-GENERATION SEGREGATION ANALYSIS

### [PHI-2019-127 study](#)

Five generations of DP915635 maize (F1, T2, T3, T4, and T5 generations) were evaluated using polymerase chain reaction (PCR) analyses and herbicide-tolerance testing to confirm Mendelian inheritance of genotype and phenotype.

#### Planting and Leaf Sample Collection

More than 100 seeds per generation were planted in separate pots and grown in a controlled environment under standard environmental conditions for producing maize plants. After germination, each generation was thinned to a final population of 100 healthy plants prior to any sampling or analysis. Due to insufficient germination, an additional planting was conducted for the T3 generation to enable a total of 100 plants for subsequent analyses.

One leaf sample per plant was collected at the V2-V4 growth stage (occurs when the leaflets on the second, third, or fourth leaf node, respectively, have unrolled). Each sample consisted of three leaf punches collected into one bullet tube and placed on dry ice until transferred to a freezer ( $\leq -10$  °C) until analysis. Individual plant and corresponding leaf samples were uniquely labeled to allow a given sample to be tracked back to the originating plant.

#### Genotypic Analysis

DNA extraction was performed for the collected leaf samples. The extracted samples were analyzed using real-time quantitative PCR (qPCR) assays to confirm the presence or absence of event DP-915635-4 and the *ipd079Ea*, *mo-pat*, and *pmi* genes.

#### Phenotypic Analysis

A glufosinate herbicide treatment was applied after PCR leaf punch sample collection, when plants were at the V3-V4 growth stages (occurs when the leaflets on the third or fourth leaf node, respectively, have unrolled). The spray mixture consisted of Ignite 280 SL containing 2.34 pounds of glufosinate per gallon (0.28 kg ai/L) as well as ammonium sulfate at a rate of approximately 3.0 lb/A (3.4 kg/ha). No other adjuvants or additives were included in the spray mixture. Ignite 280 SL was applied at a target rate of 32 fl oz/A (2.34 L/ha) with a total spray volume of approximately 15-20 gal/A (187 L/ha), using a spray chamber to simulate a broadcast (over-the-top) application. Actual application rates were within 90-110% of the target herbicide application rate.

Four to six days after herbicide application, each plant was visually evaluated for herbicide tolerance in which presence of herbicide injury corresponded to an herbicide-susceptible phenotype and absence of herbicide injury corresponded to an herbicide-tolerant phenotype.

### Statistical Analysis

A chi-square analysis was performed at the 0.05 significance level on the segregation results of each DP915635 maize generation to compare the observed segregation ratio to the expected segregation ratio (1:1 for the the F1 generation and 3:1 for the T2 and T3 generations). This analysis tested the hypothesis that the introduced traits segregated according to the Mendelian rules of inheritance. The critical value to reject the hypothesis at the 5% level is 3.84. Chi-square testing was not performed for the T4 and T5 generations because all plants were identified as positive (i.e., not segregating) as expected for a homozygous generation.

## APPENDIX D. METHODS FOR SANGER SEQUENCING ANALYSIS

### [PHI-2019-245 study](#)

#### Test and Control Substances

The test substance in the study was defined as seeds from DP915635 maize of the T4 generation. The control substance was defined as seed from a non-genetically modified (non-GM) maize line, PHR03, that has a similar genetic background to the test substance but does not contain the DP915635 maize insertion.

#### DNA Extraction and Quantification

Genomic DNA was extracted from pooled leaf tissue of equal amounts from 10 DP915635 maize plants and a separate pool of leaf tissue from two control maize plants.

Genomic DNA was extracted from finely ground maize leaf tissue using a urea lysis buffer, purified using phenol/chloroform/isoamyl alcohol (25:24:1) separation, RNase treatment, DNA precipitation, and spooling. For DP915635 maize, approximately 0.5 grams of leaf tissue was collected from each of 10 plants, pooled, and ground into a fine powder for DNA extraction. For control maize, approximately 0.5 grams of leaf tissue was collected from each of two plants, pooled, and ground into a fine powder for DNA extraction.

The presence of the DP915635 insertion in the extracted genomic DNA from the DP915635 maize plants and the absence in the extracted DNA from the control maize were further confirmed by event-specific quantitative real-time PCR.

#### Polymerase Chain Reaction (PCR) Amplification of the Insert and Flanking Genomic Regions in DP915635 Maize

Nine overlapping PCR fragments (**A, B, C, D, E, F, G, H, and I**) spanning the insert and the 5' and 3' flanking border regions were amplified from the genomic DNA of DP915635 maize. The non-GM control maize DNA was also used in amplification reactions under the same PCR conditions to serve as a negative control.

PCR fragments were generated using 100 ng of genomic DNA (with the exception of Fragment **C** which used 200 ng) as a template with primers at a concentration of 0.5  $\mu$ M (with the exception of Fragment **F** which used 0.2  $\mu$ M), in a 50  $\mu$ l reaction volume. A high-fidelity enzyme, Phusion<sup>TM</sup> Hot Start II High-Fidelity DNA Polymerase, was used for all fragments except Fragment **D**, which used high-fidelity enzyme Phusion<sup>TM</sup> High-Fidelity DNA Polymerase in GC buffer. PCR conditions were optimized for successful amplification of the targeted fragments (Table D.1).

Two independent PCR reactions for each amplified fragment were performed. A no-template control and DNA from the control substance were also run to verify the purity of the reagents and the specificity of the PCR fragment. PCR products were separated on an agarose gel and visualized under ultraviolet (UV) light.

**Table D.1. PCR Amplification Conditions**

Cycle	Thermal Cycle Conditions <sup>a</sup> for PCR Fragments Generated from DP915635 Maize								
	A	B	C	D	E	F	G	H	I
1x	98°C 2'	98°C 2'	98°C 2'	98°C 30"	98°C 2'				
30x	98°C 15"	98°C 15"	98°C 15"	98°C 10"	98°C 15"				
	64°C 15"	64°C 15"	62°C 15"	66-68°C <sup>b</sup>	65°C 10"	68°C 15"	65°C 12"	64°C 15"	57°C 15"
	72°C 1'15"	72°C 1'30"	72°C 1'45"	10"	72°C 1'	72°C 3'	72°C 2'15"	72°C 1'30"	72°C 1'30"
1x	72°C 10'	72°C 10'	72°C 10'	72°C 3'	72°C 10'				
	4°C ∞	4°C ∞	4°C ∞	4°C ∞	4°C ∞	4°C ∞	4°C ∞	4°C ∞	4°C ∞
Enzyme / Buffer System	Phusion High Fidelity II	Phusion High Fidelity II	Phusion High Fidelity II	Phusion GC	Phusion High Fidelity II				

<sup>a</sup> Cycle time is indicated in minutes (') and seconds (").

<sup>b</sup> One reaction used 66 °C annealing temperature and the other used 68°C.

### Cloning of PCR Products

PCR products from two independent PCR reactions for each PCR fragment were separately cloned into pCRTM Blunt II TOPO® vectors using Zero Blunt® TOPO® PCR Cloning Kit for Sequencing (Invitrogen).

At least five colonies from each transformation were chosen for plasmid DNA isolation. Plasmid DNA was isolated from the resulting bacterial culture using QIAprep Spin Miniprep Kit (Qiagen) and digested with restriction enzymes to confirm the presence of the cloned insert before sequencing. The purified plasmid DNA was quantified using a spectrophotometer.

### Sanger DNA Sequencing

Six positive clones (three from each of the two independent PCR reactions) for each PCR fragment were sequenced by Sanger sequencing using M13 forward and reverse primers and multiple internal sequencing primers. The overlapping PCR fragments of the DP915635 insert and flanking genomic regions were sequenced in both forward and reverse directions to cover every nucleotide by Sanger sequencing (Eurofins).

Fragment F contains three consecutive copies of the *sb*-RCC3 enhancers. Each enhancer contains an *Xmn* I site, and the enhancers are separated by *Bst* BI and *Sal* I sites. Sequencing occurred in two steps. First, PCR product fragment F (6057 bp) was cloned into Topo Blunt II PCR vector (3519 bp). Six positive clones (three from each of the two independent PCR reactions) were sequenced using primers binding to unique regions of the cloned fragment (the the *sb-gkaf* terminator, *zm*-PCOa promoter, the intervening sequence regions between the enhancers, and the Topo Blunt II PCR vector sequence) to determine adjacent regions within the intact fragment.

Next, each of the 6 clones containing fragment F were digested with *Xmn* I, producing 4 unique fragments in 2 bands (an approximately 5 kb band containing F1 and the Topo Blunt II PCR vector, and a second bands containing three approximately 1.5 kb bands F2, F3, and F4). The approximately 5 kb and 1.5 kb bands were separately gel isolated. The purified lower DNA band containing fragments F2, F3, F4 was divided into three aliquots. Each aliquot was further digested using a different combination of enzymes to digest two of the three remaining fragments (defined as Digestion 2) shown Table D.2. The gel-purified fragments F1, F2, F3, and F4 were separately sequenced. A detailed diagram of fragment F, including the restriction enzyme sites, is provided in Figure D.1.

**Table D.2. Restriction Enzyme Digests of Topo Clone DNA Containing PCR Fragment F**

DNA	Products of <i>Xmn</i> I Digestion	Restriction Enzymes for Digestion 2	Products of Digestion 2 <sup>a</sup>
Ligated Fragment F (6,057 bp Fragment F PCR product + 3,519 bp Topo Blunt II PCR vector)	<b>Approximately 5 kb band F1</b> + Topo Blunt II PCR vector (4958 bp)	<b>NA</b>	<b>NA</b>
	<b>Approximately 1.5 kb band F2</b> (1,587 bp), <b>F3</b> (1,594 bp), <b>F4</b> (1,437 bp)	<i>Sal</i> I and <i>Bae</i> I	<b>F2</b> (1,587 bp)
		<i>Bst</i> BI and <i>Bae</i> I	<b>F3</b> (1,594 bp)
		<i>Bst</i> BI and <i>Sal</i> I	<b>F4</b> (1,437 bp)

<sup>a</sup> The resulting fragment is the one not cut by the enzyme in the Restriction Enzymes for Digestion 2 column. Note that after the initial F1 digestion and gel isolation and purification, no further digestion was done on this product.

Sequencher® Version 4.8 software (Gene Codes Corporation) was used to analyze and assemble the sequences with default parameters. Low-quality data and vector sequences were trimmed from the 5' and 3' ends of each trace file when necessary. The sequences from the six clones were used to determine the consensus sequence for each PCR fragment. All reads were manually reviewed, and any ambiguous nucleotide was visually verified from the original chromatograms and compared with sequence reads from the other clones to make a final base call.

The final consensus sequence for the DP915635 insert and flanking genomic regions was generated by combining the overlapping individual consensus sequences of the PCR fragments. The final consensus sequence determined for DP915635 maize was compared with the sequence of the landing pad region of PHP73878 and the T-DNA of PHP83175.

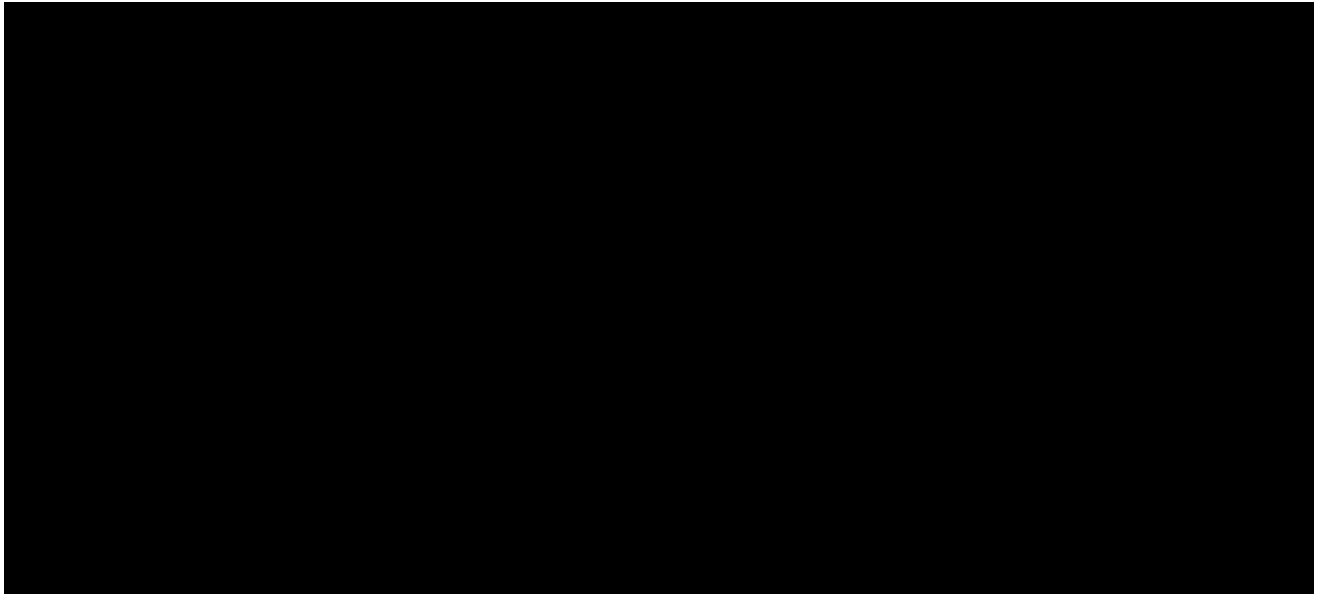


**Figure D.1. Map of Fragment F Indicating Restriction Enzyme Cut Sites**

PCR product fragment F (6057 bp) was cloned into Topo Blunt II PCR vector (3519 bp) and was sequenced in two steps. First, six positive clones (three from each of the two independent PCR reactions) were sequenced using primers binding to unique regions of the cloned fragment to determine adjacent regions within the intact fragment. Next, each of the 6 clones containing the fragment F were digested with XmnI, producing 4 unique fragments (an approximately 5kb F1 fragment with the Topo Blunt II PCR vector and three approximately 1.5 kb fragments F2, F3, F4). After gel separation and isolation, the the purified lower DNA band containing fragments F2, F3, F4 was divided into three aliquots. Each aliquot was further digested using a different combination of enzymes to digest two of the three remaining fragments. Fragment F2 was isolated from the approximately 1.5 kb band when fragments F3 and F4 were digested with Sal I and Bae I. Fragment F3 was isolated from the approximately 1.5 kb band when fragments F2 and F4 were digested with Bst BI and Bae I. Fragment F4 was isolated from the approximately 1.5 kb band when fragments F2 and F3 were digested using Bst BI and Sal I. The gel-purified fragments F1, F2, F3, and F4 were separately sequenced.

## APPENDIX E. METHODS FOR CHARACTERIZATION OF IPD079EA PROTEIN

[PHI-2020-146](#), [PHI-2019-187](#), [PHI-2020-030](#), [PHI-2020-165](#), [PHI-2020-175](#), [PHI-2020-174](#), [PHI-2019-224](#) studies

### Test Materials

*Plant-Derived IPD079Ea Protein:* IPD079Ea protein was isolated from DP915635 maize leaf tissue. The tissue samples were collected at the V9 growth stage (the stage when the collar of the ninth leaf becomes visible; Abendroth et al., 2011) from plants grown at a field location in Johnston, IA, USA. The tissue was lyophilized, homogenized and stored at  $\leq -50$  °C. The IPD079Ea protein was extracted from lyophilized maize tissue by homogenization with a Waring blender using chilled phosphate-buffered saline containing polysorbate 20 (PBST) extraction buffer (20 ml buffer per g tissue). The sample extract was then filtered through cheesecloth and clarified by centrifugation prior to purification by immunoaffinity chromatography. The immunoaffinity column was prepared by coupling an IPD079Ea protein mouse monoclonal antibody (24G10.D10.F3) to AminoLink Plus Coupling Gel. Elutions 2-5 from the immunoaffinity purification were concentrated into one sample using a centrifugal concentrator (30K Vivaspin Turbo 4; Sartorius) and buffer exchanged to a volume of approximately 120  $\mu$ l. Following extraction, purification, and concentration, the final volume in the concentrator was estimated and 50% 2X NuPAGE LDS sample buffer, 20% 10X NuPAGE DTT Sample Reducing Agent, and 30% ultrapure (American Society for Testing and Materials [ASTM] Type 1) water (referred to as water) was added to the concentrated sample. The sample in the concentrator was heated for 2-5 minutes at 70-100 °C and then transferred to a microcentrifuge tube. The sample was then heat treated at 90-100 °C for 5 ( $\pm$ 1) minutes and stored frozen at  $\leq -10$  °C.

*Microbially Derived IPD079Ea Protein:* IPD079Ea protein was produced at Pioneer Hi-Bred International, Inc. using a microbial expression system. The protein was expressed in an *E. coli* protein expression system as a fusion protein with an N-terminal His tag. The tagged protein was purified using Ni-NTA affinity chromatography. The fusion tag was cleaved with thrombin and the thrombin was removed using heparin Sepharose column chromatography. Tangential flow filtration was used to change the buffer to 50 mM ammonium bicarbonate. After lyophilization and mixing, a lot number was assigned.

### SDS-PAGE Analysis

Maize-derived prepared IPD079Ea protein samples were re-heated for 5 minutes at 90-100 °C, diluted as applicable, and then loaded into 4-12% Bis-Tris gels. Pre-stained protein molecular weight markers (Precision Plus Protein Dual Xtra Standards) were loaded into each gel to provide a visual verification that migration was within the range of the predicted molecular weight. Electrophoresis was conducted using a pre-cast gel electrophoresis system with MES SDS running buffer and NuPAGE Antioxidant at a constant 200 volts (V) for 35 minutes. Upon completion of electrophoresis, the gels were removed from the gel cassettes and used for Coomassie staining, western blot analysis, protein glycosylation analysis, or sample preparation for N-terminal amino acid sequencing and peptide mapping.

For the microbially derived samples, a 5.0-mg lyophilized IPD079Ea protein sample was solubilized in 3.85 ml of 1X LDS sample buffer (25% 4X NuPAGE LDS Sample Buffer, 10% 10X NuPAGE Sample Reducing Agent containing DTT, and 65% ASTM [American Society for Testing and Materials] Type 1 water [referred to as water]), dispensed into

aliquots, and heated at 90-100 °C for 5 minutes. The aliquots of solubilized IPD079Ea protein were diluted as applicable prior to loading for SDS PAGE analysis. Following dilution, samples were stored frozen (-80 °C freezer unit) until SDS-PAGE analysis. The prepared protein samples were analyzed using 4-12% Bis-Tris gels. For Coomassie staining and glycosylation staining, 1 µg of IPD079Ea protein was loaded. For western blot analysis, 5 ng of IPD079Ea protein was loaded. For mass spectrometry analyses, 4 µg of IPD079Ea protein was loaded. Pre-stained protein molecular weight markers (Precision Plus Protein Dual Xtra Standards) were also loaded into the gels to provide a visual verification that migration was within the expected range of the predicted molecular weight. Electrophoresis was conducted using a Mini-Cell Electrophoresis System with 1X MES SDS running buffer at a constant 200 volts (V) for 35 minutes. Upon completion of electrophoresis, the gels were removed from the gel cassettes and used for Coomassie staining, western blot analysis, protein glycosylation analysis, or sample preparation for mass spectrometry of chymotryptic peptides.

For Coomassie staining of maize and microbially derived samples, gels were washed with water two-three times for a minimum of 5 minutes each and were stained with GelCode Blue Stain Reagent for approximately 60-90 minutes. Following staining, the gel was de-stained with water four times for a minimum of 5 minutes each or until the gel background was clear. Proteins were detected as blue-colored bands on the gels. The gel image was captured electronically using an imaging system. For the microbially derived samples, densitometry analysis of the gel was conducted to evaluate the purity of the IPD079Ea protein based on the relative intensity of the IPD079Ea protein band within the lane using an imaging software.

#### Western Blot Analysis

Following SDS-PAGE, the resulting gel was assembled into a nitrocellulose or mini nitrocellulose iBlot Gel Transfer Stack. An iBlot Gel Transfer Device was used to transfer proteins from the gel to the nitrocellulose membrane for 7 minutes with a pre-set program (P3).

Following protein transfer, the membrane was blocked in PBST containing 5% weight/volume (w/v) non-fat dry milk for approximately 60 minutes at ambient laboratory temperature. Before the blocking step, the membrane was washed with PBST three times for 1 minutes each to reduce the background. The blocked membrane was incubated in an IPD079Ea polyclonal antibody 15H3 (Pioneer Hi-Bred International, Inc.) diluted 1:5,000 (maize-derived) or 1:10,000 (microbially derived) in PBST containing 1% w/v non-fat dry milk for 60 minutes at ambient temperature. Following primary antibody incubation, the membrane was washed with PBST four times for 5 minutes each. The membrane was incubated in a secondary antibody (anti-mouse IgG horseradish peroxidase conjugate, Promega Corporation) diluted 1:10,000 in PBST containing 1% w/v non-fat dry milk for 60 minutes at ambient laboratory temperature. The membrane was then washed with PBST four times for 5 minutes each. The blot remained in PBST prior to incubating with a chemiluminescent substrate for 5 minutes. The chemiluminescent signal and the pre-stained markers were detected and captured using an imaging system.

#### Peptide Mapping by Mass Spectrometry

Following SDS-PAGE, Coomassie staining, and imaging of the gels, the IPD079Ea protein band was excised from each sample lane and stored frozen at  $\leq -5$  °C. Samples were reduced with DTT, alkylated with iodoacetamide, and then subsequently digested with trypsin or chymotrypsin. The digested samples were separated on an ACQUITY UPLC (Waters Corporation) fitted with a Cortecs UPLC C18 1.6 µm Column (2.1 x 100 mm) (Waters Corporation) by gradient elution. Eluent from the column was directed into an electrospray source, operating in positive mode,

on a TripleTOF 5600+ hybrid quadrupole-time of flight (TOF) mass spectrometer (AB Sciex). The resulting MS data were processed using MS Data Converter (Beta 1.3) to produce a peak list. The peak list was used to perform an MS/MS ion search (Mascot Software version 2.6.1 or version 2.7.0) and match peptides from the expected IPD079Ea protein sequence ([Perkins et al., 1999](#)). The following search parameters were used: peptide and fragment mass tolerance,  $\pm 0.1$  Da; fixed modifications, cysteine carbamidomethyl; variable modifications, methionine oxidation; maximum missed cleavages, 1 for trypsin and 2 for chymotrypsin. The Mascot-generated peptide ion score threshold was  $>13$  which indicates identity or extensive homology ( $p < 0.05$ ). The combined sequence coverage was calculated with GPMW version 12.1 or 12.11.0.

#### N-Terminal Amino Acid Sequencing Analysis

Following SDS-PAGE, Coomassie staining, and gel imaging using the methods as described above, the resulting gel was incubated in cathode buffer (60 mM Tris, 40 mM CAPS, 0.075% SDS, pH 9.6) for 10-20 minutes. An Immobilon-P PVDF membrane was briefly wetted in 100% methanol, followed by immersion in anode buffer (60 mM Tris, 40 mM CAPS, 15% methanol, pH 9.6) for 10-20 minutes. A Trans-Blot SD Semi-Dry Electrophoretic Transfer Cell system was used to transfer proteins from the gel to the membrane at 10 V or 12 V for 45 minutes.

Following transfer of the maize-derived protein, the membrane was washed with water three times for at least 5 minutes each, stained with GelCode Blue stain reagent for 5-10 minutes, and then destained with water to visualize the IPD079Ea protein. A band containing the maize-derived IPD079Ea protein was excised and stored frozen at  $\leq -5$  °C. Following transfer of the microbially derived protein, the membrane was stained with GelCode Blue stain reagent for 10 minutes and then destained with water to visualize the IPD079Ea protein band. The bands containing the maize-derived IPD079Ea protein were excised and stored frozen at  $\leq -5$  °C.

Bands were analyzed using Edman degradation (Edman sequencing). Ten cycles of Edman sequencing were performed using a Shimadzu PPSQ-51A sequencer. During each cycle, the N-terminal amino acid was sequentially derivatized with phenylisothiocyanate (PITC), cleaved with trifluoroacetic acid, and converted to PTH-amino acid which was identified through chromatography. LabSolutions Software was used to automatically identify the N-terminal sequence.

#### Glycoprotein Analysis

A Pierce Glycoprotein Staining Kit was used to determine whether the IPD079Ea protein was glycosylated. The IPD079Ea protein, a positive control protein (horseradish peroxidase), and a negative control protein (soybean trypsin inhibitor) were run by SDS-PAGE as described above.

Following electrophoresis, the gel was washed with water twice for 5 minutes each wash, fixed with 50% methanol for 30-35 minutes, and washed twice with 3% acetic acid for 10-15 minutes each wash. The gel was then incubated with oxidizing solution for 15-20 minutes and washed three times with 3% acetic acid for 5-7 minutes each wash. The gel was incubated with glycoprotein staining reagent for 15-20 minutes and then incubated in a reducing reagent for 5-7 minutes. The gel was then washed one to three times with 3% acetic acid for 5-7 minutes each wash and then rinsed once or twice in water for 5 minutes. Glycoproteins were detected as magenta-colored bands on the gel.

Following glycoprotein detection, the image of the gel was captured electronically. The same gel was then stained with GelCode Blue stain reagent for approximately 60 minutes followed by three washes with water (minimum 5

minutes each wash) to visualize all protein bands. The image of the GelCode stained gel was then captured electronically.

#### Bioactivity Bioassay

The biological activity of the IPD079Ea protein was evaluated by conducting a 7-day bioassay using *Diabrotica virgifera virgifera* (western corn rootworm; Coleoptera: Chrysomelidae), a species sensitive to the IPD079Ea protein. *D. virgifera virgifera* (western corn rootworm; Coleoptera: Chrysomelidae) eggs were obtained from Pioneer Hi-Bred International, Inc. (Johnston, IA, USA) and their identity was recorded by study personnel.

The *D. virgifera virgifera* bioassay utilized a generalized randomized block design containing 3 blocks. Each block consisted of a 24-well bioassay plate and contained 10 replicates from each of the following treatments for a target of 30 individuals per treatment:

Treatment 1: Bioassay Control Diet (containing a dosing solution of ultrapure water)

Treatment 2: Test Diet (targeting 50 ng IPD079Ea protein per mg diet wet weight)

An IPD079Ea protein stock solution was prepared by solubilizing the test substance in ultrapure water and stored frozen (-80 °C freezer unit) until use. To prepare the test dosing solution, the stock solution was allowed to thaw and then diluted in ultrapure water to a concentration of 69.9 ng/μl. The bioassay control dosing solution consisted of ultrapure water. Dosing solutions were prepared on Day 0 and Day 4 of the *D. virgifera virgifera* bioassay and maintained chilled on wet ice until use. The carrier for the *D. virgifera virgifera* bioassay consisted primarily of Stonefly Heliiothis diet. On each day of diet preparation, each dosing solution was combined with carrier at a 2.51:1 ratio (i.e., 2.51 ml of dosing solution to 1 g carrier) to generate Treatments 1 and 2.

*D. virgifera virgifera* eggs were incubated in an environmental chamber until the eggs hatched. *D. virgifera virgifera* neonates were used in the bioassay within 24 hours of hatching. On Day 0 of the bioassay, approximately 300 μl (i.e., 1 g of wet diet equated to 1 ml of wet diet) of freshly prepared diets were dispensed into individual wells of 24-well bioassay plates. One *D. virgifera virgifera* neonate was placed in each well containing diet, each bioassay plate was sealed with heat-sealing film and two small holes were poked over each well to allow for ventilation. The bioassay was conducted in an environmental chamber set at 21°C, 65% relative humidity, and continuous dark for 7 days. On Day 4, new bioassay plates were prepared with fresh diet as described for Day 0, living *D. virgifera virgifera* larvae were transferred to the new plates, missing or dead larvae were recorded, and the freshly prepared plates were placed in the environmental chamber. After 7 days, the bioassay was complete, mortality was assessed, and surviving larvae were individually weighed. Only wells that contained one organism were included in the total number of observed individuals; organisms recorded as missing from a well, or wells containing more than one organism, were excluded from statistical analysis.

The bioassay acceptability criterion indicated the bioassay may be repeated if the combined number of dead and missing organisms exceeds 30% for the bioassay control diet (Treatment 1) group.

#### Thermolability Analysis

*D. virgifera virgifera* larvae were exposed via oral ingestion to one of the following six treatments:

- Treatment 1: Bioassay Control Diet containing ultrapure water
- Treatment 2: Control Diet containing the unheated IPD079Ea protein dosing solution
- Treatment 3: Test Diet containing IPD079Ea protein dosing solution incubated at 25 °C
- Treatment 4: Test Diet containing IPD079Ea protein dosing solution incubated at 50 °C
- Treatment 5: Test Diet containing IPD079Ea protein dosing solution incubated at 75 °C
- Treatment 6: Test Diet containing IPD079Ea protein dosing solution incubated at 95 °C

Dosing solutions were prepared on the day of diet preparation for the *D. virgifera virgifera* bioassay. The bioassay control dosing solution consisted of ultrapure water. To generate the bulk IPD079Ea protein dosing solution for Treatments 2-6, the test substance was thawed under chilled conditions and then diluted in ultrapure water to the appropriate IPD079Ea protein concentration (4750 µg/ml). Aliquots were dispensed into Eppendorf Protein LoBind tubes for heat treatment for 30-35 minutes using a heat block set to obtain temperatures (± 5 °C) of 25 °C, 50 °C, 75 °C, and 95 °C. One vial was left chilled (2-8 °C or on wet ice) as an unheated control treatment. The unheated control diet and each test diet contained a targeted concentration of 50 ng IPD079Ea protein per mg diet wet weight. Treatments were arranged in a generalized randomized block design with a total of 10 blocks. Each block consisted of a 24-well bioassay plate and contained 3 replicates from each treatment. Each diet was provided to a target of 30 individual *D. virgifera virgifera*, with the exception of Treatment 2 which had a target of 24 replicates following an infestation error. The bioassay was conducted in an environmental chamber set at 21 °C, 65% relative humidity, and continuous dark. Organisms were refed on Day 4. After 7 days, the bioassay was complete, final mortality was assessed, and surviving organisms were individually weighed.

The bioassay acceptability criteria were as follows: (1) the combined number of dead and missing organisms must not be greater than 30% for the bioassay control diet (Treatment 1) group, and (2) the mortality of the unheated control diet (Treatment 2) group must exceed 80%. The *D. virgifera virgifera* bioassay met both acceptability criteria. An enzyme-linked immunosorbent assay (ELISA) verified the homogeneity and stability under bioassay storage conditions of the IPD079Ea protein in Treatment 2 and concentration of the IPD079Ea protein dosing solution. The absence of IPD079Ea protein in the bioassay control dosing solution was also verified.

Statistical analyses of data were conducted using SAS software, Version 9.4. Fisher's exact test was used to determine if the mortality rate of *D. virgifera virgifera* fed diets containing the heated IPD079Ea protein (Treatments 3, 4, 5 and 6) was smaller than the mortality rate of those fed the control diet with unheated IPD079Ea protein (Treatment 2). The corresponding hypothesis test was

$$H_0: m_T - m_C = 0 \quad \text{vs.} \quad H_a: m_T - m_C < 0$$

Where  $m_T$  indicates the mortality rate of *D. virgifera virgifera* fed diets containing the heated IPD079Ea protein (Treatments 3, 4, 5 and 6), and  $m_C$  indicates the mortality rate of *D. virgifera virgifera* fed the control diet with unheated IPD079Ea protein (Treatment 2)

As described previously, Treatment 2 had fewer data points than the other treatments (21 total observations compared to 28-30 total observations for Treatments 1, 3, 4, 5, and 6). This reduced sample size for the unheated control treatment reduces the power of the comparisons between the test treatments and Treatment 2; however, if differences between the test entries and the unheated control are sufficiently large, Fisher's exact test will have sufficient power to detect them. The observed mortality rates suggest that despite the reduced sample size for Treatment 2, the comparison used had sufficient power, and additional observations of the unheated control would be very unlikely to change the conclusions of Fisher's exact test. A significant difference was established if the P-value was < 0.05. SAS PROC MULTTEST was utilized to conduct the Fisher's exact test.

#### Digestibility in Simulated Gastric Fluid (SGF)

Test and control solutions were prepared as follows:

- The gastric control solution was prepared fresh on the day of use and was comprised of 0.2% weight per volume (w/v) NaCl in 0.7% volume per volume (v/v) HCl with a pH of ~1.2.
- The pepsin digestion solution, referred to as simulated gastric fluid (SGF), was prepared fresh on the day of use by dissolving pepsin (Sigma-Aldrich) into gastric control solution. The SGF was prepared so that the pepsin to protein ratio of the final digestion mixture was 10 units of pepsin per  $\mu\text{g}$  of test protein.
- The test substance consisted of IPD079Ea protein solubilized from a lyophilized powder.
- To prepare the stock solutions for each of the control proteins (BSA and  $\beta$ -lactoglobulin), a sub-sample of 5.0 mg powder was weighed into an individual tube and solubilized by adding 1 ml of water (for a final protein concentration of 5 mg/ml).
- The final concentration of the protein and pepsin in the control digestion mixtures was 0.25 mg/ml IPD079Ea protein or control protein and 2500 units/ml pepsin.

An IPD079Ea protein pepsin digestion time-course was conducted. SGF solution (1,895  $\mu\text{l}$ ) was dispensed into a 7-ml glass vial and placed in a 37 °C water bath for 2 -5 minutes prior to the addition of 105  $\mu\text{l}$  of IPD079Ea protein test substance at Time 0. The digestion reaction mixture was mixed constantly using a stir bar and a submersible magnetic stirrer.

A 120- $\mu\text{l}$  sub-sample of the IPD079Ea protein digestion reaction mixture was removed from the vial at the following analytical time points ( $\pm$  10 seconds): 0.5, 1, 2, 5, 10, 20, 30, and 60 minutes. The sub-samples were inactivated by adding them to pre-labeled tubes containing 139  $\mu\text{l}$  of a pre-mixed sample solution (consisting of 48  $\mu\text{l}$  stop solution, 65  $\mu\text{l}$  NuPAGE 4X LDS sample buffer, and 26  $\mu\text{l}$  NuPAGE 10X sample reducing agent) and heating to 90-100 °C for 5 minutes prior to storage in a freezer set at -20 °C.

To prepare control digestion samples at 1 and 60 minutes, a 114- $\mu\text{l}$  sample of the digestion solution was pre-warmed in a 37 °C water bath for 2-5 minutes prior to adding 6  $\mu\text{l}$  of the test substance, control protein stock solution, or water. The tubes were incubated in the water bath for the allotted time and then inactivated by mixing with 139  $\mu\text{l}$  of the pre-mixed sample solution.

The Time 0 control reaction mixtures were prepared by first neutralizing 114  $\mu$ l of the digestion solution with 139  $\mu$ l of the pre-mixed sample solution, and then adding 6  $\mu$ l of the IPD079Ea protein test substance, control protein stock solution, or water to the appropriate tube and mixing. Following digestion and inactivation, all control reaction mixtures were heated at 90-100 °C for 5 minutes prior to storage in a freezer (-20 °C freezer unit).

Control digestion samples included in the SGF assay are provided in Table E.1.

**Table E.1. Control Samples for Simulated Gastric Fluid (SGF) Digestibility Analysis**

Protein	Digestion Solution	Digestion Time(s)
None (Water) - SGF Control	SGF	0 min, 60 min
BSA	SGF	0 min, 1 min, 60 min
$\beta$ -Lactoglobulin	SGF	0 min, 1 min, 60 min
IPD079Ea	SGF	0 min
IPD079Ea	Water	0 min, 60 min
IPD079Ea	Gastric Control Solution (No Pepsin)	60 min

#### SDS-PAGE Analysis

The IPD079Ea protein digestion time-course samples and control samples were removed from frozen storage, heated at 90-100 °C for 5 minutes, and loaded (10  $\mu$ l /well) into 4-12% Bis-Tris gels for SDS-PAGE analysis. Pre-stained protein molecular weight markers (Precision Plus Dual Xtra Standards) were also loaded into the gels to provide a visual verification that migration was within the expected range of the predicted molecular weight. Electrophoresis was conducted using a pre-cast gel electrophoresis system with 1X MES SDS running buffer at a constant 200 volts (V) for 35 minutes.

Upon completion of electrophoresis, the gels were removed from the gel cassettes for use in Coomassie staining or western blot analyses. For protein staining, the gels were washed three times for 5 minutes each with water and stained with GelCode Blue Stain Reagent for 60 minutes. Following staining, the gels were destained with water four times for a minimum of 5 minutes each or until the gel background was clear. Proteins were detected as blue-colored bands on the gels. The gel image was captured electronically using an imaging system.

#### Western Blot Analysis

The IPD079Ea protein digestion time-course samples were also analyzed by western blot. Following SDS-PAGE, one of the resulting gels was assembled into a nitrocellulose (NC) iBlot Gel Transfer Stack. An iBlot Gel Transfer Device was used to transfer proteins from the gel to the NC membrane for 7 minutes with a pre-set program (P3). Following protein transfer, the membrane was blocked in phosphate-buffered saline containing polysorbate 20 (PBST) containing 5% weight/volume (w/v) non-fat dry milk for 50 minutes at ambient laboratory temperature. Before and after the blocking step, the membrane was washed with PBST three times for 5 minutes each to reduce the background. The blocked membrane was incubated for 46 minutes at ambient laboratory temperature with an

IPD079Ea polyclonal antibody 12032 (Pioneer Hi-Bred International, Inc.) diluted 1:100,000 in PBST containing 1% (w/v) non-fat dry milk. Following primary antibody incubation, the membrane was washed in PBST three times for 5 minutes each. The membrane was incubated for 48 minutes at ambient laboratory temperature with a secondary antibody (anti-rabbit IgG, horseradish peroxidase conjugate; Promega Corporation) diluted 1:100,000 in PBST containing 1% (w/v) non-fat dry milk. The membrane was washed in PBST three times for 5 minutes each. The blot remained in PBST prior to incubating with a chemiluminescent substrate for 5 minutes. The chemiluminescent signal and the pre-stained markers were detected and captured using an imaging system.

#### Digestibility in Simulated Intestinal Fluid (SIF)

Test and control solutions were prepared as follows:

- The pancreatin digestion solution, referred to as simulated intestinal fluid (SIF), was prepared fresh on the day of use by dissolving pancreatin (Sigma-Aldrich) into intestinal control solution (I-Con 1X buffer) to a final concentration of 0.5% weight per volume (w/v) pancreatin and 50 mM  $\text{KH}_2\text{PO}_4$ .
- The test substance consisted of IPD079Ea protein solubilized from a lyophilized powder
- To prepare the stock solutions for each of the control proteins (BSA and  $\beta$ -lactoglobulin), a sub-sample of 5.0 mg of powder was weighed into an individual tube for each control and solubilized by adding 1 ml of water (to a target protein concentration of 5 mg/ml).
- The final concentration of the protein and pancreatin in the SIF reaction mixture was 0.25 mg/ml IPD079Ea protein and 0.5% (w/v) pancreatin.

An IPD079Ea protein pancreatin digestion time-course was conducted. SIF solution (1,895  $\mu\text{l}$ ) was dispensed into a 7-ml glass vial and placed in a 37 °C water bath for 2-5 minutes prior to the addition of 105  $\mu\text{l}$  of IPD079Ea protein test substance at Time 0. The digestion reaction mixture was mixed constantly using a stir bar and a submersible magnetic stirrer.

A 120- $\mu\text{l}$  sub-sample of the IPD079Ea protein digestion reaction mixture was removed from the vial at the following analytical time points ( $\pm 10$  seconds): 0.5, 1, 2, 5, 10, 20, 30, and 60 minutes. The sub-samples were inactivated by adding them to pre-labeled tubes containing 64  $\mu\text{l}$  of pre-mixed sample solution (consisting of 46  $\mu\text{l}$  NuPAGE 4X LDS Sample Buffer and 18  $\mu\text{l}$  NuPAGE 10X Sample Reducing Agent) and heating to 90-100 °C for 5 minutes prior to storage in a freezer set at -20 °.

To prepare control digestion samples at 1 and 60 minutes, a 114  $\mu\text{l}$  sample of the digestion solution was pre-warmed in a 37 °C water bath for 2-5 minutes prior to adding 6  $\mu\text{l}$  of the IPD079Ea protein test substance, control protein stock solution, or water. The tubes were incubated in the water bath for the allotted time and then inactivated by mixing with 64  $\mu\text{l}$  of the pre-mixed sample solution.

The time zero control reaction mixtures were prepared by first neutralizing 114  $\mu\text{l}$  of the digestion solution with 64  $\mu\text{l}$  of the pre-mixed sample solution, and then adding 6  $\mu\text{l}$  of the IPD079Ea protein test substance, protein stock solution, or water to the appropriate tube and mixing.

Following digestion and inactivation, all control reaction mixtures were heated at 90-100 °C for 5 minutes prior to storage in a freezer set at -20 °C.

Control digestion samples included in the SIF assay are provided in Table E.2.

**Table E.2. Control Samples for Simulated Intestinal Fluid (SIF) Digestibility Analysis**

Protein	Digestion Solution	Digestion Time(s)
None (Water) - SIF Control	SIF	0 min, 60 min
BSA	SIF	0 min, 1 min, 60 min
$\beta$ -Lactoglobulin	SIF	0 min, 1 min, 60 min
IPD079Ea	SIF	0 min
IPD079Ea	Water	0 min, 60 min
IPD079Ea	Intestinal Control Solution (No Pancreatin)	60 min

#### SDS-PAGE Analysis

The IPD079Ea protein digestion time-course samples and control samples were removed from frozen storage, heated at 90-100 °C for 5 minutes, and loaded (10  $\mu$ l /well) into 4-12% Bis-Tris gels for SDS-PAGE analysis. Pre-stained protein molecular weight markers (Precision Plus Dual Xtra Standards) were also loaded into the gels to provide a visual verification that migration was within the expected range of the predicted molecular weight. Electrophoresis was conducted using a pre-cast gel electrophoresis system with 1X MES SDS running buffer at a constant 200 volts (V) for 35 minutes.

Upon completion of electrophoresis, the gels were removed from the gel cassettes for use in Coomassie staining or western blot analyses. For protein staining, the gels were washed three times for 5 minutes each with water and stained with GelCode Blue Stain Reagent for 60 minutes. Following staining, the gels were destained with water four times for a minimum of 5 minutes each or until the gel background was clear. Proteins were detected as blue-colored bands on the gels. The gel image was captured electronically using an imaging system.

#### Western Blot Analysis

The IPD079Ea protein digestion time-course samples were also analyzed by western blot. Following SDS-PAGE, one of the resulting gels was assembled into a nitrocellulose (NC) iBlot Gel Transfer Stack. An iBlot Gel Transfer Device was used to transfer proteins from the gel to the NC membrane for 7 minutes with a pre-set program (P3). Following protein transfer, the membrane was blocked in phosphate-buffered saline containing polysorbate 20 (PBST) containing 5% weight/volume (w/v) non-fat dry milk for 50 minutes at ambient laboratory temperature. Before and after the blocking step, the membrane was washed with PBST three times for 5 minutes each to reduce the background. The blocked membrane was incubated for 50 minutes at ambient laboratory temperature with an IPD079Ea polyclonal antibody 12032 (Pioneer Hi-Bred International, Inc.) diluted 1:100,000 in PBST containing 1% (w/v) non-fat dry milk. Following primary antibody incubation, the membrane was washed in PBST three times for 5 minutes each. The membrane was incubated for 45 minutes at ambient laboratory temperature with a secondary antibody (anti-rabbit IgG, horseradish peroxidase conjugate; Promega Corporation) diluted 1:100,000 in PBST containing 1% (w/v) non-fat dry milk. The membrane was washed in PBST four times for 5 minutes each. The blot

remained in PBST prior to incubating with a chemiluminescent substrate for 5 minutes. The chemiluminescent signal and the pre-stained markers were detected and captured using an imaging system.

#### Digestibility in sequential digestion in simulated gastric fluid (SGF) and simulated intestinal fluid (SIF)

Test solutions were prepared as follows:

- A concentrated (i.e., 2X) pepsin digestion solution, referred to as simulated gastric fluid (SGF), was prepared fresh on the day of use by solubilizing pepsin (Sigma-Aldrich) in a previously prepared 2X gastric control solution. The final concentration of gastric control solution in SGF was 0.2% weight per volume (w/v) NaCl and 0.7% volume per volume (v/v) HCl ; pH ~1.2. The SGF was prepared so that the pepsin to protein ratio of the final digestion mixture was 10 units of pepsin per  $\mu\text{g}$  of test protein.
- A concentrated (i.e., 2.5X) pancreatin digestion solution, referred to as simulated intestinal fluid (SIF), was prepared fresh on the day of use by solubilizing pancreatin (Sigma-Aldrich) in 2.5X intestinal control solution (2.5X I-Con). The final concentration of intestinal control solution in SIF was 50 mM  $\text{KH}_2\text{PO}_4$ , with a pH of ~7.5. Pancreatin content in SIF was adjusted so that there was approximately 0.5% (w/v) pancreatin in the final digestion reaction mixture.
- The pre-mixed sample solutions used to inactivate samples were prepared fresh on the day of use. The solution for SGF reactions was prepared by mixing 1200  $\mu\text{l}$   $\text{Na}_2\text{CO}_3$  stop solution, 1625  $\mu\text{l}$  NuPAGE 4X LDS Sample Buffer, and 650  $\mu\text{l}$  NuPAGE Sample Reducing Agent. The solution for SIF reactions was prepared by mixing 1150  $\mu\text{l}$  NuPAGE 4X LDS Sample Buffer and 450  $\mu\text{l}$  NuPAGE Sample Reducing Agent.
- The test substance consisted of IPD079Ea protein solubilized from a lyophilized powder.

#### In Vitro Pepsin Digestion

A control sample (IPD079Ea in SGF Time 0) was prepared by first inactivating 60  $\mu\text{l}$  of 2X SGF and 49  $\mu\text{l}$  water in 139  $\mu\text{l}$  of pre-mixed SGF sample solution and then adding 12  $\mu\text{l}$  of IPD079Ea protein test substance to the neutralized SGF. The neutralized sample was heated for 5 minutes at 90-100  $^\circ\text{C}$  and stored on ice until transfer to freezer storage ( $\leq -10$   $^\circ\text{C}$ ).

An SGF-only control sample without IPD079Ea protein test substance (SGF Control 10 minutes) was prepared by mixing 60  $\mu\text{l}$  2X SGF and 49  $\mu\text{l}$  water in a tube and pre-warming at 37  $^\circ\text{C}$  for 2-5 minutes. A volume of water (12  $\mu\text{l}$ ) was added to the tube and the tube was allowed to incubate in a 37  $^\circ\text{C}$  water bath for 10 minutes ( $\pm 10$  seconds). After incubation, the sample was inactivated by neutralization with 139  $\mu\text{l}$  of pre-mixed SGF sample solution. The neutralized sample was heated for 5 minutes at 90-100  $^\circ\text{C}$  and stored on ice until transfer to freezer storage ( $\leq -10$   $^\circ\text{C}$ ).

An aliquot (1 ml) of the 2X SGF solution and 790  $\mu\text{l}$  water were dispensed into a 7-ml glass vial and pre-warmed in the 37  $^\circ\text{C}$  water bath for 2-5 minutes prior to addition of the 210  $\mu\text{l}$  IPD079Ea protein test substance. The SGF digestion reaction mixture was incubated and mixed constantly using a stir bar and submersible stir plate for 10 minutes ( $\pm 10$  seconds) after adding the IPD079Ea protein test substance. At the end of the time period, a 1.5-ml sample of the IPD079Ea SGF digestion reaction mixture was transferred to a separate vial and inactivated by neutralization with 0.3 ml of 0.5 N NaOH. This sample was used for the sequential SIF digestion.

A 120- $\mu$ l control sample (IPD079Ea in SGF 10 minutes) was taken out from the SGF digestion reaction mixture at the end of 10 minutes ( $\pm$  10 seconds) and inactivated by neutralization with 139  $\mu$ l of pre-mixed SGF sample solution. The neutralized sample was heated for 5 minutes at 90-100 °C and stored on ice until transfer to freezer storage ( $\leq$  -10 °C).

#### Sequential Pancreatin Digestion

A SIF control sample (IPD079Ea 10 minutes SGF Time 0 SIF) was prepared by mixing 48  $\mu$ l 2.5X SIF with 64  $\mu$ l of pre-mixed SIF sample solution and then heating for 5 minutes at 90-100 °C. A sub-sample (72  $\mu$ l) of the neutralized IPD079Ea SGF digestion reaction mixture was added to the heat-inactivated SIF control sample and then heated again for 5 minutes at 90-100 °C.

For the sequential SIF digestion time course, a 1.2-ml sample of the neutralized IPD079Ea SGF digestion reaction mixture was dispensed into a 7-ml glass vial and placed in the 37 °C water bath for 2-5 minutes prior to addition of 800  $\mu$ l 2.5X SIF solution. The SIF digestion reaction mixture was mixed constantly using a stir bar and a submersible stir plate.

A 120- $\mu$ l sub-sample of the SIF digestion reaction mixture was removed from the vial at each of the following analytical time points ( $\pm$  10 seconds): 0.5, 1, 2, 5, 10, 20 and 30 minutes. Each sub-sample was neutralized by adding it to a pre-labeled tube containing 64  $\mu$ l of pre-mixed SIF sample solution. The neutralized samples were inactivated by heating at 90-100 °C for 5 minutes.

After neutralization and heating, all SIF reaction samples were stored on ice and then transferred to freezer storage ( $\leq$  -10 °C).

#### SDS-PAGE Analysis

The digestion samples were removed from frozen storage, heated at 90-100 °C for 5 minutes, and loaded (10  $\mu$ l/well) into a 4-12% Bis-Tris gel for SDS-PAGE analysis. Pre-stained protein molecular weight markers (Precision Plus Dual Xtra Standards) were also loaded into the gel to provide a visual estimate of molecular weight. Electrophoresis was conducted using a pre-cast gel electrophoresis system with 1X MES SDS running buffer at a constant 200 volts (V) for 35 minutes.

Upon completion of electrophoresis, the gel was removed from the gel cassette and washed three times for 5 minutes each with water and stained with GelCode Blue Stain Reagent for 77 minutes. Following staining, the gel was destained with water four times for a minimum of 5 minutes each or until the gel background was clear. Proteins were detected as blue-colored bands on the gel. The gel image was captured electronically using an imaging system.

## APPENDIX F. METHODS FOR CHARACTERIZATION OF PAT PROTEIN

### [PHI-2020-147 study](#)

#### Test Materials

PAT protein was isolated from DP915635 maize leaf tissue. The tissue samples were collected at the V9 growth stage (the stage when the collar of the ninth leaf becomes visible; Abendroth et al., 2011) from plants grown at a field location in Johnston, IA, USA. The tissue was lyophilized, homogenized and stored at  $\leq -50$  °C.

The PAT protein was extracted from lyophilized maize tissue by homogenization in a pre-chilled Waring blender vessel using chilled phosphate-buffered saline containing polysorbate 20 (PBST) extraction buffer (500 ml buffer per 30 g tissue per batch). The sample extract was then filtered through cheesecloth, clarified by centrifugation, and fractionated using ammonium sulfate (AS) precipitation. Beginning at 0% AS saturation and using an online calculator by EnCor Biotechnology Inc. (Encor Biotechnology, 2020), AS was slowly added to the sample extract while stirring until 45% AS saturation was reached. The sample was centrifuged and the AS process was repeated with the supernatant, this time beginning at 45% AS saturation and progressing to 60%. The sample was centrifuged again, the supernatant was discarded, and the fractionated pellets were solubilized in phosphate-buffered saline and buffer exchanged using Econo-Pac 10DG columns from BioRad.

The sample after buffer exchange was further purified by immunoaffinity chromatography. The immunoaffinity column was prepared by coupling a PAT monoclonal antibody (2C10.D5.G8) to AminoLink Plus Coupling Gel. Elutions 2-5 from the immunoaffinity purification were collected separately and immediately neutralized with 1M Tris buffer, pH 8.

The PAT protein was further purified by ion exchange purification using a Q Sepharose column. Elutions 2-4 from immunoaffinity purification were pooled, diluted in 50 mM Tris pH 8, and then added to the column containing the Q ion exchange resin. Collected fractions from elutions 2-5 were concentrated into one sample using a centrifugal concentrator (10K Vivaspin; Sartorius) and buffer exchanged to a volume of approximately 130  $\mu$ l.

Following extraction, purification, and concentration, the final volume in the concentrator was estimated and 25% 2X NuPAGE LDS sample buffer and 10% 10X NuPAGE DTT Sample Reducing Agent was added to the concentrated sample. The sample in the concentrator was heated for 2-5 minutes at 70-100 °C and then transferred to a microcentrifuge tube. The sample was then heat treated at 90-100 °C for 5 ( $\pm$ 1) minutes and stored frozen at  $\leq -10$  °C.

#### SDS-PAGE Analysis

The maize-derived PAT protein sample was re-heated for 5 minutes at 90-100 °C, diluted as applicable, and then loaded into 4-12% Bis-Tris gels. Pre-stained protein molecular weight markers (Precision Plus Protein Dual Xtra Standards) were loaded into each gel to provide a visual verification that migration was within the range of the predicted molecular weight. For SDS-PAGE and western blot analysis, the PAT protein reference substance was also re-heated for 5 minutes at 90-100 °C, diluted in 1X LDS/DTT to approximately the same concentration as the maize-derived protein, and loaded into the gel. Electrophoresis was conducted using a pre-cast gel electrophoresis system with MES SDS running buffer and NuPAGE Antioxidant at a constant 200 volts (V) for 35 minutes. Upon completion of electrophoresis, the gels were removed from the gel cassettes and used for Coomassie staining, western blot

analysis, protein glycosylation analysis, or sample preparation for N-terminal amino acid sequencing and peptide mapping.

For Coomassie staining, the gel was washed with water 2 times for 5 minutes each and stained with GelCode Blue Stain Reagent for 60 minutes. Following staining, the gel was de-stained with water 4 times for at least 5 minutes each until the gel background was clear. Proteins were stained as blue-colored bands on the gel. The gel image was captured electronically using an imaging system (Bio-Rad ChemiDoc MP).

#### Western Blot Analysis

Following SDS-PAGE, the resulting gel was assembled into a nitrocellulose (NC) iBlot Gel Transfer Stack. An iBlot Gel Transfer Device was used to transfer proteins from the gel to the NC membrane for 7 minutes with a pre-set program (P3).

Following protein transfer, the membrane was blocked in PBST containing 5% weight/volume (w/v) non-fat dry milk for 60 minutes at ambient laboratory temperature. Before and after the blocking step, the membrane was washed with PBST 3 times for 1 minute each to reduce the background. The blocked membrane was incubated for 60 minutes at ambient laboratory temperature with a PAT monoclonal antibody 22H2.G4 (Pioneer Hi-Bred International, Inc.) diluted 1:5000 in PBST containing 1% w/v non-fat dry milk. Following primary antibody incubation, the membrane was washed 4 times in PBST for 5 minutes each. The membrane was incubated for 60 minutes at ambient laboratory temperature with a secondary antibody (anti-mouse IgG, horseradish peroxidase conjugate; Promega Corporation) diluted 1:10,000 in PBST containing 1% non-fat dry milk. The membrane was washed 4 times with PBST for 5 minutes each. The blot remained in PBST prior to incubating with a chemiluminescent substrate for 5 minutes. The chemiluminescent signal and the pre-stained markers were detected and captured using an imaging system.

#### Peptide Mapping by Mass Spectrometry

Following SDS-PAGE, Coomassie staining, and gel imaging using the methods as described above, two PAT protein bands were excised from a gel and stored frozen at  $\leq -5$  °C. The protein in each gel slice was reduced with DTT, alkylated with iodoacetamide, and then subsequently digested with trypsin or chymotrypsin. The digested samples were separated on an ACQUITY UPLC (Waters Corporation) fitted with a Cortecs UPLC C18 1.6  $\mu$ m Column (2.1 x 100 mm) (Waters Corporation) by gradient elution. Eluent from the column was directed into an electrospray source, operating in positive mode, on a TripleTOF 5600+ hybrid quadrupole-TOF mass spectrometer (AB Sciex). The resulting MS data were processed using MS Data Converter (Beta 1.3) to produce a peak list. The peak list was used to perform an MS/MS ion search (Mascot Software version 2.7.0) and match peptides from the expected PAT protein sequence (Perkins et al., 1999). The following search parameters were used: peptide and fragment mass tolerance,  $\pm 0.1$  Da; fixed modifications, cysteine carbamidomethyl; variable modifications, methionine oxidation; and maximum missed cleavages, 1 for trypsin and 2 for chymotrypsin. The Mascot-generated peptide ion score threshold was  $>13$  which indicates identity or extensive homology ( $p < 0.05$ ). The combined sequence coverage was calculated with GPMW version 12.11.0.

### N-Terminal Amino Acid Sequencing Analysis

Following SDS-PAGE, Coomassie staining, and gel imaging, the resulting gel was incubated in cathode buffer (60 mM Tris, 40 mM CAPS, 0.075% SDS, pH 9.6) for 10-20 minutes. An Immobilon-P PVDF membrane was wetted in 100% methanol for 30 seconds, followed by immersion in anode buffer (60 mM Tris, 40 mM CAPS, 15% methanol, pH 9.6) for 10-15 minutes. A Trans-Blot SD Semi-Dry Electrophoretic Transfer Cell system was used to transfer proteins from the gel to the membrane at 12 V for 45 minutes. Following protein transfer, the membrane was washed with water three times for 5 minutes each, stained with GelCode Blue stain reagent for 5 minutes, and then destained with water to visualize the PAT protein. A band containing the maize-derived PAT protein was excised and stored frozen at  $\leq -5$  °C. The band was analyzed using a Shimadzu PPSQ-51A sequencer. Ten cycles of Edman sequencing were performed. During each cycle, the N-terminal amino acid was sequentially derivatized with phenylisothiocyanate (PITC), cleaved with trifluoroacetic acid, and converted to PTH-amino acid which was identified through chromatography. LabSolutions Software was used to automatically identify the N-terminal sequence.

### Glycoprotein Analysis

The Pierce Glycoprotein Staining Kit was used to determine whether the maize-derived PAT protein was glycosylated. The PAT protein, a positive control protein (horseradish peroxidase), and a negative control protein (soybean trypsin inhibitor), were run by SDS-PAGE as described above.

Following electrophoresis, the gel was washed with water twice for 5 minutes each wash, fixed with 50% methanol for 30-35 minutes, and washed twice with 3% acetic acid for 10-15 minutes each wash. The gel was then incubated with oxidizing solution for 15-20 minutes and washed three times with 3% acetic acid for 5-7 minutes each wash. The gel was incubated with glycoprotein staining reagent for 15-20 minutes and then incubated in a reducing reagent for 5-7 minutes. The gel was then washed with 3% acetic acid once for 5 minutes and then rinsed in water once for 5 minutes. Glycoproteins were detected as magenta colored bands on the gel.

Following glycoprotein detection, the image of the gel was captured electronically. The same gel was then stained with GelCode Blue stain reagent for 60 minutes followed by three washes with water for 5 minutes each to visualize all protein bands. The image of the GelCode stained gel was then captured electronically.

## APPENDIX G. METHODS FOR CHARACTERIZATION OF PMI PROTEIN

### [PHI-2020-166 study](#)

#### Test Materials

PMI protein was isolated from DP915635 maize root tissue. The tissue samples were collected at the R1 growth stage (the stage when silks become visible; Abendroth et al., 2011) from plants grown at a field location in Johnston, IA, USA. The tissue was lyophilized, homogenized and stored at  $\leq -50$  °C.

The PMI protein was extracted from lyophilized maize tissue by homogenization in a pre-chilled Waring blender vessel using chilled phosphate-buffered saline containing polysorbate 20 (PBST) extraction buffer with EDTA-free Complete Protease Inhibitors (20 ml buffer per g tissue). The sample extract was then filtered through cheesecloth, clarified by centrifugation, filtered through a 0.45  $\mu\text{m}$  PES vacuum filter unit, and fractionated using ammonium sulfate (AS) precipitation. Beginning at 0% AS saturation and using an online calculator by EnCor Biotechnology Inc. (Encor Biotechnology, 2020), AS was slowly added to the sample extract while stirring until 45% AS saturation was reached. The sample was centrifuged and the AS process was repeated with the supernatant, this time beginning at 45% AS saturation and progressing to 60%. The sample was centrifuged again, the supernatant was discarded, and the fractionated pellets were stored frozen ( $-80$  °C freezer unit).

To prepare the sample for immunoaffinity purification, the pellets were solubilized and buffer exchanged in phosphate-buffered saline using a desalting column from BioRad. The eluted fraction was further purified by immunoaffinity chromatography. The immunoaffinity column was prepared by coupling rabbit polyclonal antibody (R164) anti-PMI to AminoLink Plus Coupling Gel. Elutions 2-4 from the immunoaffinity purification were concentrated into one sample using a centrifugal concentrator (30K Vivaspin Turbo 4; Sartorius) and buffer exchanged to a volume of approximately 100  $\mu\text{l}$ .

Following extraction, purification, and concentration, the final volume in the concentrator was estimated and an equal volume of 2X NuPAGE LDS sample buffer with Reducing Agent was added to the concentrated sample. The sample in the concentrator was heated for 2-5 minutes at 70-100 °C and then transferred to a microcentrifuge tube. The sample was then heat treated at 90-100 °C for 5 ( $\pm 1$ ) minutes and stored frozen at  $< -10$  °C.

#### SDS-PAGE Analysis

The maize-extracted PMI sample stored at  $\leq -10$  °C was re-heated for 2-5 minutes at 90-100 °C and then loaded into 4-12% Bis-Tris gels. The PMI reference substance was prepared in NuPAGE LDS sample buffer with reducing reagent and then heated for 5 ( $\pm 1$ ) minutes at 90-100 °C. The reference substance was then diluted to approximate the same concentration as the maize-extracted PMI sample and loaded into the gels, as applicable. Prestained protein molecular weight markers (Precision Plus Protein Dual Xtra Standards) were loaded into each gel to provide a visual verification that migration was within the range of the predicted molecular weight. Electrophoresis was conducted using a pre-cast gel electrophoresis system with MES SDS running buffer and NuPAGE Antioxidant at a constant 200 volts (V) for 35 minutes.

Upon completion of electrophoresis, the gels were removed from the gel cassettes and used for Coomassie staining, western blot analysis, protein glycosylation analysis, or sample preparation for peptide mapping and N-terminal amino acid peptide identification by LC-MS analysis.

For Coomassie staining, the gel was washed with ultrapure (American Society for Testing and Materials [ASTM] Type 1) water (referred to as water) 3 times for 5 minutes each and stained with GelCode Blue Stain Reagent for 60 minutes. Following staining, the gel was de-stained with water 3-4 times for at least 30 minutes each until the gel background was clear. Proteins were stained as blue-colored bands on the gel. The gel image was captured electronically using an imaging system (Bio-Rad ChemiDoc MP).

#### Western Blot Analysis

Following SDS-PAGE, the resulting gel was assembled into a nitrocellulose (NC) iBlot Gel Transfer Stack. An iBlot Gel Transfer Device was used to transfer proteins from the gel to the NC membrane for 7 minutes with a pre-set program (P3).

Following protein transfer, the membrane was blocked in PBST containing 5% weight/volume (w/v) non-fat dry milk for 45 minutes at ambient laboratory temperature. Before and after the blocking step, the membrane was washed with PBST for 1 minute to reduce the background. The blocked membrane was incubated for 60 minutes at ambient laboratory temperature with a PMI monoclonal antibody (13D11.F11.C12) conjugated to horseradish peroxidase diluted 1:10,000 in PBST containing 1% w/v non-fat dry milk. Following primary antibody incubation, the membrane was washed 3 times in PBST for 5 minutes each. The blot remained in PBST prior to incubating with a chemiluminescent substrate for 5 minutes. The chemiluminescent signal and the pre-stained markers were detected and captured using an imaging system.

#### Peptide Mapping and N-Terminal Peptide Identification by LC-MS

Following SDS-PAGE, Coomassie staining, and gel imaging using the methods as described above two PMI protein bands were excised from a gel and stored frozen at  $\leq -5$  °C. The protein in each gel slice was reduced with DTT, alkylated with iodoacetamide, and then subsequently digested with trypsin or chymotrypsin. The digested samples were separated on an ACQUITY UPLC (Waters Corporation) fitted with a Cortecs UPLC C18 1.6  $\mu\text{m}$  column (2.1 x 100 mm; Waters Corporation) by gradient elution. Eluent from the column was directed into an electrospray source, operating in positive mode, on a TripleTOF 5600+ hybrid quadrupole-TOF mass spectrometer (AB Sciex). The resulting MS data were processed using MS Data Converter (Beta 1.3) to produce a peak list. The peak list was used to perform an MS/MS ion search (Mascot Software version 2.7.0) and match peptides from the expected PMI protein sequence (Perkins et al., 1999). The following search parameters were used: peptide and fragment mass tolerance,  $\pm 0.1$  Da; fixed modifications, cysteine carbamidomethyl; variable modifications, methionine oxidation and acetylation of the protein N-terminal amino acid; maximum missed cleavages, 1 for trypsin and 2 for chymotrypsin. The Mascot-generated peptide ion score threshold was  $> 13$  which indicates identity or extensive homology ( $p < 0.05$ ). The combined sequence coverage was calculated with GPMW version 12.11.0.

#### Glycoprotein Analysis

The Pierce Glycoprotein Staining Kit was used to determine whether the PMI protein was glycosylated. The PMI protein, a positive control protein (horseradish peroxidase), and a negative control protein (soybean trypsin inhibitor), were run by SDS-PAGE as described above.

Following electrophoresis, the gel was washed with water twice for 5 minutes each wash, fixed with 50% methanol for 30-35 minutes, and washed twice with 3% acetic acid for 10-15 minutes each wash. The gel was then incubated

with oxidizing solution for 15-20 minutes and washed three times with 3% acetic acid for 5-7 minutes each wash. The gel was incubated with glycoprotein staining reagent for 15-20 minutes and then incubated in a reducing reagent for 5-7 minutes. The gel was then washed with 3% acetic acid three times for 5 minutes each followed by three washes in water for 5 minutes each. Glycoproteins were detected as magenta colored bands on the gel.

Following glycoprotein detection, the image of the gel was captured electronically. The same gel was then stained with GelCode Blue stain reagent for 60 minutes followed by 3 washes with water (at least 5 minutes each) to visualize all protein bands. The image of the GelCode stained gel was then captured electronically.

## APPENDIX H. METHODS FOR TRAIT EXPRESSION ANALYSES

### [PHI-2019-015 study](#)

#### Field Trial Experimental Design

A multi-site field trial was conducted during the 2019 growing season at six sites in commercial maize-growing regions of the United States (one site in each of Iowa, Nebraska, and Pennsylvania, and two sites in Illinois) and Canada (one site in Ontario). A randomized complete block design with four blocks was utilized at each site. Procedures employed during the field trial to control the introduction of experimental bias included randomization of maize entries within each block and uniform maintenance treatments across each plot area.

#### Sample Collection

The following tissue samples were collected: Root (V6, V9, R1, and R4 growth stage), leaf (V9, R1, and R4 growth stages), pollen (R1 growth stage), forage (R4 growth stage), and grain (R6 growth stage). Growth stages are described in Table H.1. One sample per plot was collected for each tissue set. All samples were collected from impartially selected, healthy, representative plants to minimize potential bias.

**Table H.1. Maize Growth Stage Descriptions**

Growth Stage	Description
V6	The stage when the collar of the sixth leaf becomes visible.
V9	The stage when the collar of the ninth leaf becomes visible.
R1	The stage when silks become visible.
R4	The stage when the material within the kernel produces a doughy consistency.
R6	Typical grain harvest would occur. This stage is regarded as physiological maturity.

Note: Growth stages ([Abendroth et al. 2011](#)).

Samples were collected as follows:

- Each root sample was obtained by cutting a circle 10-15 in. (25-38 cm) in diameter around the base of the plant to a depth of 7-9 in. (18-23 cm). The roots were thoroughly cleaned with water and removed from the plant. No above ground brace roots were included in the sample. The root tissue was cut into sections of 1 in. (2.5 cm) or less in length and collected to fill no more than 50% of a pre-labeled vial.
- Each leaf sample was obtained by pruning the youngest, healthy leaf that had emerged at least 8 in. (20 cm) from the whorl of the plant. The tissue was cut into sections of 1 in. (2.5 cm) or less in length and collected into a pre-labeled vial.
- Each pollen sample was obtained by bagging and shaking a selected tassel to dislodge the pollen. The tassel selected for sampling had one-half to three-quarters of the tassel's main spike shedding pollen. For some plots, pollen may have been pooled from multiple plants within the same plot in order to collect the

appropriate amount. The pollen was screened for anthers and foreign material, and then collected in a pre-labeled vial.

- Each forage sample was obtained by cutting one plant approximately 4-6 in. (10-15 cm) above the soil surface line. The stalk and ear were chopped into sections of 3 in. (7.6 cm) or less in length and the leaves were cut into sections of 12 in. (30 cm) or less in length and collected into a pre-labeled, plastic-lined, cloth bag. The plants selected for forage sampling contained self-pollinated ears.
- Each grain sample was obtained by husking and shelling the grain from one selected ear. The selected ear was a primary ear that had previously been self-pollinated. For each sample, a representative sub-sample of 15 kernels was collected into an individual pre-labeled vial.

### Sample Processing, Shipping, and Storage

Each sample was uniquely labeled with a sample identification number and barcode for sample tracking by site, entry, block, tissue, and growth stage. Samples were placed on dry ice within 10 minutes of collection in the field and transferred to frozen storage ( $\leq -10$  °C freezer unit) until shipment. Samples were then shipped frozen to Pioneer Hi-Bred International, Inc. for processing and analysis. Upon arrival, samples were stored frozen ( $\leq -10$  °C freezer unit).

Forage samples were coarsely homogenized on dry ice prior to lyophilization. All samples were lyophilized under vacuum until dry. Following lyophilization, pollen samples were stored frozen ( $-20$  °C freezer unit) until analysis and root, leaf, forage, whole plant, and grain samples were finely homogenized and stored frozen ( $-20$  °C freezer unit) until analysis.

During lyophilization, a malfunction of the lyophilizer occurred that affected the following samples: 20 samples of R1 leaf for DP915635 maize; 24 samples of R1 root for herbicide-treated DP915635 maize; and four samples of R4 root for DP915635 maize. Protein concentration results for the affected samples will not be reported as the integrity of the samples was considered to be compromised by the lyophilizer malfunction.

### Protein Concentration Determination

The concentrations of IPD079Ea, PAT, and PMI proteins were determined using quantitative enzyme-linked immunosorbent assay (ELISA) methods that have been internally validated to demonstrate method suitability.

Processed tissue sub-samples were weighed at the following target weights: 5 mg for pollen; 10 mg for leaf; 20 mg for grain and root; and 30 mg for forage. Samples were extracted with 0.60 ml of chilled phosphate-buffered saline containing polysorbate 20 (PBST). All extracted samples were centrifuged, and then supernatants were removed and prepared for analysis. Experimental bias was controlled through the use of replicate testing, appropriate assay controls, and pre-determined data acceptability criteria.

### *ELISA Methods*

ELISA methods were performed as follows:

- *IPD079Ea Protein ELISA Method:* Prior to analysis, samples were diluted as applicable in PBST. Standards (typically analyzed in triplicate wells) and diluted samples (typically analyzed in duplicate wells) were incubated in a plate pre-coated with an IPD079Ea-specific antibody. Following incubation, unbound substances were washed from the plate and the bound IPD079Ea protein was incubated with a different IPD079Ea specific-antibody conjugated to the enzyme horseradish peroxidase (HRP). Unbound substances were washed from the plate. Detection of the bound IPD079Ea antibody complex was accomplished by the addition of substrate, which generated a colored product in the presence of HRP. The reaction was stopped with an acid solution and the optical density (OD) of each well was determined using a plate reader.
- *PAT Protein ELISA Method:* Prior to analysis, samples were diluted as applicable in PBST. Standards (typically analyzed in triplicate wells) and diluted samples (typically analyzed in duplicate wells) were co-incubated with a PAT specific antibody conjugated to the enzyme HRP in a plate pre-coated with a different PAT specific antibody. Following incubation, unbound substances were washed from the plate. Detection of the bound PAT antibody complex was accomplished by the addition of substrate, which generated a colored product in the presence of HRP. The reaction was stopped with an acid solution and the OD of each well was determined using a plate reader.
- *PMI ELISA Method:* Prior to analysis, samples were diluted as applicable in PBST. Standards (typically analyzed in triplicate wells) and diluted samples (typically analyzed in duplicate wells) were incubated in plate pre-coated with a PMI-specific antibody. Following incubation, unbound substances were washed from the plate and the bound PMI protein was incubated with a different PMI-specific antibody conjugated to the enzyme HRP. Unbound substances were washed from the plate. Detection of the bound PMI-antibody complex was accomplished by the addition of substrate, which generated a colored product in the presence of HRP. The reaction was stopped with an acid solution and the OD of each well was determined using a plate reader.

#### *Calculations for Determining IPD079Ea, PAT, and PMI Protein Concentrations*

SoftMax Pro GxP (Molecular Devices) microplate data software was used to perform the calculations required to convert the OD values obtained for each set of sample wells to a protein concentration value.

A standard curve was included on each ELISA plate. The equation for the standard curve was derived by the software, which used a quadratic fit to relate the OD values obtained for each set of standard wells to the respective standard concentration (ng/ml).

The sample concentration values were adjusted for a dilution factor expressed as 1:N by multiplying the interpolated concentration by N.

Adjusted Concentration = Interpolated Sample Concentration x Dilution Factor

Adjusted sample concentration values obtained from SoftMax Pro GxP software were converted from ng/ml to ng/mg sample weight as follows:

$$\text{Sample Concentration (ng protein/mg sample weight)} = \text{Sample} \times \frac{\text{Extraction Buffer Volume (ml)}}{\text{Sample Target Weight (mg)}}$$

Concentration  
(ng/ml)

---

The reportable assay lower limit of quantification (LLOQ) in ng/ml was calculated as follows:

Reportable Assay LLOQ (ng/ml) = (lowest standard concentration - 10%) x minimum dilution

The LLOQ, in ng/mg sample weight, was calculated as follows:

$$\text{LLOQ} = \text{Reportable Assay LLOQ (ng/ml)} \times \frac{\text{Extraction Buffer Volume (ml)}}{\text{Sample Target Weight (mg)}}$$

#### Statistical Analysis

Statistical analysis of the IPD079Ea, PAT, and PMI protein concentration results consisted of the calculations of means, ranges, and standard deviations. Individual sample results below the LLOQ were assigned a value equal to half of the LLOQ for calculation purposes.

## APPENDIX I. METHODS FOR NUTRIENT COMPOSITION ANALYSIS

### PHI-2019-016/021 study

#### Field Trial Experimental Design

A multi-site field trial was conducted during the 2019 growing season at eight sites in commercial maize-growing regions of the United States (two sites in Illinois and one site in each of Iowa, Indiana, Nebraska, Pennsylvania, and Texas) and Canada (one site in Ontario). Each site included DP915635 maize, control maize, and four of the following non-GM commercial maize lines: 5513, P0506, 35A52, P0604, P0760, 5883, P0993, 5939, 5828, P1151, P1197, 6158, P0928, P1105, P1345, P1319, P1395, P1422, 33Y74, and 6575 maize (collectively referred to as reference maize). A randomized complete block design with four blocks was utilized at each site. An herbicide treatment of glufosinate was applied to DP915635 maize. Procedures employed during the field trial to control the introduction of experimental bias included randomization of maize entries within each block and uniform maintenance treatments across each plot area.

#### Sample Collection

One forage sample (R4 growth stage) and one grain sample (R6 growth stage) were collected from each plot. Each forage sample (combination of three plants) was obtained by cutting the aerial portion of the plants from the root system approximately 4-6 in. (10-15 cm) above the soil surface line; the plants were chopped into sections of 3 in. (7.6 cm) or less in length, pooled, and approximately one-third of the chopped material was collected in a pre-labeled, plastic-lined, cloth bag. Each grain sample was obtained from five ears at typical harvest maturity from self-pollinated plants; the ears were husked and shelled, and the pooled grain was collected into a large, plastic, resealable bag and then placed into a pre-labeled, plastic-lined, cloth bag.

All samples were collected from impartially selected, healthy, representative plants to minimize potential bias. Reference maize and control maize samples were collected prior to the collection of DP915635 maize samples to minimize the potential for contamination. Each sample was uniquely labeled with a sample identification number and barcode for sample tracking, and is traceable by site, entry, block, tissue, and growth stage. Samples were placed into chilled storage (e.g., coolers with wet ice, artificial ice, or dry ice) after collection and, within three hours of collection, transferred to a freezer ( $\leq -10$  °C). Samples were shipped frozen from each site to EPL Bio Analytical Services (EPL BAS; Niantic, IL, USA) for nutrient composition analyses.

#### Nutrient Composition Analyses

The forage and grain samples were analyzed at EPL BAS. Experimental bias was controlled through the use of the same sample identification numbers assigned to the originally collected samples, the use of pre-set data acceptability criteria, sample randomization prior to homogenization, and through the arrangement of samples for analyses without consideration of sample identity. The following nutrient composition analytes were determined:

- *Forage proximate, fiber, and mineral composition:* moisture\*, crude protein, crude fat, crude fiber, acid detergent fiber (ADF), neutral detergent fiber (NDF), ash, carbohydrates, calcium, and phosphorus

- \*moisture data were used to convert corresponding analyte values for a given sample to a dry weight basis, and were not included in subsequent statistical analysis and reporting of results.
- *Grain proximate and fiber composition:* moisture, crude protein, crude fat, total dietary fiber (TDF), crude fiber, acid detergent fiber (ADF), neutral detergent fiber (NDF), ash, and carbohydrates
  - \*moisture data were used to convert corresponding analyte values for a given sample to a dry weight basis, and were not included in subsequent statistical analysis and reporting of results.
- *Grain fatty acid composition:* lauric acid (C12:0), myristic acid (C14:0), palmitic acid (C16:0), palmitoleic acid (C16:1), heptadecanoic acid (C17:0), heptadecenoic acid (C17:1), stearic acid (C18:0), oleic acid (C18:1), linoleic acid (C18:2),  $\alpha$ -linolenic acid (C18:3), arachidic acid (C20:0), eicosenoic acid (C20:1), eicosadienoic acid (C20:2), behenic acid (C22:0), and lignoceric acid (C24:0)
- *Grain amino acid composition:* alanine, arginine, aspartic acid, cysteine, glutamic acid, glycine, histidine, isoleucine, leucine, lysine, methionine, phenylalanine, proline, serine, threonine, tryptophan, tyrosine, and valine
- *Grain mineral composition:* calcium, copper, iron, magnesium, manganese, phosphorus, potassium, sodium, and zinc
- *Grain vitamin composition:*  $\beta$ -carotene, vitamin B1 (thiamine), vitamin B2 (riboflavin), vitamin B3 (niacin), vitamin B5 (pantothenic acid), vitamin B6 (pyridoxine), vitamin B9 (folic acid),  $\alpha$ -tocopherol,  $\beta$ -tocopherol,  $\gamma$ -tocopherol, and  $\delta$ -tocopherol
  - Note: an additional analyte (total tocopherols) was subsequently calculated as the sum of the  $\alpha$ -,  $\beta$ -,  $\gamma$ -, and  $\delta$ -tocopherol values for each sample for use in statistical analysis and reporting of results
- *Grain secondary metabolite and anti-nutrient composition:* *p*-coumaric acid, ferulic acid, furfural, inositol, phytic acid, raffinose, and trypsin inhibitor

Nutrient composition analytical methods and procedures are summarized in Table I.1.

**Table I.1. Methods for Compositional Analysis**

Nutritional Analyte	Method
Moisture	The analytical procedure for moisture determination was based on a method published by AOAC International. Samples were assayed to determine the percentage of moisture by gravimetric measurement of weight loss after drying in a forced air oven (forage) and a vacuum oven (grain).
Ash	The analytical procedure for ash determination was based on a method published by AOAC International. Samples were analyzed to determine the percentage of ash by gravimetric measurement of the weight loss after ignition in a muffle furnace.
Crude Protein	The analytical procedure for crude protein determination utilized an automated Kjeldahl technique based on a method provided by the manufacturer of the titrator unit (Foss-Tecator) and AOAC International. Ground samples were digested in the presence of a catalyst. The digestate was then distilled and titrated with a Foss-Tecator Kjeltec Analyzer unit.
Crude Fat	The analytical procedure for crude fat determination was based on methods provided by the American Oil Chemists' Society (AOCS) and the manufacturer of the hydrolysis and extraction apparatus (Ankom Technology). Samples were hydrolyzed with 3N hydrochloric acid at 90 °C for 80 minutes for forage and 60 minutes for grain. The hydrolysates were extracted with a petroleum ether/ethyl ether/ethyl alcohol solution at 90 °C for 60 minutes. The ether extracts were evaporated and the fat residue remaining determined gravimetrically.
Carbohydrates	The carbohydrate content in maize forage and grain on a dry weight basis was calculated using a formula obtained from the United States Department of Agriculture " <i>Energy Value of Foods</i> ," in which the percent dry weight of crude protein, crude fat, and ash was subtracted from 100%.
Crude Fiber	The analytical procedure for crude fiber determination was based on methods provided by the manufacturer of the extraction apparatus (Ankom Technology), AOAC International, and the AOCS. Samples were analyzed to determine the percentage of crude fiber by digestion and solubilization of other materials present.
Neutral Detergent Fiber	The analytical procedure for neutral detergent fiber (NDF) determination was based on a method provided by the manufacturer of the extraction apparatus (Ankom Technology), AOAC International, and the <i>Journal of AOAC International</i> . Samples were analyzed to determine the percentage of NDF by digesting with a neutral detergent solution, sodium sulfite, and alpha amylase. The remaining residue was dried and weighed to determine the NDF content.
Acid Detergent Fiber	The analytical procedure for acid detergent fiber (ADF) determination was based on a method provided by the manufacturer of the extraction apparatus (Ankom Technology) and AOAC International. Samples were analyzed to determine the percentage of ADF by digesting with an acid detergent solution and washing with reverse osmosis water. The remaining residue was dried and weighed to determine the ADF content.
Total Dietary Fiber	The analytical procedure for the determination of total dietary fiber in grain was based on methods provided by the manufacturer of the extraction apparatus (Ankom Technology), AOAC International, and the manufacturer of the protein titrator unit (Foss-Tecator). Duplicate samples were gelatinized with heat stable $\alpha$ -amylase, enzymatically digested with protease and amyloglucosidase to remove protein and starch, respectively, and then soluble dietary fiber precipitated with ethanol. The precipitate (residue) was quantified gravimetrically. Protein analysis was performed on one of the duplicate samples while the other duplicate sample was analyzed for

Nutritional Analyte	Method
	ash. The weight of the protein and ash was subtracted from the weight of the residue divided by sample dry weight.
Minerals	The analytical procedure for the determination of minerals is based on methods published by AOAC International and CEM Corporation. The maize forage minerals determined were calcium and phosphorus. Additional grain minerals determined were copper, iron, magnesium, manganese, potassium, sodium, and zinc. The samples were digested in a microwave based digestion system and the digestate was diluted using deionized water. Samples were analyzed by inductively coupled plasma optical emission spectroscopy (ICP-OES).
Tryptophan	The analytical procedure for tryptophan determination was based on an established lithium hydroxide hydrolysis procedure with reverse phase ultra performance liquid chromatography (UPLC) with ultraviolet (UV) detection published by the <i>Journal of Micronutrient Analysis</i> .
Cystine and Methionine	The analytical procedure for cystine and methionine determination was based on methods obtained from Waters Corporation, AOAC International, and <i>Journal of Chromatography A</i> . The procedure converts cystine to cysteic acid and methionine to methionine sulfone, after acid oxidation and hydrolysis, to the 6-aminoquinolyl-N-hydroxysuccinimidyl carbamate derivatives which are then analyzed by reverse phase UPLC with UV detection.
Additional Amino Acids	Along with tryptophan, cystine, and methionine, 15 additional amino acids were determined. The analytical procedure for analysis of these amino acids was based on methods obtained from Waters Corporation and the <i>Journal of Chromatography A</i> . The procedure converts the free acids, after acid hydrolysis, to the 6-aminoquinolyl-N-hydroxysuccinimidyl carbamate derivatives, which are analyzed by reverse phase UPLC with UV detection.
Fatty Acids	The analytical procedure for determination of fatty acids was based on methods published by AOAC International and AOCS. The procedure converts the free acids, after ether extraction and base hydrolysis, to the fatty acid methyl ester (FAME) derivatives, which are analyzed by gas chromatography with flame ionization detection (GC/FID). Results are reported as percent total fatty acids but presented in the raw data as percent fresh weight.
Thiamine (Vitamin B1) and Riboflavin (Vitamin B2)	The analytical procedure for the determination of thiamine (vitamin B1) and riboflavin (vitamin B2) was based on a method published by the American Association of Cereal Chemists (AACC). The samples were extracted with 10% acetic acid/4.3% trichloroacetic acid solution. A 50-fold dilution was performed and then the samples were analyzed by reverse phase high pressure liquid chromatography (HPLC) tandem mass spectrometry (MS/MS).
Niacin (Vitamin B3)	The analytical procedure for the determination of niacin (vitamin B3) was based on a method published by the AACC. Niacin (vitamin B3) was extracted from the sample by adding deionized (DI) water and autoclaving. A tube array was prepared using three different dilutions of the samples. This tube array was inoculated with <i>Lactobacillus plantarum</i> and allowed to incubate for approximately 18 to 22 hours. After incubation, the bacterial growth was determined using a spectrophotometer at an absorbance of 660 nm. The absorbance readings were compared to a standard curve generated using known concentrations of nicotinic acid.

Nutritional Analyte	Method
Pantothenic Acid (Vitamin B5)	The analytical procedure for the determination of pantothenic acid (vitamin B5) was based on a method from AOAC International. Pantothenic acid (vitamin B5) was determined using a microbiological assay. Pantothenic acid (vitamin B5) was extracted from the sample by adding an acetic acid buffer solution and autoclaving. The pH was adjusted and a tube array was prepared using three different dilutions of the samples. This tube array was inoculated with <i>Lactobacillus plantarum</i> and allowed to incubate for approximately 18-22 hours. After incubation, the microbial growth was determined using a spectrophotometer at an absorbance of 660 nm. The absorbance readings were compared to a standard curve generated using known concentrations of D-pantothenic acid hemicalcium salt.
Pyridoxine (Vitamin B6)	The analytical procedure for the determination of pyridoxine (vitamin B6) was based on a method from the AACC. Pyridoxine (vitamin B6) was determined using a microbiological assay. Pyridoxine (vitamin B6) was extracted from the sample by adding sulfuric acid and autoclaving. The pH was adjusted and a tube array was prepared using four different dilutions of the samples. This tube array was inoculated with <i>Saccharomyces cerevisiae</i> and allowed to incubate for approximately 18-22 hours. After incubation, the microbial growth was determined using a spectrophotometer at an absorbance of 600 nm. The absorbance readings were compared to a standard curve generated using known concentrations of pyridoxine hydrochloride.
Total Folate as Folic Acid (Vitamin B9)	The analytical procedure for determination of total folate as folic acid was based on a microbiological assay published by the AACC. Samples were hydrolyzed and digested by protease and amylase enzymes to release the folate from the grain. A conjugase enzyme was used to convert the naturally occurring folypolyglutamates. An aliquot of the extracted folates was mixed with a folate and folic acid free microbiological growth medium. The mixture was inoculated with <i>Lactobacillus casei</i> . The total folate content was determined by measuring the turbidity of the <i>Lactobacillus casei</i> growth response in the sample and comparing it to the turbidity of the growth response with folic acid standards using a spectrophotometer at 600 nm.
Total Tocopherols	The analytical procedure for determination of tocopherols was based on methods from the <i>Journal of the American Oil Chemists' Society</i> and <i>Analytical Sciences</i> . Alpha-, beta-, gamma-, and delta-tocopherols were extracted with hot hexane and the extracts were analyzed by normal phase UPLC with fluorescence detection.
β-Carotene	The analytical procedure for determination of beta-carotene was based on a method published by AOAC International. Samples were extracted using a 40:60 acetone:hexane with tert-butylhydroquinone (TBHQ) solution then analyzed by HPLC-UV.
Trypsin Inhibitor	The analytical procedure for the determination of trypsin inhibitor was based on a method published by the AOCS. Trypsin inhibitor was extracted with sodium hydroxide. Trypsin was added to the extracts to react with trypsin inhibitor. The residual trypsin activity was measured with a spectrophotometer using the chromogenic trypsin substrate Benzoyl-DL-arginine-p-nitroanilide hydrochloride (BAPNA). The amount of trypsin inhibitor was calculated based on the inhibition of trypsin activity.
Inositol and Raffinose	The analytical procedure for the determination of inositol and raffinose was based on a gas chromatography (GC) method published in the <i>Handbook of Analytical Derivatization Reactions</i> , an AACC method, and a method from the <i>Journal of Agricultural and Food Chemistry</i> . Extracted inositol and raffinose were analyzed by reverse phase HPLC with refractive index detection.
Furfural	The analytical procedure for the determination of furfural was based on methods

Nutritional Analyte	Method
	published in the <i>Journal of Agricultural and Food Chemistry</i> . Ground maize grain was analyzed for furfural content by reverse phase HPLC with UV detection.
<i>p</i> -Coumaric and Ferulic Acid	The analytical procedure for the determination of <i>p</i> -coumaric and ferulic acids was developed based on methods published in <i>Journal of Agricultural and Food Chemistry</i> and <i>The Journal of Chemical Ecology</i> . Ground maize grain was analyzed to determine the amounts of <i>p</i> -coumaric acid and ferulic acid by separating the total content of phenolic acids using reverse phase HPLC and UV detection.
Phytic Acid	The analytical procedure for the determination of phytic acid was based on a method published by AOAC International. The samples were analyzed to determine the amount of phytic acid by extracting the phytic acid with dilute hydrochloric acid (HCl) and isolating it using an aminopropyl silica solid phase extraction column. Once isolated and eluted, the phytic acid was analyzed for elemental phosphorus by ICP-OES.

#### Statistical Analysis of Nutrient Composition Data

Prior to statistical analysis, the data were processed as follows:

- *LLOQ Sample Values*: For statistical analysis, nutrient composition values reported as below the assay lower limit of quantification (LLOQ) were each assigned a value equal to half the LLOQ.
- *Conversion of fatty acid assay values*: The raw data for all fatty acid analytes were provided by EPL BAS in units of percent fresh weight (%FW). Any fatty acid values below the %FW LLOQ were set to half the LLOQ value, and then all assay values were converted to units of % total fatty acids for statistical analyses. For a given sample, the conversion to units of % total fatty acids was performed by dividing each fatty acid analyte value (%FW) by the total fresh weight of all fatty acids for that sample; for analyte values below the LLOQ, the half LLOQ value was used as the analyte value. Half LLOQ values were also included in the total fresh weight summations. After the conversion, a fixed LLOQ value was not available for a given individual fatty acid analyte on the % total fatty acids basis.
- *Calculation of additional analytes*: One additional analyte (total tocopherol) was calculated for statistical analyses. The total amount of tocopherol for each sample was obtained by summing the assay values of  $\alpha$ -tocopherol,  $\beta$ -tocopherol,  $\gamma$ -tocopherol, and  $\delta$ -tocopherol in the sample. If the assay value of an individual analyte was below the LLOQ for a given sample, half of the LLOQ value was used in computing the total. The total was considered below the LLOQ only when all the individual analytes contributing to its calculation were below the LLOQ.

Statistical analyses were conducted using SAS software, Version 9.4 (SAS Institute, Inc.). The following rules were implemented for each analyte:

- If both DP915635 maize and the control maize had < 50% of samples below the LLOQ, then an across-site mixed model analysis would be conducted.
- If, either DP915635 maize or the control maize had  $\geq$  50% samples below the LLOQ, but not both entries had 100% of samples below the LLOQ across sites, then Fisher's exact test would be conducted. The Fisher's exact test assessed whether there was a significant difference (P-value < 0.05) in the proportion of samples below the LLOQ between these two maize lines across sites.

- If, both DP915635 maize and the control maize had 100% of samples below the LLOQ, then statistical analyses would not be performed.

#### Statistical Model for Across-Site Analysis

For a given analyte, data were analyzed using the following linear mixed model:

$$y_{ijk} = \mu_i + \ell_j + r_{k(j)} + (\mu\ell)_{ij} + \varepsilon_{ijk} \quad \text{Model 1}$$

$$\ell_j \sim iid N(0, \sigma^2_{Site}), r_{k(j)} \sim iid N(0, \sigma^2_{Rep}), (\mu\ell)_{ij} \sim iid N(0, \sigma^2_{Ent \times Site}), \text{ and } \varepsilon_{ijk} \sim iid N(0, \sigma^2_{Error})$$

where  $\mu_i$  denotes the mean of the  $i^{th}$  entry (fixed effect),  $\ell_j$  denotes the effect of the  $j^{th}$  site (random effect),  $r_{k(j)}$  denotes the effect of the  $k^{th}$  block within the  $j^{th}$  site (random effect),  $(\mu\ell)_{ij}$  denotes the interaction between the entries and sites (random effect), and  $\varepsilon_{ijk}$  denotes the effect of the plot assigned the  $i^{th}$  entry in the  $k^{th}$  block of the  $j^{th}$  site (random effect or residual). Notation  $\sim iid N(0, \sigma^2_a)$  indicates random variables that are identically independently distributed (*iid*) as normal with zero mean and variance  $\sigma^2_a$ . Subscript  $a$  represents the corresponding source of variation.

The residual maximum likelihood estimation procedure was utilized to generate estimates of variance components and entry means across sites. The estimated means are known as empirical best linear unbiased estimators (hereafter referred to as LS-Means). The statistical comparison was conducted by testing for a difference in LS-Means between DP915635 maize and the control maize. The approximated degrees of freedom for the statistical test were derived using the Kenward-Roger method ([Kenward and Roger, 2009](#)). A significant difference was identified if an P-value was  $< 0.05$ .

For each analyte, goodness-of-fit of the model was assessed in terms of meeting distributional assumptions of normally, independently distributed errors with homogeneous variance. Deviations from assumptions were addressed using an appropriate transformation or a heterogeneous error variance structure. The statistical results for transformed data were back transformed to the original data scale for reporting purposes.

#### False Discovery Rate Adjustment

The false discovery rate (FDR) method of Benjamini and Hochberg ([Benjamini and Hochberg, 1995](#); [Westfall et al., 1999](#)) was applied as a post-hoc procedure to control for false positive outcomes across all analytes analyzed using linear mixed models. A false positive outcome occurs if the difference in means between two entries is declared significant, when in fact the two means are not different. Since its introduction in the mid-1990s, the FDR approach has been widely employed across a number of scientific disciplines, including genomics, ecology, medicine, plant breeding, epidemiology, dairy science, and signal/image processing (e.g., [Pawitan et al., 2005](#); [Spelman and Bovenhuis, 1998](#)). In the FDR method, the false discovery rate is held at 5% across comparisons of multiple analytes via an adjustment to the P-value and is not inflated by the number of analytes in the comparison.

### *Interpretation of Statistical Results*

For a given analyte, when a statistically significant difference (P-value from mixed model analysis < 0.05, or Fisher's exact test P-value < 0.05) was identified in the across-site analysis, the respective range of individual values from DP915635 maize was compared to a tolerance interval. Tolerance intervals are expected to contain at least 99% of the values for corresponding analytes of the conventional maize population with a 95% confidence level ([Hong et al., 2014](#)). The tolerance intervals were derived from proprietary accumulated data from 31 multi-site field studies between 2003 and 2018. These studies consisted of a total of 167 non-GM commercial reference maize lines and 171 unique environments representative of commercial maize-growing regions in the United States, Canada, Chile, Brazil, and Argentina. The selected commercial maize lines represent the non-GM maize population with a history of safe use, and the selected environments (site and year combinations) represent maize growth under a wide range of environmental conditions (i.e., soil texture, temperature, precipitation, and irrigation) and maize maturity group zones.

If the range of DP915635 maize contained individual values outside the tolerance interval, it was then compared to the respective literature range. Literature ranges were generated from relevant crop composition data obtained from published literature ([AFSI, 2019](#); [Codex Alimentarius Commission, 2019](#); [Cong et al., 2015](#); [Lundry et al., 2013](#); [OECD, 2002](#); [Watson, 1982](#)). Literature ranges compliment tolerance intervals and in-study reference ranges in that they are composed of non-proprietary data from additional non-GM commercial maize lines and growing environments, which are not included in the proprietary database used for tolerance interval construction.

If the range of DP915635 maize contained individual values outside the literature range, it was then compared to the respective in-study reference range. In-study reference ranges were comprised of all individual values across-sites from all non-GM reference maize lines grown in this study. In-study reference data ranges compliment tolerance intervals and literature ranges in that they provide additional context of natural variation specific to the current study.

In cases when a raw P-value indicated a significant difference but the FDR adjusted P-value was > 0.05, it was concluded that the difference was likely a false positive.